Ice stream dynamics and pro-glacial lake evolution along the north-western margin of the Laurentide Ice Sheet

Victoria Helen Brown

Abstract

Ice streams drain ice sheets rapidly and are key regulators of their mass balance in both palaeo and contemporary settings. Present day ice streams can be identified, and their short-term activity monitored, by measuring the surface velocity of ice sheets. However, in order to understand their long-term behaviour, reconstructions of their activity in palaeo-ice sheets are necessary. Numerous palaeo-ice streams have been identified in the Laurentide Ice Sheet (LIS) and this has considerably refined our understanding of its dynamic behaviour and links to the ocean-climate system. In the north-west sector of the LIS, ice streaming has been hypothesised but detailed mapping of the area has not been carried out and so our understanding of palaeo-ice streaming is limited compared to other areas.

This thesis presents a new ice sheet reconstruction of the north-west sector of the LIS that incorporates ice stream activity and pro-glacial lake evolution. Mapping and analysis was carried out using a range of remote sensing imagery and Digital Elevation Models (DEMs), which enabled widespread, rapid and systematic coverage of the 800,000 km^2 study area. More than 95,000 bedforms have been mapped, including glacial lineations, eskers, moraines and palaeo-channels. These data permit the identification and classification of 272 flow-sets which have been dated using an existing ^{14}C database and relative cross-cutting relationships. Flow-sets are used to construct a robust and self-consistent ice sheet reconstruction, incorporating the activity of ice streams at a temporal resolution of up to 250-500 years.

The reconstruction reveals major changes in ice sheet configuration during Late Wisconsinan deglaciation and indicates that margin retreat was complex and dominated by the dynamic spatial and temporal evolution of seven ice stream systems. These ice streams were not synchronous but a peak in their activity occurred between 15 and 13 ka. Their location and behaviour was influenced by the availability of soft sediments, but their temporal switching was likely controlled by sub-glacial meltwater routing and ice piracy. Large proglacial lakes developed during deglaciaton but their evolution did not appear to control ice stream activity, as observed elsewhere in the ice sheet. However, major palaeo-channels are consistent with a previously hypothesised north-west drainage route for Glacial Lake Agassiz.

Ice stream dynamics and pro-glacial lake evolution along the north-western margin of the Laurentide Ice Sheet

Victoria Helen Brown

Department of Geography

Durham University

A thesis submitted in partial fulfilment of

the requirements for the degree of

Doctor of Philosophy

November 2012

Declaration and Statement of Copyright

I confirm that no part of the material presented in this thesis has previously been submitted by me or any other person for a degree in this or any other university. In all cases, where is relevant, material from the work of others has been acknowledged.

Victoria Helen Brown

Department of Geography
Durham University
November 2012

Acknowledgements

Getting me to read as a child was always a struggle and, to be honest, little has changed! Those who know me well will recall that the last fiction book I read was 'Fantastic Mr Fox' at the age of 8. So, since the days of being bribed (and I mean that!) by Mum and Dad to read about the adventures of Roger Red Hat, choosing to 'read' for a Ph.D. has perhaps been one of my more surprising choices and as much as a shock to me as anyone else! But, to have got to point of writing my acknowledgements probably means that I did find something quite interesting to read about after all! Mum and Dad: thank you for persisting with a child who has always known her own mind and I'm sorry for draining you of 20p coins (the bribe!)! You have always been there through the ups and downs and listened to endless rants along the lines of 'Arc isn't working'. I am so very grateful, even though I don't say it enough.

Studying Geography is something that you could say I fell into. First it was Dentistry, then Music but then I found my true love…colouring in! Indeed, while most Geography Ph.D. students are able to argue they do far more than colouring in, I have no defence having drawn a map containing a crazy amount of drumlins. I also must apologise to my fellow GISers who had to tolerate the constant 'click, click…click, click, click'! It has been wonderful to share the last 3 years with some great friends in the Geography Department and I am sorry for my poor excuses as regards pub trips!

Throughout my studies, Chris and Colm have provided fantastic supervision. It has been wonderful to work with them and I am incredibly grateful for their patience and support. Similarly, I must acknowledge the I.T. staff in Geography who have helped me out in many a crisis moment. Away from Durham, it was a privilege to assist Prof. Chris Burn and Dr J. Ross Mackay with fieldwork in the Western Arctic. Their love for the Arctic is truly inspirational. Chris: thank you for the opportunity to dive into the world of permafrost, see an amazing part of the world, and for your patience when I was totally convinced that a bear was going to 'get me' in my sleep!! Never trust bear spray…

I am also very grateful to Kristen Dellorey at the National Air Photo Library of Canada who assisted in the organisation of my visit and made me feel very welcome. Discussions with Julian Murton, Alan Condron, John England and Art Dyke have also proved thought-provoking, and sparked the investigation of additional avenues within this research.

Although I am not leaving Durham, I would still like to thank a number of people without whom my time as a Ph.D. student just would not have been complete! Living in Van Mildert College made life away from Geography fantastic. Thanks to everyone that I shared the 83's with!! Chad's Choir has also been a big part of my life in Durham. It has introduced me to a wonderful group of friends with whom I have shared some amazing experiences. I have gained more than I could ever have imagined from singing…including an organ-playing, physicist from Lancashire!!

Table of Contents

Table of Figures

Chapter 1: Introduction

1.1 Background and rationale

The Laurentide Ice Sheet (LIS), which covered much of northern North America during the Last Glacial Maximum (LGM), was an influential component of the earth system (Clark *et al.,* 1999; Clark and Mix, 2002). During the LGM, the LIS accounted for 35 % of global ice volume and was the largest ice mass to completely disappear in response to the last glacial-interglacial transition (Siddall and Kaplan, 2008). The maximum extent of the LIS is shown below in Figure 1-1. At a continental scale, the LIS influenced atmospheric circulation by providing a permanent source of Arctic air to the mid-latitudes (Oerlemans and van der Veen, 1984; Clark *et al.*, 1999). The changing configuration of the ice sheet during deglaciation also determined the location of pro-glacial lakes and their subsequent drainage routeways which delivered freshwater to the oceans (Boulton *et al.,* 1985; Teller *et al.,* 2005). This influenced the salinity balance of the Thermohaline circulation and, therefore, had implications for global climate (Fairbanks, 1989; Bond *et al.,* 1993). Furthermore, the ice sheet was significant because, at the LGM, it contained enough freshwater to raise global mean sea level by between 76 and 85 m (Clark and Mix, 2002). At its maximum extent, it was coalescent with the Cordilleran Ice Sheet to the west and to the Innuitian Ice Sheet in the Canadian High Arctic to the north (Dyke *et al.,* 2002). Fulton and Prest (1987) estimate that, during the LGM, the LIS covered between 10.2 and 11.3 x 10^6 km^2.

The geometry of the LIS was complex and featured a number of dynamic sub-systems, including ice streams (see Figure 1-1). According to Patterson (1994), an ice stream is defined as “a region of grounded ice sheet in which the ice flows much faster than in regions on either side” (Patterson, 1994, p. 16). As such, ice streams have the ability to rapidly drain large volumes of ice and thus dominate ice sheet mass balance and their response to climate change (Stokes and Clark, 2001, Bennett, 2003, Pritchard *et al.*, 2009). Present day ice streams can be identified, and their short-term activity monitored, by measuring the surface velocity of ice sheets (e.g. Lucchitta and Ferguson, 1986; Bindschadler and Scambos, 1991; Joughin *et al.,* 2012). However, in order to understand their long-term behaviour (including location, timing, geometry and mechanisms of flow) and thus provide analogues for contemporary ice stream activity, reconstructions of their activity in palaeo-ice sheets are necessary by examining the geomorphological and sedimentological record. Our knowledge of ice stream operation can also be used to inform numerical ice sheet/ice stream models of both palaeo and

contemporary glacial environments, with the aim of more accurately predicting ice sheet and/or ice stream activity (e.g. Stokes and Tarasov, 2010).

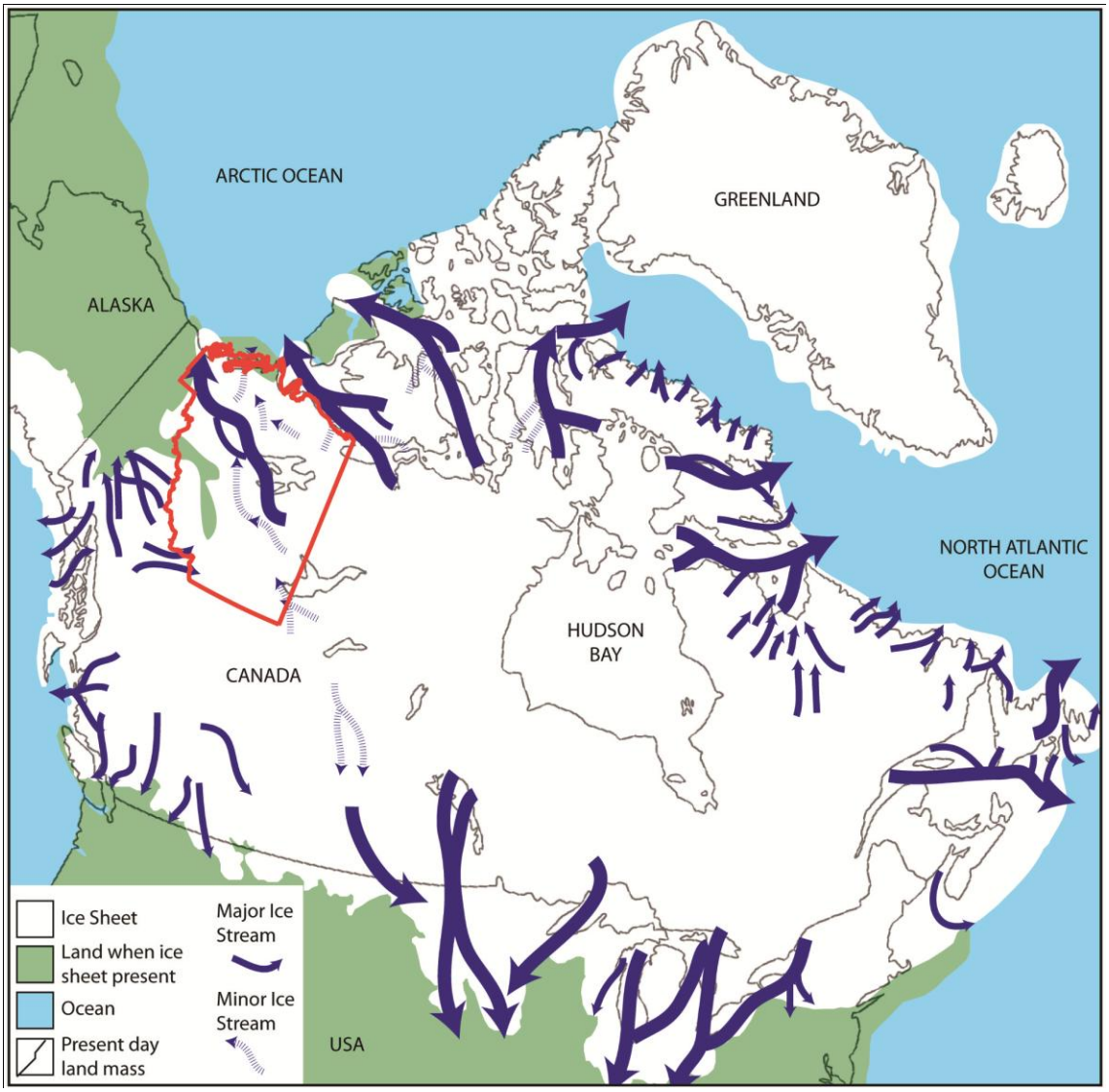

Figure 1-1: The location of ice streams within the LIS during the Late Wisconsinan. The figure was compiled from the LGM (21.4 cal. ka BP) ice margin of Dyke et al. (2003), and the location of reconstructed palaeo-ice streams as shown in Kleman and Glasser (2007). While reconstructions of many of these ice streams have previously been published (see Patterson, 1998; Stokes et al., 2009; De Angelis and Kleman, 2007), some remain only hypothesised (e.g. those flowing north-west on the north-west Canadian mainland).

The investigation of palaeo-ice streams also provides a unique opportunity to understand ice sheet basal processes. In contemporary settings, ice stream beds remain largely inaccessible, with only a limited number of investigations having been carried out (see Engelhardt and Kamb, 1997 and King *et al.,* 2009). Furthermore, while King *et al.* (2009) provide imagery of the ice-bed interface beneath Rutford Ice Stream, West Antarctica, the spatial coverage of the imagery is limited (see Chapter 2, Section 2.4.3). However, palaeo-ice stream beds are much

more accessible. This counteracts problems associated with the extrapolation of small-scale studies as analogues for much larger ice stream processes (Stokes and Clark, 2001). It can also aid our understanding of the controls on ice stream activity, and, in particular, the causes of ice stream onset and shut-down (Stokes and Clark, 2001; Winsborrow *et al.,* 2010).

Palaeo-ice streams have been identified and reconstructed in numerous palaeo-ice sheets, including those which covered Fennoscandia, the British Isles and North America (Winborrow *et al.,* 2004; Boulton and Hagdorn, 2006; Kleman and Glasser, 2007; Phillips *et al.,* 2010; Rydningen *et al.,* 2012; Winsborrow *et al.,* 2012). In the LIS, evidence for palaeo-ice streams has been comprehensively documented and compiled by Winsborrow *et al.* (2004). However, in the north-west LIS, ice streaming has been hypothesised, but the timing of ice stream activity has, prior to the reconstruction presented in Chapter 5, remained largely unknown. Indeed, Beget (1987) suggests that the LIS was characterised by a low profile ice surface and streaming flow, based on drift limits along the western Cordillera. Streaming has also been reported in the north-west LIS by Kleman and Glasser (2007), Winsborrow *et al.* (2004) and Clark (*unpublished*, cited in Winsborrow *et al.,* 2004). Furthermore, Prest *et al.* (1968) provide a continental map at a scale of 1:5,000,000 which indicates a complex bedform arrangement in the north-west sector of the LIS. However, the map does not identify areas of cross-cutting bedforms which are vital for accurate palaeo-ice sheet reconstruction (cf. Kleman and Börgstrom, 1996). More recently, Shaw *et al.* (2010) have reconstructed ice flowlines for this sector of the LIS, but a map which identifies individual bedforms, and therefore provides the basis for a definitive regional ice sheet reconstruction, is yet to be constructed. Figure 1-1 provides a compilation of the reconstructed and hypothesised ice streams within the LIS as suggested by Kleman and Glasser (2007). In the north-west LIS, the hypothesised ice streams of Clark (*unpublished,* cited in Winsborrow *et al.,* 2004) form a complex network which includes one large sinuous ice stream, and a number of minor ice streams. However, as previously noted, detailed and systematic geomorphological evidence for these ice streams has not hitherto been documented.

According to Dyke *et al.* (2003), since the LGM, ice stream activity in the LIS and overall ice sheet geometry have evolved alongside several millennial scale warming and cooling events which punctuated deglaciation. Many of these events were most widespread and rapid around the North Atlantic (Keigwin *et al.,* 1991; Bond *et al.,* 1992; Bond *et al.,* 1993; Broecker, 2000; Meissner and Clark, 2006). The events have been linked to changes in the delivery of freshwater to the North Atlantic as a result of deglacial ice sheet reorganisation; in particular that of the LIS (Leverington *et al.*, 2000; Teller *et al.*, 2002; Fisher *et al.*, 2002a; Fisher *et al.*,

2002b; Murton *et al.*, 2010). One such example is the Younger Dryas (12.86 – 11.69 ka BP), which constituted a return to full glacial conditions across much of the Northern hemisphere and is the most well documented of these events (Fawcett *et al.*, 1997; Brook and Birks, 2000). The drainage of pro-glacial lakes, in particular Glacial Lake Agassiz which formed around the margin of the LIS, has been assumed as the source of this freshwater and thus a trigger for this climatic downturn (Teller *et al.,* 2005; Smith and Fisher, 1993; Murton *et al.,* 2010). However, the precise location of freshwater delivery to the oceans remains debated with a number of different drainage routes proposed (east to the North Atlantic through the Gulf of St Lawrence, south to the Gulf of Mexico, north-west to the Arctic Ocean, or subglacially into Hudson Bay) (cf. Teller *et al.,* 2002; Teller *et al.,* 2005; Murton *et al.,* 2010; Fisher *et al.,* 2002a; Smith and Fisher, 1993). This study area is, therefore, directly relevant to this debate because the study area forms the north-west drainage routeway. A robust reconstruction of pro-glacial lake evolution around the LIS during deglaciation, and in particular along the north-west margin of the LIS is, therefore, required for two reasons: 1; to assess the viability of a north-west outlet for Glacial Lake Agassiz, and 2; to investigate the link between pro-glacial lake evolution and ice stream activity in the north-west sector of the LIS.

1.2 Aims and objectives

The thesis has two overarching aims.

1. To map the glacial geomorphology of the north-west sector of the LIS in order to identify the tracks of possible palaeo-ice streams, and provide a robust reconstruction of their activity from the LGM through to deglaciation.
2. To reconstruct the evolution of pro-glacial lakes along the north-west margin of the LIS during Late Wisconsinan deglaciation and thus test the concept of a north-west drainage routeway for Glacial Lake Agassiz (cf. Teller *et al.,* 2002; Smith and Fisher, 1993; Fisher *et al.,* 2002).

In order to fulfil these aims, the following specific objectives have been developed.

a. To map the glacial geomorphology of the study area using a range of remote sensing products including Landsat ETM+, ASTER and aerial photography (Chapter 4).
b. To use the geomorphological map produced in objective 1 to identify discrete ice flow sets, including those potentially formed by palaeo-ice streams, based on previously published criteria (Stokes and Clark, 1999) (Chapter 5).

c. To embed each flow set into the deglaciation of the LIS using the ice margins of Dyke *et al.* (2003) and to reconstruct their temporal activity during deglaciation (Chapter 5).

d. To merge a Digital Elevation Model (DEM) of North America with the patterns of solid earth deformation throughout deglaciation, and flood the resulting DEM to establish the location of pro-glacial lakes and identify possible spillways for lake drainage (Chapter 6).

1.3 Study area

The study area spans the border between the Northwest Territories (NWT) and Nunavut, Canada (see Figure 1-2). The region largely consists of low lying plains which are occupied by a series of major river systems and two large lakes: Great Bear Lake and Great Slave Lake (see Figure 1-3). Away from the Yukon Mountains, summits attain a relatively subdued maximum altitude of ~ 480-500 m. Physiographically, the study area spans four key areas: the Western Cordillera, Interior Plains, Precambrian Shield and Arctic Coastal Plain (Vincent, 1989). The largest of these geological areas is the metamorphosed Precambrian Canadian Shield which encircles Hudson Bay in the east and has minimal sediment cover. In contrast, to the west, the majority of the study area occupies the Interior Plains. This region is dominated by thick, soft-sediment marine and fluvial sequences, deposited by rivers and shallow inland seas (Reed *et al.*, 2003). The westernmost portion of the study area occupies the Canadian Cordillera; an area of mountainous terrain consisting of the deformed margin of the North American Craton (Vincent, 1989). In the north, the Arctic Coastal Plain is a lowland area of continuous permafrost which stretches along the coast of northern Canada from Meighen Island in the east to Alaska in the west (Côté and Burn, 2002, Murton, 1996).

The last glaciation of north-west mainland Canada was during the Late Wisconsinan, when ice reached its maximum extent ~ 21 cal. ka BP (Dyke *et al.,* 2003). In the west, ice was buttressed against the Yukon, Richardson and Mackenzie Mountains and, according to Duk-Rodkin and Lemmen (2000), this was the most extensive glaciation of the Quaternary. The ice margin reconstructions from Dyke *et al.* (2003) indicate a relatively stable offshore ice margin until ~ 16.2 cal. ka BP. Rapid eastward retreat of the ice margin then followed until the area became ice free around 11.5 cal. ka BP (Dyke *et al.*, 2003). As noted previously, Beget (1987) suggests that the north-west mainland sector of the LIS was characterised by a low profile ice sheet which underwent streaming flow during the Late Wisconsinan. Kleman and Glasser (2007) and Winsborrow *et al.* (2004), after Clark (*unpublished*, cited in Winsborrow *et al.,* 2004) have also hypothesised ice stream activity in this sector of the ice sheet based on localised inspections of

the region's glacial geomorphology. In addition, Prest *et al.* (1968), in the Glacial Map of Canada, indicate that large portions of the study area are occupied by groups of highly elongate bedforms which, according to Stokes and Clark (1999), are a key criterion for the identification of palaeo-ice stream beds (see Chapter 2, Section 2.3).

The maximum extent of pro-glacial lakes along the north-western margin of the LIS during the Late Wisconsinan has been documented by Craig (1965) and Smith and Fisher (1993). Based on geomorphological evidence, two major pro-glacial lakes have been identified; Glacial Lake McConnell and Glacial Lake Mackenzie (see location maps in Chapter 2). However, their evolution during deglaciation since the LGM is yet to be established. As noted, the study area is significant with respect to pro-glacial lakes because Glacial Lake Agassiz may have drained north-west, through the study area, and into the Arctic Ocean (cf. Teller *et al.,* 2002; Teller *et al.,* 2005; Smith and Fisher, 1993; Murton *et al.,* 2010) (for location, see Chapter 2). This may have triggered climatic downturns such as the Younger Dryas and the 8.2 cal. ka BP event by interrupting ocean circulation (Teller *et al.,* 2002; Teller *et al.,* 2005; Condron and Winsor, 2011). Indeed, Condron and Winsor (2011) indicate that a north-west drainage routeway for Glacial Lake Agassiz would have been the most effective means of interrupting North Atlantic Deep Water formation, thus initiating climate change. Moreover, Murton *et al.* (2010) have identified sedimentological evidence for two major flood events along the Mackenzie River valley, through Glacial Lakes McConnell and Mackenzie, around the time of the Younger Dryas. A possible drainage routeway via the Clearwater-Athabasca spillway has also been hypothesised. An extended discussion of the glacial history of the north-west sector of the LIS and previous reconstructions of pro-glacial lakes, is provided in Section 2.5 of Chapter 2.

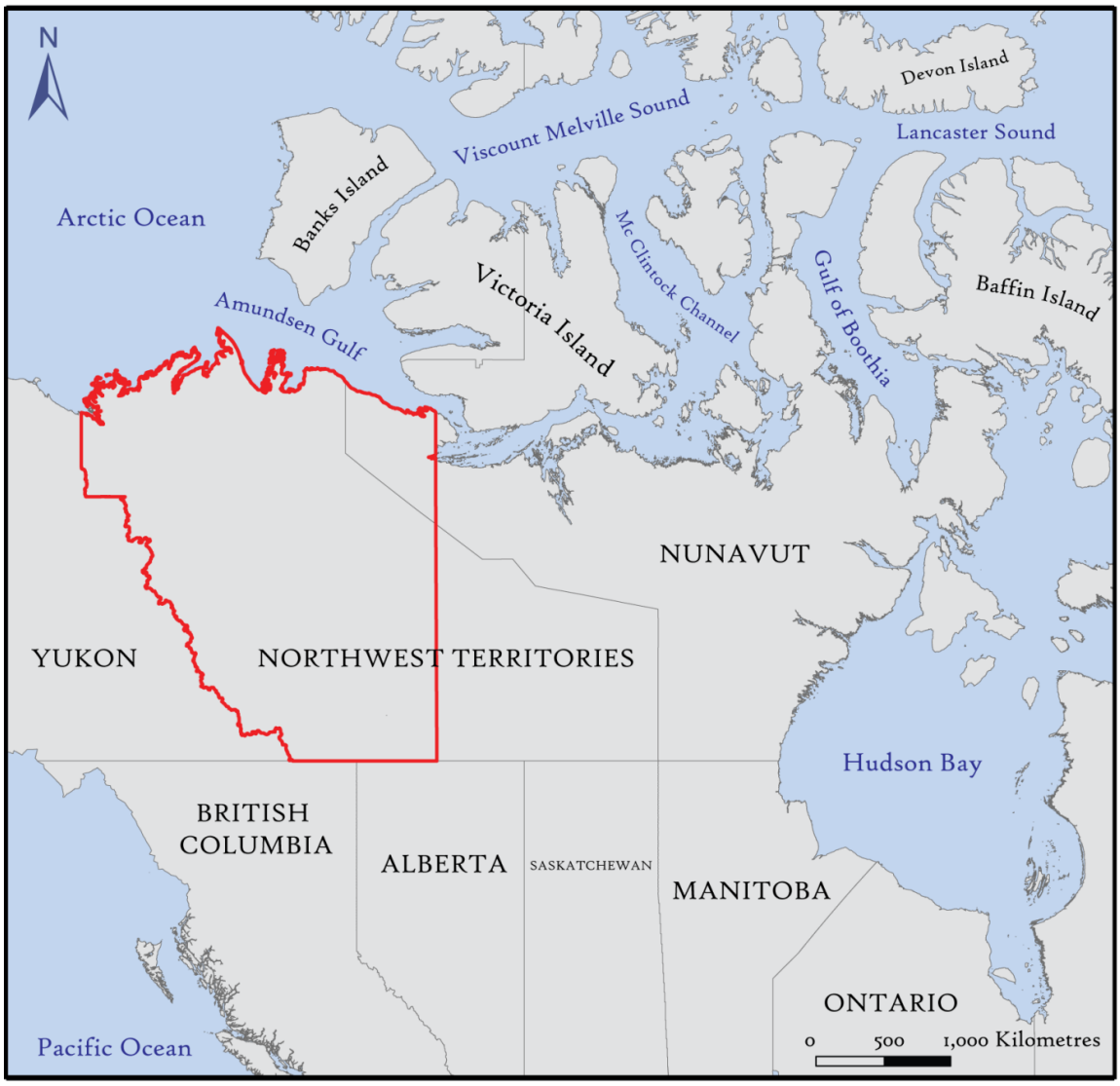

Figure 1-2: The location of the study area within NWT and Nunavut, Canada (highlighted by the red line). The study area is ~ 800,000 km2 which is more than three times the size of the British Isles. The red box highlighted here is shown on Figure 1-3

Figure 1-3: The location and physiography of the study area within NWT and Nunavut, Canada (highlighted by the red line). All locations noted in this thesis are labelled on this figure.

1.4 Thesis structure

Following the introduction, **Chapter 2** is a synthesis of the literature about the identification, reconstruction, and dynamics of palaeo-ice streams within the LIS. The influence of ice streams on ice sheet mass balance is then discussed along with previous work within the study area. It is concluded that, in order to gain insights into the behaviour of ice streams over millennial timescales, it is necessary to investigate and reconstruct the activity of palaeo-ice streams in past ice sheets. The second part of this chapter discusses the evolution of pro-glacial lakes around the LIS which includes an outline of the possible drainage routeways of Glacial Lake Agassiz.

Chapter 3 details the methods and is split into three sections which correspond to the results in Chapters 4, 5 and 6. First, this chapter presents the methods employed in the construction of the geomorphological map and reviews the various types of imagery available from which to map. The second section provides an overview of the processes of flow-set identification, ice stream identification and the construction of a regional reconstruction of ice sheet dynamics. The final section of Chapter 3 presents the method followed in the reconstruction of pro-glacial lake evolution along the LIS margin.

The presentation of a geomorphological map (see fold-out and CD) of the study area follows in **Chapter 4**. This map is accompanied by examples of the mapped geomorphology as visualised on Landsat ETM+ imagery. The contents of Chapter 4, including the geomorphological map, are also published in Brown *et al.* (2011). In **Chapter 5**, the mapped geomorphology is used to decipher the first regional reconstruction of ice stream activity in the north-west LIS. Flow-sets are then identified on the basis of bedform morphology and spatial distribution, and embedded behind the ice margins of Dyke *et al.* (2003). These ice margins were established from > 4000 radiocarbon dates from across North America (71 within the study area) and were modified to account for the newly documented geomorphology (see Chapter 4). This chapter culminates in the identification of ice streams in the north-west sector of the LIS.

Chapter 6 provides a continental scale reconstruction of pro-glacial lake evolution along the mainland margin of the LIS at 27 timesteps from 21.4 to 7.7 cal. ka BP. The purpose of this reconstruction is to compare the formation of pro-glacial lakes with the temporal and spatial distribution of ice streams while also establishing the viability of a north-west outlet for Glacial Lake Agassiz.

Chapter 7 is the discussion, which draws together the themes of the thesis by comparing the evolution of ice streams with that of pro-glacial lakes. This chapter places the findings of Chapters 4, 5 and 6 in the context of global environmental change during Late Wisconsinan deglaciation. Having established the behaviour of ice streams in the north-west sector of the LIS during deglaciation, Chapter 7 also considers the factors controlling the location and timing of ice streaming such as subglacial topography, geology and the thermal regime of the LIS.
Chapter 8 summarises the major conclusions of this thesis.

Chapter 2: A review of Laurentide Ice Sheet dynamics, ice stream activity and the significance of pro-glacial lakes

2.1 Introduction

This chapter begins by discussing the definition of an 'ice stream' before outlining the various types of ice streams and the controls on their operation. Examples are drawn from contemporary settings such as Antarctica and Greenland. While it is important to understand the behaviour of contemporary ice streams, observations are only possible over decadal time-scales. However, the beds of palaeo-ice streams provide a means of reconstructing longer term ice stream activity and are therefore valuable analogues for future ice stream/ice sheet activity. This chapter reviews previous reconstructions of palaeo-ice streams within the Laurentide Ice Sheet before focusing on the ice sheet history and ice stream activity in the north-west sector of the ice sheet. The final part of the chapter discusses our current knowledge of pro-glacial lake extent around the LIS, the various approaches to lake reconstructions and the significance of their drainage as a possible driver of deglacial climate variability.

2.2 What is an ice stream?

Ice streams have been recognised as sub-systems of ice sheets since the beginning of the 20th century but their impact upon ice sheet dynamics was not realised until as recently as 1981 by Denton and Hughes (Denton and Hughes, 1981). However, only in the last 50 years has a clear definition of the term 'ice stream' evolved. As outlined in Chapter 1, Patterson (1994) suggests that an ice stream is a region of grounded ice sheet in which the ice flows much faster than in regions on either side. However, earlier definitions included that of Swithinbank (1954) who stated that an ice stream is "part of an inland ice sheet in which the ice flows more rapidly than, and not necessarily in the same direction as, the surrounding ice" (Swithinbank, 1954, p. 185). Matthews (1991) also quotes Bader (1965), who suggested that an "ice stream is something akin to a mountain glacier consisting of a broad accumulation basin and a narrower outlet valley glacier; but a mountain glacier is laterally held in by rock slopes while the ice stream is contained by slower moving surrounding ice" (Bader, 1965, p. 11). These definitions

highlight the spatial extent and relative speed of ice flow within an ice stream, but do not characterise the temporal dimension of ice streaming leading to some confusion between ice streams and surge-type glaciers (see Lovell *et al.,* 2012).

2.2.1 Contemporary ice streams

The study of contemporary ice streams often involves observations of the ice surface morphology (Joughin *et al.,* 2009). Characteristic crevassing patterns, sharply delineated margins and ice which sharply converges from its catchment into a narrower channel of increased ice velocity, are typical of ice stream activity (Goldstein *et al.,* 1993; Joughin *et al.,* 2002; King *et al.,* 2009). Longitudinal profiles of the ice surface and bed are also expected to be low, and surface velocity high compared to the surrounding ice (Bindschadler and Scambos, 1991; Matthews, 1991; Bentley, 1987; Bindschadler and Vornberger, 1998). While King *et al.* (2009) record the formation of mega-scale lineations beneath the Rutford Ice Stream, West Antarctica using radio-echo sounding, observations of contemporary ice stream beds are few. Thus, palaeo-ice stream beds, which are more accessible than those of their contemporary counter-parts, have been exploited as a means of understanding ice stream operation over millennial time-scales, and used to inform predictions of future ice sheet/ice stream activity (Stokes *et al.,* 2009).

Presently, ice streams account for 10% of the volume of the Antarctic ice sheet but, along with outlet glaciers, account for 90% of the mass loss from the continent (Morgan *et al.,* 1982) (Figure 2-1). They therefore dominate the mass balance and stability of continental ice sheets by draining large volumes of ice rapidly (Bamber *et al.,* 2000; Conway *et al.*, 2002; Bennett, 2003; Payne *et al.,* 2004; Pritchard *et al.,* 2009). Bentley (1987) describes the contrast between the ice streams of West and East Antarctica. While the majority of ice streams in East Antarctica can be likened to outlet glaciers because of their locations in deep subglacial troughs, those in West Antarctica and around the Ross Sea have high width : thickness ratios and often do not coincide with topographic lows (Bentley, 1987).

While both the East Antarctic Ice Sheet (EAIS) and the West Antarctic Ice Sheet (WAIS), have undergone fluctuations in area and mass throughout their history, this has been most pronounced in the WAIS (Joughin and Alley, 2011). However, according to White *et al.* (2011), the sensitivity of the EAIS to climate fluctuations, particularly immediately following the LGM, may have been under estimated.

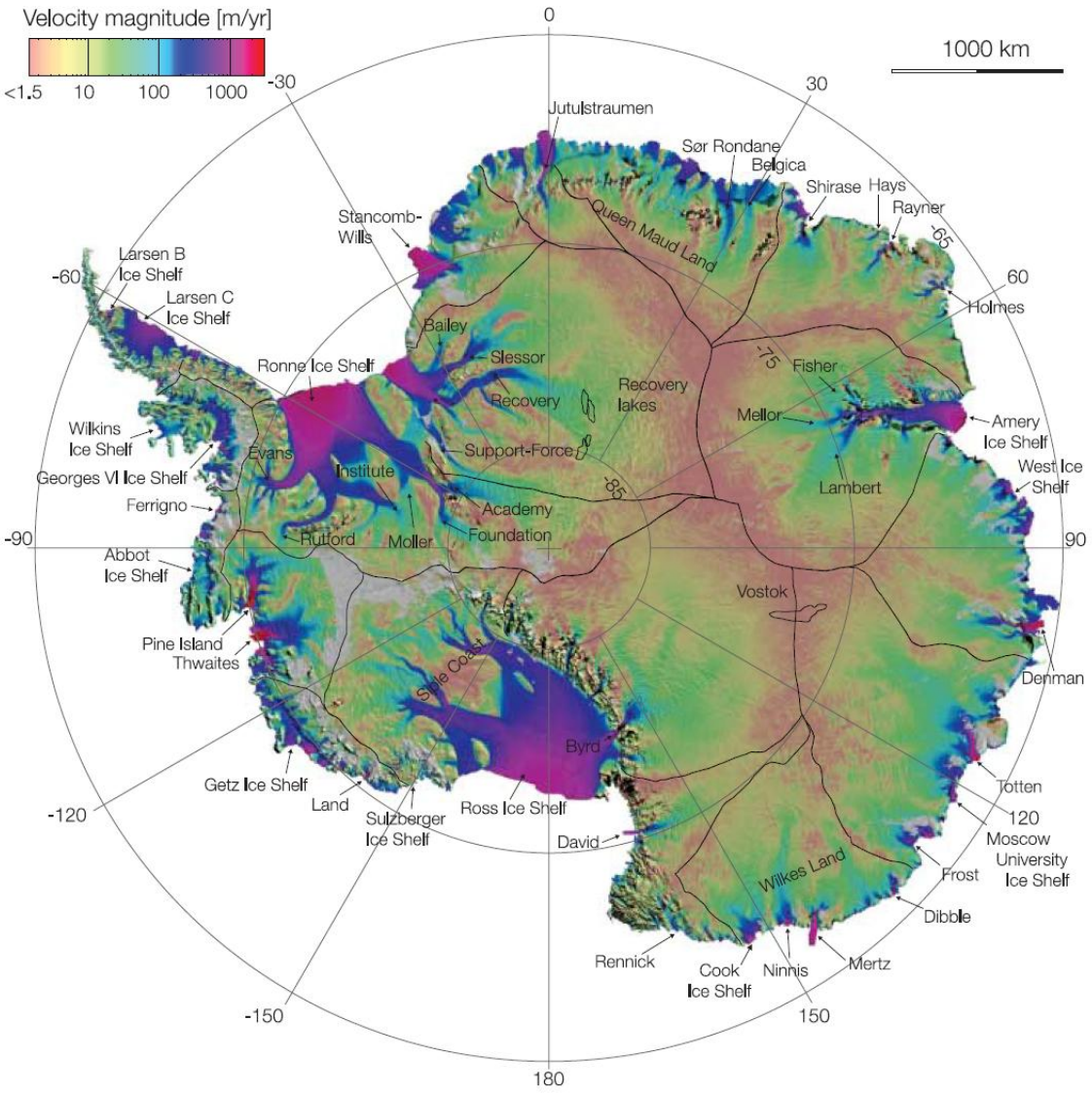

Figure 2-1: Ice velocity of the Antarctic Ice Sheet. The purple areas represent the areas of most rapid ice flow. While the coast of East Antarctica is occupied by a series of localised outlet glaciers and small ice shelves, West Antarctica contains much larger arteries of fast ice flow. The principal areas of fast ice flow in West Antarctica are in and around the Ross Ice Shelf, Ronne Ice Shelf, and in Pine Island and Thwaites Glaciers. Figure taken from Rignot et al. (2011).

2.2.2 Ice stream types

Ice streams have long been classified according to their relationship to the underlying topography as 'pure' ice streams or 'topographic' (isbrae) ice streams (Bentley, 1987; Patterson, 1994; Stokes and Clark, 1999; Bamber *et al.*, 2000; Bennett, 2003; Truffer and Echelmeyer, 2003). These two types of ice stream form either end of an ice stream continuum, under which a single ice stream can be both pure and isbrae along its length as the environment at the ice stream bed changes (Truffer and Echelmeyer, 2003). Typically, pure ice streams are relatively wide and shallow (1000 m), have low surface slopes and driving stresses, and, their location is not strongly controlled by topography, see Figure 2-2 (Patterson, 1994).

For example, several of the ice streams along the Siple Coast, West Antarctica, which terminate in the Ross Ice Shelf are pure ice streams (Bamber *et al.,* 2000). The trunks of the Whillans (ice stream B), Bindschadler (ice stream D) and MacAyeal (ice stream E) ice streams are not well constrained by topography and are focused in areas of warmer ice with thicker sediment concentrations where subglacial meltwater is more abundant (Bamber *et al.,* 2000; Bennett, 2003).

Instability in the Siple Coast ice streams has occurred and resulted in highly variable ice sheet mass balance, with at least one ice stream (the Kamb ice stream/ice stream C) having undergone recent episodic stagnation (Bentley *et al.*, 1998). The most likely reason for this stagnation was competition for water with neighbouring ice streams (water piracy) which aided streaming flow through subglacial sediment saturation and bed lubrication (Engelhardt *et al.,* 1990; Bennett, 2003; Winberry *et al.,* 2009). In contrast, 'isbrae' type ice streams, which are characterized by very high driving stresses, typically occupy deep bedrock channels and have steeper surface slopes (Figure 2-2) (Patterson, 1994). Isbrae type ice streams can also therefore be thought of as 'topographic ice streams' and, as a result of their topographic location, are stable features compared to pure ice streams (Bennett, 2003; Jacobel *et al.,* 1996). An example is the Rutford Ice Stream in West Antarctica which is 2.2 km thick and occupies a deep trough which is 1400 m below sea level at the grounding line (Smith and Murray, 2009).

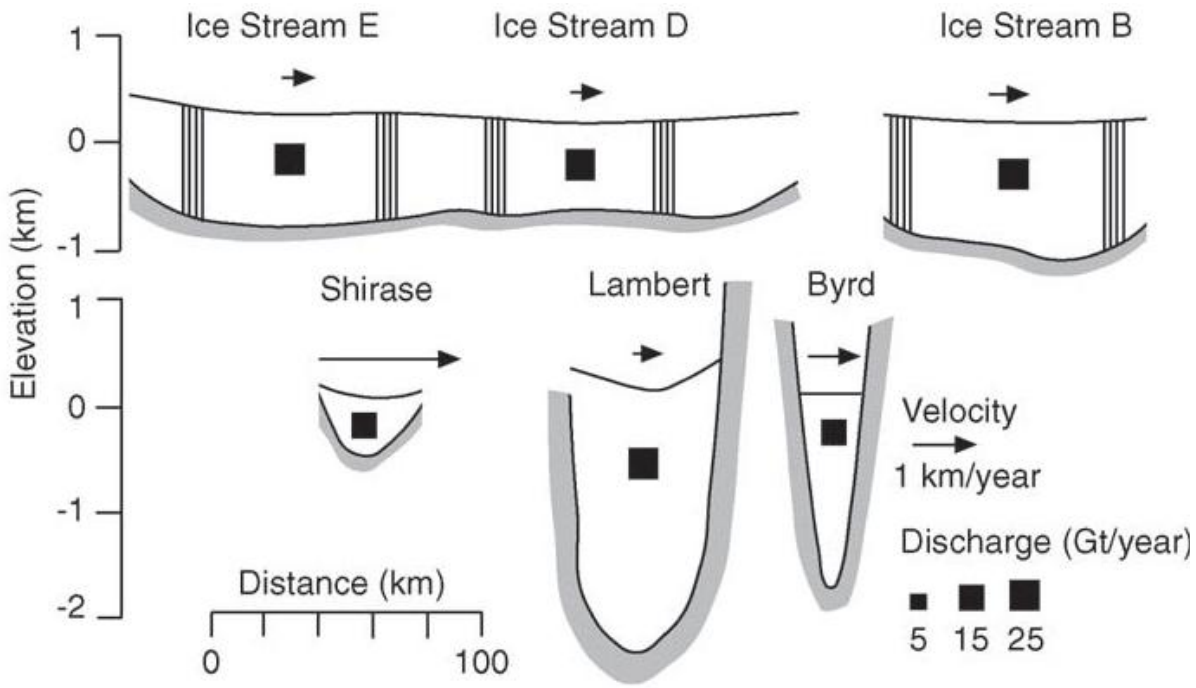

Figure 2-2: A schematic illustration of the cross-sectional profiles of topographic and pure ice streams in Antarctica. Ice Streams B, D and E are pure ice streams while the Shirase, Lambert and Byrd ice streams are topographic. Figure taken from Bennett (2003), originally modified from Bentley (1987).

Additionally, ice streams can be classified as marine or terrestrially terminating (Stokes and Clark, 1999; Truffer and Echelmeyer, 2003; Bentley, 1987). All contemporary ice streams are marine terminating with some terminating in open water e.g. Pine Island glacier in West Antarctica, but more commonly terminating in an ice shelf e.g. the Siple Coast ice streams, again in West Antarctica (Joughin *et al.*, 2009). In Antarctica, the sensitivity of ice streams and outlet glaciers to external forcing is greatly influenced by their termination in marine environments (Livingstone *et al.,* 2012). This allows ice streams to respond to both atmospheric forcing and changes in ocean circulation and therefore ocean temperature (Bamber *et al.,* 2007; Lloyd *et al.,* 2011; Young *et al.,* 2011). That said, Livingstone *et al.* (2012) note that, despite the termini or grounding line position of an ice stream being influenced by an external forcing (oceanic or atmospheric), the individual characteristics of an ice stream, such as underlying topography or surficial geology, modulate the precise timing and rate of ice stream change through time.

Spatially, the location of ice stream activity is controlled by a range of factors which have been summarised by Winsborrow *et al.* (2010). They identify seven controls on ice stream activity; topographic troughs, soft beds, abundant meltwater supply, smooth beds, high geothermal

heat flux and topographic steps. These controls are summarised in Figure 2-3 and discussed further in Chapter 7 with respect to ice stream activity in the north-west LIS.

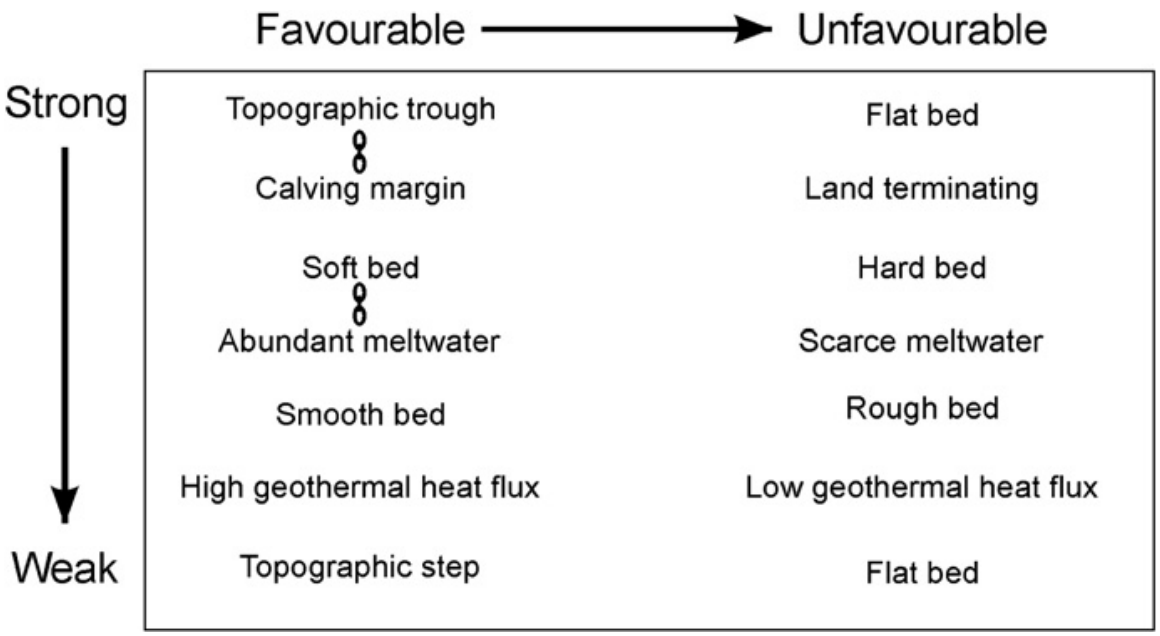

Figure 2-3: The hierarchy of controls on the location of ice streams. Taken from Winsborrow *et al.* (2010). Repeated and further discussed as Figure 7.2 in Chapter 7. The chains between factors of the left-hand side of the diagram indicate that these factors may be of equal importance.

2.3 The identification of palaeo-ice streams

A number of different approaches have been taken to investigate palaeo-ice streams, ranging from localized field investigations (Hicock, 1988) to large scale remote sensing projects such as this study and the work of De Angelis and Kleman (2008), Stokes and Clark (2004), Stokes *et al.* (2005) and others. However, each of these studies has a common component; the use of the glacial inversion method as outlined by Kleman and Borgström (1996) and Kleman *et al.* (2006). The glacial inversion method uses the distribution of glacial geomorphology to reconstruct the geometry and dynamics of an ice sheet by assuming that particular types of bedforms form under specific conditions (Kleman *et al.,* 2006). This is summarized below in Figure 2-4 and discussed further in Section 3.4 of Chapter 3.

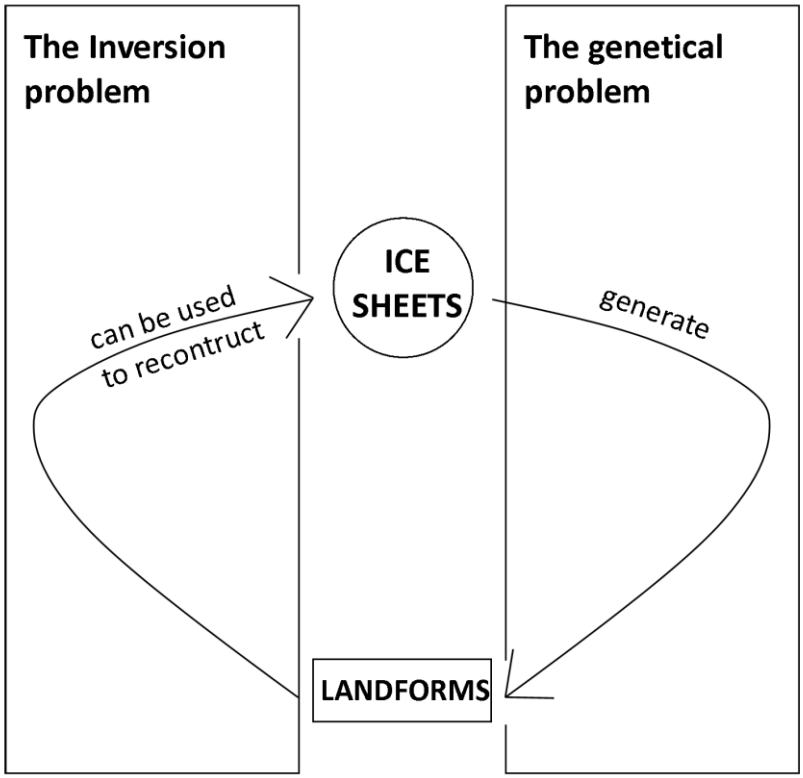

Figure 2-4: The fundamental assumption of the glacial inversion method shown schematically. The genetical problem assumes that ice sheets generate landforms while the inversion problem assumes that landforms can be used to reconstruct ice sheet behaviour. Taken from Kleman and Borgström (1996).

As noted by Evans and Twigg (2002), accurate interpretations of ancient glaciated landscapes rely heavily on our understanding of process-form relationships in contemporary glacierized regions. The 'landsystems approach' is well documented by Evans (2007), Spedding and Evans (2002), Evans and Russell (2002), Evans (2003) and Bennett *et al.* (2010). However, the earliest landsystems-type investigations include those of Speight (1963), Clayton and Moran (1974) and Fookes *et al.* (1978). This approach prioritises the assessment of groups of landforms rather than forms in isolation, and therefore allows for a regional understanding of ice sheet activity (Evans, 2007). Conceptual landsystems models have been developed for a range of glacierized terrain including an active temperate ice margin (Evans and Twigg, 2002; Benn and Lukas, 2006), a glaciated valley (Spedding and Evans, 2002; Benn *et al.,* 2003), a plateau icefield (Rea *et al.,* 2007; Golledge, 2007; Benn and Evans, 2010) and a palaeo-ice stream (Stokes and Clark, 1999; Stokes and Clark, 2001; Stokes and Clark, 2003). The latter was developed by Stokes and Clark (1999), see Figure 2-5.

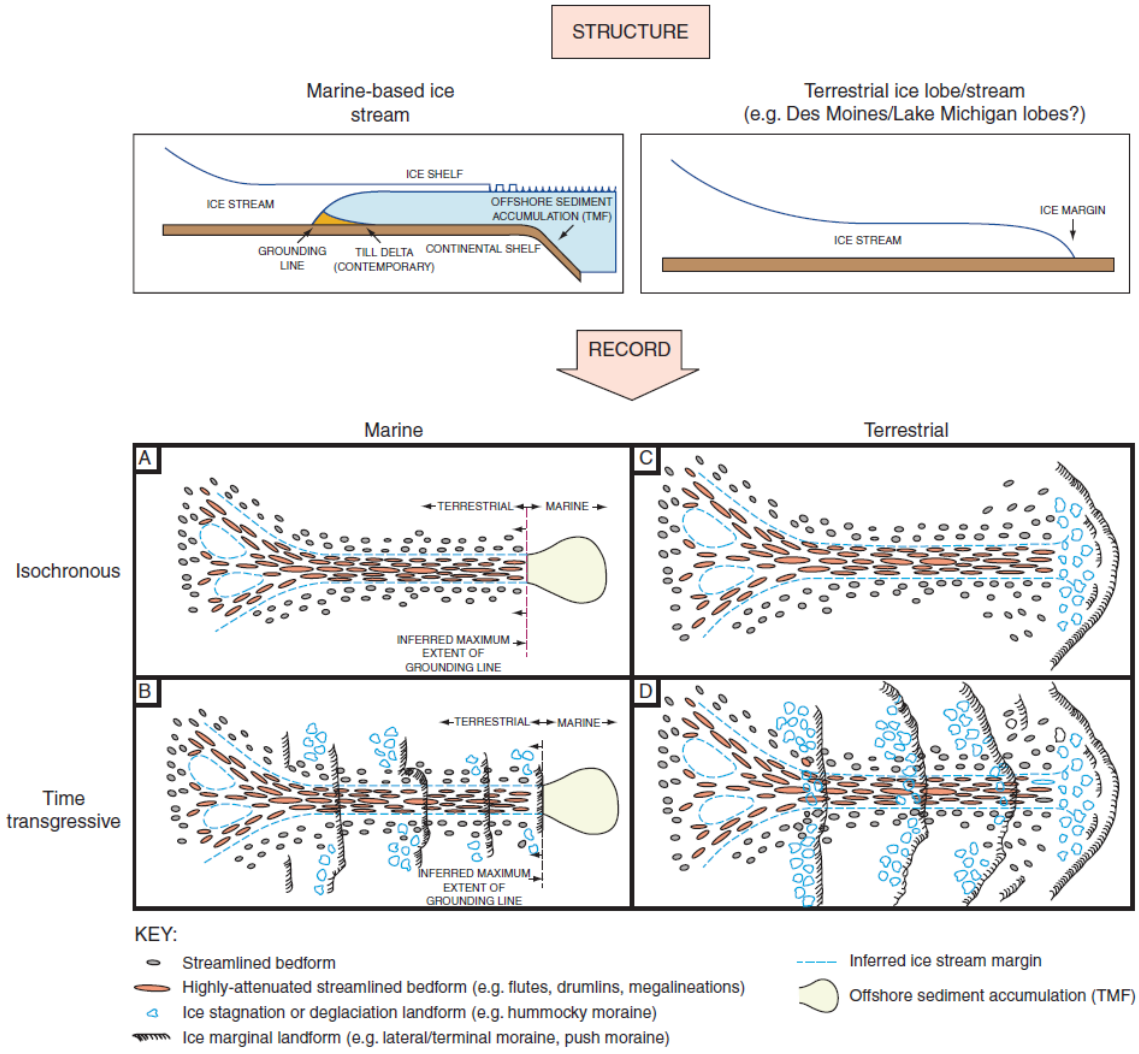

Figure 2-5: A landsystems model for ice streams showing the four end members of marine-based and terrestrial ice streams which are either isochronous/rubber stamped or time transgressive/smudged. The figure has been modified from Stokes and Clark (1999) by Evans (2007). This version of the figure is from Evans (2007).

Prior to the work of Stokes and Clark (1999), the geomorphological signature of ice stream activity was poorly understood. As a consequence, the occurrence of palaeo-ice streams was often hypothesized, but evidence for their existence based on the *systematic* examination of geomorphology was frequently lacking. The work of Stokes and Clark (1999) addresses this problem by developing criteria which they consider to be the fundamental characteristics of contemporary ice streams and which may be manifest in the geomorphological record, see Table 2.1. The individual criteria may not be exclusive indicators of palaeo-ice stream activity, but collectively, the set of criteria can be used as a basis for a palaeo-ice stream landsystems model. These criteria mostly relate only to 'pure' ice streams as it is believed that 'topographic' ice streams should be easier to infer on the basis of topography and reconstructed ice sheet geometries (Stokes and Clark, 1999).

Contemporary Ice-Stream characteristics	Proposed geomorphological signature
A. Characteristic shape and dimensions	1. Characteristic shape and dimensions. 2. Highly convergent flow patterns.
B. Rapid velocity	3. Highly attenuated bedforms (length-to-width ≥ 10:1). 4. Boothia-type erratic dispersal trains.
C. Sharply delineated shear margin	5. Abrupt lateral margins. 6. Lateral shear moraine.
D. Deformable bed conditions	7. Glaciotectonic and geotechnical evidence of pervasively deformed till. 8. Submarine till delta or sediment fan.

Table 2-1: The criteria for the identification of palaeo-ice streams outlined by Stokes and Clark (1999). The table is repeated as Table 3.2 in Chapter 3.

2.4 Palaeo-ice streams in the Laurentide Ice Sheet

Early work on the location of palaeo-ice streams within the LIS was carried out by Denton and Hughes (1981), who assumed that the location of palaeo-ice streams coincided with topographic troughs. Marshall *et al.* (1996) also reconstructed ice stream activity at a coarse, continental scale over North America again based on topography, but also on the location of soft (deformable) sediments. A wide variety of ice streams have been identified in the LIS which are indeed located in topographic troughs and in regions of abundant soft sediment. However a number of 'anomalous' ice streams have also been identified (Patterson, 1998). Each of these broad categories will be discussed in turn below.

2.4.1 Canadian Archipelago: topographic ice streams

The majority of large palaeo-ice streams in the Canadian Archipelago were marine terminating, topographic ice streams, having occupied deep marine troughs (Figure 1-1). Stokes *et al.* (2009) have reconstructed a palaeo-ice stream in M'Clintock Channel which is thought to have operated between 10.4 and 10.0 cal. ka BP. The ice stream was ~ 720 km long with a surface area of 162,000 km^2, and originated from the Keewatin Dome on the western side of Hudson Bay (Stokes and Clark, 2001; Stokes *et al.,* 2009). Within M'Clintock Channel, pre-existing unconsolidated drift encouraged fast ice flow through subglacial sediment deformation. However, the shut-down of the ice stream was initiated by increased basal friction as the ice stream cut down through the subglacial sediment to reach bedrock. According to Stokes and Clark (2001), the M'Clintock Channel ice stream was unable to generate its own lubricating sediment in sufficient quantities that the life-cycle of the ice stream was predetermined by the

initial sediment thickness at the bottom of the channel. Assuming that the M'Clintock Channel Ice Stream was comparable in size to the Hudson Strait Ice Stream and flowing at a similar velocity (roughly 4 km a^{-1}), in 200 years of operation it may have drained around 80,000 km^3 of ice. This may have significantly affected the dynamics of the Keewatin sector of the LIS during a period of rapid deglaciation (Stokes *et al.,* 2009).

The M'Clintock Channel Ice Stream was the deglacial phase of a much larger ice stream which extended into M'Clure Strait across the Storkerson Peninsula (Stokes *et al.,* 2005) (Figure 2-6). This much more extensive phase of ice streaming extended along M'Clure Strait to the edge of the continental shelf and was episodically active between 30 and 10 cal. ka BP. Stokes *et al.* (2005) and Darby *et al.* (2002) suggest that the M'Clure Strait ice stream may have played a key role in four large ice export events at 12.9, 15.6, 22 and 29.8 ^{14}C ka BP (Darby *et al.,* 2002). These events roughly coincide with Heinrich Events in the North Atlantic, but it is unclear whether ice streaming preceded the Heinrich Events or *vice versa* (Darby *et al.,* 2002; Stokes *et al.,* 2005; Kaplan *et al.,* 2001).

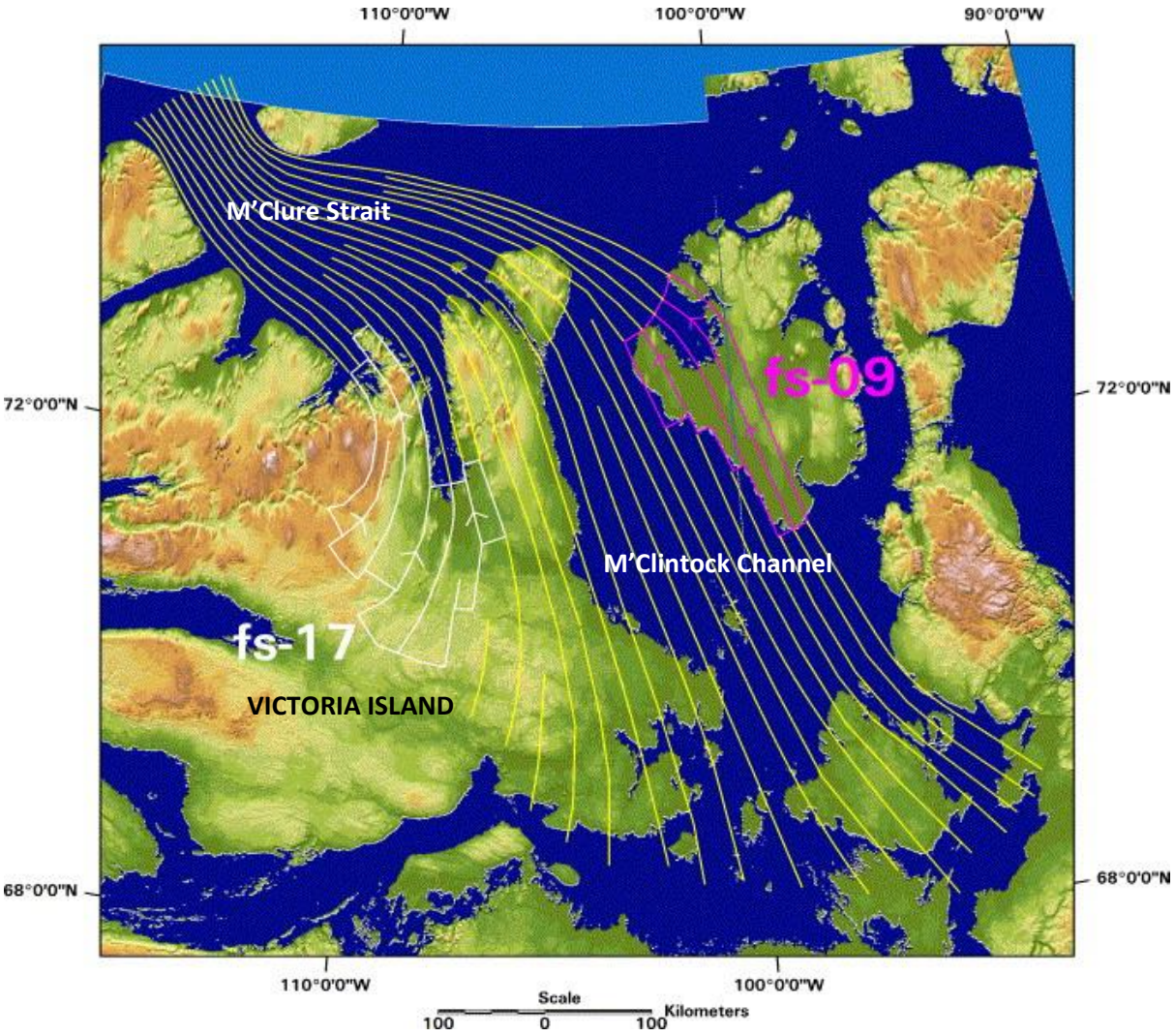

Figure 2-6: The spatial extent of the M'Clintock Channel - M'Clure Strait palaeo-ice stream. Extensive geomorphological evidence for ice stream activity is documented by Storrar and Stokes (2007) on Victoria Island, Stokes (2000) and Stokes et al. (2009). Figure taken from Stokes et al. (2009).

A further major topographic ice stream has been identified to the south-west of Victoria Island in Amundsen Gulf (Stokes *et al.,* 2006). Flow-sets with a convergent arrangement of MSGLs with abrupt lateral margins indicate that, at its maximum, the ice stream was 1000 km long and 130 km wide. Geomorphological evidence on Wollaston Peninsula and on the Canadian mainland indicates that the ice stream reorganized several times during ice sheet retreat with its final phase of activity occurring between 11 and 10 ka BP (Stokes *et al.,* 2006). This coincides with the demise of ice stream activity in M'Clintock Channel. A series of much smaller palaeo-ice streams have also been identified by Stokes *et al.* (2005) on north-western Victoria Island, at least two of which drained into the M'Clure Strait Ice Stream around Richard Collinson Inlet. Another three small palaeo-ice streams have been identified on Prince of Wales Island by Stokes *et al.* (2005), De Angelis and Kleman (2007) and Dyke *et al.* (1982). The

regional impact of extensive ice streaming in the western Canadian Archipelago may have been key to the development of Arctic Ocean ice shelves and the delivery of meltwater to the Arctic Ocean during the Late Pleistocene (Tarasov and Peltier, 2005; Winsborrow *et al.,* 2004; Stokes *et al.,* 2006).

2.4.2 The lobes of the southern LIS: terrestrially terminating ice streams

Clark (1992), Patterson (1997) and Patterson and Boerboom (1999) all record evidence of palaeo-ice streaming around the southern margin of the LIS during deglaciation, see Figure 2-7. The Des Moines and James Lobes both had low longitudinal ice-surface profiles and occupied pre-existing topographic lowlands. According to Patterson (1997), the lobes re-advanced rapidly and repeatedly during deglaciation. Indeed, the LIS margin positions of Dyke *et al.* (2003) depict the changing configuration of these lobes through Late Wisconsinan deglaciation. Based on the modest ice thicknesses modelled by Clark (1992), Patterson (1997) indicates that the re-advance of the Des Moines Lobe ~ 14 cal. ka BP, would have required a very large ice flux in order to redevelop the lobe in less than 1000 years. This ice flux would have had to be comparable to that of the present day Ice Stream B in Antarctica (Patterson, 1997).

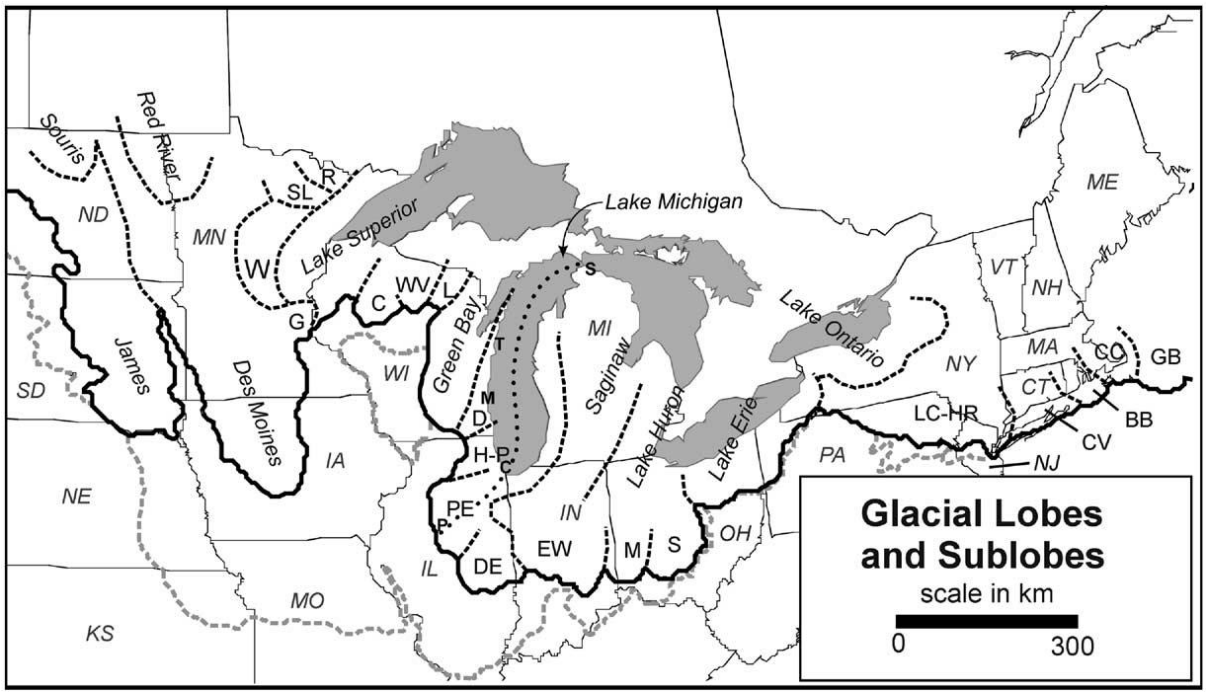

Figure 2-7: The ice lobes of the southern LIS during the Late Wisconsinan. Major lobes are labelled and sub-lobes are as follows: G = Grantsburg, W = Wadena, SL = St. Louis, R = Rainey, C = Chippewa, WV = Wisconsin Valley, L = Langlade, D = Delevan, H-P = Harvard-Princeton, PE = Peoria, DE = Decatur, EW = East White,M = Miami, S = Scioto, LC = Lake Champlain, HR = Hudson River, CV = Connecticut Valley, BB = Buzzards Bay, CC = Cape Cod, GB = Georges Bank. The light grey dashed line shows the margin position at the LGM. The southern margin maintained its lobate shape throughout deglaciation. Figure taken from Mickelson and Colgan (2003).

Ross *et al.* (2009) and Ó Cofaigh *et al.* (2010) have identified a complex subglacial landscape in southern Saskatchewan where coherent patterns of landforms have been grouped together to reveal two distinct and cross-cutting palaeo-ice stream landsystems. One palaeo-ice stream flowed south-west (the Maskwa ice stream) while the other flowed south-east (the Buffalo ice stream). The Maskwa ice stream is represented by discontinuous geomorphology in a linear corridor, which crosses pre-glacial valleys and the associated topographic highs with little disturbance to its operation. The ice stream was, therefore, relatively thick and basal shear stresses high. In contrast, the Buffalo ice stream was constrained by topography. However, landform evidence suggests that this ice stream was much more unstable and shifted position several times during its life cycle. The Buffalo ice stream fed into the James Lobe and was therefore potentially crucial to the development and sustenance of the southern lobes of the LIS (Ross *et al.*, 2009).

Further west in Alberta, Evans *et al.* (2008) have identified a number of 'fast-flow' tracks separated by inter-lobate and inter-stream moraine belts which include overridden transverse

ridges and overprinted flow-sets indicative of the margin between two neighbouring palaeo-ice streams which advanced in southern and central Alberta. Unlike the ice streams found elsewhere in the LIS, the ice streams and outlet glaciers of the southern lobes terminated in terrestrial settings, and underwent continual re-arrangement (both advance and retreat) during overall deglaciation. In the LIS, it therefore appears that the terrestrially terminating ice streams along the southern margin of the ice sheet responded much more rapidly to climate, or atmospheric temperature changes, particularly during the early stages of deglaciation (Evans *et al.*, 2008). Conversely, termination in marine settings can be thought to have a modulating effect on ice stream/outlet glacier response to changes in climate (Livingstone *et al.,* 2012; Evans *et al.,* 2008).

Further east, five palaeo-ice streams for which evidence exists but their extent remains undefined have been identified in James Bay and Placentia Bay (Shaw, 2003; Veillette, 1995), and as part of the Lake Michigan, Lake Superior and Simcoe Lobes (Boyce and Eyles, 1991; Jennings, 2006; Clark, 1992). More recently, Hess and Briner (2009) have found new evidence for fast ice flow in three distinct zones within the New York drumlin field around Lake Ontario. However, the chronology of this fast ice flow and the formation of the drumlin field under a palaeo-ice stream or a surging outlet glacier remains uncertain (Hess and Briner, 2009). Topographic palaeo-ice streams were also present in the Gulf of St Lawrence and St George's Bay (Shaw, 2003). Both of these ice streams were active during the LGM when a calving margin in the Gulf of St Lawrence aided ice draw-down and therefore high velocity streaming flow (Winsborrow *et al.,* 2004; Shaw, 2003). Uncertainty surrounding the timing of ice stream activity is not only problematic in the south-east LIS, but across the whole ice sheet. Moreover, the distribution of radiocarbon dates across North America, as documented by Dyke *et al.* (2003), is not consistent. In particular, additional radiocarbon dates are required in order to refine the chronology of the ice margin throughout the Canadian Archipelago, along the north-west margin, and as noted above, around the Great Lakes.

2.4.3 Eastern sector of the LIS: 'anomalous' ice streams

Evidence for palaeo-ice streaming in the Foxe / Baffin and Labrador / Ungava regions of the LIS has been well documented (De Angelis and Kleman, 2007; De Angelis and Kleman, 2005; De Angelis and Kleman, 2008; Dyke and Morris, 1988) (Figure 2-8). On Baffin Island and in the Gulf of Boothia, glaciation during the Late Wisconsinan was dominated by frozen bed conditions on the high plateaus with ice streams in the troughs constrained by the topography (De Angelis and Kleman, 2007). From the LGM to 7 ka BP, radial ice-flow from an ice dome centred on the eastern Foxe Basin occurred during overall deglaciation. Sometime between 6 and 7 ka BP

large portions of the remaining Foxe/Baffin sector of the LIS catastrophically collapsed and wet-based deglaciation ensued (De Angelis and Kleman, 2007). This period also saw the development of palaeo-ice streams in areas characterized by loosely defined, relatively flat and wide valleys, the floors of which are dominated by soft Palaeozoic carbonates. Kaplan *et al.* (2001) note, with particular reference to the palaeo-ice stream in Cumberland Sound, that as a result of their topographic setting, palaeo-ice streams in the region had very low surface gradients and driving stresses. Rapid switches between different ice stream configurations caused individual ice streams to become transient features of a retreating ice sheet (De Angelis and Kleman, 2007; Dyke and Morris, 1988).

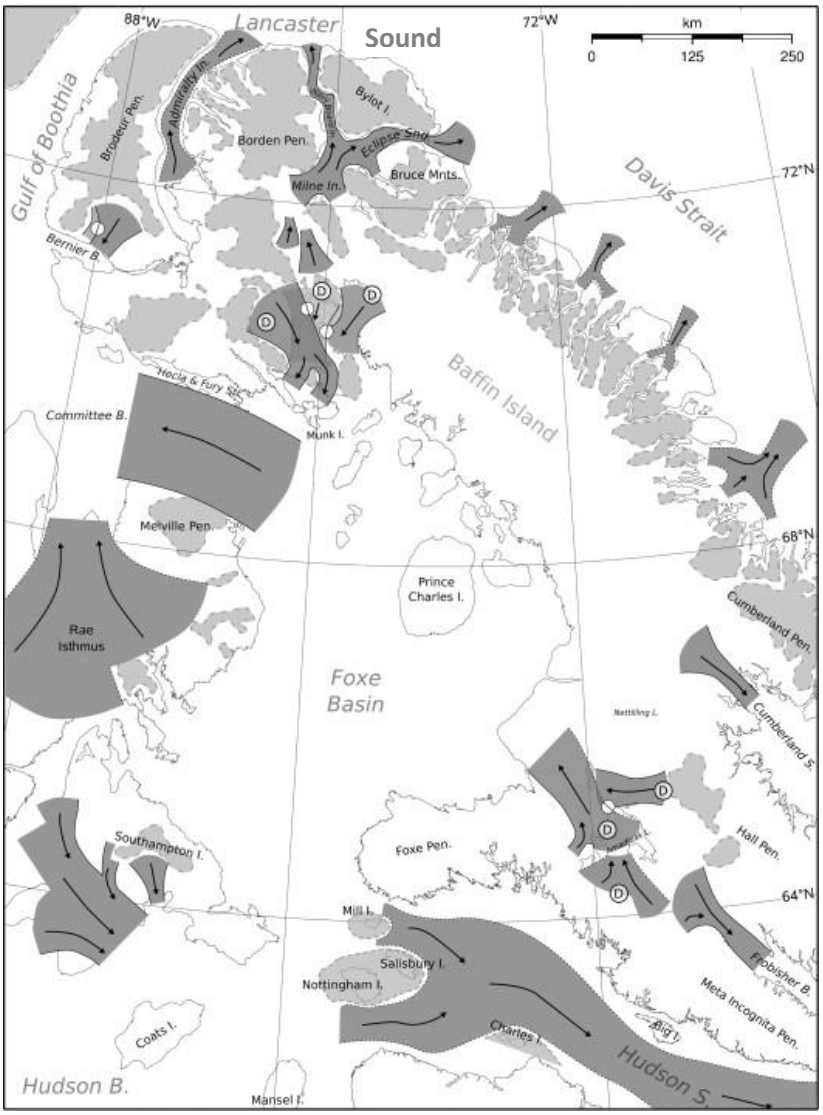

Figure 2-8: Palaeo-ice streams in the Foxe/Baffin sector of the LIS. Cold based ice is denoted by the light grey colouring while area of ice streaming are shown in dark grey. Ice streams marked with a 'D' are thought to be of deglacial age. The figure was taken from De Angelis and Kleman (2007).

By far the largest palaeo-ice stream in the eastern LIS was the Hudson Strait palaeo-ice stream (Figure 2-8). However, following the work of Marshall and Clarke (1997), the evidence for palaeo-ice streaming in the strait has been re-examined (Andrews and MacLean, 2003; Ross *et al.,* 2011). It is widely accepted that Heinrich events emanating from the eastern sector of the LIS have produced layers of ice-rafted debris known as 'Heinrich layers' in the Hudson Strait and North Atlantic (Andrews and MacLean, 2003). Based on the estimated sedimentation rates required for their formation, it has been suggested that these layers are the product of low gradient palaeo-ice streams in Hudson Strait (Kaplan *et al.,* 2001). However, geomorphological evidence to support this is lacking or ambiguous. Indeed, De Angelis and Kleman (2007) conclude that, aside from the striae evidence of Blake (1966), Laymon (1992) and Manley (1996), little evidence exists on emerged land to support the existence of a palaeo-ice stream flowing parallel to the long axis of Hudson Strait. The presence of submerged lineations across the mouth of Hudson Strait, as noted by Kleman *et al.* (2001) can therefore be explained by an ice stream which was confined to the deepest parts of Hudson Strait with cold-based ice in marginal areas. Much higher resolution sonar images are now required in order to visualize potential evidence for palaeo-ice streaming in the deepest parts of Hudson Strait.

Typically, throughout the LIS, palaeo-ice streams occupy topographic troughs and areas of abundant soft sediment. However, west of Hudson Bay, Stokes and Clark (2003; 2004), find evidence for an 'anomalous' pure ice stream which was underlain by the solid crystalline bedrock of the Canadian Shield: the Dubawnt Lake Palaeo-ice Stream. The geomorphological signature of the Dubawnt Lake palaeo-ice stream is striking and dominated by extensive MSGL, see Figure 2-9. Although smaller than the large palaeo-ice streams occupying the marine troughs around Victoria Island, the Dubawnt Lake palaeo-ice stream was over 450 km long and 140 km wide with a catchment area of 190,000 km^3 (Stokes and Clark, 2004). For comparison, the catchment of the modern Whillans ice stream in West Antarctica is estimated at 163,000 km^2. Operation of the Dubawnt lake palaeo-ice stream was short-lived, having occurred between 9 and 8.2 cal. ka BP. While the regional topography and sediment supply do not appear to control the operation of streaming flow near Dubawnt Lake, Stokes and Clark (2003) also note that, with an average bed gradient of 0.004°, bed slope is also unlikely to have contributed to streaming flow. Rather, the location of the Dubawnt Lake palaeo-ice stream was dictated by the development of a pro-glacial lake along the ice margin which caused calving, ice draw-down and increased subglacial water pressures which aided streaming flow (Stokes and Clark, 2003, 2004), see Figure 2-10.

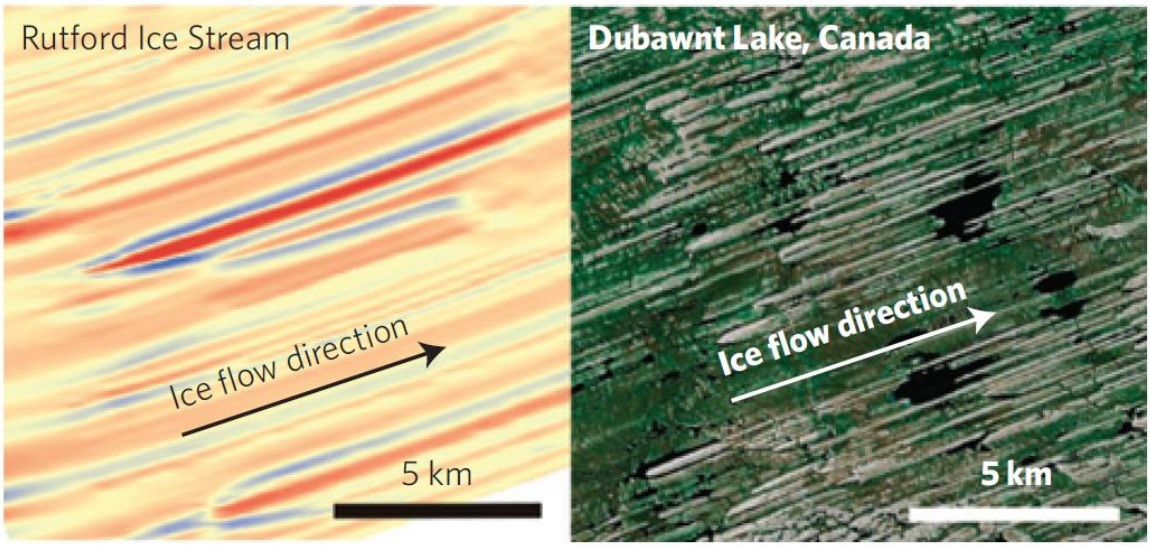

Figure 2-9: The similarity between the ancient geomorphological signature of the Dubawnt Lake palaeo-ice stream (right) compared to the bedforms below the present day Rutford ice stream, Antarctica (left). MSGL are abundant in both images. Figure taken from King et al. (2009).

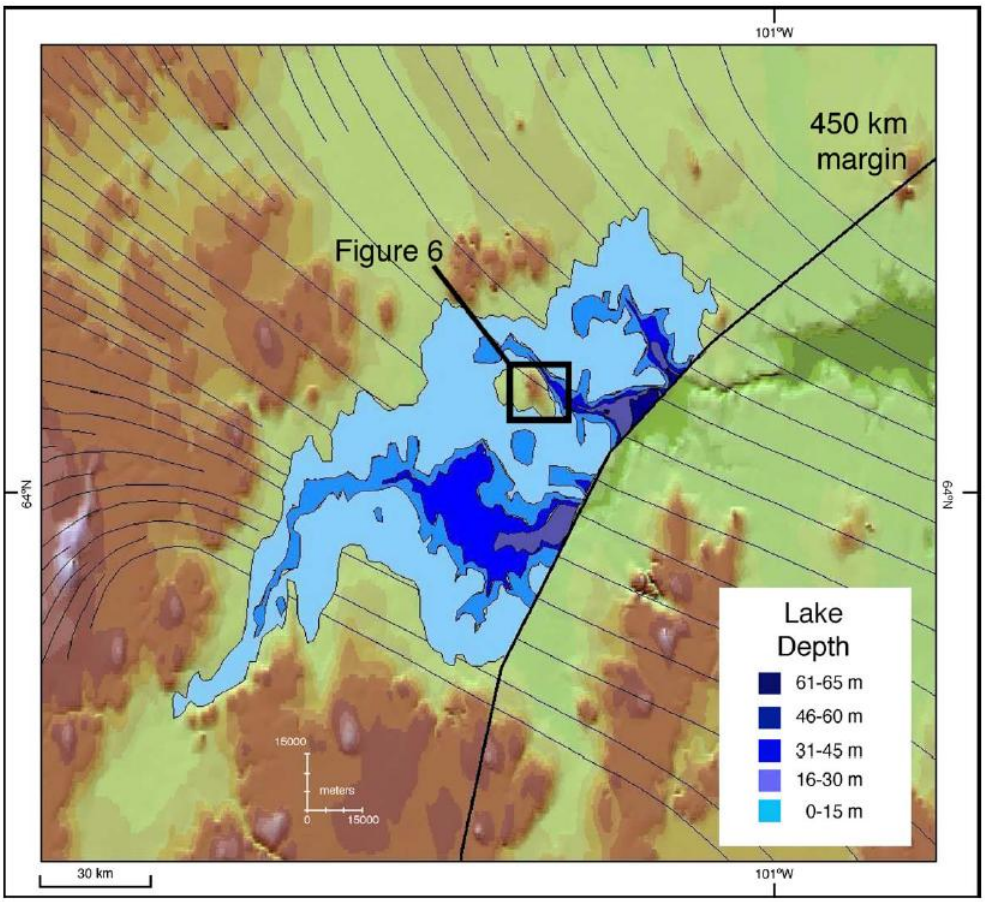

Figure 2-10: The location and bathymetry of inferred pro-glacial lakes forming along the margin of the LIS near the Dubawnt Lake palaeo-ice stream. The flow-lines of the ice stream are shown in dark blue. The lake reaches a maximum of 68 m depth. Figure taken from Stokes and Clark (2005).

Other ice streams which are located on solid crystalline bedrock include eight ice streams which supplied ice to southern Ungava Bay (Jansson *et al.,* 2003). The geomorphological signature of these palaeo-ice streams covers an area of 260,000 km^2 south of Ungava Bay and includes convergent drumlins, crag-and-tails and flutes. The flow-sets constructed from this geomorphological imprint require similar ice sheet configurations and are therefore suggested to have formed during consecutive flow events (Jansson *et al.*, 2003). The above discussion demonstrates that, while many ice streams have been reconstructed in the LIS, the timing of their activity frequently remains uncertain. Furthermore, while some palaeo-ice stream reconstructions are based on comprehensive regional geomorphological mapping, others rely on localised chronological controls or sedimentological evidence. Therefore, in order to produce a self-consistent account of ice streams throughout the LIS, a number of key gaps need to be addressed. One such gap is the north-west LIS, which is the focus of this thesis.

Recent attempts to model the location and timing of ice streams in the LIS have been carried out by Stokes and Tarasov (2010), see Figure 2-11. The model successfully reproduces all of the large marine-terminating ice streams in the LIS which occupied deep topographic troughs (see Section 2.4). However, while the model captures some of the major terrestrially terminating ice streams, not all are depicted. Indeed, around the southern margin of the LIS where robust evidence for ice stream activity exists (see Patterson, 1998; Evans *et al.,* 2008; Ross *et al.,* 2009), the model fails to reproduce high ice velocities comparable to those shown further north. Stokes and Tarasov (2010) indicate that the dynamics of the southern lobes of the LIS were strongly controlled by basal hydrology. It is anticipated, therefore, that the incorporation of basal hydrology into the model may lead to improved replication of previously documented streaming flow in this region (Stokes and Tarasov, 2010). At a continental scale, ice stream activity is modelled throughout the Canadian Archipelago which agrees with the reconstructions of England *et al.* (2009), Stokes *et al.* (2009), Stokes (2000), Stokes *et al.* (2005) and Stokes and Clark (2001). Higher velocity flow, probably of an order comparable to ice streaming, is also shown in Hudson Strait (Andrews and MacLean, 2003), the Gulf of St Lawrence (Occhietti, 1989; Hicock, 1988) and throughout the mainland north-west sector of the LIS (Clark, *unpublished*; Winsborrow *et al.,* 2004; Beget, 1987). The latter is located within the study area, as outlined in Chapter 1 of this thesis, and appears as one of the most pronounced areas of streaming flow within the LIS, see Figure 2-11. As noted in Chapter 1, despite hypothesised ice streaming in this sector of the ice sheet, ice stream activity is yet to be confirmed via a robust interrogation of the geomorphological record.

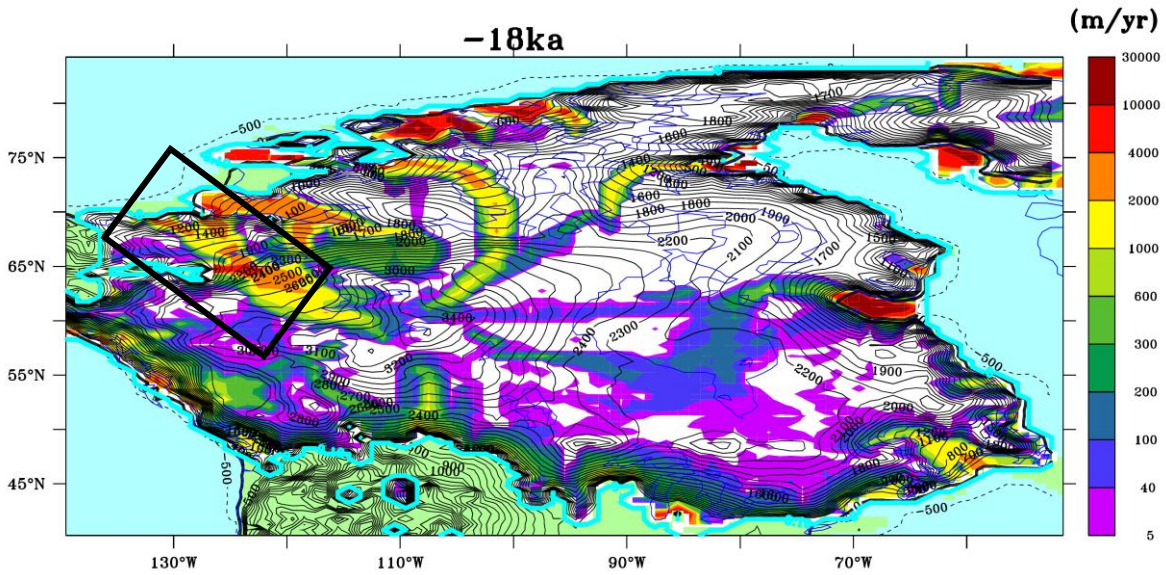

Figure 2-11: Modelled velocities in the LIS at 18 cal. ka BP according to Stokes and Tarasov (2010), showing the location of palaeo-ice streams. Note the intense streaming velocities in the study area (black box).

2.5 The glacial history of the north-west LIS

The last continental glaciation of western NWT was during the Late Wisconsinan, when ice reached its maximum extent ~ 21 cal. ka BP (Dyke *et al.,* 2003). According to Duk-Rodkin and Lemmen (2000), this was the only continental ice to reach as far west as the Rocky Mountains during the Quaternary. However, since the Late Pliocene, north-west Canada has been affected by several montane and continental glaciations (Barendregt and Duk-Rodkin, 2004, Dallimore and Matthews, 1997, England *et al.*, 2009). Early ideas about the extent of the 'last Laurentide glaciation' were outlined by Bostock (1948) who, on the basis of aerial photograph interpretation, suggested that the western limit of the last glaciation was located along the eastern flank of the Richardson Mountains and north-westward to near Herschel Island. This limit was refined but not greatly modified by the subsequent studies of Hughes (1972) and Rampton (1982). Locally this glacial period was named the Hungry Creek Glaciation based on evidence from the Bonnet Plume Basin; a basin within the Peel River catchment on the eastern side of the Mackenzie Mountains (Denton and Hughes, 1981). Following work in northern Yukon, Rampton (1982) preferred to term this the 'Buckland glaciation'. While Denton and Hughes (1981) assigned an age of ~ 30 ka to the Hungry Creek Glaciation, Rampton (1982) considered the Buckland glaciation to be of Early Wisconsinan age despite the similar geometry of their most extensive ice limits. Both ice limits were identified based on the limit of subtle morainic topography, kame terraces and the local maximum elevation of erratics (Hughes, 1972). Indeed, the earlier work of Mackay (1959) attributed the formation of

Herschel Island, an ice-thrust feature, to the Early Wisconsinan which matches with the extent of the Buckland glaciation outlined by Rampton (1982), Rampton (1988) and Bostock (1948).

Dating campaigns and the compilation of radiocarbon dates from across North America by Dyke *et al.* (2003) have more confidently ascertained the extent of the most recent Late Wisconsinan glaciation in north-west Canada. While previous reconstructions have depicted just a single maximum ice extent, Dyke *et al.* (2003) present a time-series of ice margins at 500 year intervals from the Late Wisconsinan maximum until deglaciation. These reconstructions are an update of Dyke and Prest (1987) and Dyke *et al.* (1982) and indicate an ice sheet which engulfed the regional topography with ice consistently in excess of 850 m thick in the north-west sector of the LIS (Duk-Rodkin and Lemmen, 1995). Following the Late Wisconsinan maximum, Dyke *et al.* (2003) indicate a relatively stable offshore ice margin until ~ 16.2 cal. ka BP. An ice-free corridor then formed between the Laurentide and Cordilleran ice sheets along the foot of the Yukon Mountains ~ 14.25 cal. ka BP after which rapid eastward ice retreat is envisaged until the area became ice free around 11.5 cal. ka BP (Dyke *et al.,* 2003).

In the same region, Rampton (1988) indicates that the Sitidgi Stade in which the ice margin was located on the southern side of the Mackenzie delta, was the most extensive Late Wisconsinan ice extent in the region. However, the ice margin reconstructions from Dyke *et al.* (2003) indicate much more extensive ice at the Late Wisconsinan maximum with ice located well offshore. This was confirmed by Duk-Rodkin and Hughes (1995) who deemed the Sitidgi Stade ice margin to be a sub-lobe and a deglacial phase of the north-west LIS. This agrees with the work of Vincent (1989) who recognised that the Sitidgi Stade was not the most extensive phase of Late Wisconsinan ice in the region and assigned it an age of 13 ^{14}C ka BP (15.60 cal. ka BP). However, around the Mackenzie Delta, the Sitidgi Stade margin is almost identical to the more extensively chronologically controlled 14.25 cal. ka BP margin of Dyke *et al.* (2003). It is therefore believed to be at least 1000 years younger than that suggested by Vincent (1989).

Early work on the extent of Late Wisconsinan ice in north-west Canada also reconstructed ice margins at 12, 11 and 10 ^{14}C ka BP. Despite these margins being labelled as 'speculative' by Vincent (1989), in general they show agreement, at least in terms of geometry, with ice margins from the time-series of Dyke *et al.* (2003) (see Chapter 5). In particular, the Tutsieta/Kelly Lake Phase; a margin position suggested by Vincent (1989), and earlier by Hughes (1987), to have occurred ~ 12 ^{14}C ka BP (14.10 cal. ka BP), is comparable to the similarly dated ice margin of Dyke *et al.* (2003). This 14.10 cal. ka BP margin is also comparable in geometry to that of Mackay (1958), who illustrated the 'Great Bear Lake Ice Lobe' in the

north-west LIS. While Mackay (1958) did not assign an absolute age to the identified ice margin, he did attribute it to the 'last ice advance'.

According to Rutter (1974), Late Wisconsinan ice margin positions in the region are marked extensively by meltwater channels. Craig (1960) also notes that the retreating ice built spectacular systems of end moraines along with extensive hummocky moraine and ice contact deposits. The most well-developed of these moraines is, according to Hughes (1987), located north and north-west of Great Bear Lake and known as the Kelly Lake Moraine (Vincent, 1989). Indeed, the Glacial Map of Canada from Prest *et al.* (1968), documents the distribution of very long end moraines, some within nested sequences, along with extensive hummocky moraine, particularly in the north around the Melville Hills. Prest *et al.* (1968) accompany these moraines with abundant indications of ice flow orientation, which attest to the extensive and complex glacial geomorphological signature present throughout north-west Canada. These ice flow indicators suggest that ice principally flowed north-west. A lobe of ice then formed over the present day Mackenzie Delta and tongues of ice extended more than 40 km into the adjacent mountains up the Keele, Mountain and Arctic Red River valleys (Vincent, 1989). One feature of the Hungry Creek glacial limit which is visible in the reconstructions of Dyke *et al.* (2003) from the early stages of Late Wisconsinan deglaciation, is a tongue of ice which extended into the Bonnet Plume area as outlined by Denton and Hughes (1981) and Duk-Rodkin and Hughes (1995). This lobe dammed a pro-glacial lake between itself and the adjacent mountains up to an elevation of 560 m; Glacial Lake Hughes (Duk-Rodkin and Hughes, 1995).

Despite the apparent robustness of the ice margin chronology set out by Dyke *et al.* (2003), Tarasov *et al.* (2012) highlight the need for more accurate assessments of its errors, particularly with respect to the locations of offshore ice margins. Indeed, the limited changes to the ice margin geometry in the north-west LIS during the early stages of deglaciation may require some refinement.

2.5.1 Ice streams in the north-west LIS

Along the north-western margin of the LIS, Beget (1987) provides evidence for an unusually thin ice sheet based on drift limits traced for hundreds of kilometres along the western Cordillera (Figure 2-12 and Figure 2-13). This may be partly due to deformation of the low strength subglacial sediments found around the Mackenzie River delta, but also a result of high retreat rates during deglaciation (Beget, 1987). According to Beget (1987), rapid retreat of this sector of the LIS following the LGM may have been enhanced by the presence of climatically

sensitive ice streams. Kleman and Glasser (2007) and Winsborrow *et al.* (2004), citing Clark (*unpublished*, cited in Winsborrow *et al.,* 2004), also hypothesise that palaeo-ice streams were present in the mainland north-west LIS during the Late Wisconsinan. In particular, Kleman and Glasser (2007) depict a small ice stream on the northern side of Great Bear Lake; the Haldane Ice Stream, see Figure 2-14. In addition, a longer, more sinuous ice stream is suggested to have flowed north-west along the eastern side of the Yukon Mountains (see Figure 1-1 and Figure 2-12). In total, five ice streams have been hypothesised in the north-west mainland sector of the LIS which are documented below in Table 2.2 (Clark, *unpublished*). However, as should be noted from the table below, evidence for these ice streams remains unpublished and the timing of operation either unknown or only loosely assigned as 'deglacial'.

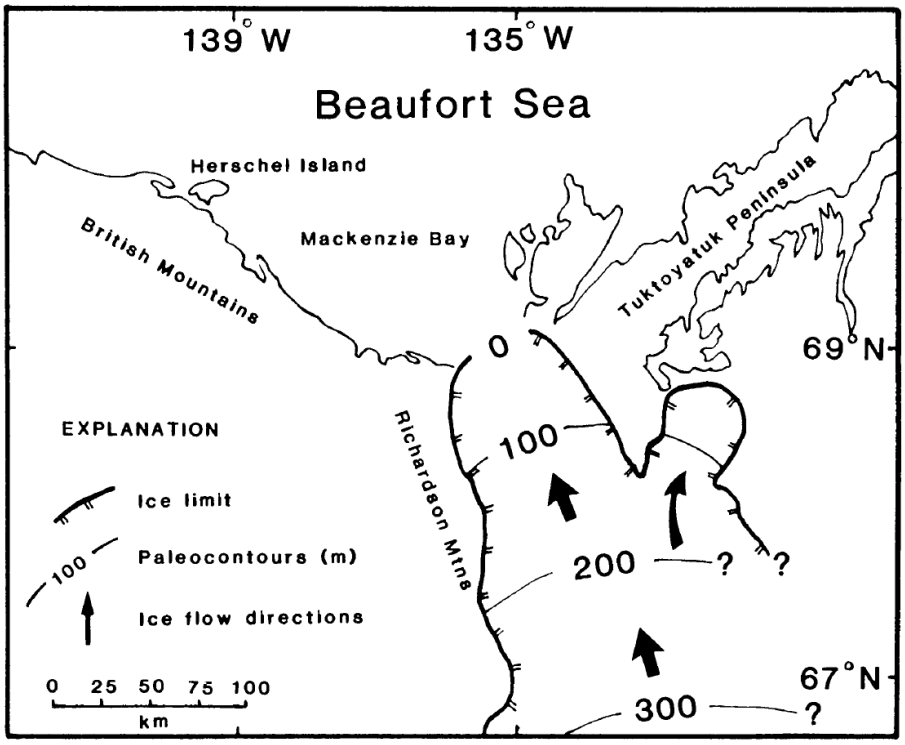

Figure 2-12: The configuration and surface contours of Late Wisconsinan ice in the vicinity of the present day Mackenzie delta during the Sitidgi Stade. Taken from Beget (1987).

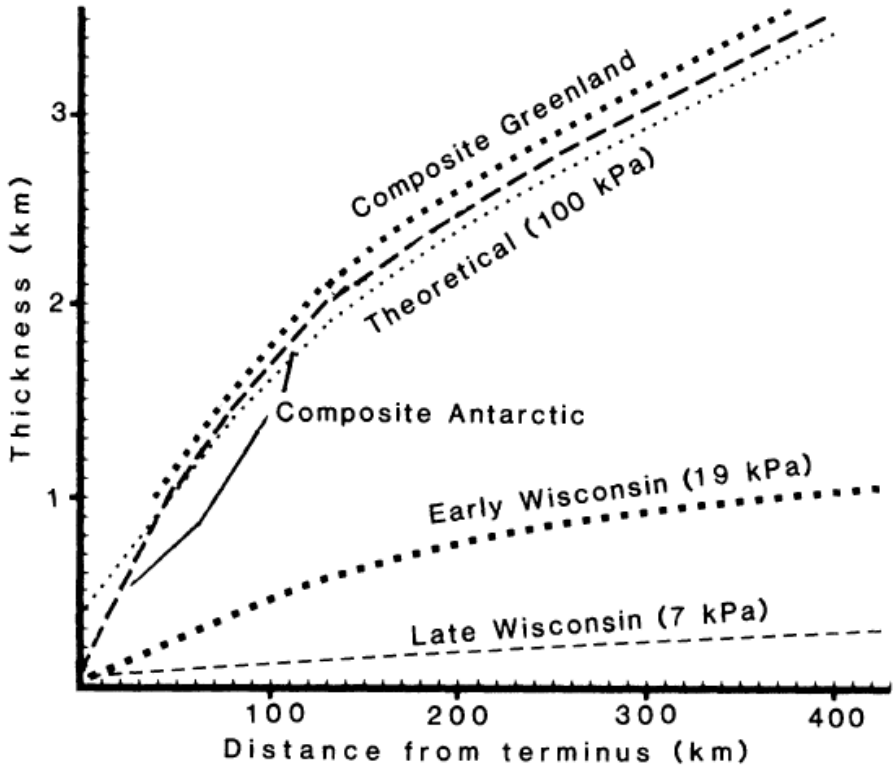

Figure 2-13: The cross-sectional profile of the north-west lobe of the LIS shown in Figure 1-1 during the Early and Late Wisconsinan, compared to that of the present day Greenland and Antarctic Ice Sheets. The Late Wisconsinan north-west LIS was particularly thin. Taken from Beget (1987).

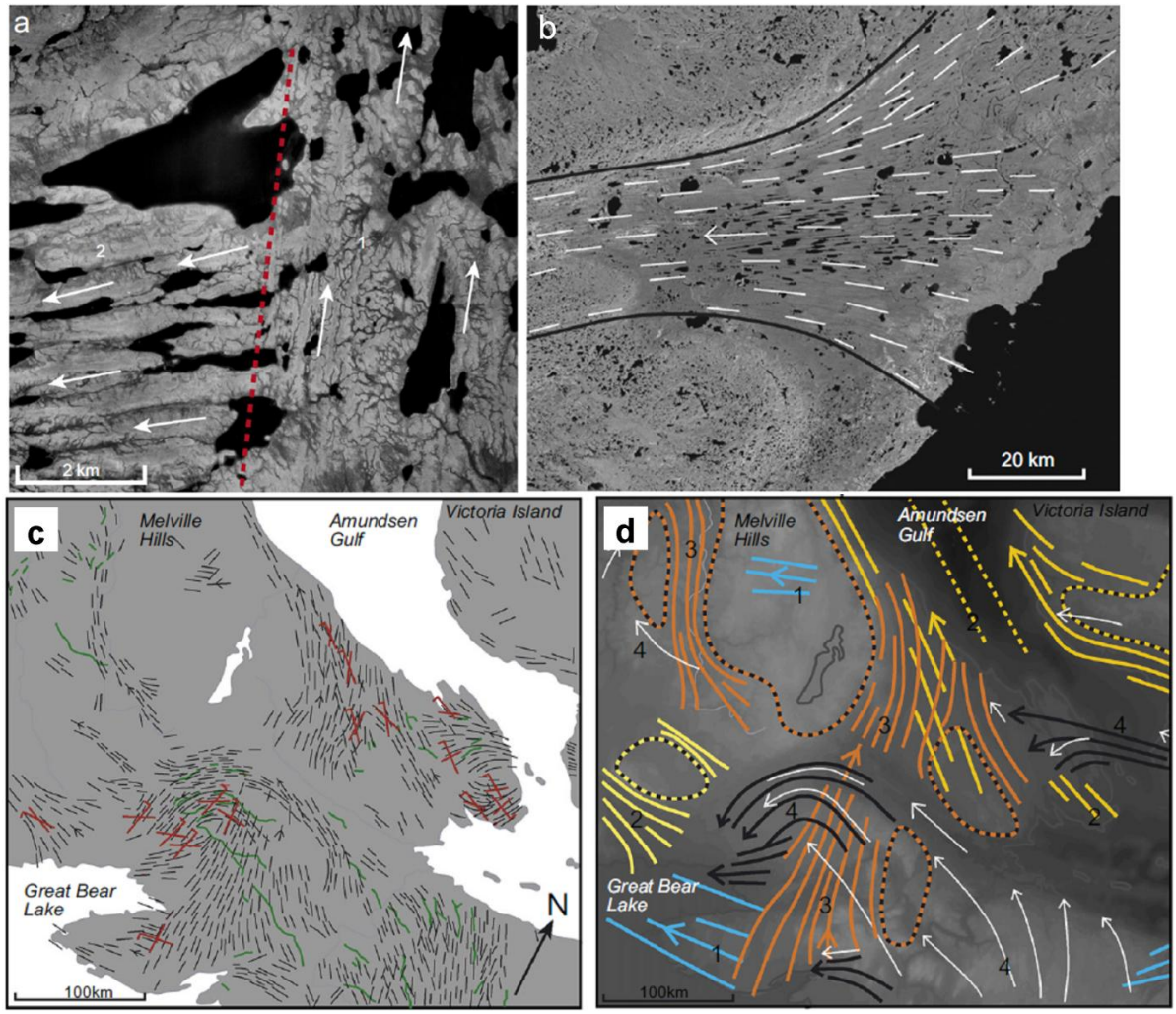

Figure 2-14: Evidence of ice streaming in the Mackenzie valley, north-west Canada. (a) Cross-cutting lineations near Great Bear Lake are separated by a sharp lateral margin between thawed bed conditions on the right (the younger landforms) and frozen bed on the left (the older landforms). (b) The head convergence of the Haldane Ice Stream northwest of Great Bear Lake. Lineations converge to form the main trunk of the ice stream which is ~ 25 km wide. (c) Glacial lineations and eskers north of Great Bear Lake. Black = lineations: Green = eskers: Red = crossing lineations. (d) Ice flow patterns deduced from Figure 2-15a. Black = lineations: Yellow and Orange = flow events with corresponding frozen bed patches (dashed line): Blue = older flow phases: White = deglacial flow. The oldest event is labelled 1 and the youngest with 4. Taken from Kleman and Glasser (2007).

Ice stream	References	Nature of evidence	Timing
Mackenzie (1)	Clark (unpublished)	Mega-scale glacial lineations in a major topographic trough.	Unknown
Anderson (2)	Clark (unpublished)	Mega-scale glacial lineations form a coherent flow-set with abrupt lateral margins.	Unknown
Horton (3)	Clark (unpublished)	Mega-scale glacial lineations, characteristic flow-set shape and shear margin moraines.	Deglacial
Haldane (4)	Clark (unpublished)	Topography and bedforms indicate a convergent onset zone feeding the main trunk. Elongate bedforms create a coherent flow-set with abrupt lateral margins marked by a suite of shear margin moraines.	Deglacial
Great Bear (5)	Clark (unpublished)	Mega-scale glacial lineations and characteristic flow-set shape.	Deglacial

Table 2.2: Palaeo-ice streams within the study area, which have previously been documented and for which a well-defined footprint exists. Table modified from Winsborrow et al. (2004).

Detailed mapping of the whole of the Mackenzie corridor has not been carried out beyond the coarse scale map of Prest *et al.* (1968). However, Clark (unpublished, cited in Winsborrow *et al.,* 2004), and Kleman and Glasser (2007),have depicted the presence of a complex pattern of overprinted and cross cutting landforms indicative of palaeo-ice streaming, particularly around Great Bear Lake in the vicinity of the Haldane palaeo-ice stream (Figure 1-1 and Figure 2-14). Cross-cutting bedforms highlight the contrast between areas affected by different basal thermal regimes and many of the criteria identified by Stokes and Clark (1999) (see Table 2.1) can be identified in this region: convergent bedforms, highly elongate bedforms and groups of bedforms with abrupt lateral margins. Along with the observations of Kleman and Glasser (2007), the complex arrangement of bedforms, particularly on the northern side of Great Bear Lake, suggests that multiple changes in ice flow orientation occurred in this sector of the LIS during deglaciation (cf. Prest *et al.,* 1968). Furthermore, frozen-bed patches were episodic throughout deglaciation and typically occupied topographic highs (Kleman and Glasser, 2007). Their presence may also have contributed to the distribution of ice streams in the north-west LIS in the absence of significant topographic control along the Mackenzie River valley.

2.5.2 Pro-glacial lake evolution along the north-western margin of the LIS

In their reconstruction of LIS ice margins, Dyke *et al.* (2003) also depict the extent of pro-glacial lakes. These have largely been derived from previously published evidence, particularly with respect to the maximum lake extent. In the north-west LIS, pro-glacial lake extent is based largely on field evidence presented by Craig (1965). However, it has been known for much longer that pro-glacial lakes occupied the basins of Great Slave Lake, Great Bear Lake and Lake Athabasca along the north-western margin of the LIS during deglaciation (see McConnell, 1890; Bell, 1990; Cameron, 1922; Raup, 1946 and Craig, 1960). Glacial Lake McConnell was the

largest of these lakes. According to Craig (1965), Glacial Lake McConnell formed during deglaciation as a result of either the changing configuration of the ice margin which caused drainage routeways to be dammed by ice, or, differential isostatic depression which caused a reversal of drainage.

The most widespread evidence for the existence of pro-glacial lakes along the north-west LIS margin is strandlines. Early observations of strandlines (McConnell, 1890) found that, around the basin of the present day Great Slave Lake, strandlines in the west were at lower elevations than those in the east. This phenomenon was attributed to 'changes in elevation', presumably of the land, or the damming of lakes by ice by McConnell (1890). Assuming that strandlines of the same age were correctly traced around the basin of Great Slave Lake and west to Fort Simpson, from west to east the difference in strandline elevation is 425 feet (130 m), which equates to ~ 2 feet per mile (38 cm per 1 km). The probable maximum extent of Glacial Lake McConnell is shown below in Figure 2-15. Strandlines demarcate the extent of Glacial Lake McConnell and indicate that the lake extended west along the present day valley containing the outflow from Great Slave Lake, to ~ 100 km beyond Fort Simpson. Water then exploited the lowland topography between lakes Great Slave and Great Bear along the western edge of the Canadian Shield, to form a 100 km wide lake corridor. The northern end of Glacial Lake McConnell occupied the basin of Great Bear Lake and covered an area not dissimilar in plan-view to that of the present day lake (Craig, 1965). As shown in Figure 2-15, the lake also extended south beyond the study area to Lake Athabasca and west along the valley of the Peace River. The configuration of Glacial Lake McConnell depicted by Craig (1965) is similar to that of Lemmen *et al.* (1994).

Figure 2-15: The extent of Glacial Lake McConnell based on strandline evidence. Figure taken from Craig (1965).

To the west of Glacial Lake McConnell, Smith (1992) found evidence for the formation of a lake along the route of the present day Mackenzie River based on the location of strandlines, dunes and sedimentological evidence. The lake, named Glacial Lake Mackenzie connected with Glacial Lake McConnell at the western most end of the Great Bear Lake basin (Figure 2-16). The lake was 800 km long with an average width of 15 km. However, it reached 75 km wide in the north. Near the connection with Glacial Lake McConnell, the lake was at least 80 m deep. The timing of lake formation remains uncertain but Smith (1992) suggests that the lake had formed by 11,760 cal. years BP with drainage having occurred ~ 10,290 cal. years BP when the lake incised a limestone barrier near Fort Good Hope and sediment filling of the lake occurred.

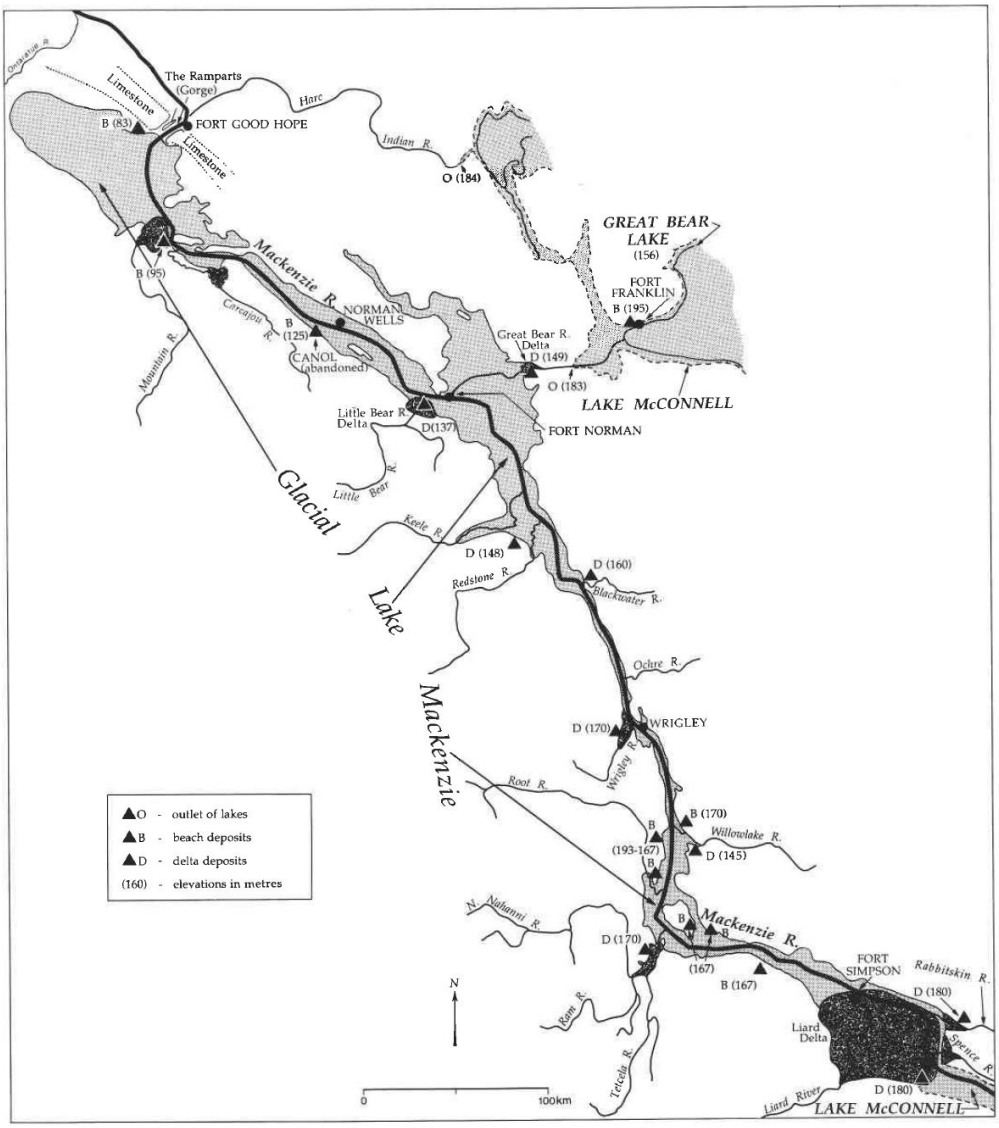

Figure 2-16: The extent of Glacial Lake Mackenzie based on the maximum elevation of raised beaches and extent of deltaic deposits. Figure taken from Smith (1992).

Further west, Hughes (1987) provides a reconstruction of Glacial Lake Old Crow and Glacial Lake Hughes. These were ice dammed lakes which formed when the ice margin was buttressed against the base of the Yukon/Richardson Mountains. Unlike the pro-glacial lakes reconstructed in the east, these lakes occupied mountainous terrain and an overflow from Lake Hughes to Lake Old Crow is noted by Lauriol *et al.* (2010) ~ 15,120 ^{14}C years BP (Figure 2-17).

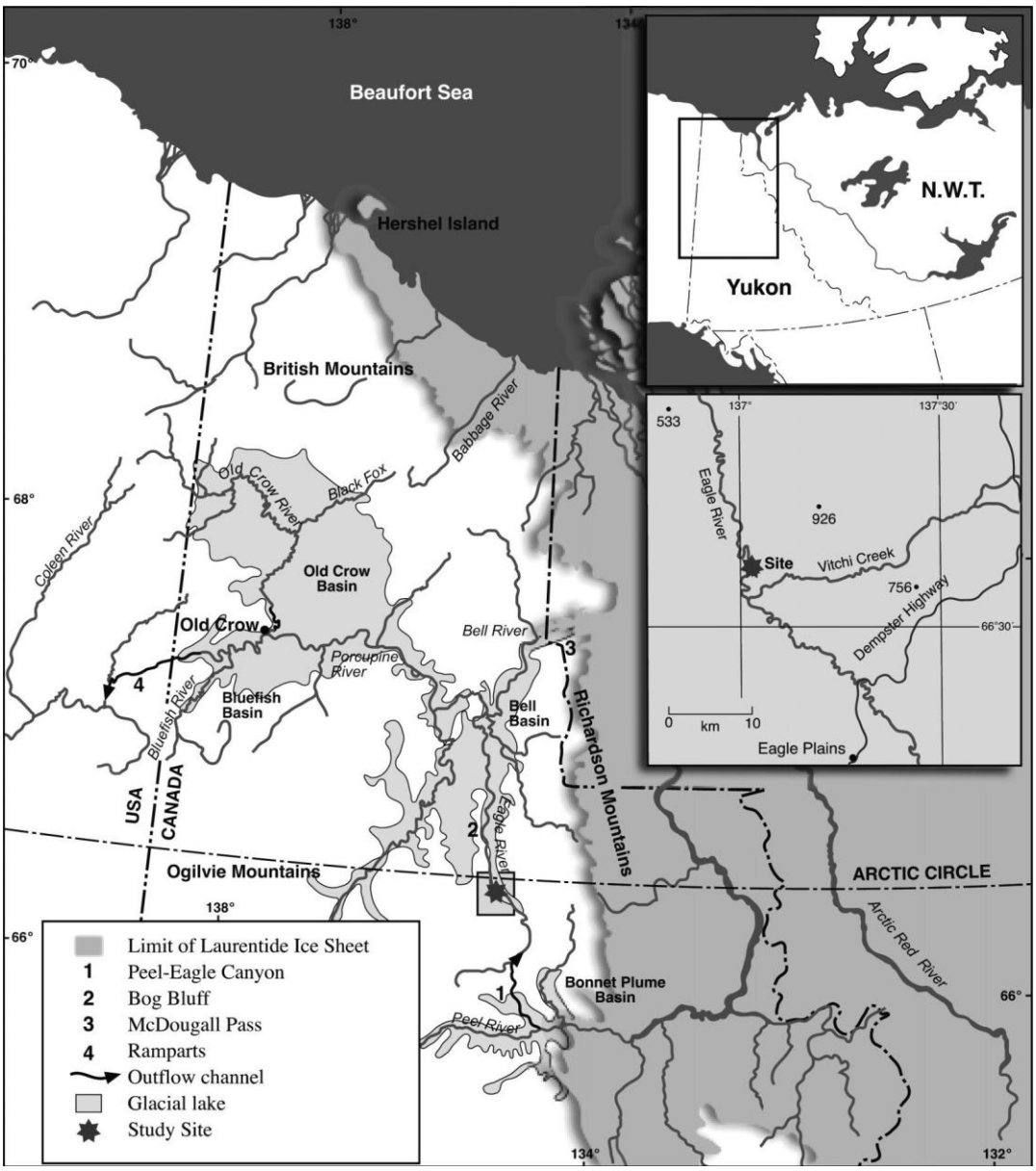

Figure 2-17: The extent of Glacial Lakes Old Crow and Hughes according to Lauriol et al. (2010). Glacial Lake Hughes is the lake which occupies the valley of the Peel River and is marked with a '1'. Glacial Lake Old Crow was located further north in Old Crow Basin. Figure taken from Lauriol et al. (2010).

Aside from the maximum extent of Glacial Lake McConnell provided by Craig (1965), Dyke *et al.* (2003) provide an indication of how pro-glacial lakes evolved during deglaciation. This was achieved by the extrapolation of mapped strandlines based on the work of Craig (1960; 1965), Duk-Rodkin and Hughes (1995), Smith (1992; 1994), Teller and Kehew (1994) and Lemmen *et al.* (1994). Lakes began to form along the mainland north-west margin of the LIS, in the western end of the basin now occupied by Great Bear Lake, ~ 14.10 cal. ka BP. This followed the opening of the ice free corridor between the Laurentide and Cordilleran Ice Sheets along the foot of the Yukon Mountains; a period when meltwater is likely to have been abundant (Dyke *et al.,* 2003). Much larger pro-glacial lakes had developed along the north-west margin

of the LIS by ~ 12.7 cal. ka BP and by ~ 11.45 cal. ka BP, pro-glacial lakes had begun to exploit the basin occupied by Great Slave Lake. The lakes reached their maximum extent ~ 10.72 cal. ka BP by which time, Laurentide ice had retreated east and the study area was ice-free (Dyke *et al.,* 2003).

2.6 The drainage of pro-glacial lakes surrounding the LIS

Three major cooling events punctuated Late Wisconsinan deglaciation: the Younger Dryas (12.9-11.5 cal. ka BP), the Preboreal Oscillation (PBO) (11.5 cal. ka BP) and the 8.2 cal. ka BP cold event (Meissner and Clark, 2006). These climate oscillations are recorded in the δO^{18} record from the Greenland Ice Core Project 2 (GRIP2). The cause of the events is uncertain, but many attribute their occurrence to the varying drainage regime of Glacial Lake Agassiz (GLA) and other pro-glacial lakes surrounding the LIS during deglaciation which may have altered global ocean circulation (Leverington *et al.*, 2000).

The changing geometry of the LIS during deglaciation along with the associated differential isostatic rebound, caused the configuration of pro-glacial lakes around the LIS and their drainage routeways to evolve. Four major drainage routeways for the LIS pro-glacial lakes have been identified: the Mississippi River, the St Lawrence River and a north-west routeway into the Arctic Ocean (Fisher *et al.,* 2002; Leverington *et al.,* 2000; Teller *et al.*, 2005) (Figure 2-18). A further sub-glacial drainage routeway into Hudson Bay has also been identified (Teller *et al.*, 2005). The hypothesised drainage chronology for each of these outlets is shown below in Table 2.3. As shown in Figure 2-18, the largest of the pro-glacial lakes which surrounded the LIS during the Late Wisconsinan was Glacial Lake Agassiz (Fisher, 2003). The lake occupied the southern margin of the LIS and, according to early records, the area of the lake was 110,000 square miles and the level of the lake was approximately 700 feet (215 m) above the present level of Lake Winnipeg (Warren, 1895).

Drainage period (cal. ka BP)	Drainage period (^{14}C ka BP)	Routeway	Destination
13.49 – 12.73	11.7 – 10.9	South: Mississippi River	Gulf of Mexico
12.73 – 11.72	10.9 – 10.1	East: St Lawrence River	North Atlantic
11.72 – 10.65	10.1 – 9.4	North-west: Mackenzie River	Arctic Ocean
10.65 – 8.45	9.4 – 7.7	East: St Lawrence River	North Atlantic
8.45	7.7	North-east: Hudson Bay	Hudson Bay » North Atlantic

Table 2.3: A summary of the proposed drainage history of pro-glacial lakes along the mainland margin of the LIS during Late Wisconsinan deglaciation, see also Figure 2-18. Adapted from Teller et al. (2005). The radiocarbon ages have been taken from Teller et al. (2005) while the calibrated ages were obtained using the INTCAL 06 curve.

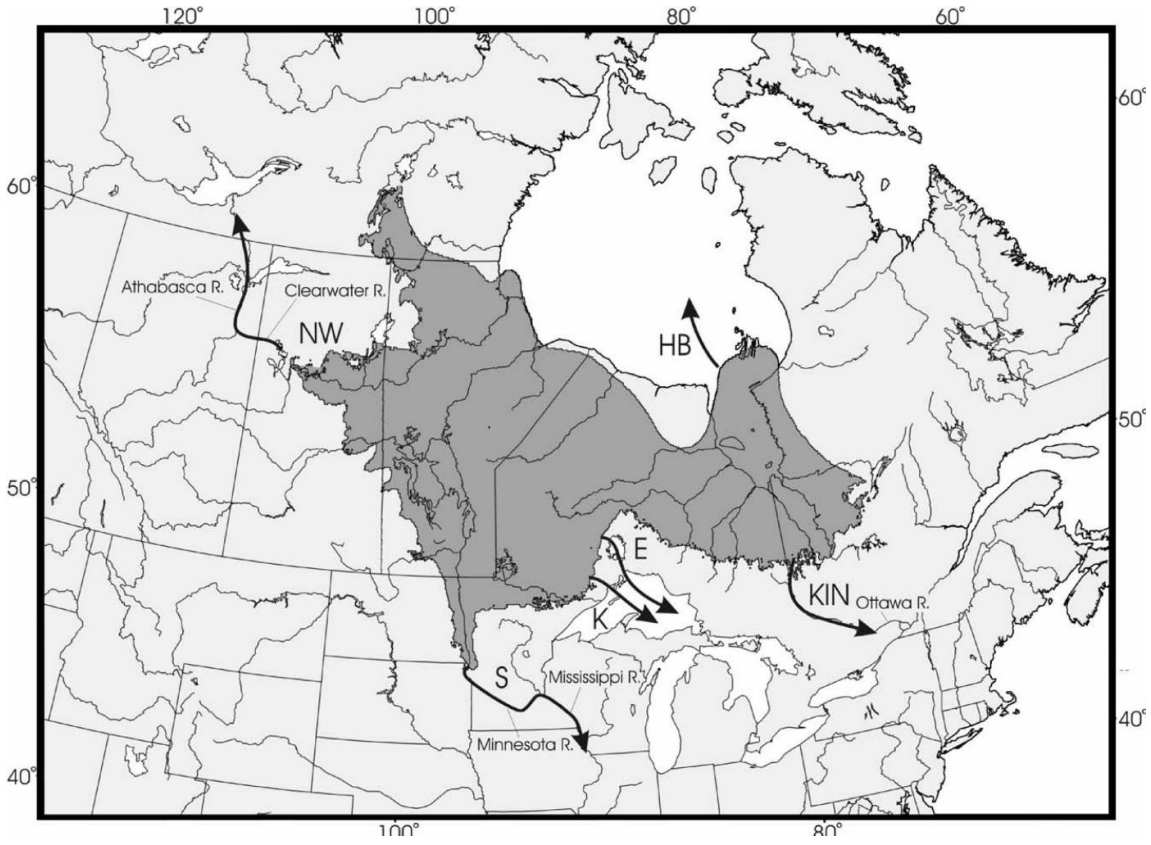

Figure 2-18: The drainage routeways of Glacial Lake Agassiz (GLA). GLA attained its maximum size ~ 9.4 14C ka BP and covered an area of > 260,000 km^2 with 22,000 km^3 of water. The area of GLA is represented by the dark shaded grey area. NW = Mackenzie Valley to Arctic Ocean: S = Mississippi Valley to Gulf of Mexico: K = eastern outlet through Thunder Bay: E = eastern outlet through Nipigon basin: KIN = Kinojevis outlet, HB = Hudson Bay to North Atlantic. Note, outlets K, E and KIN all exit through the St Lawrence valley and into the North Atlantic. Taken from Teller et al. (2005).

The precise timing and routing of pro-glacial lake drainage is critical to our understanding of the controls on global climate change. If drainage preceded major climate events, the impact of the release of large volumes of freshwater into the oceans upon ocean circulation will have varied depending on the location of its delivery (Teller *et al.,* 2005; Condron and Winsor, 2011). It has long been assumed that the freshwater released from pro-glacial lakes around the LIS during deglaciation, via the St Lawrence River, moved rapidly eastward into the deep sub-polar North Atlantic to inhibit North Atlantic Deep Water (NADW) formation (Alley and Águstsdóttir, 2005). This reduced convective oceanic heat transport and ultimately weakened the poleward heat transport of the Atlantic Meridional Overturning Circulation (AMOC), and abrupt climate cooling resulted (Alley and Águstsdóttir, 2005). This concept has been used to explain the climatic down-turns of the Younger Dryas (YD), Preboreal Oscillation (PBO) and 8.2 cal. ka BP event (Barber *et al.,* 1999; Teller *et al.,* 2002; Clarke *et al.,* 2009; Lewis *et al.,* 2012). However, Condron and Winsor (2011) indicate that water released from these locations instead occupied narrow coastal flows and continued south into the sub-tropical North Atlantic gyre (20-40°N). Their model, with an ~ 18 km resolution, indicates that little or no freshwater would be routed to the Nordic Seas to interrupt NADW formation if released into the oceans via the St Lawrence River, Mississippi River or via Hudson Bay (Condron and Winsor, 2011). While Condron and Winsor (2011) focuses on the 8.2 cal. ka BP event, periods of water discharge into the North Atlantic, particularly via the St Lawrence River earlier in deglaciation, may have been directed to similar locations irrespective of their magnitude. Examples include discharge events around the time of MWP-1A and the Younger Dryas (Rohling and Pälike, 2005; Peltier, 2005; Broecker *et al.,* 2010).

2.7 The north-west drainage of pro-glacial lakes

Until recently, the idea of a north-western outlet for Glacial Lake Agassiz received little consideration. However, the discovery of extensive fluvial boulder gravel deposits along the Mackenzie River, the oversized lower Clearwater and Athabasca valleys, and the anomalously large Late Pleistocene Athabasca delta – first identified by Rhine and Smith (1988) – initiated further investigation into a north-western outlet for Glacial Lake Agassiz by Fisher (1993) and Smith and Fisher (1993). Smith and Fisher (1993) interpret the poorly-sorted to massive, coarse-grained boulder gravel as a high velocity flood deposit. They conclude that Glacial Lake Agassiz discharged through a north-western outlet involving drainage through the Clearwater valley into Glacial Lake McConnell, then Glacial Lake Mackenzie before reaching the Arctic Ocean via the Mackenzie River and delta as shown in Figure 2-19 (Couch and Eyles, 2008).

Tarasov and Peltier (2006) provide a surface meltwater drainage chronology for the deglaciation of the North American ice complex (Laurentide, Innuitian and Cordilleran ice sheets) during the Late Wisconsinan glacial maximum. This chronology indicates that the southern outlet through the Mississippi valley and into the Gulf of Mexico was abandoned around the onset of the Younger Dryas. However, in almost all of the model runs, the model of Tarasov and Peltier (2006) indicates an active north-west outlet from Glacial Lake Agassiz around the time of the Younger Dryas. Indeed, Fisher (2007) indicates that the north-west outlet was abandoned between 9.07 and 9.59 ^{14}C ka BP (10,220 and 10,810 cal. yr. BP) with a best estimate of 9.45 ^{14}C ka BP (10,650 cal. yr. BP).

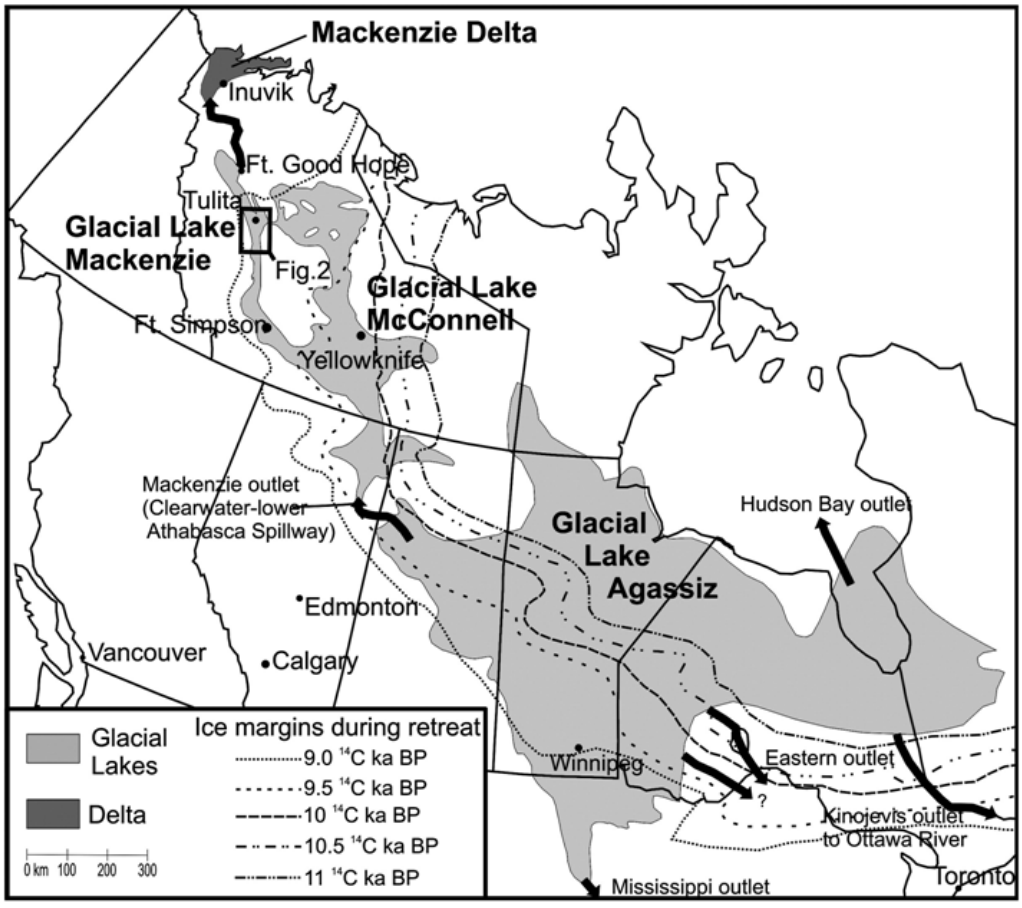

Figure 2-19: The locations and maximum extent of glacial lakes Agassiz, McConnell and Mackenzie along the margin of the LIS at various stages of deglaciation (taken from Couch and Eyles, 2008). The effect of Glacial Lake Mackenzie, and possibly Glacial Lake McConnell, may have been to trap fine sediment allowing sediment-poor water to enter the oceans and therefore enhance the effect of outflow through the north-west outlet on the Thermohaline Circulation.

Most recently, the north-west outlet for pro-glacial lakes has received attention from Murton *et al.* (2010), who identify sedimentological evidence for two floods along the Mackenzie River around the time of the Younger Dryas. The source of these floods was the pro-glacial lakes along the southern and north-western margin of the LIS, including Glacial Lake Agassiz, and the timing of the floods was dictated by the geometry of the LIS margin on the western side of the Athabasca lowlands, around the Alberta - NWT border. In this region, the LIS re-advanced ~ 11.5 cal. ka BP. However, prior to this, at ~ 12.9 cal. ka BP, Murton *et al.* (2010) suggest that the ice margin of Dyke *et al.* (2003) be shifted < 50 km east. This would have allowed for increased outflow from pro-glacial lakes toward the north-west through the Mackenzie River valley. The subsequent re-advance, blocked the outflow from the lakes to the north-west, before overall retreat of the ice margin towards the east resumed and the north-west drainage routeway was reopened. Murton *et al.* (2010) suggest that these floods are represented by two fluvial gravels located downstream of the Athabasca lowlands and along the Arctic Ocean coast. The gravel units have been dated using optically stimulated luminescence (OSL) to between 13.0 and 11.7 cal. ka BP, and 11.7 and 9.3 cal. ka BP. Murton *et al.* (2010) therefore reject the hypothesis that routing of deglacial meltwater from Lake Agassiz at the start of the Younger Dryas switched from the southern outlet solely to the eastern outlet. Rather they favour a north-west outlet and support the hypothesis that this drainage may have triggered the Younger Dryas (Murton *et al.,* 2010). This supports the much earlier work of Smith and Fisher (1993).

Indeed, returning to the model of Condron and Winsor (2011) and Condron and Winsor (*unpublished*), the most effective place to deposit water into oceans in order to disrupt the formation of NADW is through the north-west routeway, into the Arctic Ocean. This routeway distributes water throughout the Canadian Archipelago and, through a combination of eddy activity off the southern tip of Greenland and increased sea-ice flux out of Fram Strait, an increased portion of freshwater from LIS pro-glacial lakes is able to accumulate in the Nordic Seas and penetrate deep into the North Atlantic to inhibit NADW formation (Condron and Winsor, 2011). A robust reconstruction of pro-glacial lake evolution along the north-western margin of the LIS, along with possible links to the neighbouring Glacial Lake Agassiz, is therefore crucial to inform future debate about the plausibility, location, timing and ultimately impact of freshwater drainage on palaeo-oceanography.

2.8 Summary

- Ice streams are present in the present day Antarctic and Greenland ice sheets and are instrumental in ice sheet mass balance. Currently, in Antarctica, ice streams account for 10 % of the surface area of the Antarctic ice sheet and, along with outlet glaciers, account for 90 % of the mass loss from the continent.
- While we can observe the activity of contemporary ice streams over short timescales, the study of palaeo-ice streams allows for reconstructions of their behaviour over millennial timescales. These reconstructions can be used to inform predictions about the activity of contemporary ice streams under present and future climate change.
- A set of criteria have been developed by Stokes and Clark (2001) to aid the identification of palaeo-ice streams. These criteria include groups of highly elongate bedforms with abrupt lateral margins, convergent and divergent patterns of bedforms and lateral shear margin moraines. The criteria are based on the principles of the Glacial Inversion Method of Kleman and Borgström (1996) which suggests that the spatial arrangement of glacial geomorphology can be used as a basis for inferring past glacial environments.
- Palaeo-ice streams were present throughout the LIS during the Late Wisconsinan. Topographic ice streams were present throughout the Canadian Archipelago (see Stokes *et al.,* 2009) and also occurred in the Foxe/Baffin (eastern) sector of the LIS (see De Angelis and Kleman, 2007). Major ice streams along the southern margin of the LIS were terrestrially terminating (Patterson, 1998). Ice streams have been hypothesised in the north-west sector of the LIS by Clark (*unpublished*, cited in Winsborrow *et al.,* 2004), Winsborrow *et al.* (2010) and Stokes and Tarasov (2010), but remain unconfirmed.
- Craig (1965) and Smith (1993) provide detailed reconstructions of pro-glacial lakes along the north-western margin of the LIS. However, these reconstructions are based purely on field evidence and do not account for changes in solid earth deformation during deglaciation. These studies report the presence of extensive pro-glacial lakes including Glacial Lake McConnell and Glacial Lake Mackenzie.
- Pro-glacial lakes around the LIS drained via four principal routeways as outlined by Teller *et al.* (2005): through the Mississippi River (south), the St Lawrence River (east), north-west to the Arctic Ocean or sub-glacially through Hudson Bay. The precise timing and location of lake drainage may have had important implications for palaeo-oceanography.

- A north-west drainage routeway for pro-glacial lakes remains debated but has been hypothesised by Murton *et al.* (2010) based on the presence of extensive fluvial boulder gravels along the Mackenzie River and Arctic Ocean coast. A regional reconstruction of pro-glacial lakes is now required which uses a DEM as a base in order to investigate the plausibility and timing of a north-west routeway and complement the work of Murton *et al.* (2010).

Chapter 3: Methods

3.1 Introduction

This chapter is divided into three parts. Part 1 documents the methods employed in the mapping. This includes a justification for mapping remotely rather than in the field, and a discussion of the various types of spaceborne and airborne imagery from which mapping was undertaken. Part 2 documents the method used to produce the reconstruction of ice stream activity presented in Chapter 5. Finally, Part 3 details the methods used to reconstruct pro-glacial lakes, as shown in Chapter 6.

Part 1: Geomorphological mapping

Approaches to glacial geomorphological mapping are numerous and include mapping in the field (ground survey) (Mitchell and Riley, 2006), mapping from airborne imagery (Evans *et al.,* 2006; Evans *et al.,* 2007) or, as is the case here, mapping primarily from spaceborne satellite imagery (Smith *et al.,* 2006; Livingstone *et al.,* 2008; Storrar and Stokes, 2007). This section will discuss the relative merits of each approach to glacial geomorphological mapping before elaborating on the method used in this thesis.

3.2 Remote sensing

Remote sensing is the science of collecting and interpreting information about an area without being physically in contact with it and has revolutionized glacial geomorphological mapping, and therefore vastly increased our knowledge of the dynamics of former ice masses (Smith and Knight, 2011; Jansson and Glasser, 2005). In many cases, remote sensing also enables users to investigate beyond the spectral range of human perception i.e. beyond the visible range of the electromagnetic spectrum. A wide range of remote sensing products and imagery are available including those from both airborne and spaceborne devices. For geomorphological mapping, spaceborne satellite imagery is particularly advantageous as it allows for rapid and systematic coverage of large areas at a variety of scales, which could not be achieved using aerial photography or by ground survey. More specifically, satellite imagery can also be manipulated, principally using different band combinations, to enhance the visualisation of a landscape and, consequently, a greater number of geomorphological features can be identified (Clark, 1997). An additional benefit is that satellite imagery is, increasingly, becoming freely available while aerial photography remains more costly to obtain. A combination of spaceborne and airborne

imagery (Landsat ETM+, ASTER, GTOPO-30 and aerial photography) was used to map the glacial geomorphology presented in Chapter 4, each of which is briefly reviewed below. The large size of the study area (~ 800,000 km^2) and the cost associated with carrying out fieldwork meant that this was not possible. As such, all mapping was carried out remotely to provide a self-consistent map of the glacial geomorphology.

3.2.1 Landsat ETM/ETM+

Landsat 7 is the most recently launched satellite in the Landsat Program. The satellite has seven bands, which simultaneously record emitted radiation from the Earth's surface in the blue-green (band 1), green (band 2), red (band 3), near-infrared (band 4), mid-infrared (bands 5 and 7), and the far-infrared (band 6) portions of the electromagnetic spectrum (Lillesand *et al.*, 2008; Olsen, 2007). The satellite is also fitted with an Enhanced Thematic Mapper Plus (ETM+), which provides an extra panchromatic band (band 8). This band produces panchromatic images with a higher spatial resolution of 15 m (Lillesand *et al.,* 2008). As noted by Jansson and Glasser (2005) and Smith *et al.* (2006), Landsat ETM+ enables the user to identify a greater number of glacial lineations than possible on earlier imagery such as Landsat TM. This makes Landsat ETM+ a highly valuable tool in geomorphological mapping (Storrar and Stokes, 2007; Smith *et al.,* 2006; De Angelis, 2007). Examples of Landsat ETM+ are shown in Figure 3-1.

Freely available Landsat Enhanced Thematic Mapper (ETM+) images were obtained from the Global Landcover Facility (GLCF) (http://glcf.umiacs.umd.edu/index.shtml) and imported into Erdas Imagine 9.3 and ArcGIS 9.3 for manipulation. Once downloaded, the Landsat ETM+ scenes were projected into Universal Transverse Mercator (UTM) zone 10 North and the band combinations were adjusted in order to optimise the visualisation of the geomorphology. In order to avoid bias in the mapping process, landforms were identified at a range of scales and using a variety of band combinations (Smith *et al.,* 2006). False colour imagery with a band combination of 6, 5, 2 (R, G, B) was found to be the most beneficial for mapping. Figure 3-1 provides examples of glacial lineations as viewed on Landsat ETM+ under four different band combinations, while Figure 3-2 and Figure 3-3 show the location of the Landsat (ETM+ and TM) tiles which cover the study area.

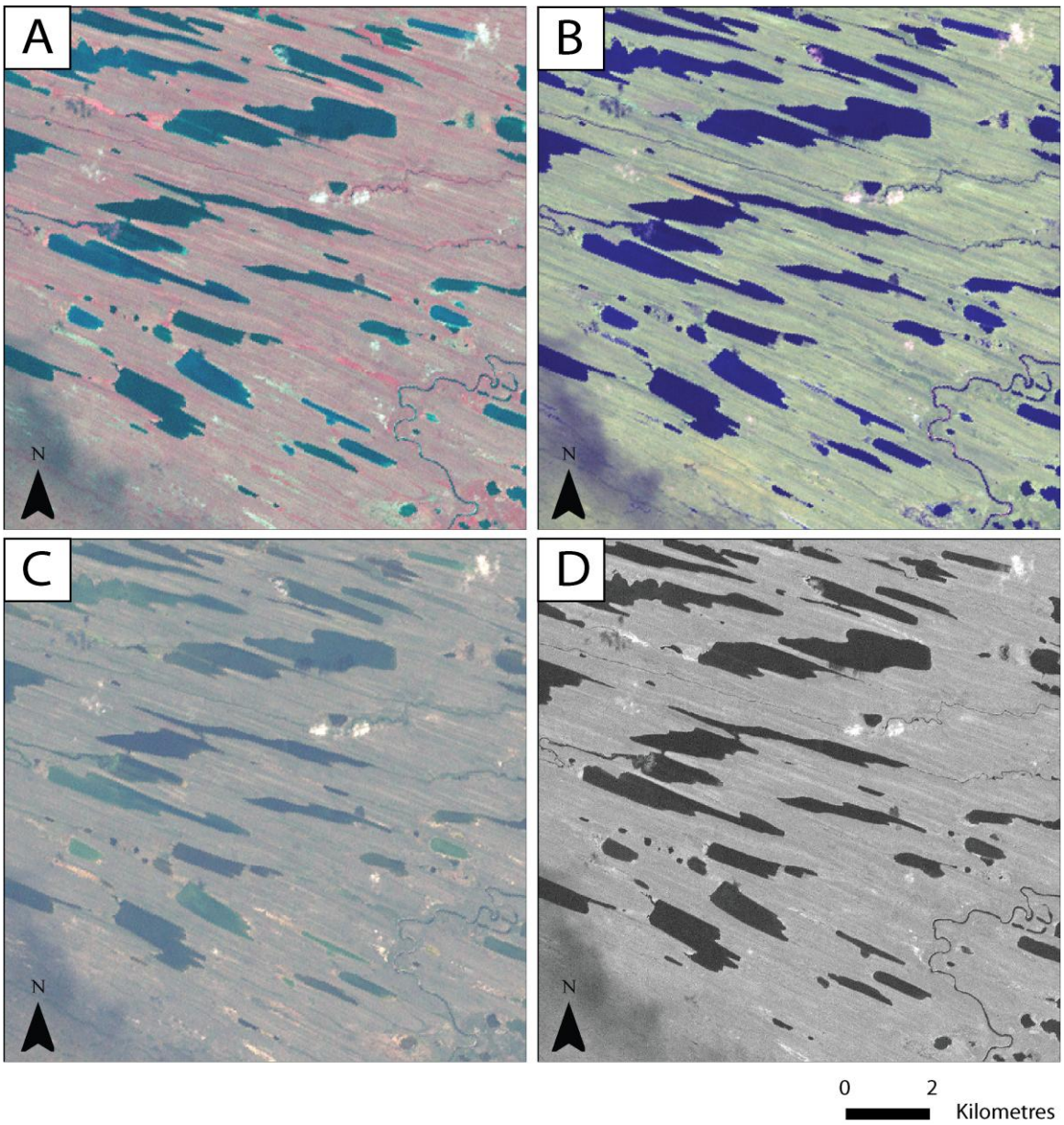

Figure 3-1: Examples of spaceborne imagery used in the mapping process. A) Landsat ETM+, band combinations 4, 3, 2: B) Landsat ETM+, band combinations 6, 5, 2: C) Landsat ETM+, band combinations 3, 2, 1: D) Landsat ETM+, band 8. The images depict glacial lineations along the northern shore of Great Bear Lake. The bedforms are best visualised in A and B rather than the true colour composite shown in C. The higher resolution, band 8 imagery was particularly useful when mapping smaller features and features which were closely spaced.

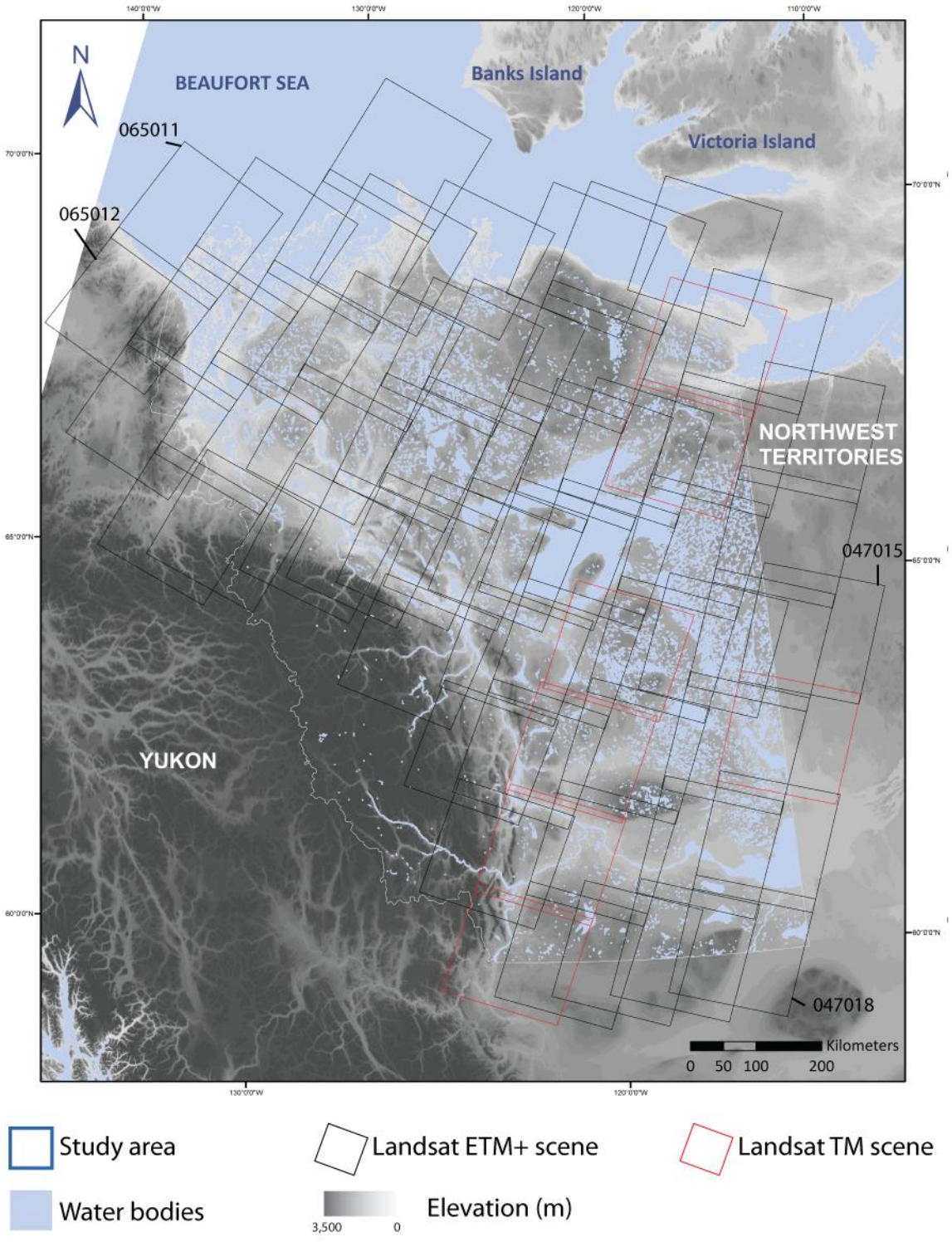

Figure 3-2: The location of the Landsat ETM+ and Landsat TM (and selected path and row numbers) used to produce the geomorphological map.

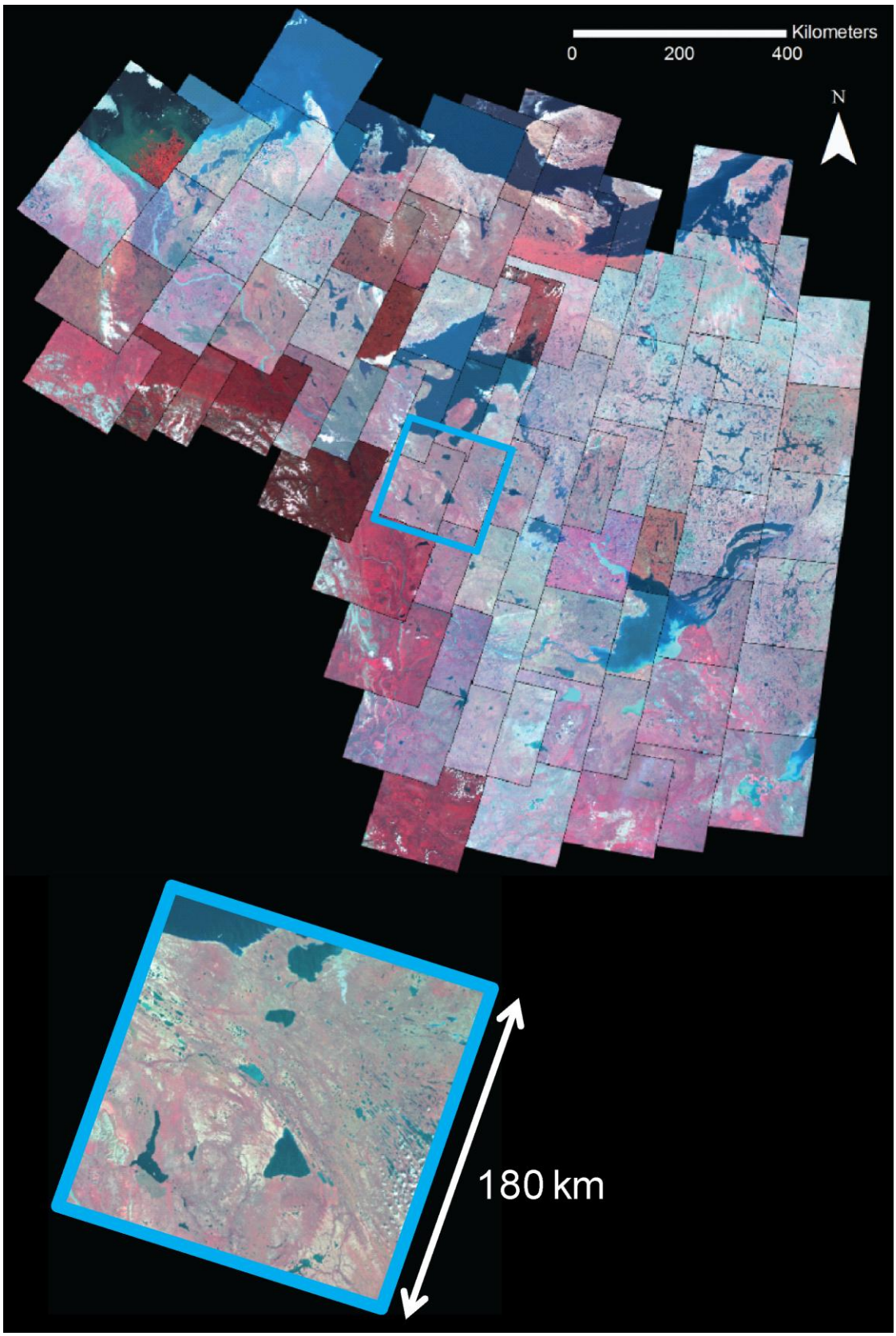

Figure 3-3: The Landsat ETM+ and Landsat TM tiles which cover the study area with band combinations 4,3,2 (R, G, B). Each tile is 180 km by 180 km.

3.2.2 ASTER

Mounted on board TERRA, a satellite launched in 1999, the ASTER sensor produces multi-spectral images in 14 bands. Of the 14 bands comprising ASTER imagery, three bands are in the visible and near infrared spectral range (0.5-1.0 µm) and have a spatial resolution of 15 m (the same as the single panchromatic band of the Landsat ETM+ imagery). This makes ASTER imagery better for geomorphological mapping in areas where it is necessary to view a greater amount of detail, for example in areas of complex esker distribution. However, the scene size of ASTER imagery is smaller (120 by 150 km) than that of Landsat ETM+ making it more computationally resource heavy for geomorphological mapping over large areas. Furthermore, Landsat ETM+ has been widely proven to be of sufficient resolution to undertake geomorphological mapping (see Storrar and Stokes, 2007; Smith *et al.*, 2006; De Angelis, 2007). As a result, the majority of the mapping was carried out from Landsat ETM+, but in areas where, for example, cloud obscured the imagery, ASTER imagery was used as an alternative.

3.2.3 Aerial photography

Aerial photography was used in areas where the complexity of the geomorphology could be detected but not resolved by the Landsat ETM+/TM or ASTER imagery, and in areas where cloud obscured the other imagery. The photography was sourced from the National Air Photograph Library (NAPL) of Canada in Ottawa who provided hard copies of the photography at a variety of scales in black and white for use within their offices. However, the cost of obtaining copies of the photography that could be returned to the UK limited their use.

3.2.4 GTOPO-30

Digital Elevation Models (DEMs) provide a representation of earth's surface elevation. The use of DEMs across a range of disciplines over the past 50 years has revolutionized approaches to geographical research (Smith *et al.,* 2006). However, until recently DEMs were incredibly costly to source, required intense and lengthy processing times, or were not available at spatial resolutions suitable for glacial geomorphological mapping (Smith *et al.,* 2006). A number of products are now available freely including the GTOPO30 DEM, SRTM-90 DEM and ASTER GDEM that provide data at horizontal resolutions of 900 m, 90 m and 30 m, and vertical resolutions of 10 m, < 16 m and < 20 m respectively.

While DEMs with horizontal resolutions of 90 or 900 m provide general visualizations of the regional topography and have indeed been widely used (e.g. Storrar and Stokes, 2007; De Angelis, 2007), it is impossible for them to resolve landforms of a size comparable to eskers or

drumlins. Furthermore, the vertical resolution of each of the DEMs is unsuitable for the detection of these bedforms. In this thesis, GTOPO-30 has been used as the background for the maps and reconstructions (e.g. Figure 3-2). The reason for choosing to use this apparently coarse scale DEM over the ASTER-GDEM and STRM-90 DEM was two-fold: 1), the ASTER GDEM tiles are small and vast amounts of time and processing power would have been required to mosaic enough tiles together to produce a DEM which covered the entire study area, and 2), the SRTM-90 DEM only covers land between 60°N and 56°S i.e. not the whole study area. The GTOPO-30 DEM was also used in the reconstruction of pro-glacial lakes presented in Chapter 6.

3.3 The identification of glacial geomorphology

Individual landforms were identified, interpreted and digitised manually on-screen in ArcMap 9.3 (e.g. Clark, 1997). In order to produce an accurate reconstruction of ice stream activity from the mapping, it was decided that every individual bedform should be mapped rather than just landform patterns (e.g. where areas of streamlined terrain are identified). The map, published in Brown *et al.* (2011), therefore takes a similar format to previous work on Victoria Island (Storrar and Stokes, 2007) and the central-eastern sector of the LIS (De Angelis, 2007). All imagery, and therefore geomorphology, was visualised at a variety of scales (up to the resolution of the ASTER or Landsat ETM+ band 8 imagery) in order to avoid bias within the mapping process and the band combinations were manipulated for optimum viewing (usually R, G, B = 6, 5, 2 on Landsat ETM+).

Each landform type was digitised in a separate shapefile (some as lines and some as polygons). Details of the process of landform identification are shown below in Table 3-1. Upon completion of mapping, vector layers were exported (.eps files) into Adobe Illustrator CS4 to compile the map. The map is intended for printing and visualisation at A1 size. While the initial identification of each different landform type was challenging, later in the mapping process it became apparent that each landform was often represented by a particular pattern of reflectance within the imagery. For example, eskers have sharp narrow crests and are composed of glacio-fluvial sediment, which reflects strongly as sinuous and/or fragmentary lines. While The Glacial Map of Canada (Prest *et al.*, 1968), the flowline map of Shaw *et al.* (2010) and a number of smaller scale geomorphological maps of the area (Mackay, 1963; Mackay and Matthews, 1973; Lemmen *et al.*, 1994; Duk-Rodkin and Lemmen, 2000; Kleman and Glasser, 2007) provided interesting comparisons to this mapping, it should be emphasised

that the mapping completed as part of this thesis was done in isolation and not influenced by previous work.

Landform type	*Map symbol*	*What does the mapping represent?*	*How was the landform identified on the imagery?*
Glacial lineations	Line	Crest line	Elongate bedforms, typical in groups with contrasting reflectance on either side of a linear crest line. Regular morphology and spacing often found between neighbouring bedforms.
Major moraine ridges	Polygon	Basal break of slope	Broadly linear ridges which reflect strongly along their crest line. In many cases reflectance contrasts sharply on one side of the crest line while a more gradual change in reflectance is seen on the other.
Hummocky topography	Polygon and line	Areal extent	Mottled topography in which some linearity can be distinguished but may initially appear as chaotically arranged. Strong contrasts in reflectance represent peaks and troughs.
Ribbed moraine	Polygon	Basal break of slope	Typically in groups with a regular morphological pattern of thick sinuous fingers, which contrast in their reflectance from the surrounding terrain.

Eskers	Line	Crest line	A strongly reflectant and clearly defined sinuous line owing to their composition from glacio-fluvial sands and gravels.
Palaeo-channels	Polygon	Channel edge	Branched networks of incised topography, the edges of which are defined by changes to a darker, contrasting reflectance on either side of the channel.
Lake strandlines	Line	Crest line	Sinuous, strongly reflectant lines, which mark the shorelines of former lakes. They contrast from the surrounding terrain and are often found to have contrasting terrain on either side of them.

Table 3-1: An explanation of the methods used to identify geomorphological features on Landsat ETM+/TM imagery.

Part 2: Reconstruction of ice stream activity

This section outlines the principles of the glacial inversion method (cf. Kleman and Borgström, 1996), which forms the theoretical foundation for the ice stream reconstruction presented in Chapter 5. This is followed by an outline of the Dyke *et al.* (2003) ice margin chronology and the process of embedding ice flow-sets into a temporal reconstruction of ice stream activity.

3.4 Glacial inversion method

The technique of glacial inversion uses the distribution of glacial geomorphology to reconstruct the geometry and dynamics of an ice sheet at different time steps (Kleman and Borgström, 1996). It assumes that discrete phases of ice flow produce groups of bedforms with similar morphology and orientation. Furthermore, the scheme classifies landforms according to their formative conditions e.g. ice velocity or the thermal state of the ice-bed interface (Kleman and

Borgström, 1996). Kleman *et al.* (2006) depict a five-dimensional model involving three-dimensional space, time (chronological control) and glaciological process (numerical ice sheet modelling) components. However, the scheme is based on a simple problem: how can we utilise the geomorphological record to reconstruct the behaviour of past ice sheets? The primary assumption of the glacial inversion method is that landforms produced by ice sheets can subsequently be used to reconstruct ice sheet behaviour (Figure 2-4). To aid consistency in this approach, Kleman *et al.* (1997) set out a number of fundamental building blocks upon which this assumption is based (see Table 3-2).

Assumption	*Examples*
i) The control on landform creation, preservation and destruction is the location of the phase boundary of water/ice at or under the ice-sheet (i.e. basal temperature).	Boulton (1972), Sugden (1977; 1978), Sollid and Sørbel (1994), Kleman *et al.* (2006), Kleman and Glasser (2007), Evans (2009).
ii) Basal sliding requires a thawed bed.	Weertman (1964).
iii) Lineations can only form if basal sliding occurs.	Clark *et al.* (2003), King *et al.* (2009).
iv) Lineations are created in alignment with the local flow and perpendicular to the ice-surface contours.	Boulton (1987), Clark (1993), Patterson and Hooke (1995), Clark *et al.* (2009), Stokes *et al.* (2011).
v) Frozen-bed conditions inhibit rearrangement of the subglacial landscape.	Kleman (1994), Kleman *et al.* (1994), Clark (1999).
vi) Regional deglaciation is always accompanied by the creation of a spatially coherent but metachronous system of meltwater features such as channels, eskers and deglacial lake shorelines.	Kleman (1992), Glasser *et al.* (1999), Dyke and Evans (2003), Greenwood *et al.* (2007).
vii) Eskers are formed in an inward-transgressive fashion inside a retreating ice front.	Warren and Ashley (1994), Clark and Walder (1994), Mäkinen (2003).

Table 3-2: The assumptions associated with the glacial inversion method as outlined by Kleman et al. (1997) along with published examples that use this technique.

3.5 Flow-sets

Boulton and Clark (1990a and b) introduced the concept of 'flow-sets' (also termed 'landform swarms' by Kleman and co-workers): landforms of a coherent and systematic pattern and which are interpreted to record distinct phases of ice flow (Clark, 1993, Clark *et al.*, 2000, Clark, 1999). Flow-sets can be identified based on the comparative morphology and spatial arrangement of bedforms. In particular, the parallel concordance of glacial lineations and

associated distribution of eskers and moraines. The process of flow-set construction is shown schematically in Figure 3-4.

Flow-sets can be classified as isochronous or time-transgressive. Isochronous flow-sets form quickly, with every bedform within the flow-sets being of approximately the same age. In contrast, time-transgressive flow-sets form slowly as the nearby ice margin steps back during deglaciation. The bedforms within a time-transgressive flow-set may therefore be of different ages having formed over a longer period of time than the group of bedforms in an isochronous flow-set (Clark, 1999; Kleman *et al.,* 2006). The bedforms within a time-transgressive flow-set are assumed to be younger, up-ice closer to the ice divide. The ice margin is also assumed to be located orthogonal to the ice flow orientation suggested by the geomorphology i.e. drumlins, MSGLs etc. (Clark *et al.,* 2000). The difference between isochronous and time-transgressive flow-sets is illustrated below in Figure 3-5.

The extraction of flow-sets from patchy and partially overprinted landform records, which are often present in areas occupied by palaeo-ice sheets, remains challenging. As such, Kleman and Borgström (1996), Kleman *et al.* (1997) and Kleman *et al.* (2006) assume that flow-sets which form under different conditions (e.g. during deglaciation or streaming flow) have different geomorphological signatures. Four types of flow-set are identified in the literature: wet-based deglacial, frozen-bed deglacial, ice stream or event (Kleman *et al.,* 2006). These categories provide the first stage of interpretation in the reconstruction of ice sheet and ice stream dynamics by indicating the conditions under which each flow-set formed. The characteristics of each type of flow-set will be discussed in turn below.

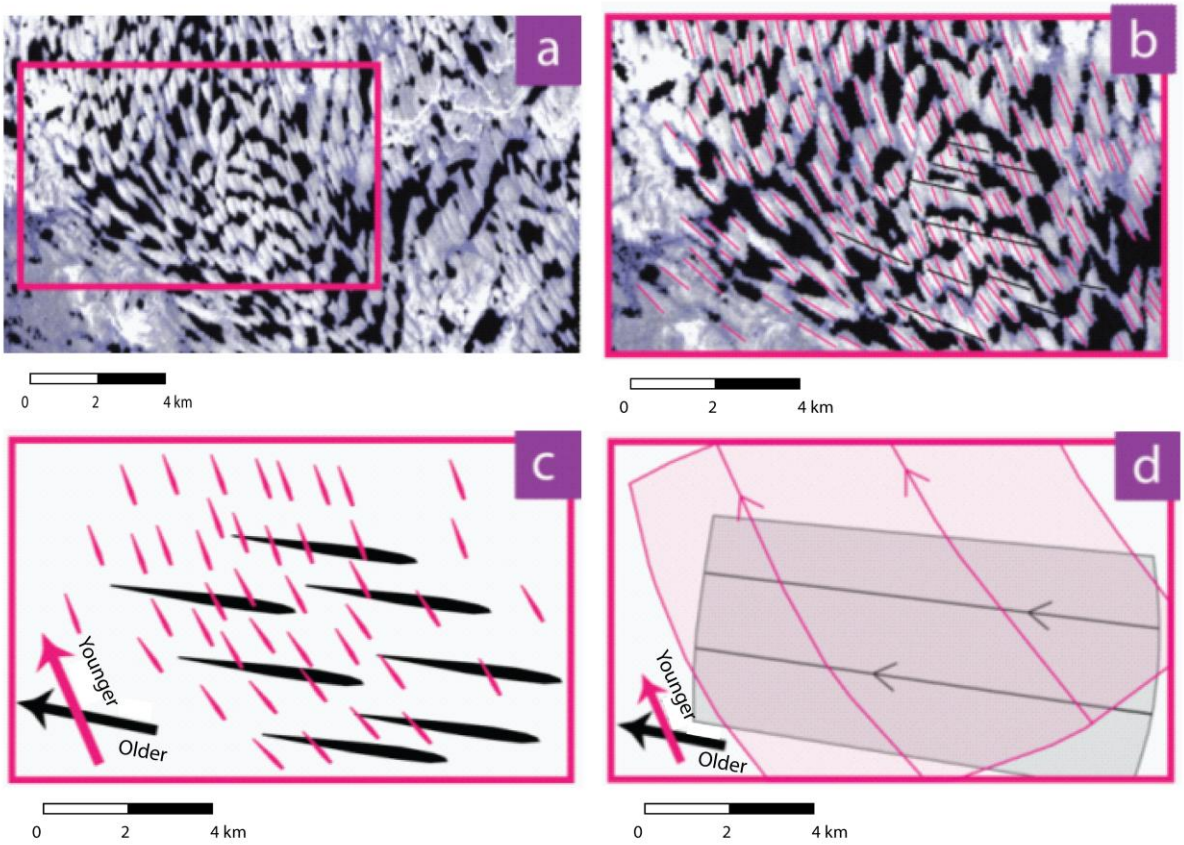

Figure 3-4: A schematic illustration of the methodology employed in the development of flow-sets. (a) an area of cross-cutting glacial lineations; (b) an example of the mapped geomorphology; (c) a schematic illustration of the mapped geomorphology and an indication of the relative age of the bedforms based on patterns of cross-cutting; (d) the flow-sets developed from the bedforms shown in (c) and their relative ages.

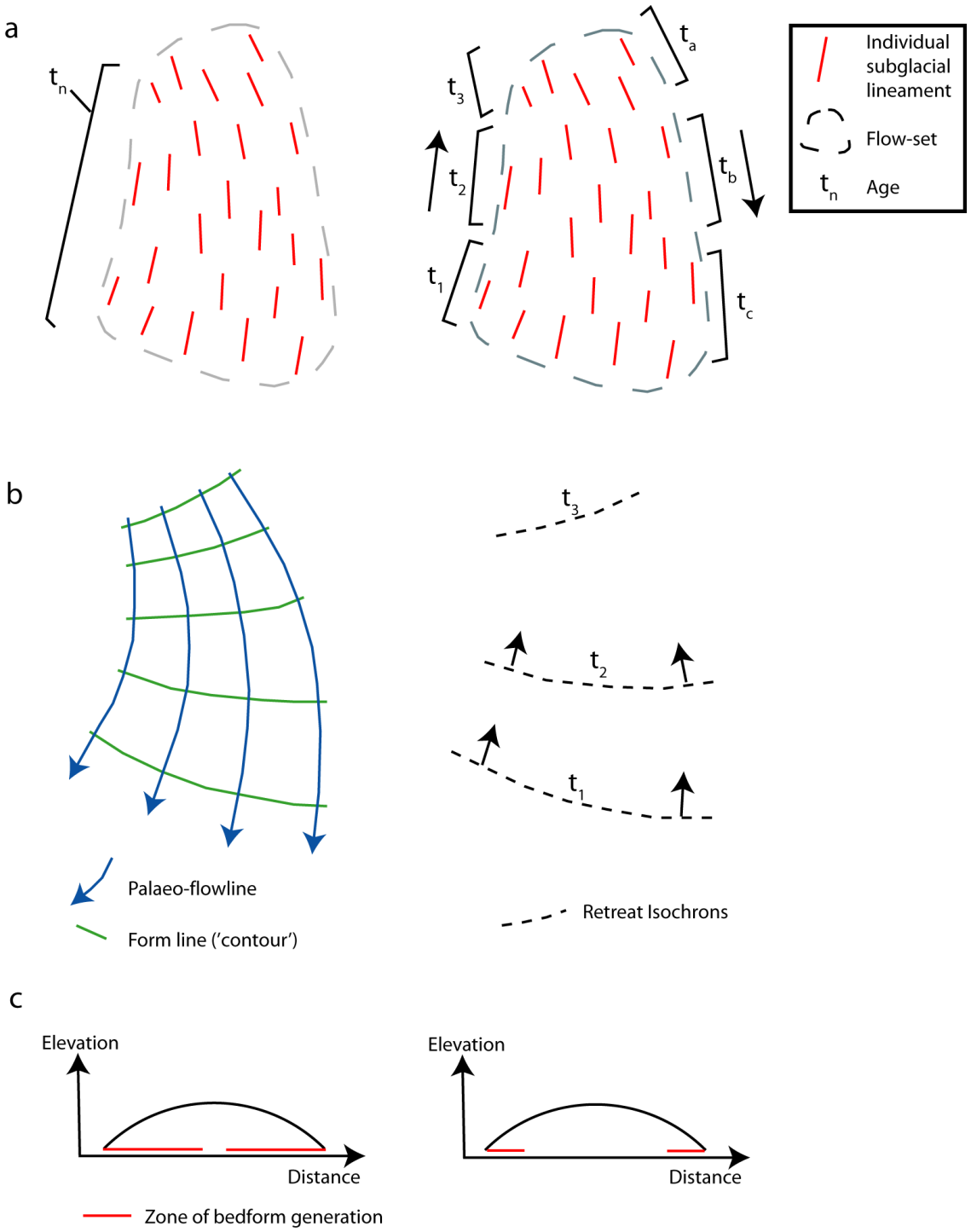

Figure 3-5: The identification of time-transgressive and isochronous flow-sets from glacial lineations. (a) A flow-set that may have formed isochronously (t_n) or time-transgressively from (t_1-t_3 or t_a-t_c). (b) Alternative modes of interpretation of such geomorphology. (c) Consequent presumptions about the glaciodynamic context, as either along extensive palaeo-flowlines or restricted to submarginal positions. Adapted from Clark (1999).

3.5.1 Wet based deglacial

Wet-based deglacial flow-sets are identified by an abundance of flow traces (i.e. glacial lineations), which are locally aligned with eskers and meltwater channels (Kleman *et al.,* 2006). Kleman *et al.* (2006) suggest that ribbed moraine may also be present if the wet-based zone

has resulted from thawing of a previously cold-based region. These flow-sets are associated with formation close to the ice margin owing to their formation under warm, wet-based conditions. They represent the inward-transgression of the wet-based zone of ice during deglaciation and may therefore be examples of flow-sets which formed time-transgressively as shown in Figure 3-5 (Kleman *et al.*, 2006).

3.5.2 Frozen-bed deglacial

This type of flow-set can be identified by the most subtle geomorphological signature of 'see-through' meltwater features imprinted on a relict glacial or non-glacial landscape which was presumably protected by cold-based ice (Kleman *et al.*, 2006). The relict surfaces may be printed on landscapes which provide evidence for older glacial events.

3.5.3 Ice stream

The geomorphological signature of ice stream activity has been well documented by Stokes and Clark (1999), Stokes and Clark (2002) and Kleman *et al.* (2006). Ice streams are typically associated with abundant, highly elongate flow traces (i.e. glacial lineations). Groups of these bedforms often have abrupt lateral margins and can be delimited by lateral shear margin moraines, see Table 2-1. Areas of convergent flow represent the transition from sheet flow to streaming flow. Land-terminating ice streams also typically have divergent terminal zones while those terminating in water do not (Stokes and Clark, 1999) (see Table 2-1). Figure 3-6 demonstrates the convergent and divergent nature of ice stream flow-sets.

3.5.4 Event

Event flow-sets are associated with sheet flow within an ice sheet. They can form many hundreds of kilometres inside the ice margin and have a geomorphological signature which includes flow traces without associated meltwater channels, or with superimposed meltwater traces, such as eskers, misaligned. This misalignment is a result of subsequent phases of deglaciation and retreat which occurred at different orientations.

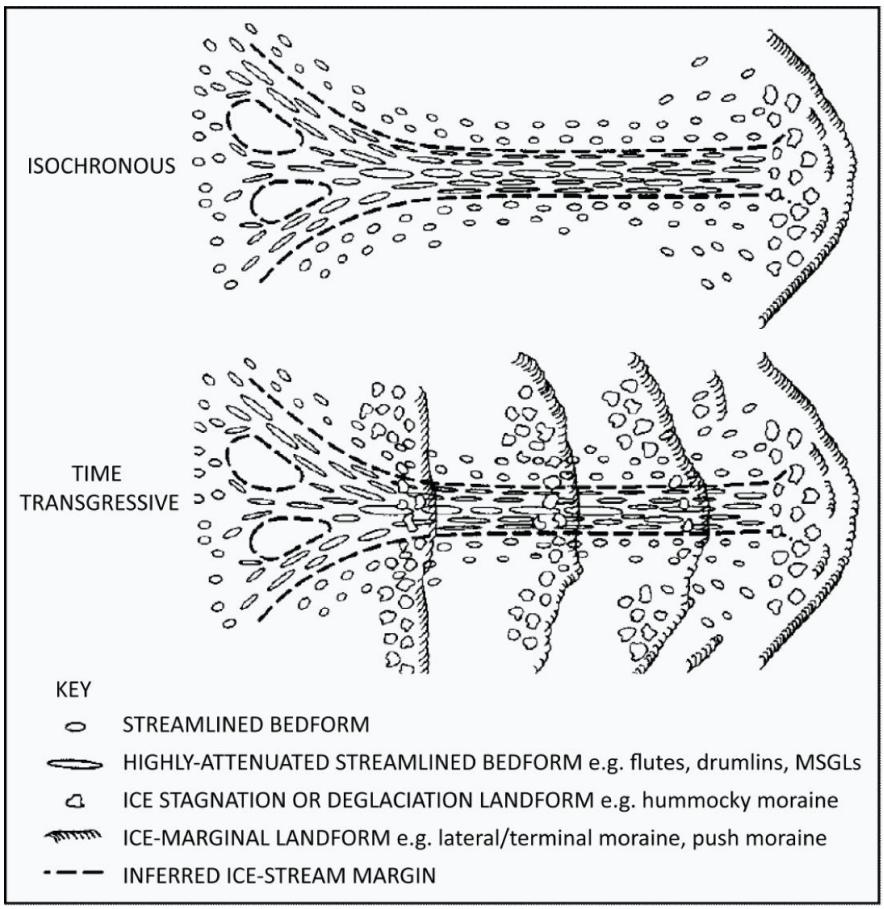

Figure 3-6: A schematic illustration of the criteria for the identification of ice stream activity as outlined in Table 3.2. Taken from Stokes and Clark (1999).

3.6 LIS margin chronology

From the LGM (21.4 cal. ka BP) to 5.75 cal. ka BP, the deglacial ice margins of the LIS at 32 timesteps have been published by Dyke *et al.* (2003) based on ~ 4000 radiocarbon dates from across North America. Dyke *et al.* (2003) is the most recent continental scale reconstruction of the LIS during the Late Wisconsinan and has therefore been used as a basis for the reconstruction of ice stream activity and pro-glacial lake evolution presented in this thesis. While all dates stated in this thesis include 2 decimal places, the dates have been directly quoted from Dyke *et al.* (2003). This includes dates in both radiocarbon and calendar years which were calibrated by Dyke *et al.* (2003) using the INTCAL98 calibration curve of Stuiver *et al.* (1998). The source material, location, and ID of each of the dates used in this thesis are presented in the Appendix. Dyke *et al.* (2003) note that the maximum error associated with the dates from which the ice margin reconstruction were derived is ± 400 years. However, Tarasov *et al.* (2012) suggest that this error should be increased to ± 1 timestep of the reconstruction. Despite this, Dyke *et al.* (2003) remains the most comprehensive reconstruction of LIS ice margins currently available. Therefore, while an extensive dating

campaign to update the margin chronology is still lacking, we favour Dyke *et al.* (2003) as the basis for the reconstructions presented in Chapters 5 and 6.

Not all of the 32 timesteps from Dyke *et al.* (2003) were used in this thesis. For the reconstruction of ice stream activity presented in Chapter 5, 20 timesteps were used spanning 21.4 cal. ka BP to 11.45 cal. ka BP (Table 3-3). This is because from 11.45 cal. ka BP, the study area shown in Chapter 1 became ice-free. However, in order to reconstruct the evolution of pro-glacial lakes more widely across the whole ice sheet (particularly with respect to Glacial Lake Agassiz) from their initial growth to demise, a further six timesteps were required. These additional timesteps extended the reconstruction of pro-glacial lakes to 8.45 cal. ka BP and are highlighted in Table 3.3. Dyke *et al.* (2003) report both radiocarbon and calendar years in their reconstructions. This thesis will henceforth refer to calendar years, which were calibrated using the INTCAL98 radiocarbon calibration curve of Stuiver *et al.* (1998) by Dyke *et al.* (2003). All margin positions are available as shapefiles from Dyke *et al.* (2003).

All uncertainties associated with the radiocarbon dates from Dyke et al. (2003) are stated in the Appendix. However, the uncertainty associated with each of the ice margins from Dyke et al. (2003) is harder to determine since each margin is based on several dates and the uncertainties associated with the ice margins are not stated in the publication of Dyke et al. (2003). However, it is suggested by Dyke (pers. comm.) and Tarasov (pers. comm.) that the uncertainty associated with each ice margin is in the order of one time-step (250-500 years). An element of quality control was established for the radiocarbon dates through consultation with the authors of Dyke *et al*. (2003). Dyke (pers. comm.) recommended the removal of 5 dates from the original Dyke *et al.* (2003) dataset due to worries about their source material, sample size or method of processing. However, it should be noted that the removal of these dates did not result in any changes to the ice margins (Dyke, pers. comm.).

Within the study area, 71 radiocarbon dates are available and have been compiled by Dyke *et al.* (2003) (see Chapter 5). While this appears to be a restricted number given the large size of the study area, the documentation of such a large number of landforms has also allowed for flow-sets to be relatively dated using cross-cutting flow patterns (cf. Boulton and Clark, 1990) with confidence in areas where absolute dates are not available (see Section 3.7). Furthermore, while a new regional dating campaign for this sector of the LIS was not within the scope of this research, several of the dates within the study area have queries associated with them. These queries were identified by Dyke *et al.* (2003) and subsequently eliminated from the reconstruction of ice stream activity. This also allowed for the identification of areas

of uncertainty within the margin chronology for this region. Such areas are discussed later in this thesis and modifications to the ice margins are made accordingly. Dyke *et al.* (2003) also note that problematic dates such as those from marl, freshwater shells, lake sediment with low organic carbon content, marine sediment, bulk samples with probable blended ages, and most deposit feeding molluscs from calcareous substrates, are excluded from the reconstruction. Many of these excluded dates were used in previous reconstructions (e.g. Dyke and Prest, 1987) but are now thought to yield ages that are too old. Unlike previous reconstructions, Dyke *et al.* (2003) also incorporate a regionally variable marine reservoir effect on dates from marine shells, rather than a uniform correction of 400 years across the continent (England and Furze, 2008; England *et al.*, 2009). Therefore, while the spatial pattern of LIS deglaciation is not dramatically dissimilar to that of Dyke and Prest (1987), a delay of 1000-2000 years is apparent.

^{14}C	Calendar
18.00	21.40
17.50	20.80
17.00	20.20
16.50	19.65
16.00	19.10
15.50	18.50
15.00	17.90
14.50	17.35
14.00	16.80
13.50	16.20
13.00	15.60
12.50	14.80
12.25	14.25
12.00	14.10
11.75	13.80
11.50	13.45
11.00	13.00
10.50	12.70
10.25	12.00
10.00	11.45
9.60	11.00
9.50	10.72
9.00	10.20
8.50	9.50
8.00	8.98
7.80	8.60
7.70	8.45

Table 3-3: The timesteps from Dyke et al. (2003) used in this thesis. The twenty timesteps shown in white are used in the reconstruction of ice stream activity presented in Chapter 5. The additional timesteps used in the reconstruction of pro-glacial lakes across the whole ice sheet (Chapter 6) are highlighted in blue.

Flow-sets were dated by two different means. The first, absolute dating, was possible where a radiocarbon date was available from material (e.g. organic matter) on top of the flow-set. This provided a minimum age before which the flow-set must have formed. It should be noted that this method assumes that the material from which the date was obtained was carefully sampled and not reworked (e.g. Stokes *et al.,* 2009). The maximum age of a flow-set was harder to obtain through absolute dating. However, in some cases, the geomorphological signature of a flow-set provided crucial evidence about the proximity of a flow-set to the ice

margin during formation. For example, wet-based deglacial flow-sets, which contain lineations with aligned eskers are likely to have formed close to the ice margin during deglaciation. As such, these flow-sets were placed close to the ice margin in the reconstruction and their maximum age was restricted by the retreat of the ice margin.

The relationship between cross-cutting bedforms also provided an important means of establishing a relatively chronology for the flow-sets. For example, a flow-set can be assigned an age relative to another by assuming that it is younger (or older) than the flow-set that it is superimposed on (or beneath) (Stokes *et al.*, 2009) (see Figure 3-4). Each flow-set was then embedded behind the ice margins of Dyke *et al.* (2003) in an up-ice position to create a reconstruction of flow-set activity throughout deglaciation. In order to fulfil the aims of this thesis, the ice stream flow-sets were then identified and patterns of ice stream activity were extrapolated between flow-sets to provide a regional ice stream history. This method has been employed by numerous authors including Stokes *et al.* (2009; 2006), De Angelis and Kleman (2007), Greenwood and Clark (2009a and b) and Clark *et al.* (2000), and is summarised in Figure 3-7.

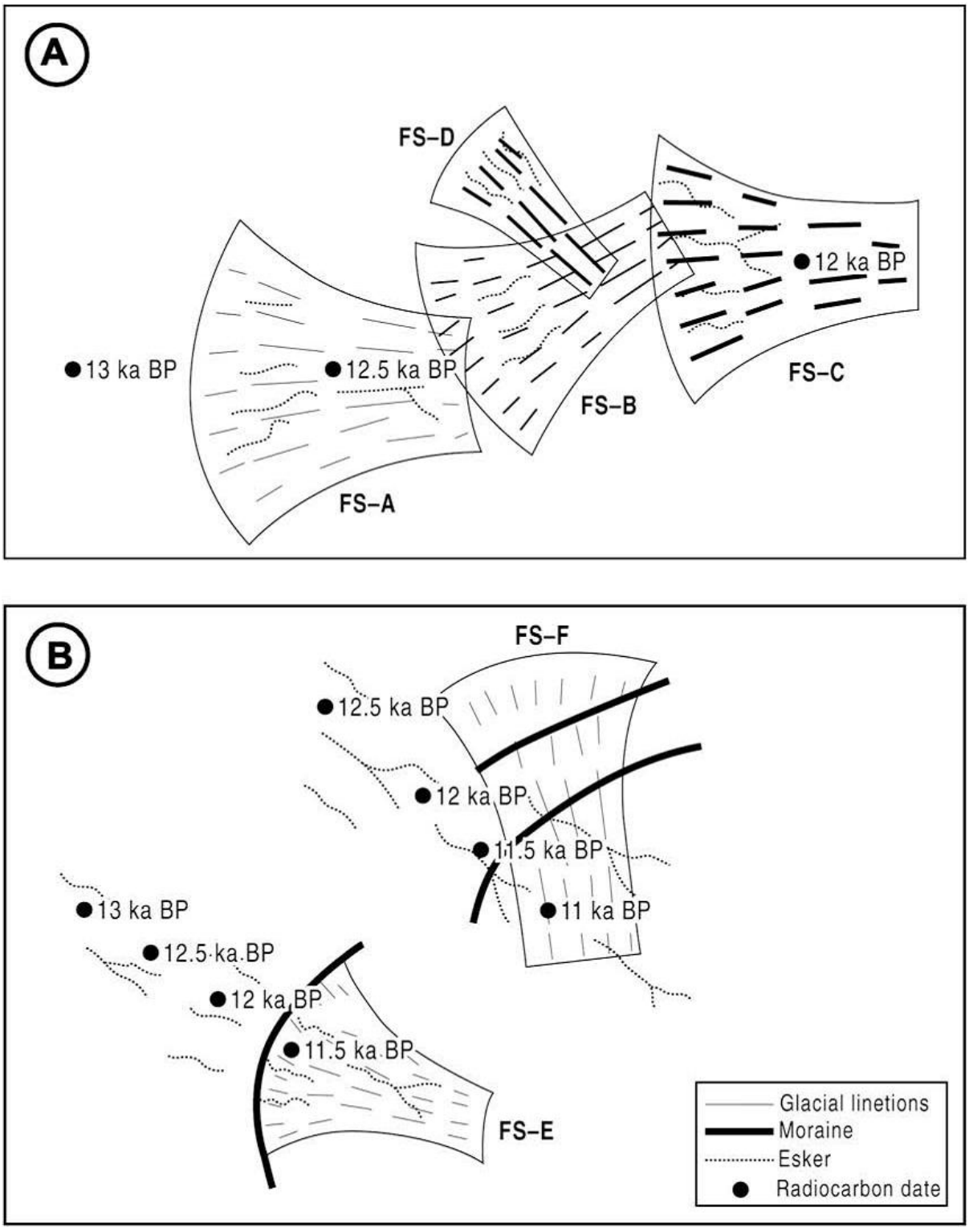

Figure 3-7: A schematic representation of the method employed in assigning minimum and maximum ages to flow-sets. In (A), the area occupied by flow-set A (FS-A) must have been deglaciated by 12.5 ka BP and so this provides a minimum age. Likewise, FS-C can be given a minimum age of 12 ka BP. FS-B is superimposed on FS-A and is cross-cut by FS-C and must therefore, have been generated at some time between 12.5 and 12 ka BP. FS-D must also have been generated between 12.5 and 12 ka BP but we also know that it is superimposed on FS-B and therefore, must be younger. We can reconstruct FS-A as a flow sometime before 12.5, followed by FS-B and then FS-D between 12.5 and 12; and then finally FS-C, before 12 ka BP. Determining whether FS-A was formed between 18 and 12.5 ka or 13 and 12.5 ka BP is more

difficult but if we know that the flow-set is a deglacial flow-set, from aligned eskers and moraines, then it is more likely that it formed during or immediately prior to deglaciation and close to the ice margin. This idea is illustrated in (B), where FS-E is a deglacial flow-set and would probably be bracketed to between 12 and 11.5 ka BP. In contrast, the event FS-F would probably be assigned a larger age bracket (e.g. 12.5-11 ka BP) because it does not fit with the esker and moraine patterns from deglaciation. Figure and caption taken from Stokes et al. (2009).

Part 3: Reconstruction of pro-glacial lakes

Previous attempts to reconstruct pro-glacial lakes have been limited to regional smaller-scale or local studies. Such studies have relied upon geomorphological evidence documented through field investigation or mapping campaigns via remotely sensed imagery (see Craig, 1985). Furthermore, determining the chronology of strandline formation often involves the extrapolation of dated strandlines across large areas. This thesis therefore approaches the reconstruction of pro-glacial lakes at a continental scale by manipulating a Digital Elevation Model (DEM) within in a Geographic Information System (GIS). Similar approaches to pro-glacial lake reconstruction have been carried out by Stokes and Clark (2004), Jansson (2003) and Lovell *et al.* (2012). This approach identifies areas where water could accumulate along the ice margin at 27 timesteps throughout Late Wisconsinan deglaciation. The various stages of this process will be elaborated upon below.

An initial reconstruction of pro-glacial lake evolution was produced for the north-west sector of the LIS. This required the shapefiles of the ice margins at each of the timesteps throughout deglaciation, and the DEM, to be cropped to the study area. However, computationally, in terms of time and resources, there was little difference between the production of a reconstruction for the north-west LIS and a reconstruction of pro-glacial lakes for the whole ice sheet. Scientifically, the connection of pro-glacial lakes along the north-west margin of the LIS to Glacial Lake Agassiz, further justified a continental-scale reconstruction of pro-glacial lakes. The continental-scale reconstruction also allows for changes in pro-glacial lake area and volume to be correlated with major climate oscillations during Late Wisconsinan deglaciation (e.g. the Younger Dryas). Furthermore, as discussed in Chapter 2, the drainage of Glacial Lake Agassiz has been implicated as a trigger for key climate events during deglaciation such as the Younger Dryas (cf. Fisher and Souch, 1998; Teller *et al.,* 2002; Teller *et al.,* 2005; Smith and Fisher, 1993). As such, it is important to consider the continental-scale patterns of freshwater routing throughout deglaciation. While ideally, the reconstruction of ice stream activity would have been extended across the whole ice sheet to match the scale of the pro-glacial lake reconstruction, this was not possible due to time constraints. In particular, the mapping from

which the ice stream reconstruction is derived, which already covers an area in excess of 800,000 km^2, would have had to be extended vastly.

3.7 Data input

3.7.1 Digital elevation models and ice margins

Four tiles of the GTOPOT30 DEM with a 900 m horizontal resolution were downloaded from the USGS website and mosaiced into a new raster in ArcGIS 9.3. Shapefiles of Laurentide Ice Sheet margins were taken from Dyke *et al.* (2003) at ~ 500 year intervals from the Last Glacial Maximum to 8.45 cal. ka BP. The ice margins from Dyke *et al.* (2003) were merged with the revised margins for the north-west sector of the LIS, as shown in Chapter 5.

Each of the shapefiles of the ice margins were then converted to individual raster files for each of the timesteps throughout deglaciation. The cell size of the raster files was set to 900 m to match the resolution of the DEM. The newly created rasterized ice margins were then given an elevation of 500 m. This height was in no way intended to imitate the true ice thickness but provided a barrier when flooding the DEM with water. By introducing a barrier against which water could pond, the method assumes that water cannot drain over the ice sheet. This assumption has previously been employed by Stokes and Clark (2004) and Jansson (2003) who also used a flooded DEM to derive pro-glacial lake extent. However, this thesis provides an advance on the method of both Stokes and Clark (2004) and Jansson (2003), because the reconstruction of pro-glacial lake evolution presented in Chapter 6 accounts for both lake bathymetry and Glacio-isostatic Adjustment (GIA). The inclusion of this additional data is discussed further below in Section 3.8.3.

3.7.2 Bathymetric data

Present day water bodies appear in the DEM as flat surfaces rather than as depressions in which water may have been able to accumulate during deglaciation. When a DEM is filled with water this means that water runs over the flat surfaces of the water bodies rather than accumulating. It was therefore necessary to incorporate the bathymetry of the two largest lakes into the DEM before flooding the DEM with water.

Nautical charts of Great Bear Lake and Great Slave Lake were obtained from the Canadian Hydrographic Service as .BSB files (compressed raster format). The charts were digitized as a series of points with associated water depths, and interpolated to produce two rasters of lake bathymetry, one for each lake. The lake bathymetry rasters were then added to the DEM at

each timestep to produce topography without major water bodies. Since the focus of this thesis remains on the north-west LIS, and because bathymetric data is not yet available for other major lake basins, bathymetric raster data was only created for the Great Bear Lake and Great Slave Lake (see Chapter 6). While many smaller lakes are also present in the study area, the bathymetry of which would ideally be incorporated into a reconstruction of pro-glacial lakes, time constraints did not allow for the collection of their bathymetric data.

3.7.3 ICE-5G

When reconstructing pro-glacial lakes, it is important to account for the effects of Glacio-isostatic Adjustment (GIA) and Solid Earth Deformation (SED) although previous studies have often ignored this (see Stokes and Clark, 2004 and Lovell *et al.,* 2012). Isostasy is the process by which deformation takes place in order to return the Earth to a state of equilibrium, while GIA, more specifically, is the temporal response of the solid Earth to mass redistribution from ice and water during a glacial cycle (Whitehouse, 2009). SED is the product of this redistribution at a fixed point in time.

During the Late Wisconsinan, crustal loading was particularly profound over North America due to the growth of major ice sheets. The growth and decay of these ice sheets further modified the pattern of SED. The Laurentide Ice Sheet (LIS) was comprised of three ice centres: Foxe/Baffin, Labrador and Keewatin (see Dyke and Prest, 1987) (see Chapter 2). The Keewatin dome to the west of Hudson Bay, was dominated by the thickest ice (3.3-4.3 km thick) and formed a 'horseshoe-shaped' rise trending north-west to south-east towards the Great Lakes (Tarasov and Peltier, 2003). Earliest retreat of the LIS during the Late Wisconsinan occurred along the terrestrially terminating southern and western margins (Dyke and Prest, 1987). By 13 cal. ka BP, the eastern LIS had also begun to retreat. However, deglaciation was much more rapid in the west than east (Bryson *et al.*, 1969, Dyke and Prest, 1987). As a result, the ice divides of the Keewatin dome migrated towards the east over the western Canadian Shield. Later in deglaciation, ice became centred on Hudson Bay and retreated towards this ice centre until its demise ~ 8.7 cal. ka BP (Carlson *et al.*, 2008, Dyke and Prest, 1987, Josenhans and Zevenhuizen, 1990).

This configuration of the LIS is reflected in the data from ICE-5G; a global ice sheet model, which provides a 3D topographic representation of the solid ice-age earth by incorporating SED (Peltier, 2004). In North America, ICE-5G indicates a depression of the solid earth across the area covered by the LIS. At 21 cal. ka BP the configuration described above caused the greatest deformation of the solid earth below the Keewatin dome, to the west of Hudson Bay (Figure

3-8). As deglaciation progressed, crustal rebound occurred as the ice thinned and ice divides migrated. This continued until the final time step of the reconstruction (8.45 cal. ka BP) (Figure 3-9). This deformation tilted the crust towards the centre of loading and therefore aided the formation of pro-glacial lakes. A correction for GIA was obtained for each timestep throughout deglaciation at a spatial resolution of 1 minute from ICE-5G (see Peltier, 2004) and added to the present day topography from GTOPO30 to produce a modified 'ice-age' DEM at 20 timesteps throughout deglaciation.

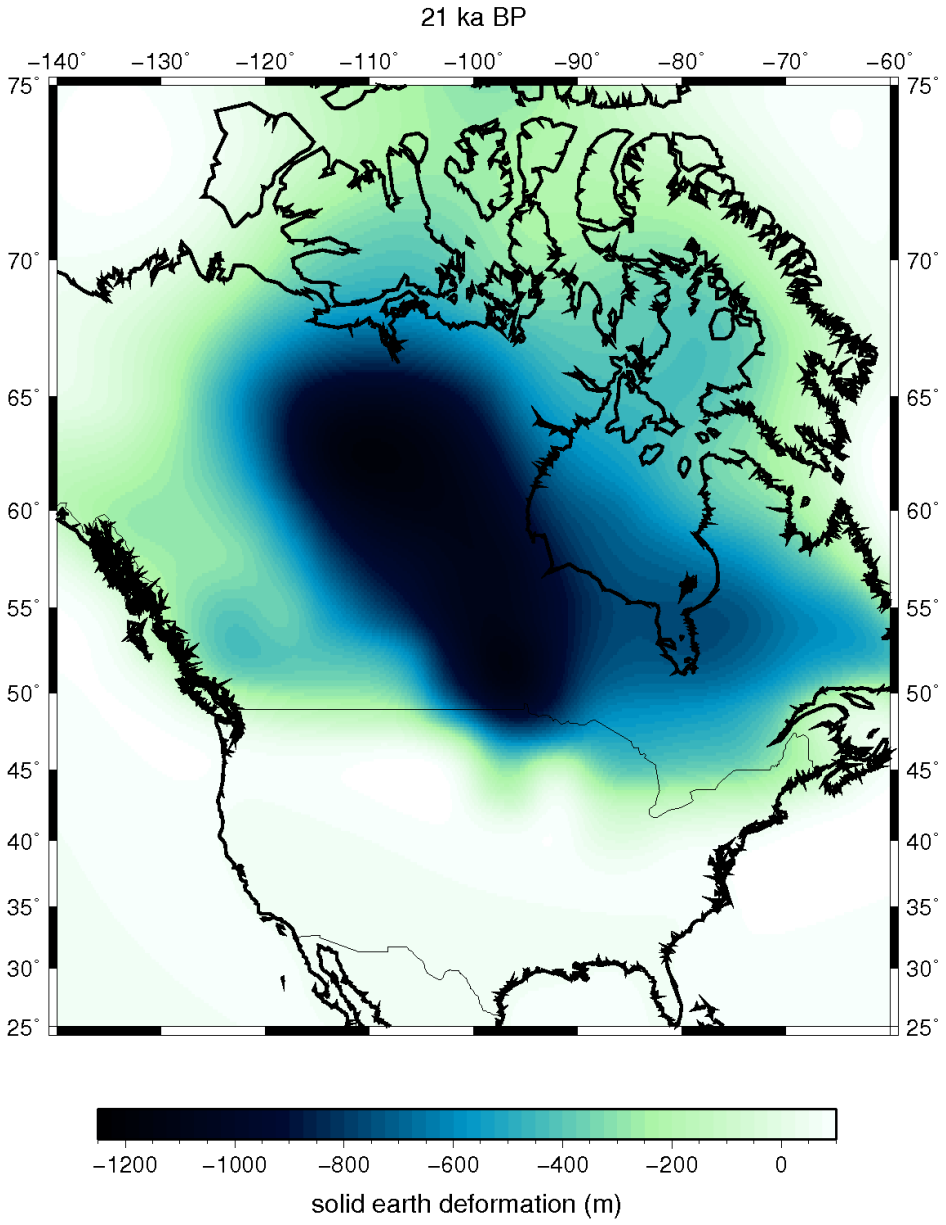

Figure 3-8: The record of solid earth deformation at 21 cal. ka BP according to ICE-5G. Deformation was centred west of Hudson Bay and, at its maximum, exceeded 1000 m. The data was plotted from ICE-5G.

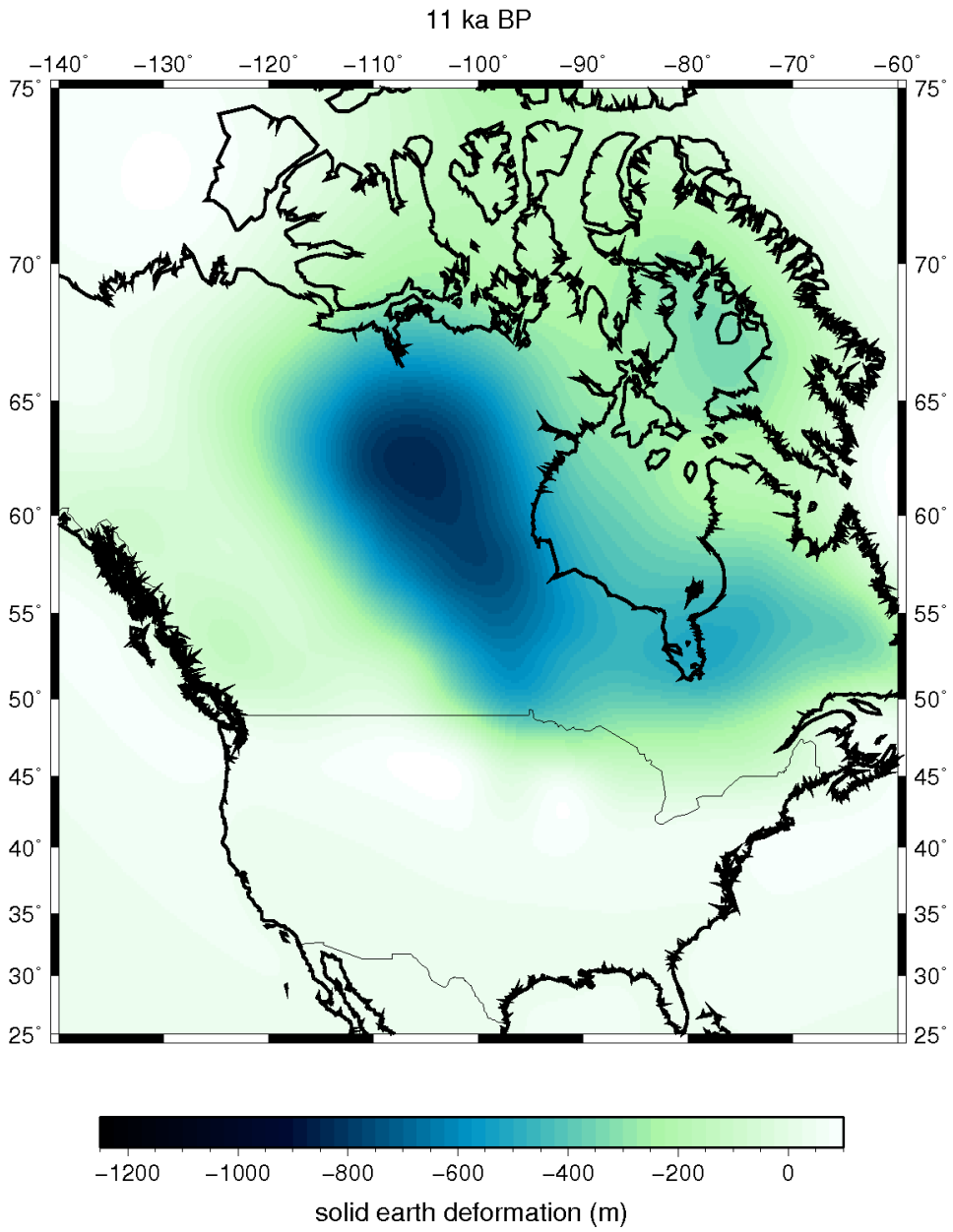

Figure 3-9: The record of solid earth deformation at 11 cal. ka BP according to ICE-5G. The maximum SED remained centred west of Hudson Bay but the area of deformation was both horizontally and vertically smaller than at 21 cal. ka BP (Figure 3-8). The data was plotted from ICE-5G.

3.8 Data processing in ArcGIS

Following the addition of lake bathymetry data for Great Bear Lake and Great Slave Lake to the DEM, the ICE-5G representations of Late Wisconsinan deglacial SED at each timestep were added to a new copy of the DEM. The newly rasterized ice margins were then mosaicked to the corresponding DEMs and the resulting DEMs were termed the 'ice-age' DEMs. An example of an 'ice-age' DEM is shown below in Figure 3-10.

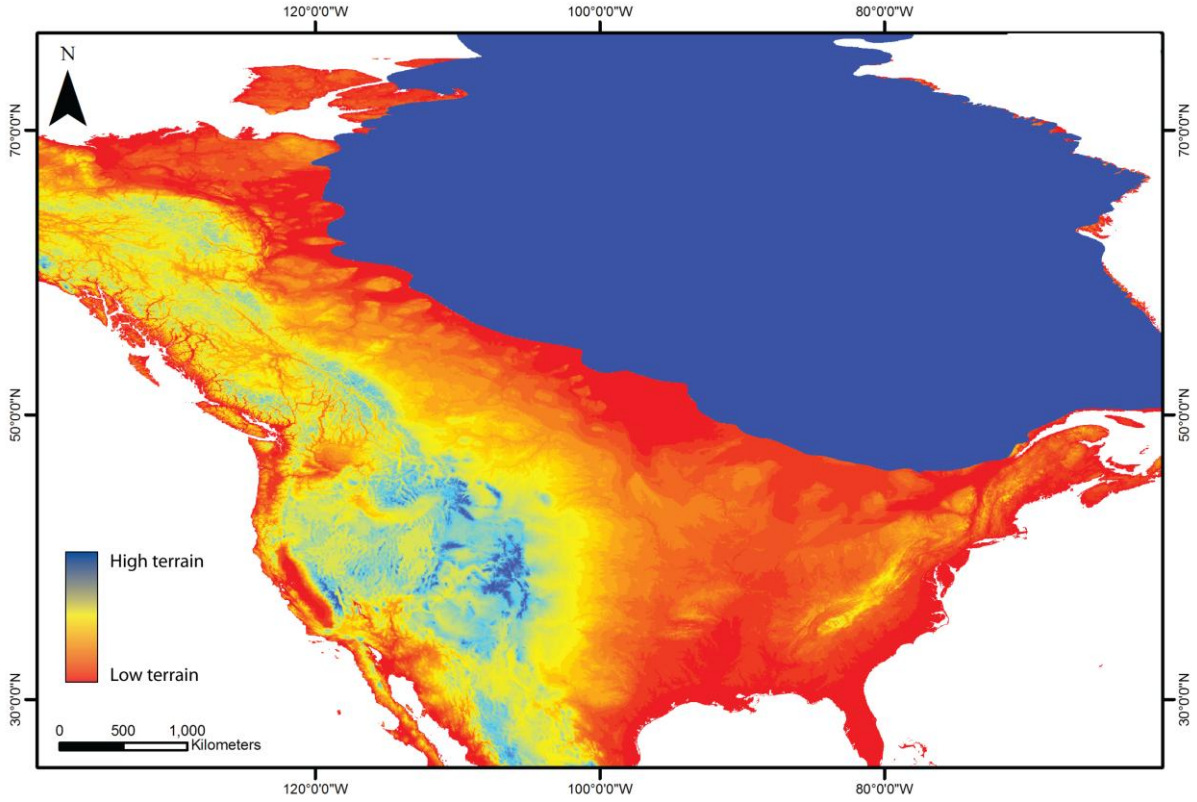

Figure 3-10: An example of an 'ice-age' DEM. The blue mass in the top-right of the image represents the elevated, rasterized ice sheet taken from Dyke et al. (2003) at 12.70 cal. ka BP. The ice was elevated to provide a barrier against which water could pond when the DEM was flooded. The low terrain around the periphery of the ice is where the water gathered to form pro-glacial lakes.

The 'ice-age' DEMs were then flooded with water using the Hydrology tools in Arc Toolbox to create a DEM which included areas where water could accumulate. In order to isolate the areas of water accumulation, the 'ice-age' DEMs were subtracted from the flooded DEMs at each of the respective timesteps. This produced a series of rasters of the flooded areas which were then converted to shapefiles. A definition query was set up in order to isolate the ponded areas that were in contact with the ice margin (i.e. the ice marginal lakes) and the queried attributes were copied to new shapefiles. The attributes within this final set of shapefiles were assumed to represent the maximum possible extent of pro-glacial lakes at each timestep during deglaciation. From these shapefiles, the area of the lakes at each timestep was calculated. However, in order to calculate the volume of the lakes it was necessary to develop the methodology further. Lake volume was required in order to draw comparisons with previously published lake volumes (see Leverington *et al.,* 2000; Teller *et al.,* 2005). However, since previous reconstructions have not accounted for SED, volume data also allowed for an assessment of the influence of SED on lake evolution.

Within Arc Toolbox, 3D Analyst provides a means of calculating the volume of a raster below a given value; in this case, the elevation. Alternatively, the default setting allows calculation of a raster's volume below the maximum altitude. This function is therefore ideal if the value below which you wish to calculate volume is constant throughout the raster. However, since the elevation of the lakes around the ice margin varies markedly, this method could not be employed. Therefore, at each timestep, the individual attributes/lakes within the lake shapefiles were extracted to new shapefiles i.e. with one attribute in each file. These files were then used as masks to extract the bathymetry of the pro-glacial lakes from the 'ice-age' DEM; again with one lake in each file (see Figure 3-10). The volume of these individual lakes was then calculated below the maximum value within each file using 3D Analyst. The volumes were exported to text files and a total lake volume for each timestep was achieved by summing the volume of all the individual lakes in each timestep. The extraction of the lake shapefiles from the 'ice-age' DEM also allowed for effective cartographic visualisation of lake bathymetry at each timestep. The process outlined in Section 3.9 is summarised in Figure 3-11 and Figure 3-12 below.

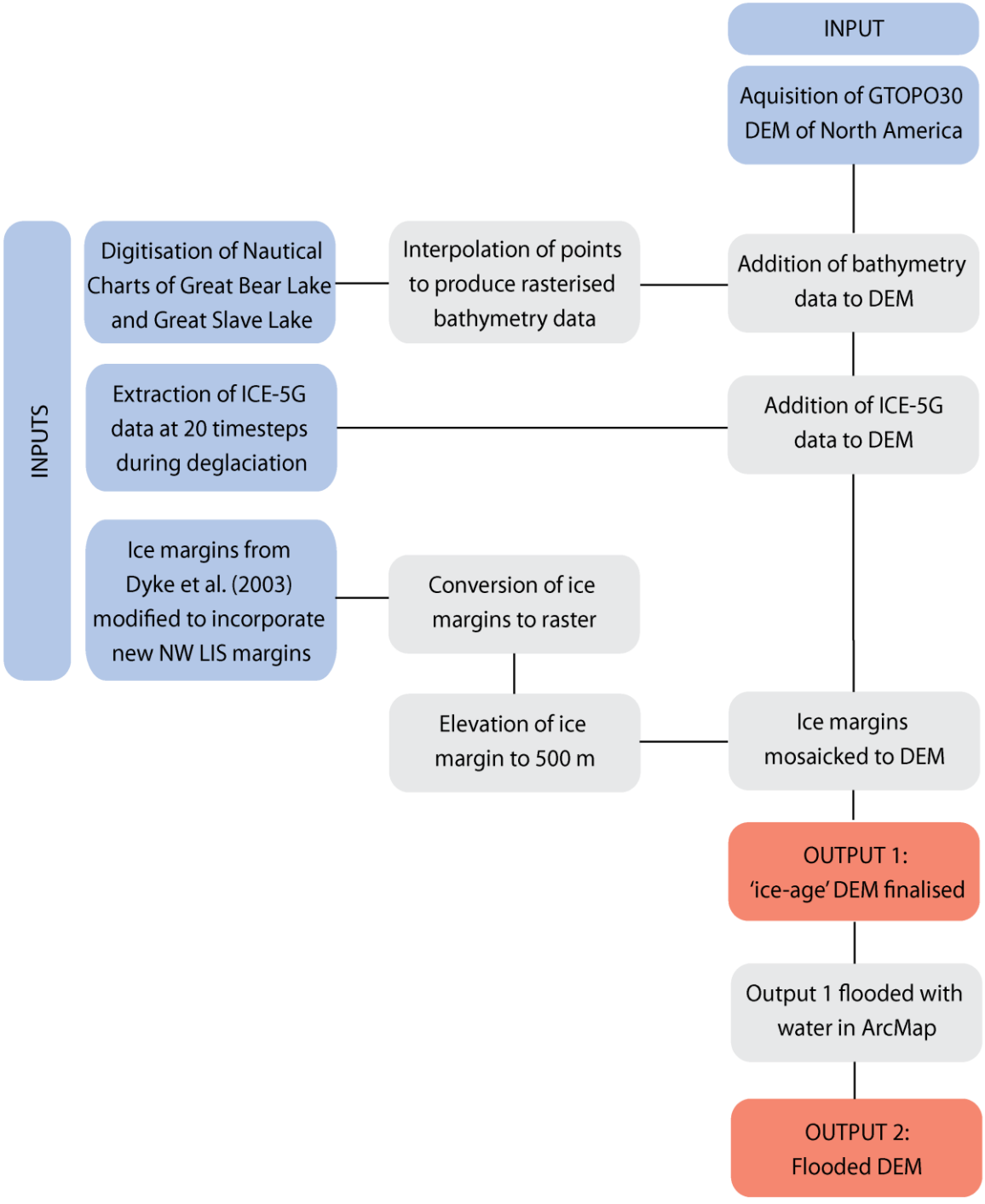

Figure 3-11: The method employed in generating the 'ice-age' DEMs and the flooded DEM. The process was repeated for each of the twenty timesteps at which pro-glacial lakes are reconstructed.

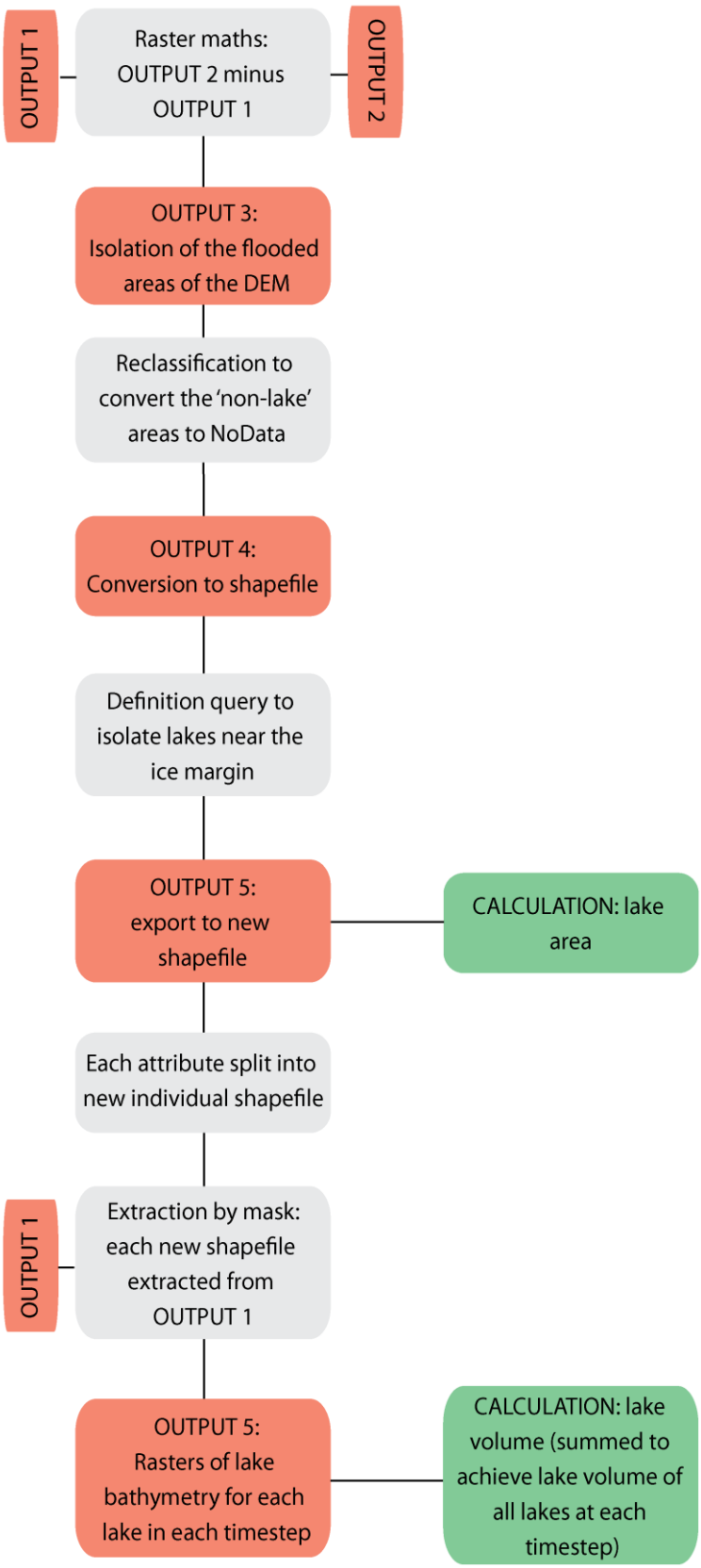

Figure 3-12: The method employed in isolating pro-glacial lakes in order to subsequently calculate lake area and volume. The process was repeated for each of the twenty timesteps at which pro-glacial lakes are reconstructed.

3.9 Summary

- Geomorphological mapping provides the foundations for the reconstruction of ice stream dynamics. Mapping was carried out remotely using a range of spaceborne and airborne imagery. This is advantageous because it allows for rapid and systematic coverage of large areas at a variety of scales.
- Six types of bedforms were mapped. Moraine ridges, ribbed moraine, hummocky moraine and large meltwater channels were mapped as polygon features while eskers and glacial lineations were mapped as polylines.
- Flow-sets represent groups of bedforms with a similar morphology and orientation which formed during the same phase of ice flow. Four different types of flow-sets are identified in the literature; ice stream, wet based deglacial and event flow-sets (Kleman *et al.*, 2006). Each type can be identified by specific geomorphological criteria. In particular, the geomorphological signature associated with areas of palaeo-ice streaming are well documented in the literature (Stokes and Clark, 1999).
- The Late Wisconsinan deglacial ice margins of the LIS have been compiled by Dyke *et al.* (2003) from ~ 4000 radiocarbon dates from across northern North America. 71 of these dates are located within the study area.
- The age of each flow-set was established by one of two means: 1), absolute dating where radiocarbon dates were located directly on top of a flow-set, or 2), relative dating based on the cross-cutting relationships of bedforms.
- Based on their age, flow-sets were embedded behind the ice margins from Dyke *et al.* (2003) at twenty timesteps throughout Late Wisconsinan deglaciation to establish the location and timing of ice streaming in the north-west LIS.
- A DEM of North-America was flooded with water using ArcGIS to establish the location of pro-glacial lakes along the mainland LIS margin. Prior to flooding, the DEM was modified by adding lake bathymetry data and an ICE-5G representation of SED to create topography comparable to that of North America at the various timesteps during the Late Wisconsinan.

Chapter 4: Geomorphological mapping

4.1 Introduction

This chapter documents the results of glacial geomorphological mapping in the study area. A total of 94,780 landforms were mapped and six landform types were identified: lineations, major moraine ridges, hummocky topography, ribbed moraine, eskers and large meltwater channels. The map of the glacial geomorphology of the north-west sector of the LIS, to which reference is made throughout this chapter, can be found, folded and on a CD inside the back cover of this thesis and is labelled as Figure 4-1. The map, and contents of this chapter, are published in Brown *et al.* (2011). As previously highlighted, this new map (Figure 4-1) is distinct from previous maps such as The Glacial Map of Canada (Prest *et al.,* 1968), the flowline map of Shaw *et al*. (2010) and other localised maps of the area, because it documents individual bedforms within the study area rather than generalised bedform or ice flow patterns. It is therefore possible to identify regions of cross-cutting bedforms which are crucial to the provision of a realistic reconstruction of ice stream activity which includes subtle but complex switches in ice flow orientation. Each landform type is discussed in turn and examples of the imagery from which the mapping was carried out are provided, see Figure 4.2. The location of the landform examples found in this chapter, are shown on Figure 4-2.

The mapped landforms provide information about ice flow orientation and dynamics, meltwater/lake drainage, and ice margin geometry. They represent the fundamental building blocks of the glacial inversion method as discussed in Chapter 3 (Kleman and Borgström, 1996, Kleman *et al.*, 2006). Although not the only approach, geomorphological mapping is an effective means by which to understand ice sheet behaviour based on the detailed spatial arrangement of landforms. The map will form the basis of the regional reconstruction of ice sheet flow patterns presented in Chapter 5.

Figure 4-1: See map and CD at back of thesis.

Figure 4-2: The location of the mapped area in the Northwest Territories and Nunavut, Canada (highlighted by the red line). All locations noted in this chapter are labelled on this figure. The black numbered boxes indicate the location of each of the figures within the study area.

4.2 Lineations

Streamlined lineations are abundant throughout the study area and range from oval-shaped hills (drumlins) to more elongate mega-scale lineations (Figure 4-3). Mean length/width ratios (elongation) of between 2:1 and 3:1 are suggested by Menzies (1979) to be characteristic of drumlin morphology. In contrast, mega-scale lineations are ridges which form in subglacial sediment, and can be longitudinally continuous for many tens of kilometres (Clark *et al.*, 2003, Clark, 1993). While Clark *et al.* (2003) and Stokes *et al.* (2012) suggest that bedforms such as these are the product of a groove-plough mechanism in which the basal ice moulds and deforms subglacial sediment, Shaw *et al.* (1984: 1987) favour a meltwater origin for drumlins/glacial lineations. Shaw *et al.* (1984: 1987: 1989) suggest that drumlins/glacial lineations result from catastrophic subglacial meltwater floods. However, we reject this hypothesis on the basis that it cannot explain the diversity of bedforms present within the study area. Furthermore, the complex arrangement of cross-cutting bedforms cannot be explained by a catastrophic flood hypothesis in which a relatively consistent flow orientation might be expected (Evans *et al.,* 2006: Ó Cofaigh *et al.,* 2010).

Lineations occupy the opposite end of the lineation landform continuum to drumlins, being much greater in length and elongation (Spagnolo *et al.,* 2012). Where landforms exhibit moderate elongation it is often challenging to distinguish drumlins from mega-scale lineations, see Figure 4-4 and Figure 4-5. For the purposes of the mapping, all streamlined bedforms with long-axes aligned parallel to the direction of ice flow have therefore been grouped together as one unit: glacial lineations.

Within the study area, lineations are up to 50 km in length (see Figure 4-3). Cross-cutting lineations are also present, as shown in Figure 4-6. The spatial distribution of the 88,536 lineations is not uniform across the study area. Lineations are abundant along the Amundsen Gulf Coast and appear in smaller groups of varying orientations north of Great Bear Lake (see the map). Conversely, higher ground remains free of lineations, possibly due to the development of cold-based ice in these areas. The most elongate landforms are identified west of Great Bear Lake roughly following the current path of the Mackenzie River in a broad zone ~ 100 km wide. Previous work on palaeo-ice sheets (e.g. Hart, 1999, Stokes and Clark, 2002) and observations from the beds of contemporary ice streams indicate that bedform elongation is related to ice velocity (King *et al.*, 2009). Areas of highly attenuated landforms are therefore assumed to delimit areas of fast ice flow within the LIS (Clark, 1993, Hart, 1999, King *et al.*, 2009, Stokes and Clark, 2002).

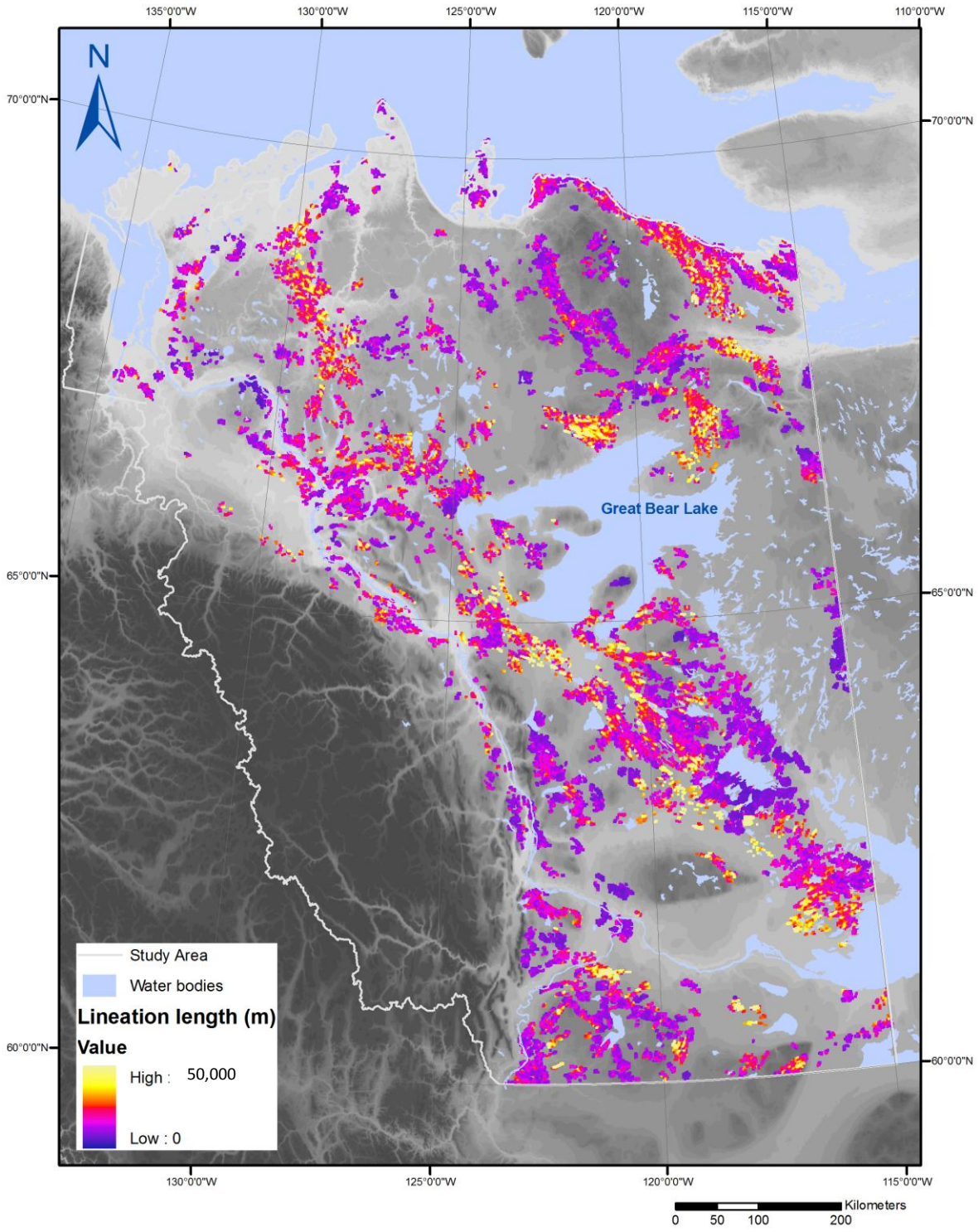

Figure 4-3: The length of glacial lineations within the study area. Each glacial lineation is shaded according to its length. The longest bedforms are shown in orange/yellow colours and are located west of Great Bear Lake, along the Amundsen Gulf coast, in the vicinity of the Anderson River, in a small corridor on the north-western shore of Great Bear Lake.

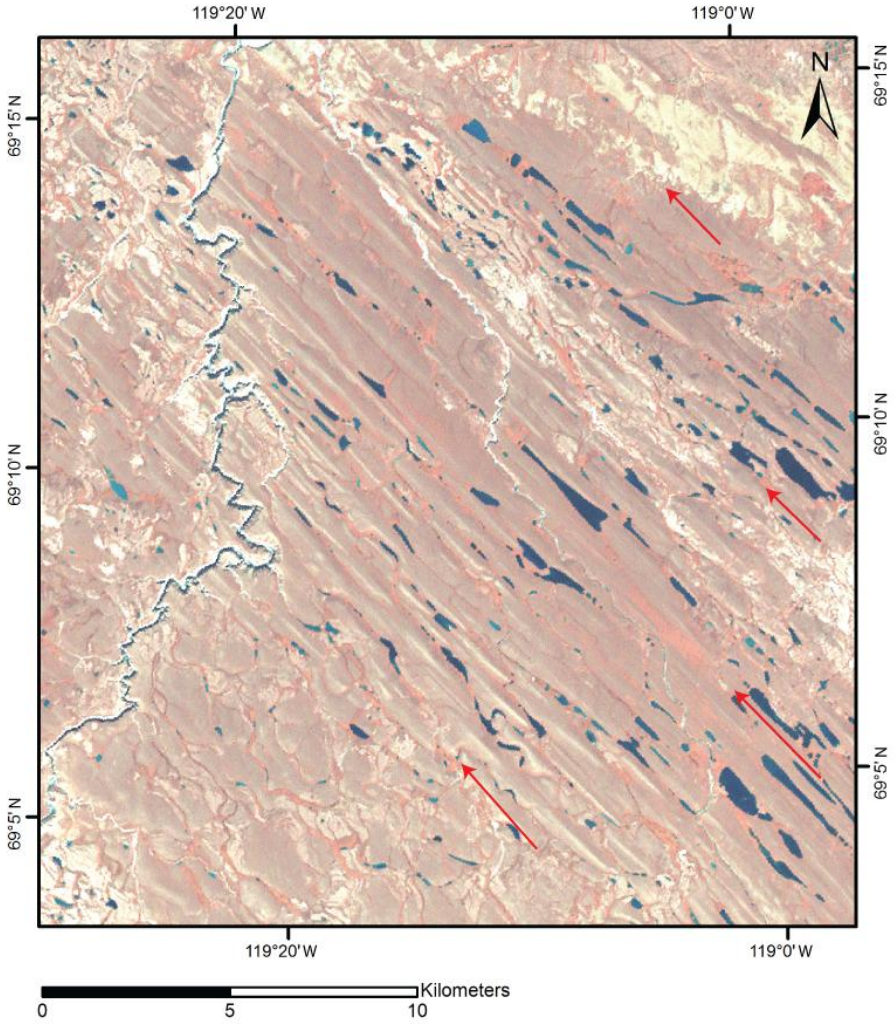

Figure 4-4: Landsat ETM+ scene (band combinations R, G, B: 4, 3, 2) showing elongate drumlinised landforms up to 4 km long along the Arctic Ocean coast. The red arrows indicate the orientation of the drumlins. Location shown on Figure 4-2.

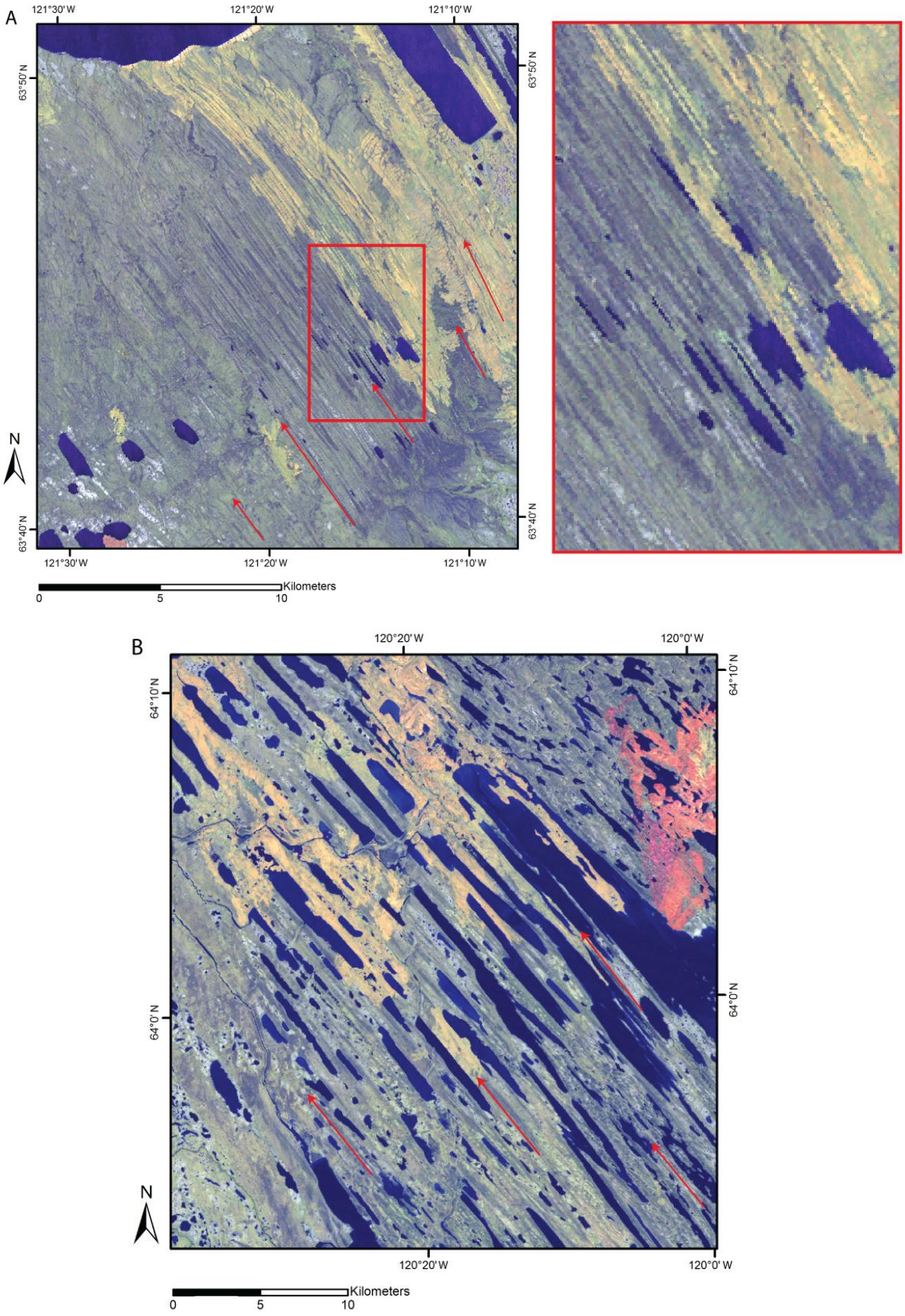

Figure 4-5: Two examples of mega-scale lineations found to the west of Great Bear Lake (Landsat ETM+ band combination R, G, B = 6, 5, 2). The changes in colour across the images are due to differences in spectral characteristics from different land covers. (a) narrow, highly elongate features which show a high degree of parallel conformity and are very closely spaced. (b) broader elongate bedforms interspersed with lakes. Bedform density is lower than in (a).

The red arrows indicate the orientation of the mega-scale lineations and also their parallel conformity. Location shown on Figure 4-2.

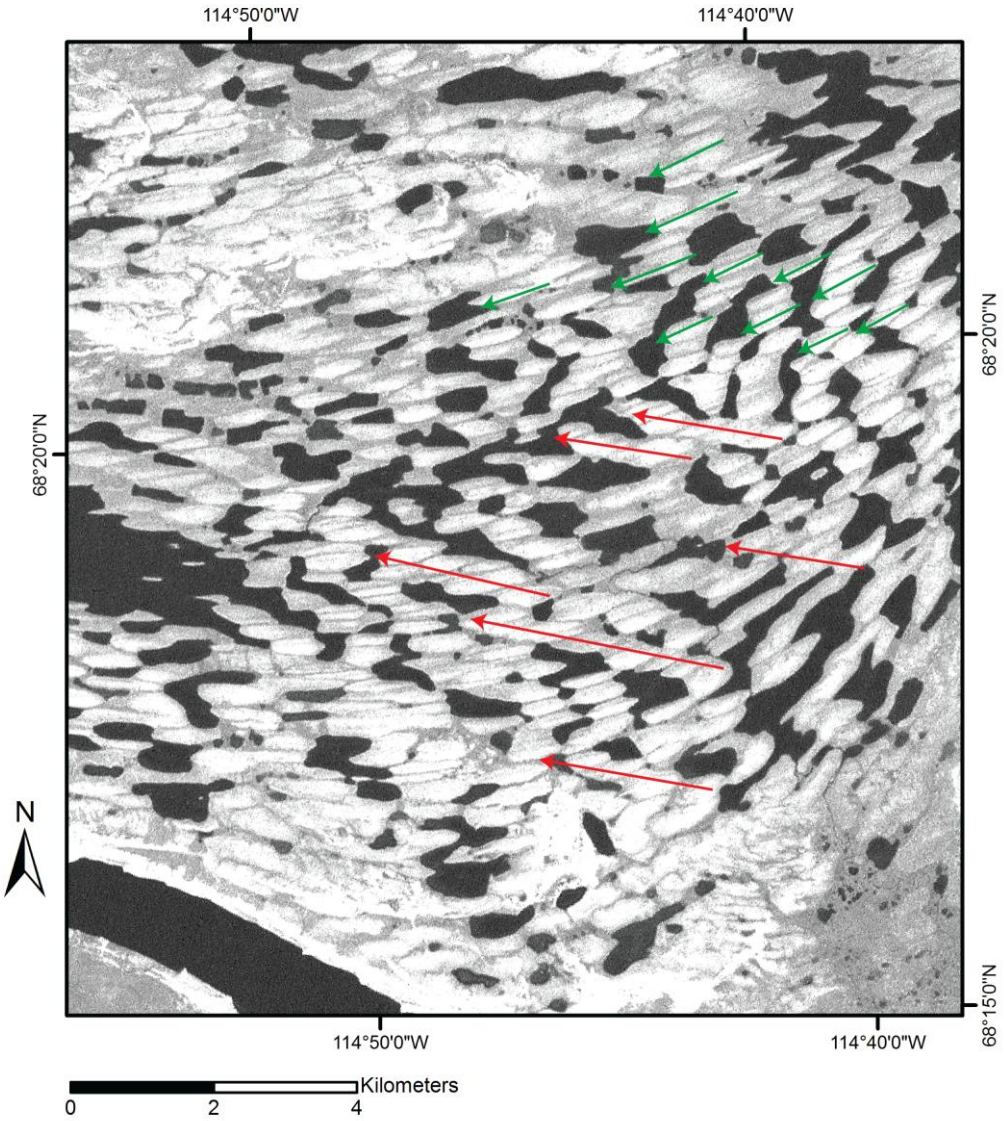

Figure 4-6: Cross-cutting bedforms along the Amundsen Gulf Coast as visualised on Landsat ETM+, band 8. Successive generations of ice flow are indicated by cross-cutting drumlins (lineations). Location shown on Figure 4-2.

4.3 Major moraine ridges

Major moraine ridges occur as curvilinear ridges both parallel and perpendicular to lineations (Figure 4-7 Figure 4-8). Although moraine ridges more commonly overprint lineations, ridges with overprinted lineations are also present. The mapped moraine ridges are typically 1-2 km wide and can be tens of kilometres long with clearly visible crestlines (Figure 4-8). 734 moraine ridges have been mapped throughout the study area but it is acknowledged that much smaller ridges probably exist that have not been mapped at this scale. At least 50% of these moraines were originally mapped by Prest *et al.* (1968) on the Glacial Map of Canada and were later

mapped by Dyke and Prest (1987). A large group of closely spaced moraine ridges has been mapped along the Beaufort Sea coast which are known locally as the Eskimo Lakes (Mackay, 1956).

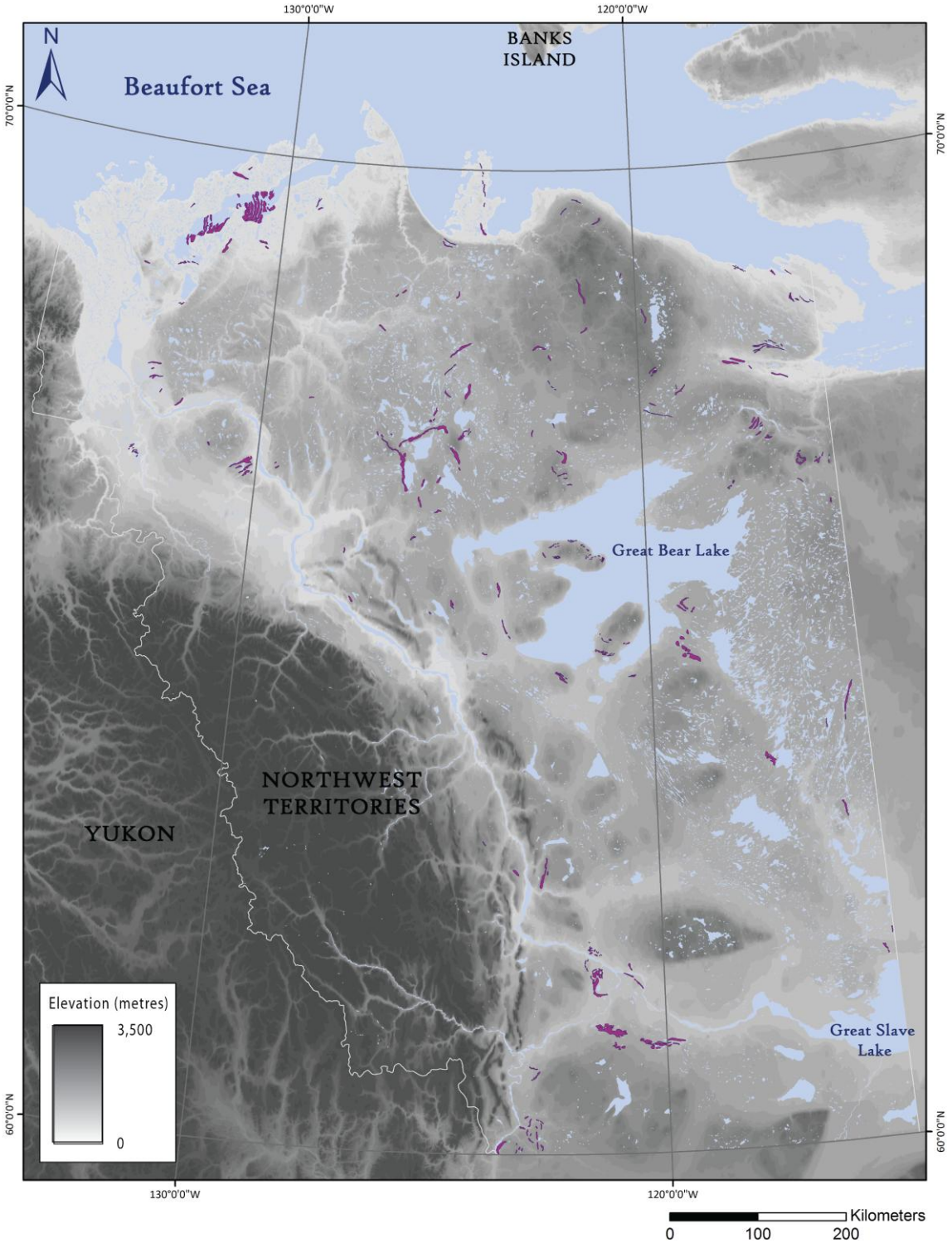

Figure 4-7: The distribution of major moraine ridges (purple) in the study area.

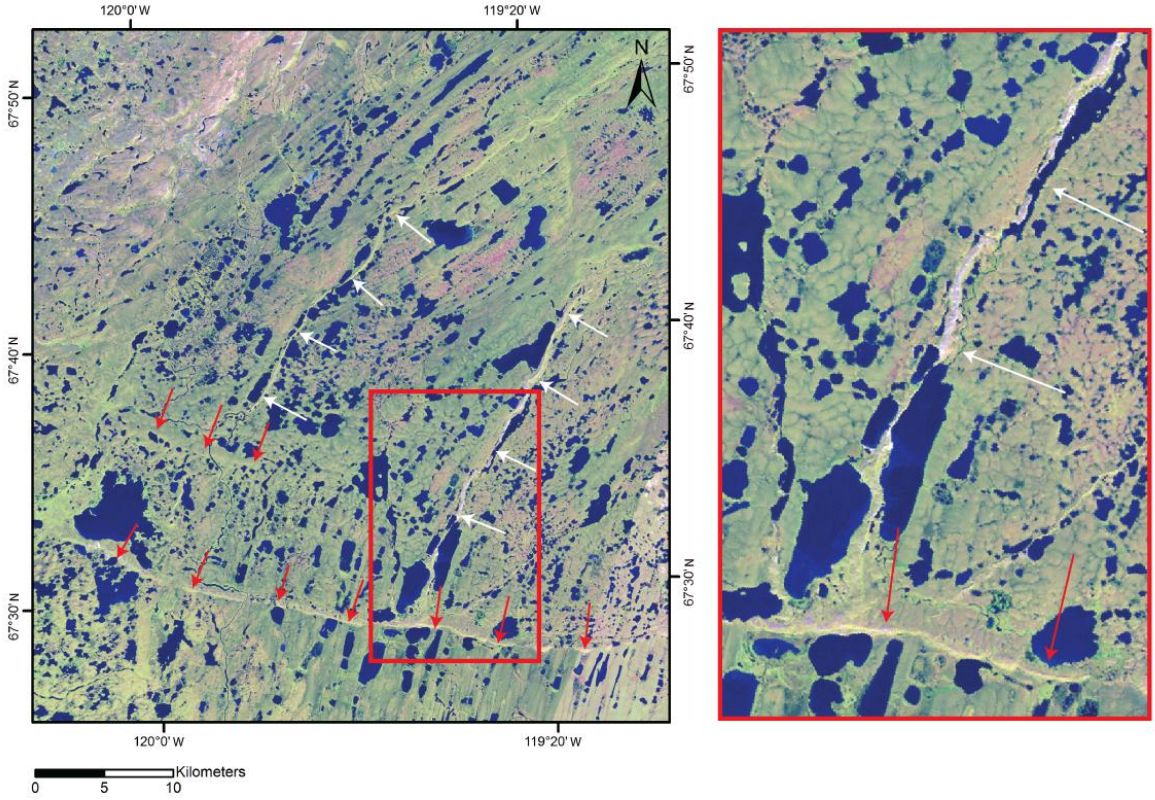

Figure 4-8: A moraine ridge trending east to west (red arrows) across a Landsat ETM+ image (band combination R, G, B = 6, 5, 2). On the western side of the image, a further shorter ridge is also visible to the north of the main ridge. Eskers also run from north to south (white arrows), perpendicular to the moraine ridges, and are surrounded by numerous lineations. The red box provides a closer view of a section of the imagery. Aside from the large esker trending north to south, a smaller esker is also visible at 45° to the main moraine ridge on the closer image. Location shown on Figure 4-2.

4.4 Hummocky topography

Hummocky topography is extensive throughout the northern part of the study area and is identified as an irregular undulating surface of peaks, and often, ponded depressions, see Figure 4-9. While visualisation of localised areas of hummocky topography reveals a largely chaotic arrangement, coarser scale visualisation often allows for the identification of regional patterns of linear organisation in some locations (cf. Dyke and Savelle, 2000). While some workers argue that hummocky topography is indicative of regional ice stagnation and down-wasting (Andersson, 1998), it is also suggested that it represents a series of complex ridges which formed during the retreat of an active ice margin (see Dyke and Savelle, 2000, Eyles *et al.*, 1999, Munro and Shaw, 1997, Munro-Stasiuk and Sjogren, 1999). Similar ridges have been reported by Storrar and Stokes (2007) on Victoria Island. Of particular note is the Melville Hills moraine complex, see Figure 4-10, which is located to the east of Paulatuk (Figure 4-2). Hummocky topography is also mapped extensively around the Mackenzie delta and the

Tuktoyaktuk Peninsula. In contrast to the Melville Hills area, this hummocky topography exhibits minimal relief and any internal ridges are completely indistinguishable.

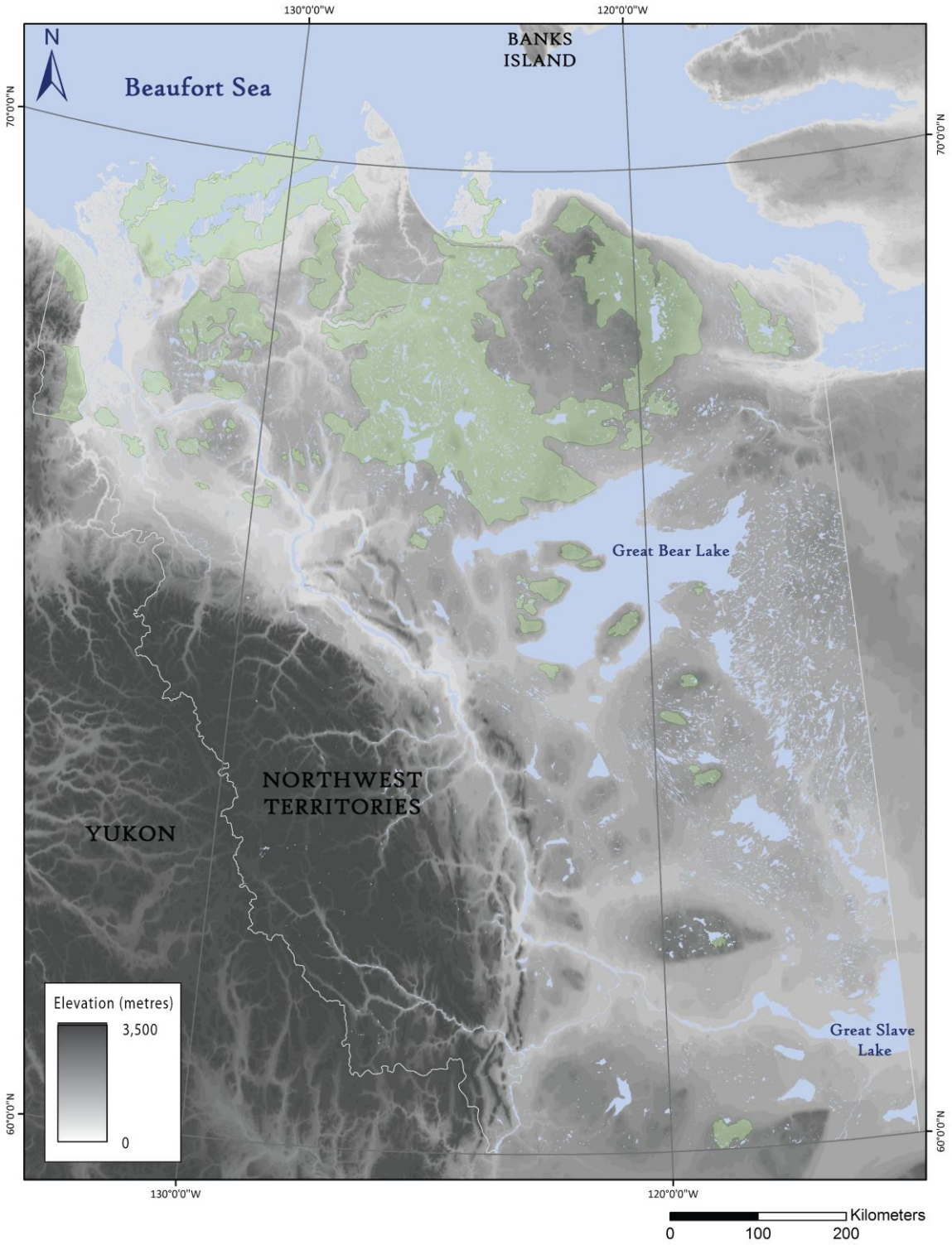

Figure 4-9: The distribution of hummocky topography (green) within the study area.

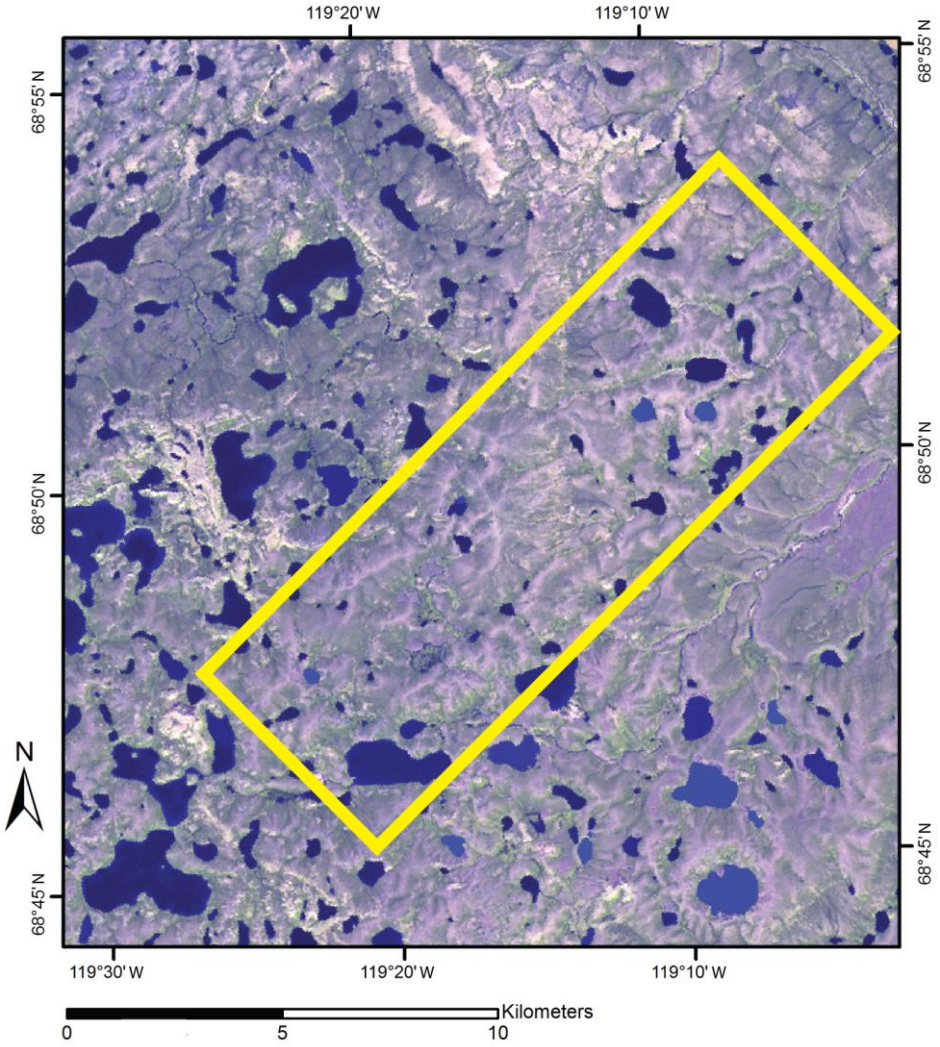

Figure 4-10: Irregular hummocky topography in the Melville Hills area as visualised on Landsat ETM+ (band combination R, G, B = 6, 5, 2). Some organisation in a north-east to south-west orientation is visible in the centre of the image (highlighted by the yellow outline box). Elsewhere on the image, the arrangement of the moraine appears more chaotic. Location shown on Figure 4-2.

4.5 Ribbed moraine

Ribbed moraine (Dunlop and Clark, 2006, Fisher and Shaw, 1992, Hattestrand and Kleman, 1999) appear as a series of morphologically similar, closely spaced ridges aligned transverse to ice flow (Figure 4-11). They are found in swarms and are most common in the east-west trending trough which extends out of Great Slave Lake towards the Yukon Mountains, see Figure 4-12. The moraines are generally orientated perpendicular to the long axis of the trough (NNE to SSW) in a similar fashion to that noted by Marich *et al.* (2005) in Newfoundland. Marich *et al.* (2005) report bedform areas of no larger than 5 km^2 for ribbed moraine which are continuous, evenly spaced and oriented parallel to one another. This is comparable to the ribbed moraine mapped here, where 82% of the bedforms have an area ≤ 5 km^2. Smaller

ribbed moraine have also been identified further east by Aylsworth and Shilts (1989) in the Keewatin sector of the LIS.

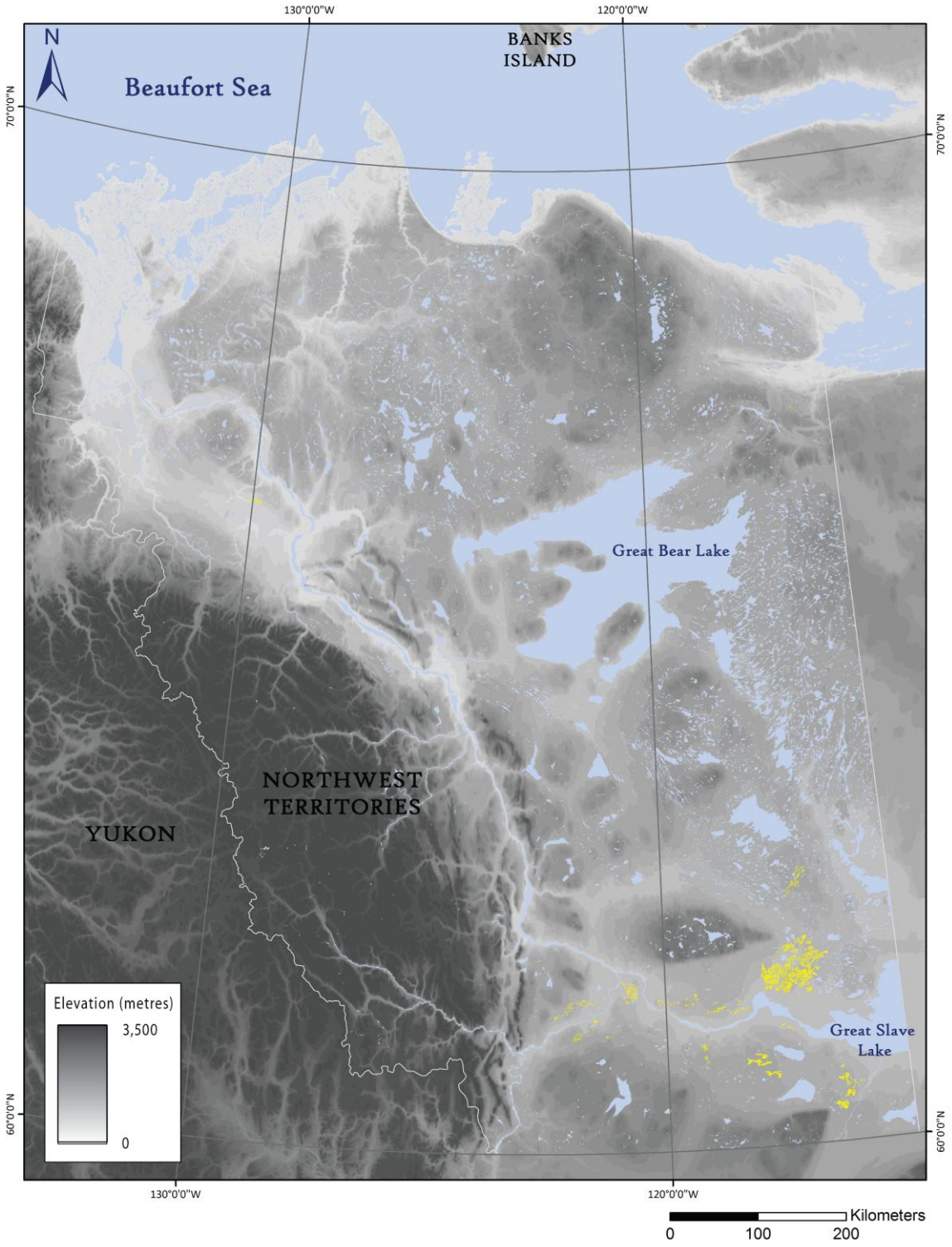

Figure 4-11: The distribution of ribbed moraine (yellow) within the study area.

A number of formative mechanisms have been invoked for ribbed moraine. Early work suggests formation in a marginal or near-marginal position (Cowan, 1968, Lundqvist, 1989).

However, since the 1980s, studies have exclusively proposed a subglacial origin (Hattestrand and Kleman, 1999, Linden *et al.*, 2008, Marich *et al.*, 2005, Möller, 2010). Most recently, Dunlop and Clark (2006) indicate that ribbed moraine results from a subglacial sediment instability which produces the regular morphology and downstream wavelength observed in areas of ribbed moraine (Dunlop *et al.*, 2008). Although their origin is still debated (see Dunlop and Clark, 2006, Hattestrand and Kleman, 1999), their presence is usually associated with a switch in the basal thermal regime and/or areas of slower-flowing ice (e.g. Fisher and Shaw, 1992, Kleman and Hättestrand, 1999, Stokes *et al.*, 2008).

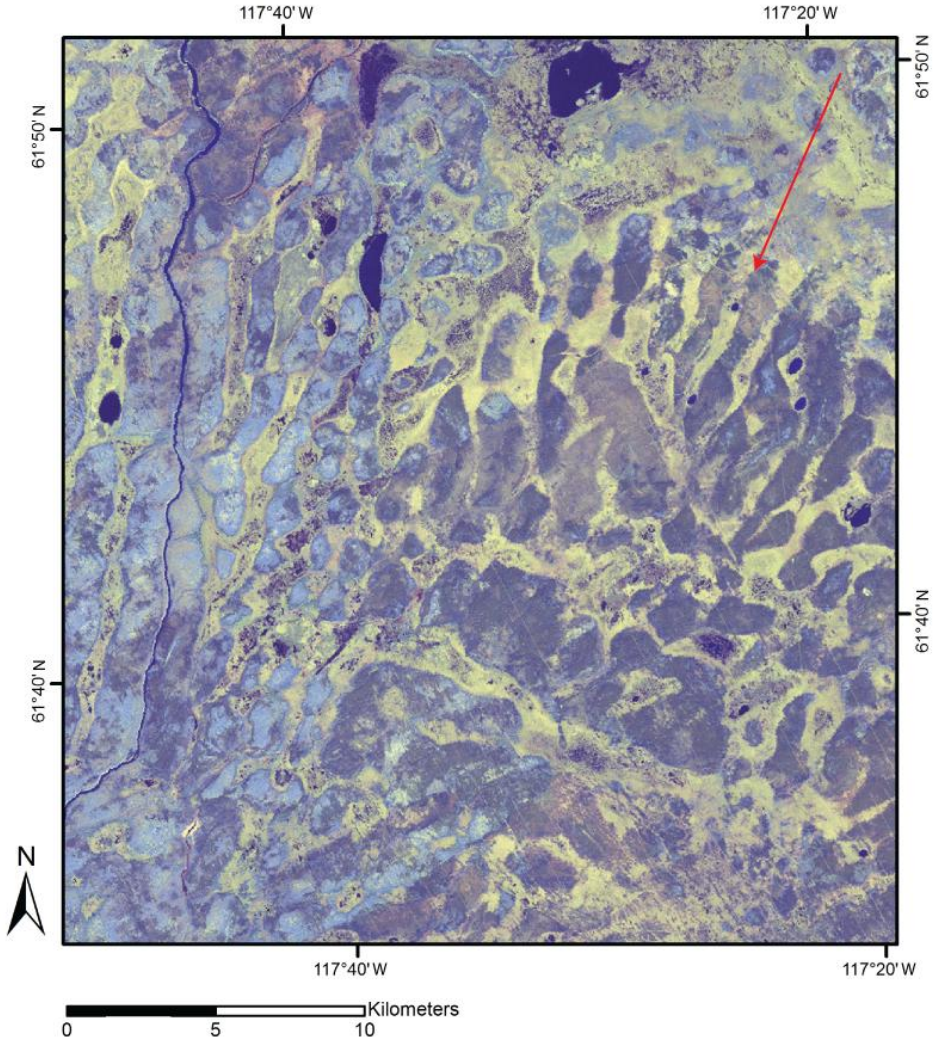

Figure 4-12: Ribbed moraine (Landsat ETM+ band combination R, G, B = 6, 5, 2) north of Great Slave Lake. This area of bedforms exhibits a regular morphology and spacing. Elsewhere, ribbed moraine occurs in smaller and more isolated areas. The arrow indicates the mean long axis orientation of the bedforms. The ribbed moraine is coloured grey and is surrounded by lighter coloured material. Location shown on Figure 4-2. It should be noted that the ribbed moraine found in the study area are much larger than typical ribbed moraine as described by Dunlop and Clark (2006).

4.6 Eskers

Eskers are elongate sinuous ridges of glacio-fluvial sand and gravel that represent the infillings of subglacial meltwater channels (Bannerjee and MacDonald, 1975). A total of 1,320 eskers have been mapped, many of which radiate outwards from the Canadian Shield, see Figure 4-13. While some eskers remain isolated and relatively linear throughout their length (e.g. Figure 4-8), others display a more complex morphology. Eskers broadly radiate away from the Canadian Shield in the east, which reflects ice flow from the Keewatin dome during the Late Wisconsinan. In the study area, eskers are often found not to be continuous but rather very fragmented.

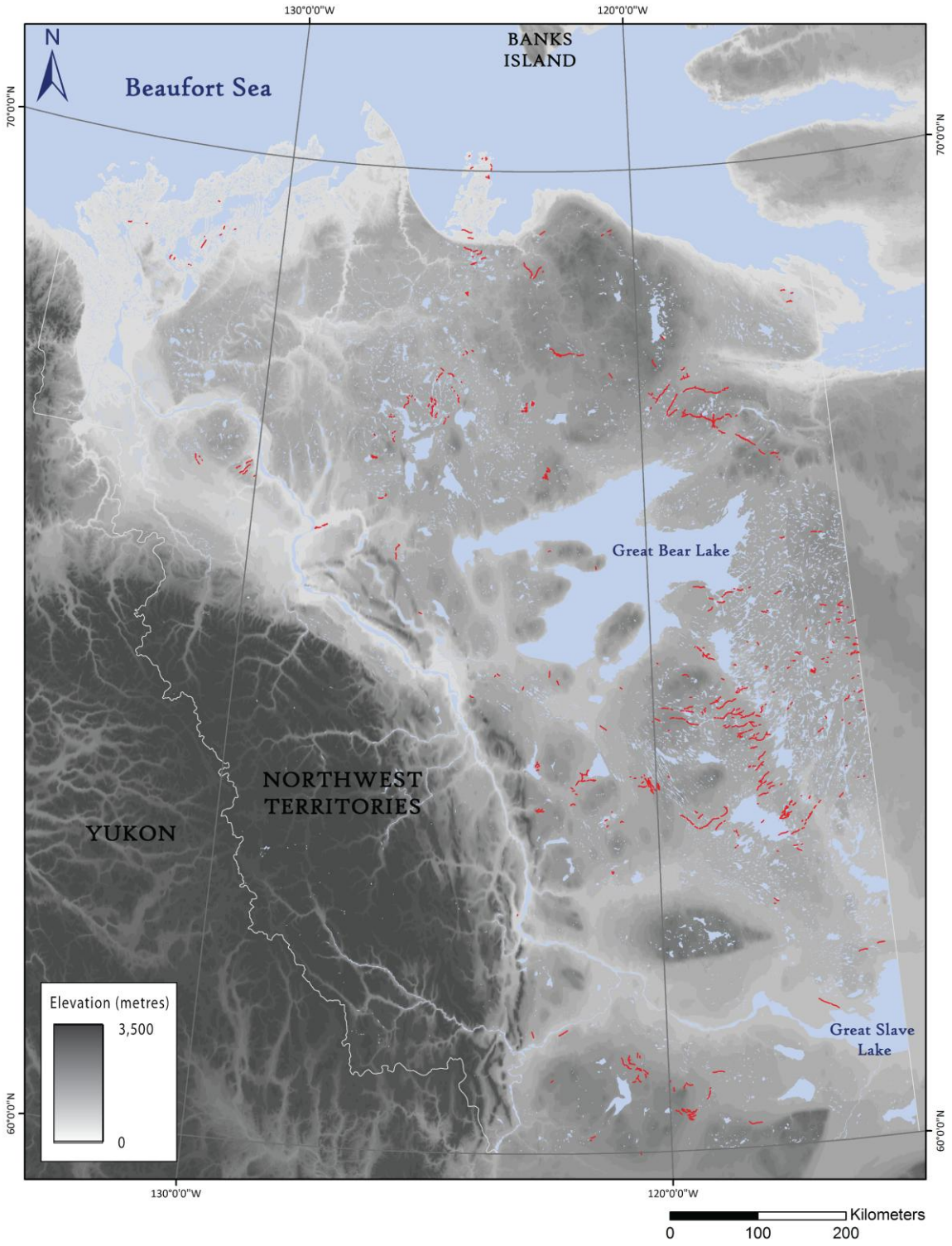

Figure 4-13: The distribution of eskers (red) within the study area.

Although eskers are often found aligned with the surrounding lineations, they are also observed perpendicular to lineations throughout the study area. They exhibit a range of lengths from 100 metres to 15 km with a mean length of 1.8 km. However, esker fragments can be traced for over 100 km (e.g. north-east of Great Bear Lake). There is a surprising lack of eskers in the north-western part of the mapped area and, where present, eskers are often

misaligned with the surrounding lineations (short, deranged eskers, see Brennand, 2000). This may reflect the complex changes in ice flow orientation and dynamics occurring here during deglaciation, but can also be attributed to the surficial geology of the region. In the east, where the Canadian Shield provides a mass of rigid substrate, drainage within channelized flow would be expected (Brennand, 2000, Clark and Walder, 1994). However, where the ice-bed interface is gently sloping and consists of deformable sediment (as is the case in the north-west part of the mapped area), a drainage network consisting of wide, shallow channels or sheet-flow may be expected (Brennand, 2000, Clark and Walder, 1994, Shreve, 1985). The formation of eskers would therefore be limited. Indeed, eskers are found to generally increase in number from west to east to west away from the Canadian Shield; a distribution which is also noted by Clark and Walder (1994).

4.7 Large meltwater channels

A series of large channels, frequently occupied by mis-fit streams, dominate the landscape in the north-western part of the mapped area, see Figure 4-14. The 46 mapped channels cover an area of 14,300 km^2. The channels are occasionally in excess of 10 km wide and form a fragmented network which cross-cuts the surrounding geomorphology, see Figure 4-15 and Figure 4-16. A series of smaller meltwater channels may also exist but the mapping was restricted to the larger channels by the resolution of the imagery and the need to create a regional geomorphological map. Major meltwater channels dissect areas of hummocky topography and a number of channels drain towards the present route of the Mackenzie River. Large meltwater channels, similar to those mapped here, have been identified by Mackay and Matthews (1973) near Fort Good Hope. These channels were cut during the early stages of deglaciation by overflow from a nearby ice-dammed lake (Mackay and Matthew, 1973).

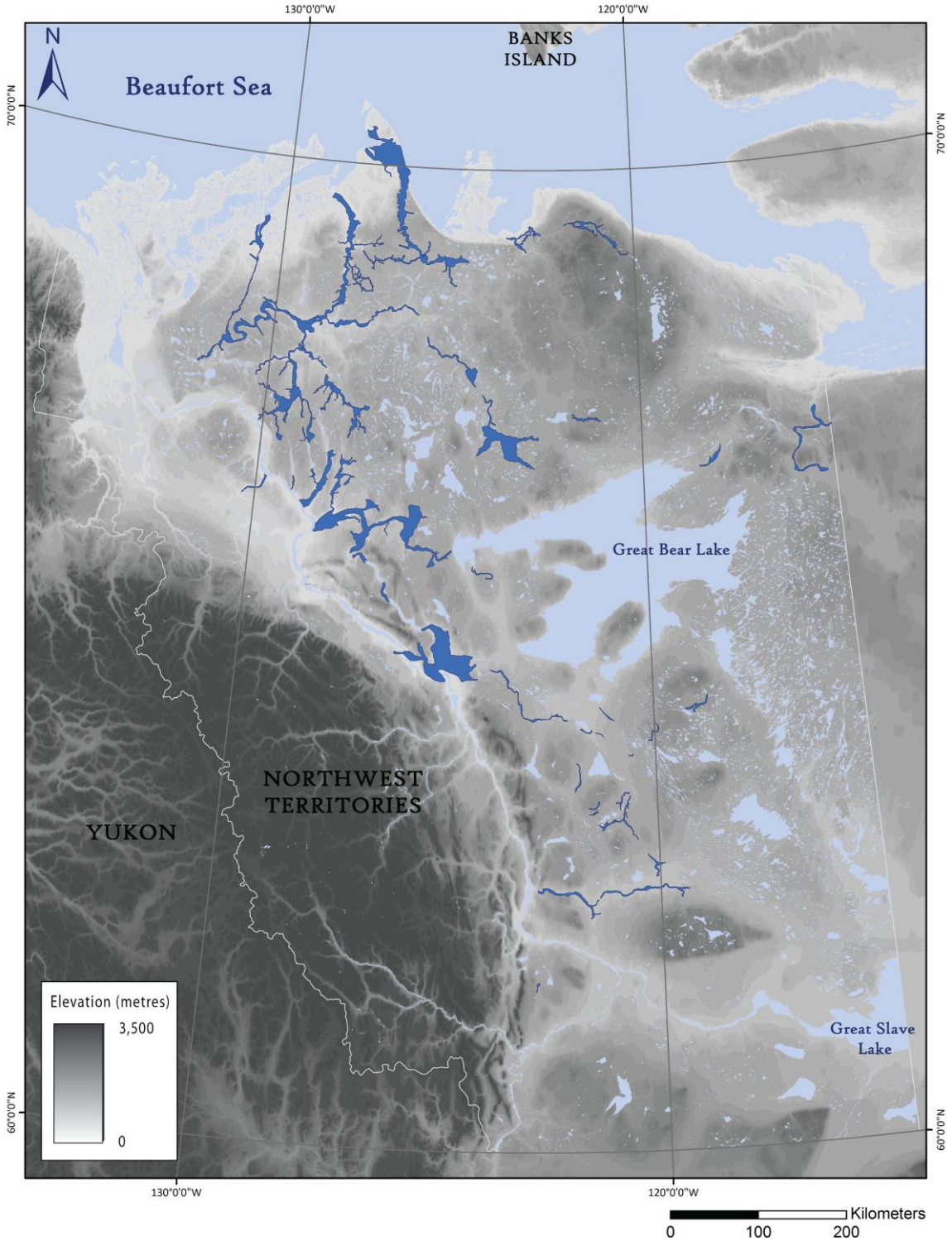

Figure 4-14: The distribution of large meltwater channels (dark blue) within the study area.

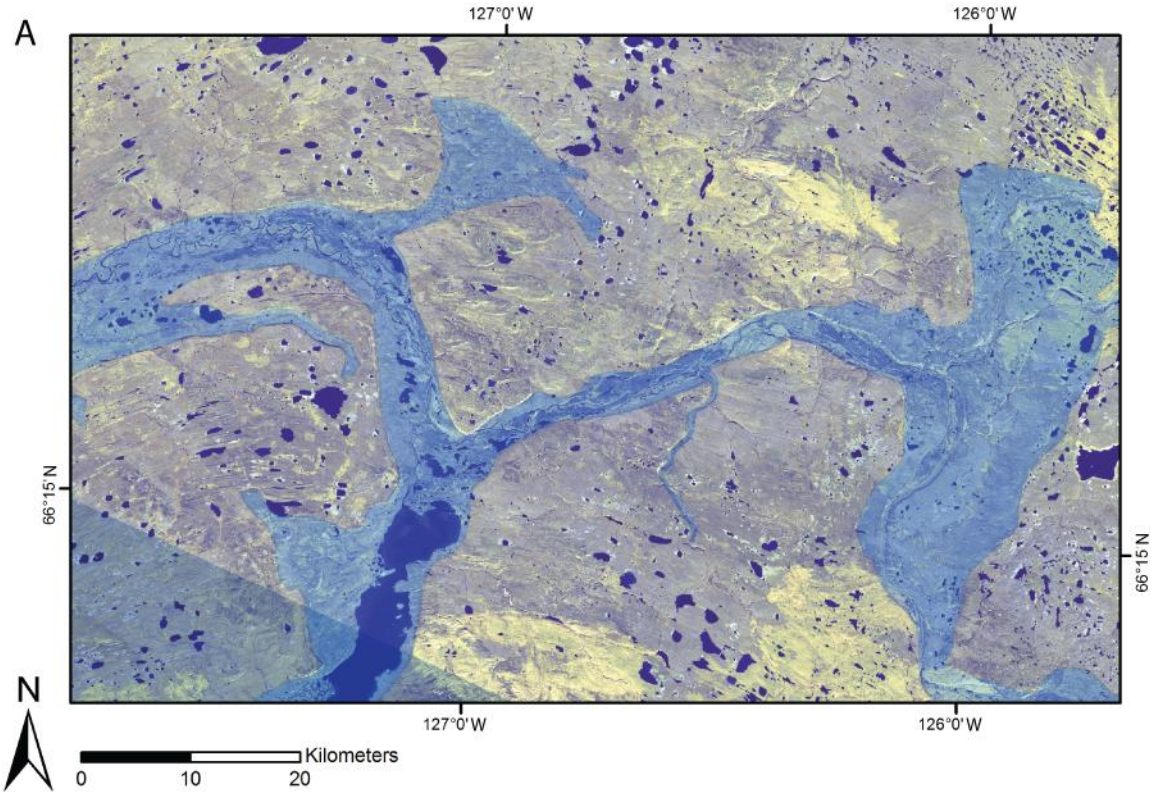

Figure 4-15: Landsat ETM+ image (band combination R, G, B = 6, 5, 2). An abandoned meltwater channel (highlighted in blue) near Fort Good Hope. The western section of this channel was originally identified by Mackay and Matthews (1973). Location shown on Figure 4-2.

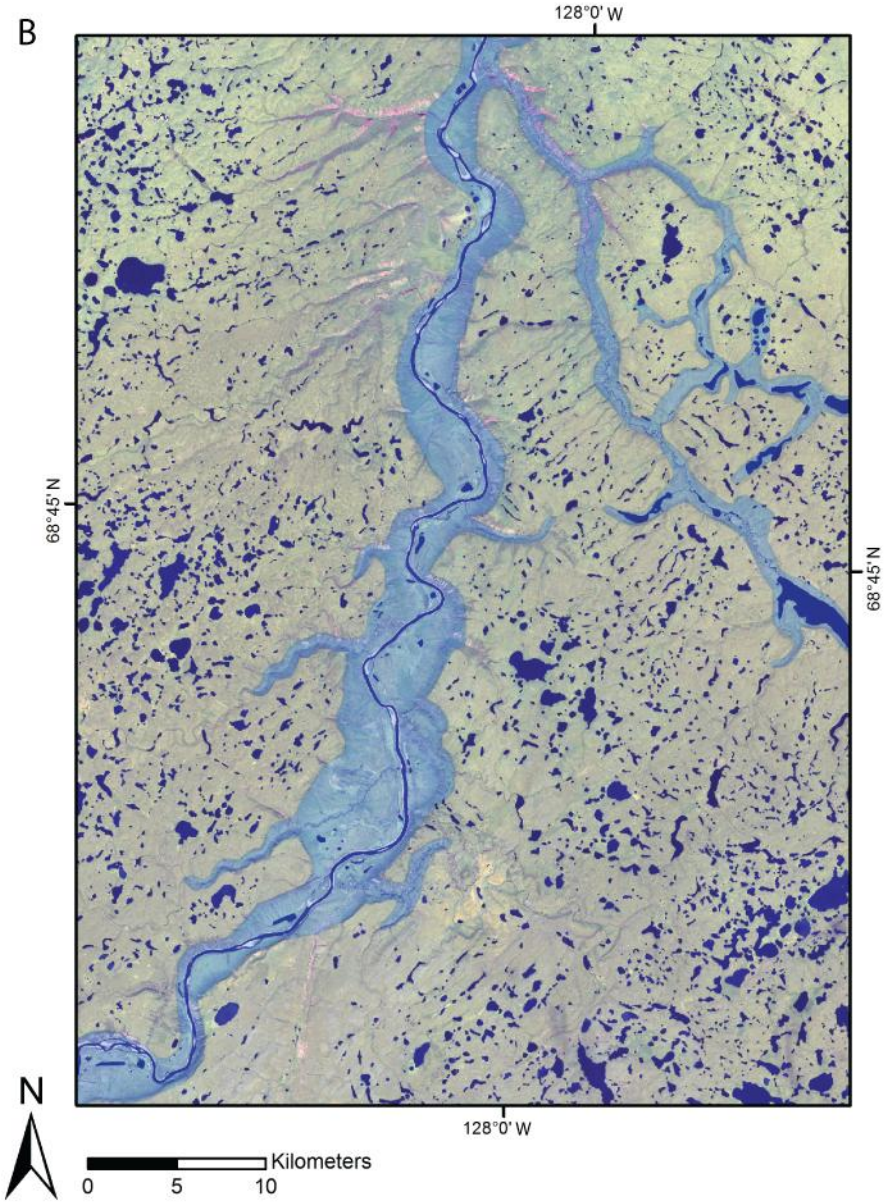

Figure 4-16: Landsat ETM+ image (band combination R, G, B = 6, 5, 2).) A channel (highlighted in blue) along the Anderson River. Location shown on Figure 4-2.

4.8 Lake strandlines

A series of lake strandlines have also been identified. They are often strongly reflected on Landsat ETM+ and are common as nested terraces which mark former lake levels. Strandlines are most abundant near Great Slave Lake, Great Bear Lake and around the western margin of the Canadian Shield. The longest of these sinuous strandlines can be traced for 82 km along the southern side of the trough which extends from the outflow of Great Slave Lake, see Figure 4-2. An example of a mapped strandline is shown on Landsat ETM+ imagery on Figure 4-17. Further discussion about the significance of these features is presented in Chapter 7.

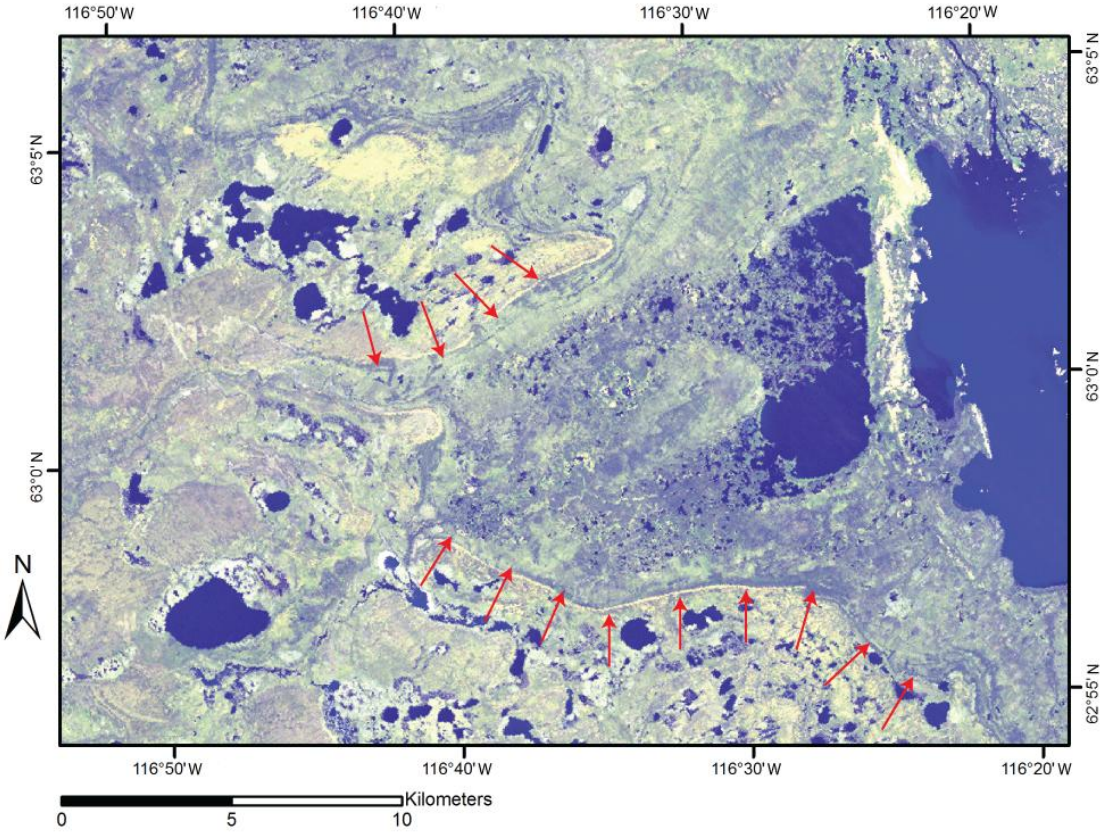

Figure 4-17: Shorelines are identified as 'terrace-like' features, which can be traced for many tens of kilometres across the landscape. The red arrows highlight a shoreline which can be found on the western side of the northern arm of Great Slave Lake (imagery: Landsat ETM+ band combination R, G, B = 6, 5, 2). Location shown on Figure 4-2.

4.9 A comparison to previously published mapping

As a whole, Figure 4-1 displays several similarities to The Glacial Map of Canada; the most comprehensive map of the glacial geomorphology of the north-west LIS prior to the publication of Brown *et al.* (2011), see Figure 4-18. Three areas are highlighted on Figure 4-18. According to The Glacial Map of Canada, area 1 on Figure 4-18 contains a corridor of glacial lineations which is sinuous from south to north. On either side this is bounded, at least in part, by areas of hummocky topography with a very limited number of eskers. Figure 4-1 also indicates a large number of highly elongate bedforms in this area which are arranged into a corridor with an abrupt lateral margin. However, unlike Figure 4-18 which indicates that the distribution of glacial lineations is even along the length of the group of bedforms, the mapping of individual bedform on Figure 4-1 indicates that this is not the case. Indeed, while the corridor of bedforms remains clear, lineations are far more densely arranged in the south-central part of this area and much less densely distributed in the north. As discussed in Chapter 5, the distribution of bedforms can have major implications for the extent of flow-sets. This

area is also cross-cut by large palaeo-channels, the extent of which cannot be fully appreciated from Figure 4-18. Furthermore, Figure 4-1 has found that the hummocky topography is more extensive than indicated on Figure 4-18.

In area 2, a similar arrangement of bedforms to The Glacial Map of Canada has been mapped on Figure 4-1. A major moraine ridge trends east to west and is accompanied by numerous eskers which are aligned with lineations, particularly on the northern side of the moraine ridge. However, Figure 4-1 indicates a greater number of bedform orientations in this region than Figure 4-18 as a result of mapping all individual bedforms rather than bedform patterns. Furthermore, the eskers are depicted on Figure 4-18 as single long sinuous features. However, according to Figure 4-1 many of these eskers are in fact several smaller ridges which cannot be traced continuously across the landscape. This is an important difference between the two maps because it may provide vital information about the genesis of the eskers (Warren and Ashley, 1994).

Area 3 contains large areas of cross-cutting bedforms, some of which lie perpendicular to each other. In the southern part of this area, the bedforms curve around from a north-east to south-west orientation to a south-east to north-west orientation (see Figure 4-18). While The Glacial Map of Canada depicts a simple broad pattern in these bedforms, the bedform arrangement indicated by Figure 4-1 is somewhat more complex. Figure 4-1 indicates that the bedforms are cross-cut by other lineations, particularly in the southern part of this area. Furthermore, the switch between areas of perpendicular bedforms is not a clear-cut as shown on Figure 4-18. This has implications for the subsequent reconstruction of ice stream activity (see Chapter 5). For example, this could have implications for flow-set extent which in turn, may influence the time-step of the reconstruction to which certain groups of bedforms are allocated. On this basis, it is possible to justify a new map of this region which documents the locations of individual bedforms rather than the overall patterns of bedform orientation.

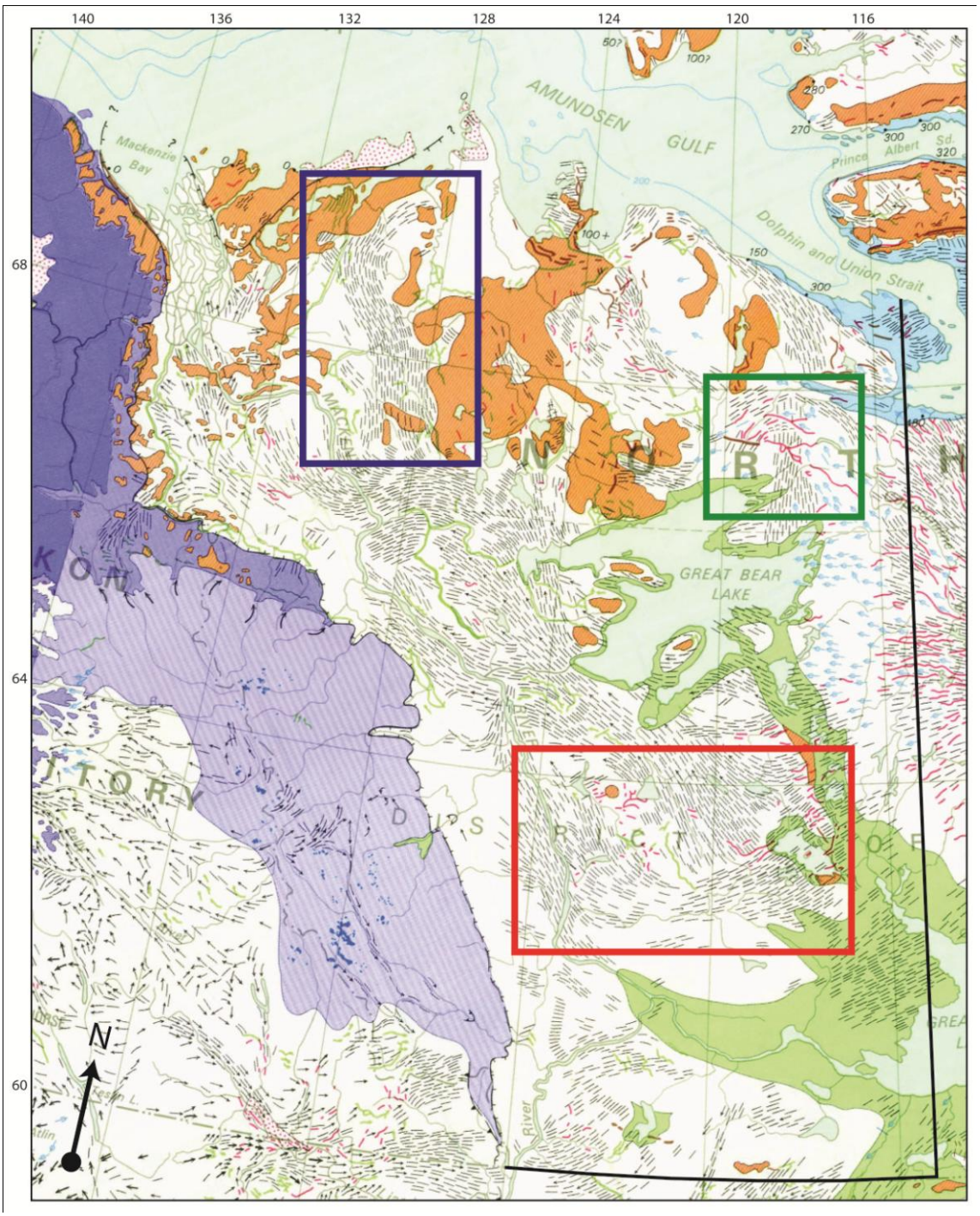

Figure 4-18: The study area as mapped on the The Glacial Map of Canada. Three areas have been highlighted which are discussed in the text. Blue box: area 1, green box: area 2, red box: area 3. The black line marks the southern and eastern margin of the study area. Longitude and latitude are given by the numbers around the outside of the map. The arrow indicates north only at the fixed point marked, this is a function of the projection of this map. Map taken from Prest et al. (1968).

4.10 Conclusions

- A large, regional scale map documents the spatial distribution of more than 94,000 landforms. Mapped features include lineations, moraine ridges, hummocky topography, ribbed moraine, eskers, and large meltwater channels.
- The spatial arrangement of bedforms indicates that the glacial geomorphology of the region is the result of temporal switches in ice flow orientation during Late Wisconsinan deglaciation and cannot have formed synchronously. In particular, complex arrangements of eskers, highly attenuated lineations and partially over-printed bedforms are present throughout the study area.
- The most attenuated bedforms are clustered in a sinuous, but fragmented corridor ~ 90 km wide, trending south-east/north-west along the western edge of Great Bear Lake towards the Arctic Ocean.
- Convergent and divergent patterns of lineations with abrupt lateral margins have also been identified around Great Bear Lake, along the Amundsen Gulf coast and in the vicinity of the Anderson River. This arrangement of bedforms provides potential evidence for palaeo-ice streaming (cf. Stokes and Clark, 1999).
- Areas of higher ground generally remain free of lineations, most notably around the Melville Hills and to the north-east of Fort Simpson.

Chapter 5: Ice sheet reconstruction

5.1 Introduction

This chapter documents the use of geomorphological evidence to reconstruct ice sheet and ice stream activity in the north-west sector of the LIS throughout Late Wisconsinan deglaciation. Sections 5.2 and 5.3 are concerned with the construction of flow-sets, while Sections 5.4 and 5.5 describe the reconstructed ice margins from Dyke *et al.* (2003) and the radiocarbon chronology used to produce these. Finally, Sections 5.6 and 5.7 provide an illustrated commentary of flow-set activity throughout deglaciation.

5.2 Flow-set identification and classification

Flow-sets or 'landform swarms' are defined as landforms of a coherent and systematic pattern which are interpreted to record distinct phases of ice flow (Clark, 1993, Clark *et al.*, 2000, Clark, 1999). Flow-sets were identified from the mapped geomorphology, see Chapter 4. To be identified as a flow-set, groups of landforms require the follows:

1. Parallel concordance: each landform was required to have a similar orientation to its neighbours.
2. Close proximity: landforms within the same flow-set needed to be closely packed, typically with a spacing of up to two or three times the dimensions of the landform.
3. Similar morphometry: neighbouring landforms within the same flow-set were required to display similar morphometry.

Based on their unique geomorphological signature, the flow-sets were assigned to one of four types: wet-based deglacial, frozen-bed deglacial, ice stream or event (Kleman *et al.,* 2006). These categories provide the first stage of interpretation in the reconstruction of ice sheet and ice stream dynamics by indicating the conditions under which each flow-set formed. The geomorphological characteristics of each type of flow-set are outlined in Chapter 3, but will also be discussed below, alongside the distribution of each flow-set type within the study area.

5.2.1 Wet-based deglacial

As outlined in Chapter 3, wet-based deglacial flow-sets are identified by an abundance of flow traces (i.e. glacial lineations) which are locally aligned with eskers and meltwater channels. They represent the inward-transgression of the wet-based zone of ice during deglaciation

(Kleman *et al.*, 2006). Wet-based deglacial flow-sets are most abundant in the southern half of the study area and are generally orientated north-east to south-west. Two large areas of wet-based deglacial flow-sets are found in the southern half of the study area; one on either side of the broad valley which contains the outflow from Great Slave Lake. Further north, these flow-sets are more isolated, smaller and more commonly trend south-east to north-west. In particular, Fs17, Fs172 and Fs79 are orientated parallel to two ice stream flow-sets; in the east, Fs82, and in the west, Fs215. Fs89 and Fs83 are located on the northern edge of Great Bear Lake and both trend north-east/south-west.

5.2.2 Frozen-bed deglacial

Frozen-bed patches are important for ice sheet stability because they laterally constrain and isolate peripheral drainage basin their ice streams (see Kleman and Glasser, 2007). I have not identified frozen-bed patches or delineated frozen-bed flow-sets. This may have been possible with higher resolution imagery which would have enabled small meltwater channels to be mapped. However, Kleman and Glasser (2007) provide a map of cold-based zones and I have no evidence to suggest that their depiction is incorrect. Indeed, some of their zones coincide with hummocky moraine or high topography which is consistent with ice stagnation (Kleman and Glasser, 2007: Kleman and Hättestrand, 1999). There is also some coincidence between the cold-based zones of Kleman and Glasser (2007) with the anomalous, possibly pre-LGM, flow-sets shown later in this chapter. This further supports the hypothesis of Kleman and Glasser (2007) that these zones were cold-based during deglaciation. Finally, it is should be acknowledged that the absence of evidence for the existence of frozen-bed patches is not evidence for the absence of warm-based ice. For example, some areas which are suggested to be cold-base could be thawed bed but be a product of largely inactive ice.

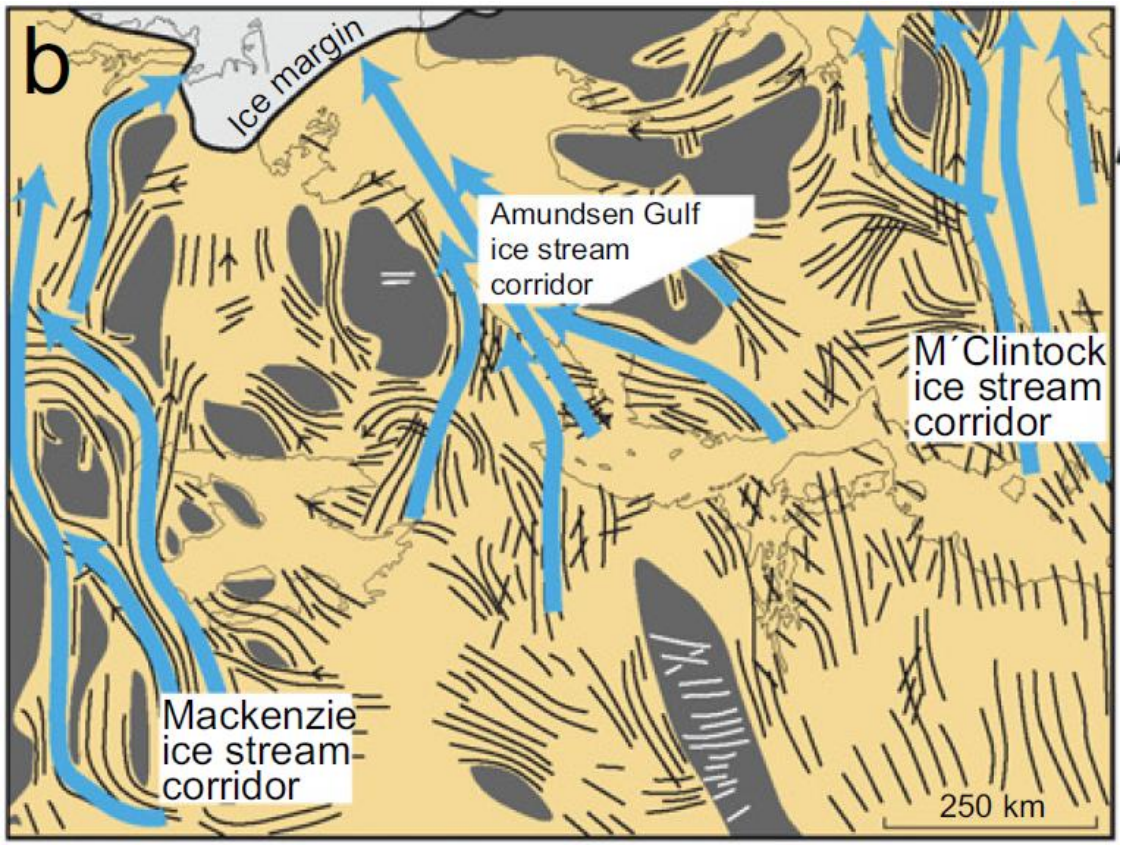

Figure 5-1: Frozen-bed patches in the north-west LIS after Kleman and Glasser (2007). A similar arrangement of frozen-bed patches is hypothesised based on the results presented in Chapter 4 of this thesis. Grey patches indicate areas of frozen-bed, the black lines provide an indication of ice flow orientation, and the blue lines highlight hypothesised ice streams.

5.2.3 Ice Stream

As noted by Stokes and Clark (1999) and Kleman *et al.* (2006), ice streams are typically associated with abundant highly elongate flow traces (i.e. glacial lineations), and groups of bedforms which often have abrupt lateral margins and can be delimited by lateral shear margin moraines. Areas of convergent flow represent the transition from sheet flow to streaming flow, and land-terminating ice streams also typically have divergent terminal zones while those terminating in water do not (Stokes and Clark, 1999). The characteristic geomorphological signature of ice stream activity is summarised in Table 2-1, and Figure 3-6. As shown in Chapter 4, in the north-west sector of the LIS, the longest bedforms are found along the Amundsen Gulf coast, near the Anderson River, around the south-western arm of Great Bear Lake and on the northern shore of Great Bear Lake. These are all areas where ice stream flow-sets have been identified (see Figure 5-2). Furthermore, the size of ice stream flow-sets in the north-west sector of the LIS is highly variable. A large ice stream flow-set lies along the Amundsen Gulf coast (Fs170) and several large ice stream flow-sets can together be traced for several hundred kilometres from ~ 64°N to the Arctic Ocean (Fs228, Fs216, Fs270

and Fs215). North of Great Bear Lake, smaller ice stream flow-sets have been identified (Fs95, Fs1, Fs88 and Fs82).

5.2.4 Event

Event flow-sets are the most common type of flow-set observed within the study area and are associated with sheet flow within an ice sheet (Kleman *et al.,* 2006). They can form many hundreds of kilometres inside the ice margin and have a geomorphological signature which includes flow traces without associated meltwater channels or aligned eskers. Within the study area, event flow-sets tend to be much smaller than the other types of flow-set and generally have a much more subtle geomorphological imprint. They coincide closely with the orientation of neighbouring flow-sets and although they largely follow a south-east to north-west orientation, a group of 26 event flow-sets also indicate a period of north-east to south-west ice flow across the northern half of the study area. This group of flow-sets are discussed further in Section 5.6.5.

5.3 Flow-set configuration

The ~95,000 landforms were used to generate 272 flow-sets (Figure 5-2). Following the construction of the flow-sets, it became apparent that the minimum number of lineations used in the demarcation of a flow-set was 12. In contrast, flow-sets such as Fs270, Fs256 and Fs228 are represented by several thousand individual bedforms.

Initial inspection of the spatial arrangement of the 272 flow-sets, in which neighbouring flow-sets often indicate perpendicular flow orientations, suggests that all 272 cannot have formed synchronously. Indeed, in order reconcile the arrangement of the flow-sets with a series of viable ice flow orientations, major changes in ice sheet flow configuration are required in this sector of the ice sheet during deglaciation. Following the construction of flow-sets, it became apparent that nearly all of the flow-sets could be accommodated in a post-LGM reconstruction, with just a small number identified as being of potentially pre-LGM origin. These older flow-sets are discussed in Section 5.6.5. The reconstruction shown in Section 5.6 documents these changes in a more detailed fashion by embedding individual flow-sets into reconstructions of the ice margin at 20 time-steps from 21.4 to 11.45 cal. ka BP.

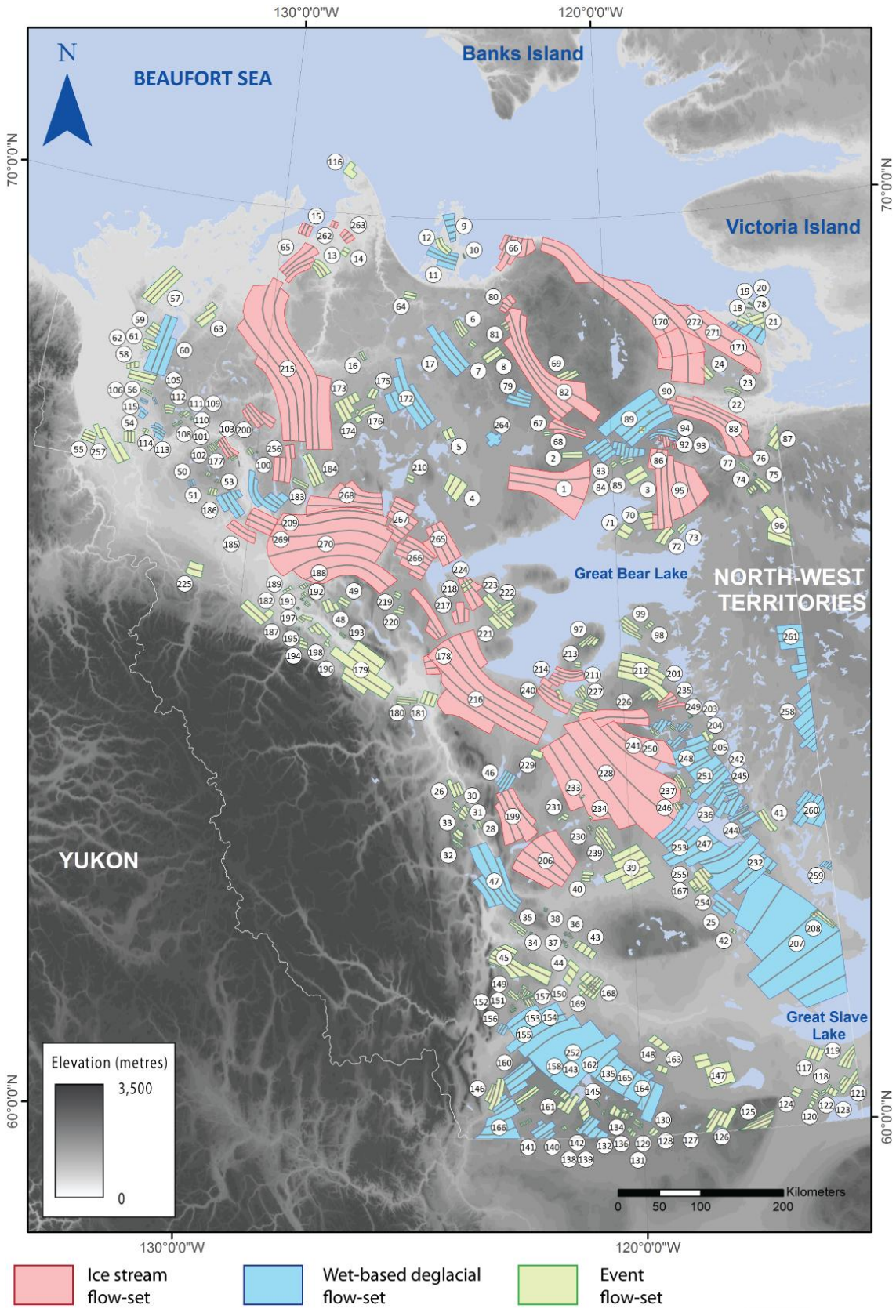

Figure 5-2: Flow-sets reconstructed from the map of glacial geomorphology which is presented in Chapter 4.

5.4 Flow-sets and ice margin chronology

Of the radiocarbon dates compiled by Dyke *et al.* (2003) for the entire LIS, 71 lie within the study area. The dates have been adjusted for regional ^{14}C marine reservoir effects (see Dyke *et al.* (2003) and Coulthard *et al.* (2010) for further information). The dates were taken from a range of organic fragments including *Hiatella arctica* (a marine mollusc, native to the Arctic Ocean), peat, wood and organic lake sediments, as detailed in the Appendix. Within the study area, the dates range from 14.92 ^{14}C ka BP to 6.97 ^{14}C ka BP onshore, with one further date of 21.6 ^{14}C ka BP offshore in Amundsen Gulf (RD12). While dates in the eastern part of the study area are often younger than those in the west, this is not a consistent trend. Indeed, this lack of consistency supports the notion that ice margin recession was not uniform. Specifically, the ice margin did not retreat steadily eastwards but instead was characterised by the formation of numerous small lobes of ice and subtle periods of ice readvance.

The radiocarbon dates are not spread uniformly across the study area (see Appendix). In the north, they are found in clusters along the Amundsen Gulf coast and on the eastern side of the Mackenzie delta along the Tuktoyaktuk Peninsula. Further south, a cluster of 11 dates is located around the foot of the Yukon Mountains between 64 and 66°N. While these dates provide a chronology suitable for the derivation of ice margin positions during deglaciation following the LGM, they by no means allow for absolute dating of every individual flow-set. As such, it has been necessary to relatively date flow-sets, particularly those in the central portion of the study area, based on the cross-cutting relationships of the bedforms in different flow-sets. For example, a flow-set without a radiocarbon date within it can be assigned a relative age if it is superimposed on, or below, a flow-set with a radiocarbon control (see Stokes *et al.*, 2009). Further details about this method can be found in Chapter 3.

5.5 Ice margin reconstruction

The ice margin reconstructions of Dyke *et al.* (2003) are based largely on the interpretation of radiocarbon dates with more limited input of geomorphological evidence. This provided a continental scale reconstruction rather than detailed regional-scale maps. It has therefore been necessary to modify the ice margin in some areas in order to i) match the ice margins with the location of major moraine ridges, ii) to account for the local topography which would be difficult to account for in a continental scale reconstruction and iii) to resolve any discrepancies with flow-set extent and the ice margin position. The revised ice margins are shown n Figure 5-3. The construction of flow-sets assumes that the bedforms within each flow-set formed under the same phase of ice flow. It was therefore necessary to ensure that, where

flow-sets could be confidently assigned an age and therefore associated with a particular margin (e.g. with a radiocarbon date or through the relative dating of cross-cutting bedforms), the whole flow-set formed behind that margin (cf. Stokes *et al.,* 2009).

New ice margins (as shown in Figure 5-3) have been assumed as an intermediate position between neighbouring younger and older ice margins. For example, the margin labelled in Figure 5-3 as '14.10 – 14.4 cal. ka BP' (because it lies between the 14.10 and 14.40 cal. ka BP ice margins from Dyke *et al.* (2003)), is assumed to date to 14.25 cal. ka BP. Similarly, the new margin between 13.45 and 14.10 cal. ka BP is assumed to date to 13.80 cal. ka BP in this reconstruction.

Two further ice margins were added to the reconstruction (shown by the long dashed lines on Figure 5-3). These additional margins allowed the reconstruction to account for relatively dated flow-sets which lack a radiocarbon control and could not be reconciled with the neighbouring younger or older margin positions. The presence of moraine ridges between the neighbouring ice margins provided further evidence for the occurrence of the margin in the positions shown for a sustained period. Two new ice margins were therefore justified despite a lack of radiocarbon control on the ice margin or relevant flow-sets.

The main modification of the Dyke *et al.* (2003) margins took place ~ 13 cal. ka BP and ~ 12.7 cal. ka BP (Figure 5-3). According to Dyke *et al.* (2003) the geometry of the ice margin around the foot of the Yukon Mountains at ~ 62°N showed little change during this period. However, the relative dating of flow-sets and the location of major moraine ridges in this area suggests that the margin may have stepped back between 13.45 and 13 cal. ka BP. Further north, smaller modifications were made to this margin to account for the topographic lows in the basin of Great Bear Lake. The 12.7 cal. ka BP margin was principally modified to account for the switching on of a flow-set near Kugluktuk (68°N and 115°W).

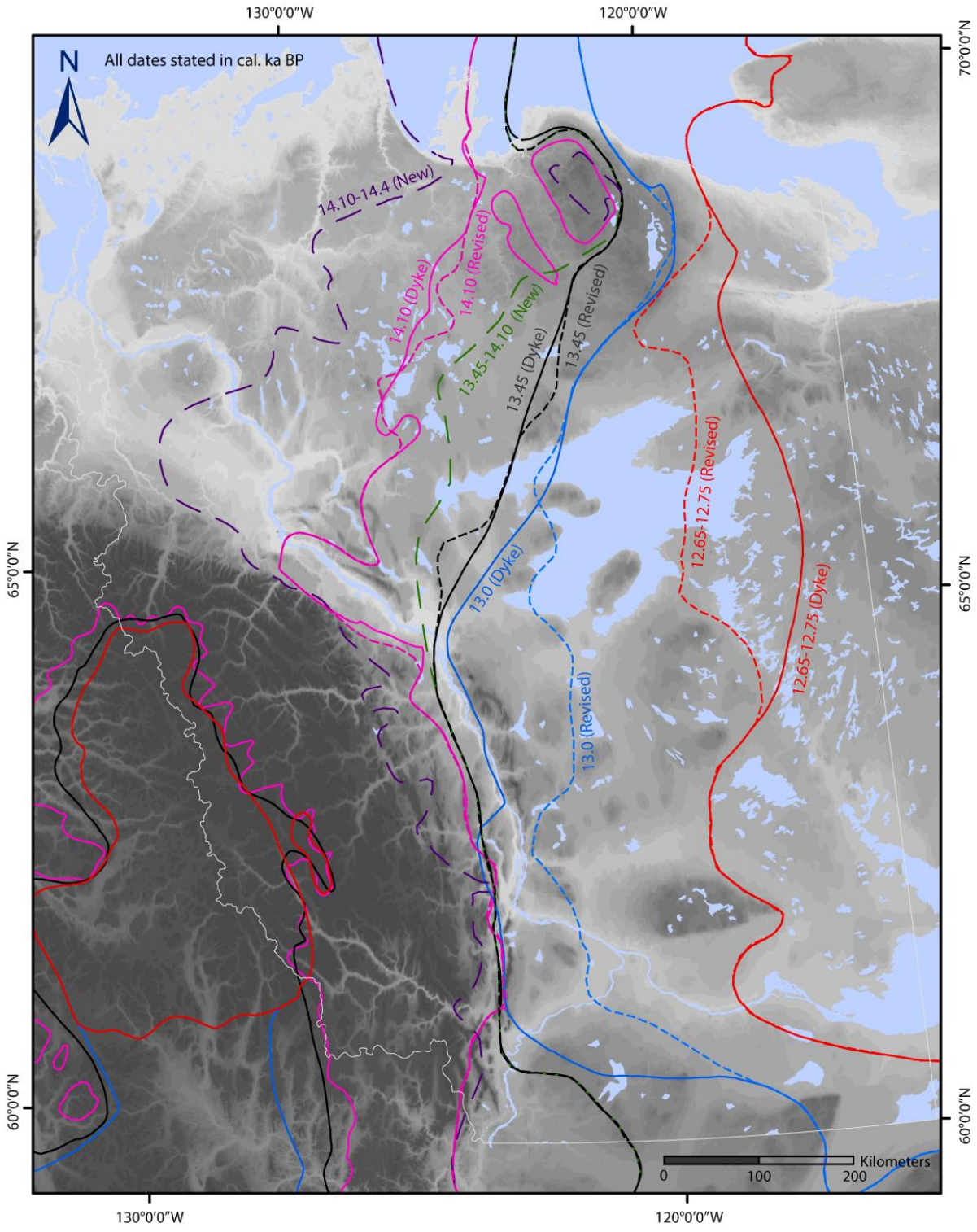

Figure 5-3: Ice margins used at the 20 time-steps for which reconstructions of ice sheet dynamics are presented. These include ice margins from Dyke et al. (2003), which have been modified as discussed above, and two new margins at 14.25 cal. ka BP and 13.80 cal. ka BP.

5.6 Ice sheet dynamics during Late Wisconsinan deglaciation

This section provides a commentary of ice sheet dynamics in the north-west sector of the LIS during Late Wisconsinan deglaciation. Ice streams were active throughout deglaciation but changed configuration as overall ice sheet retreat occurred towards the east. The reconstruction of ice stream activity shown below in Figure 5-4 is derived from the flow-sets shown above which are based on the geomorphological map presented in Chapter 4.

5.6.1 21.4 – 17.35 cal. ka BP

Dyke *et al.* (2003) indicate a stable ice margin position during the early part of deglaciation following the LGM based on the radiocarbon dates shown in Table 3-3. Between 21.4 and 17.35 cal. ka BP, a large ice lobe extended > 100 km offshore over the current Mackenzie delta, with ice flowing from south-east to north-west (Figure 5-4A-H). In Amundsen Gulf, ice flowed north-west and terminated in a lobe just beyond the western edge of the Canadian Archipelago. However, more recent work by England *et al.* (2009) suggests that, north of the study area, on the northern side of Banks Island in M'Clure Strait, the LGM ice limit was much more extensive and reached the continental shelf. Furthermore, ice, at least partly, inundated Banks Island (England *et al.,* 2009). While the reconstruction of England *et al.* (2009) has not been extended south to the study area, it is worth noting that the ice margin in Amundsen Gulf is likely to have also extended to the continental shelf edge.

According to Dyke *et al.* (2003), the western margin of the LIS occupied the foot of the Yukon Mountains during the LGM. This left an ice free corridor between ice on the eastern and western side of the mountains. The Melville Hills also remained ice free throughout deglaciation (Figure 5-4). Klassen (1971) was the first to identify an ice limit around the Melville Hills and this was later correlated with the extent of the Jesse Till, the most recent Pleistocene till found throughout the Canadian Arctic, by Vincent (1983). Dyke and Prest (1987) and Dyke *et al.* (2003) have both therefore adopted this ice limit around the Melville Hills in their reconstructions of Late Wisconsinan LIS extent.

An ice divide trending north to south was present between the Melville Hills and Great Bear Lake from the LGM until 16.80 cal. ka BP (Figure 5-4I). This separated ice to the east flowing north into Amundsen Gulf from ice flowing north-west towards the present day Anderson River. Ice divides were located by tracing ice flow-lines back up ice to the head of regions of divergent bedforms. Two large flow-sets (Fs95 and Fs170) which are comprised of abundant elongate drumlins and parallel eskers indicate streaming flow away from the Canadian Shield

to the north and along the Amundsen Gulf Coast. A smaller series of ice stream flow-sets (Fs23, Fs21 and Fs94), which indicate a similar arrangement of streaming flow in the area, have also been identified. Furthermore, Fs86 which also demarcates flow towards the Amundsen Gulf, comprises abundant flow traces but differs from nearby ice stream flow-sets because it lacks a convergent arrangement of bedforms. Six event flow-sets (Fs74, Fs75, Fs76, Fs77, Fs93 and Fs96) indicate sheet flow alongside Fs95. The flow-sets on the eastern side of the ice divide, which indicate streaming flow towards, and along, the Amundsen Gulf, agree with previously published reconstructions of a palaeo-ice stream in Amundsen Gulf based largely on mapping from the adjacent Victoria Island (Stokes and Clark, 1999, Stokes *et al.*, 2009, Stokes *et al.*, 2006). On the western side of the ice divide, two ice lobes formed during this period; one over the Mackenzie Delta and one near the Anderson River. Ice in these lobes was fed by sheet flow from the south-east. This flow is represented in our reconstruction by 72 event flow-sets and, closer to the margin, four wet-based deglacial flow-sets. This arrangement of flow-sets persisted until 19.10 cal. ka BP (Figure 5-4E).

At 18.50 cal. ka BP, Fs228 became active. This flow-set contains abundant highly elongate glacial lineations and aligned eskers which converge into a 100 km wide corridor. The onset of Fs228 marks the initiation of ice streaming on the south-western side of Great Bear Lake flowing north-west towards the Mackenzie and Anderson lobes. At 17.90 cal. ka BP (Figure 5-4G) a series of smaller ice stream flow-sets (Fs217, Fs266, Fs267, Fs269 and Fs200), which directed streaming ice towards the Mackenzie lobe, switched on. Subsequently, however, streaming flow shifted to the east towards the Anderson lobe (Fs215, Fs15, Fs65, Fs262, Fs263 and Fs256).

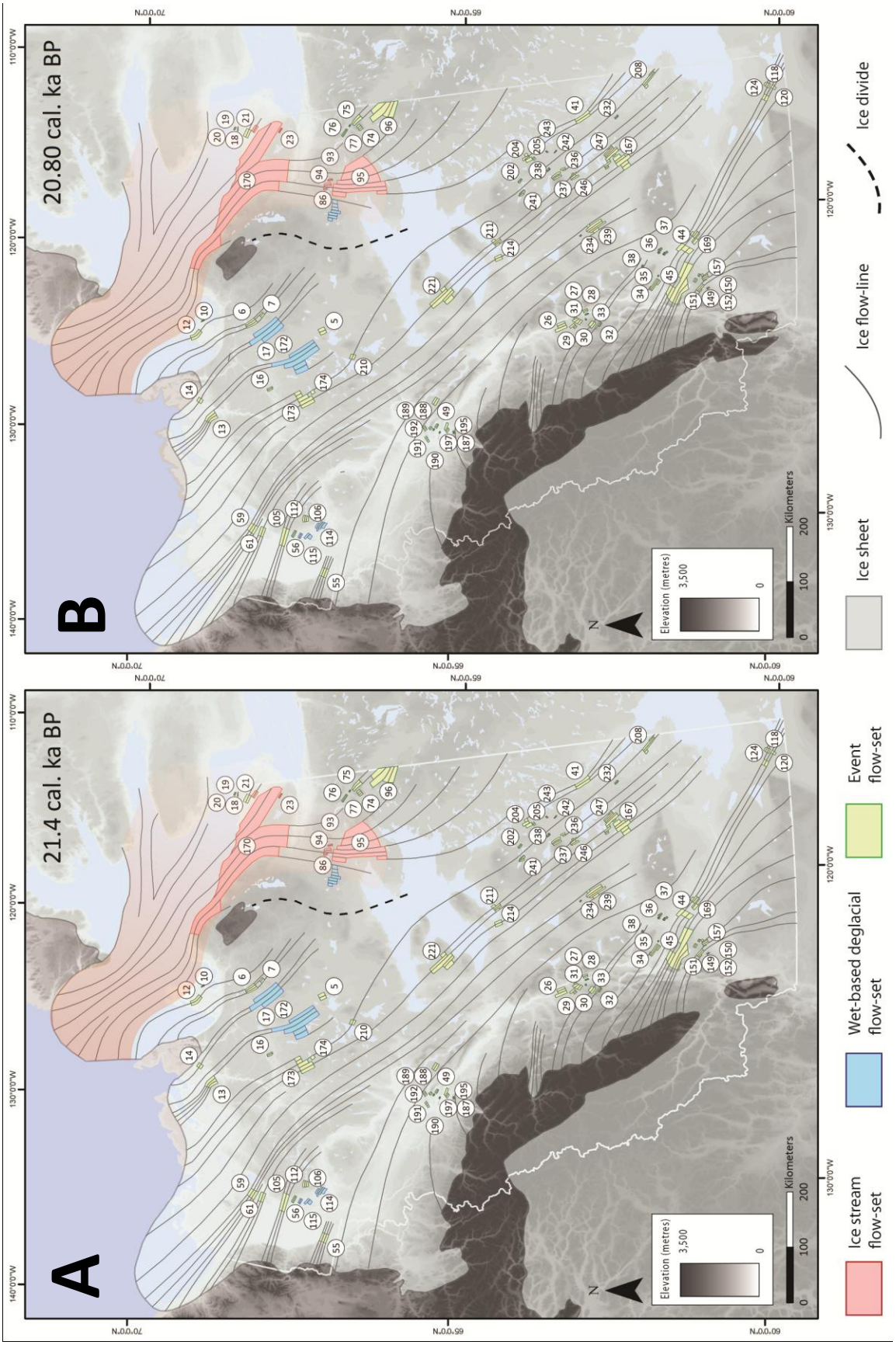

Figure 5-4: Reconstructed ice sheet and ice stream dynamics in the north-west sector of the LIS during Late Wisconsinan glaciation.

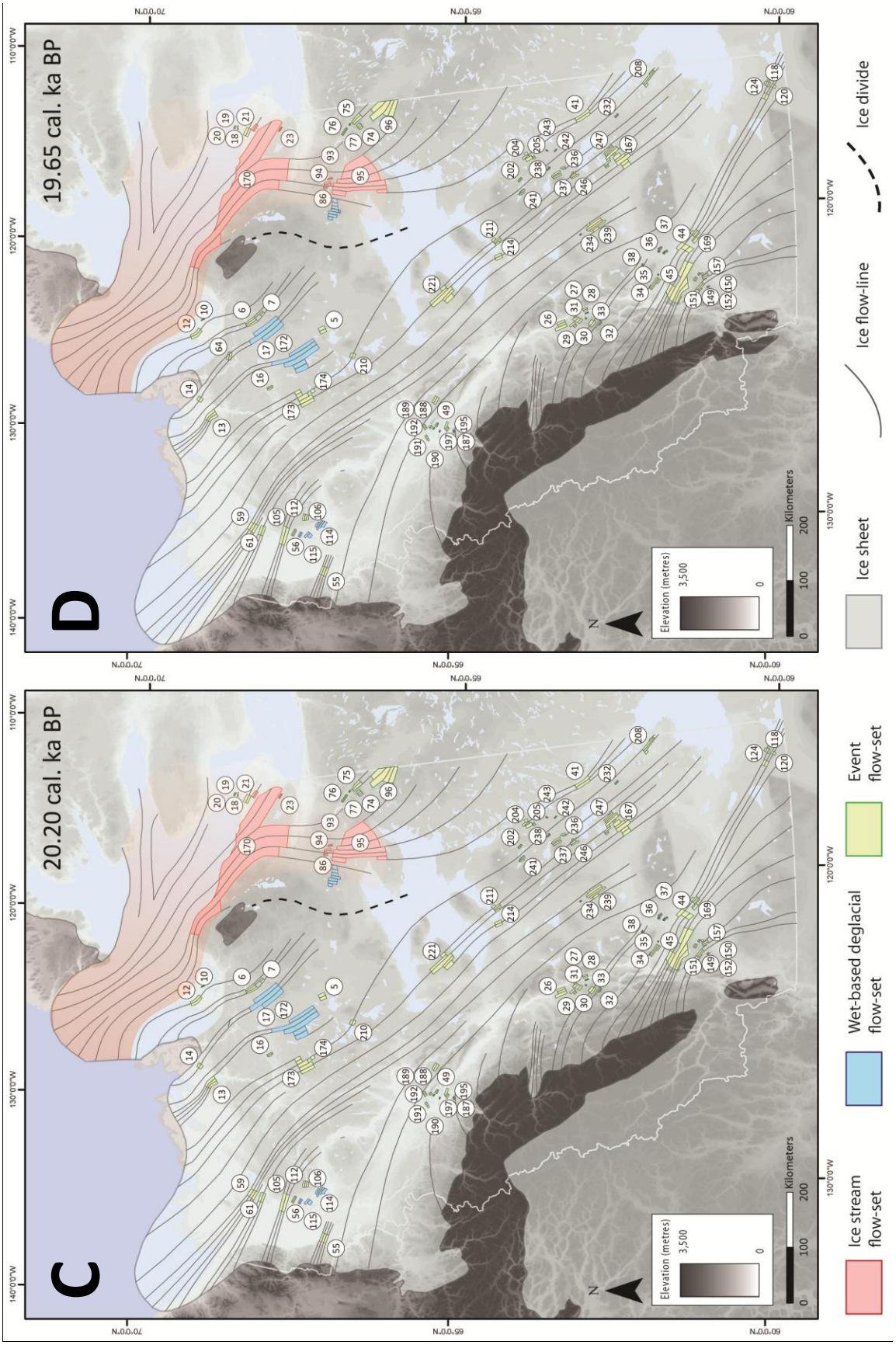

Figure 5-4 (cont.): Reconstructed ice sheet and ice stream dynamics in the north-west sector of the LIS during Late Wisconsinan glaciation.

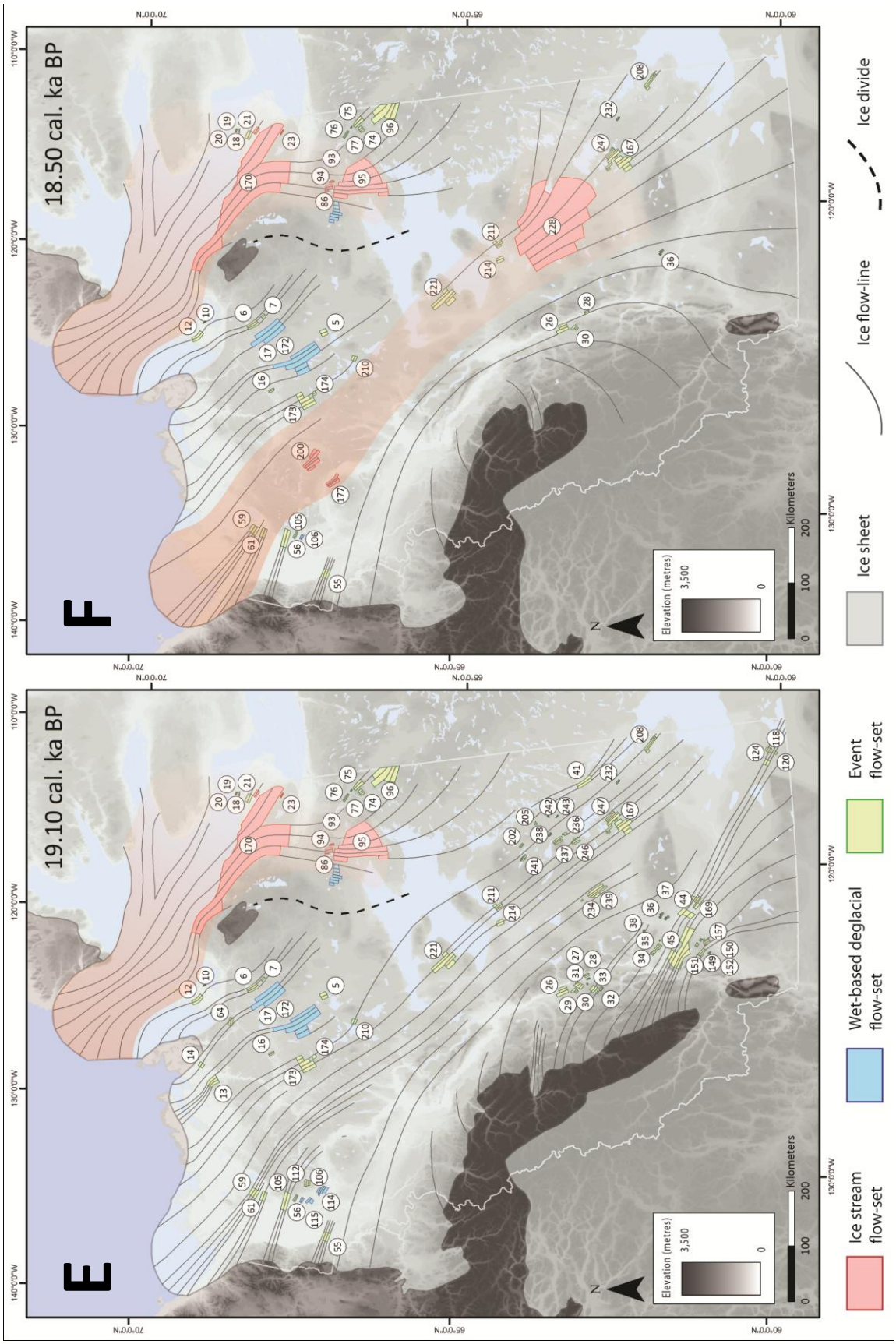

Figure 5-4 (cont.): Reconstructed ice sheet and ice stream dynamics in the north-west sector of the LIS during Late Wisconsinan glaciation.

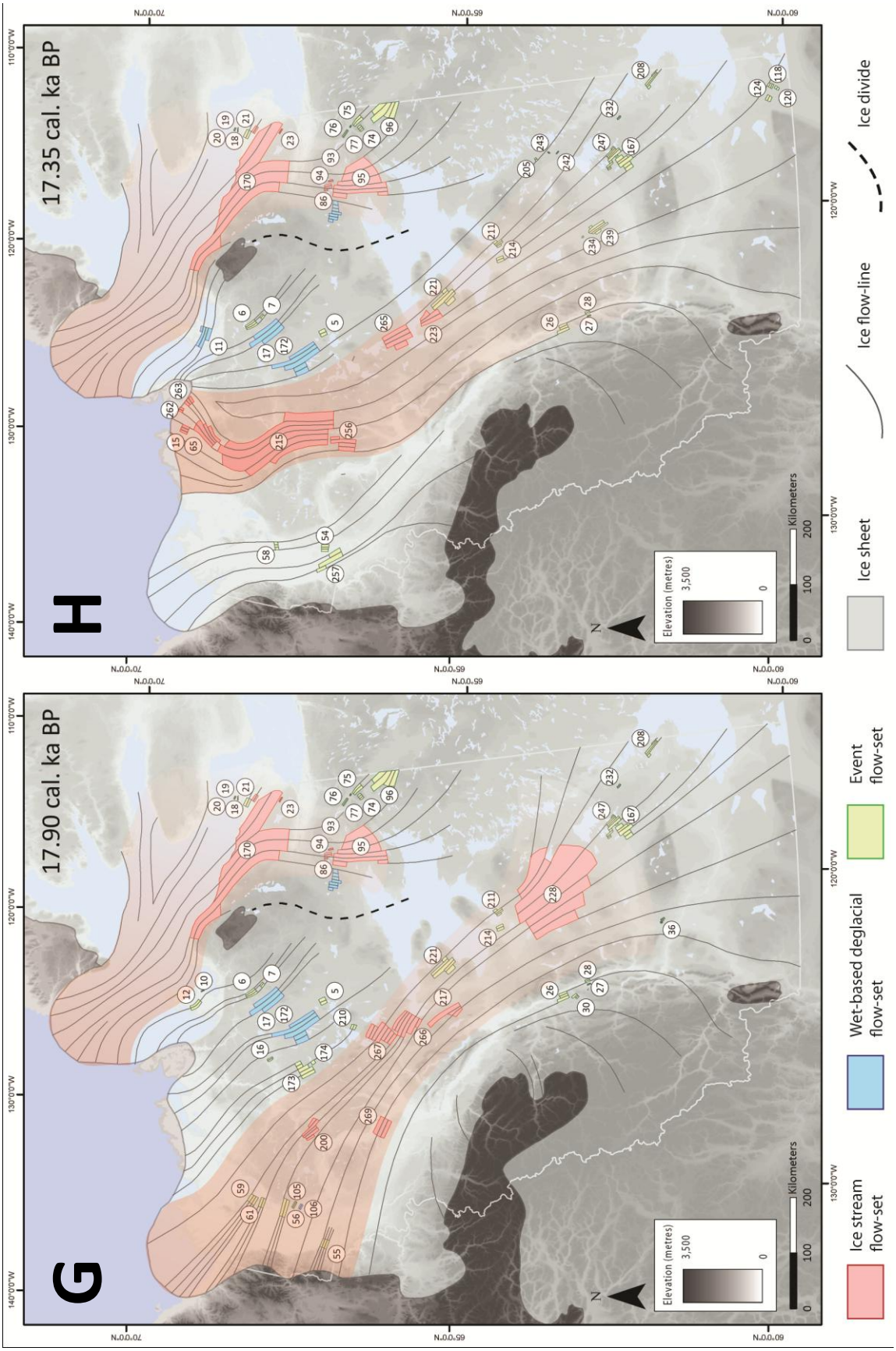

Figure 5-4 (cont.): Reconstructed ice sheet and ice stream dynamics in the north-west sector of the LIS during Late Wisconsinan glaciation.

5.6.2 17.35 – 14.8 cal. ka BP

The ice divide south of the Melville Hills persisted until 16.80 cal. ka BP alongside streaming flow towards the Anderson lobe (represented principally by Fs215, Fs15 and Fs256). Along with the loss of the Melville Hills ice divide, Fs95 subsequently became overridden by ice from the east (Figure 5-4I and J). The geomorphological signature of Fs82, which is located on the southern side of the Melville Hills, consists of abundant elongate glacial lineations, the morphology of which is similar to those along the Amundsen Gulf coast. Furthermore, the bedforms are highly convergent up-ice and divergent closer to the margin. This signature is typical of streaming flow (Stokes and Clark, 1999). Between 17.35 cal. ka BP and 16.20 cal. ka BP, the ice margin also changed markedly with the recession of ice across the Tuktoyaktuk Peninsula to the south-east and further inland near Paulatuk. The Mackenzie lobe also became much smaller during this period having retreated south-east towards the present day coast. The rate of change in ice margin geometry increased from 15.60 cal. ka BP during late Wisconsinan deglaciation and a general south-eastward and eastward retreat of ice occurred across the study area.

Between 15.60 cal. ka BP and 14.80 cal. ka BP, major ice loss from the Anderson lobe occurred. This included the whole of the area occupied by Fs215 (Figure 5-4K and L). An ice divide also developed south of Fs228 which separated ice flowing to the north from ice moving south: including ice exiting the basin now occupied by Great Slave Lake. North of this ice divide, nine flow-sets indicate the locations of streaming flow at 14.80 cal. ka BP. The most significant change post-15.60 cal. ka BP was the switching of flow from the Anderson to the Mackenzie lobes (Figure 5-4L). Streaming in the Mackenzie lobe is represented by Fs217, Fs266, Fs267, Fs268, Fs269 and Fs185. Down-ice of Fs185 in the Mackenzie Lobe, flow-sets are few in number and small, probably owing to the subsequent development of the Mackenzie Delta and extensive fluvial activity in the area which has hindered the preservation of glacial geomorphology. Of the flow-sets which are present, no further ice stream flow-sets have been identified. Instead, three wet-based deglacial flow-sets and four event flow-sets are present which indicate warm based conditions during deglaciation. However, given the limited geomorphological evidence available to delimit these flow-sets, it is possible that their full geomorphological signature has not been preserved. As such, these seven flow-sets could have been classified as ice stream flow-sets had a greater amount of geomorphological evidence been available. Indeed, Kleman *et al.* (2009) note the ambiguity associated with the genetic identification of flow-sets, especially event flow-sets. They state that many flow-sets may have origins in streaming or sheet flow but cannot be confidently assumed as such due to a lack of geomorphological evidence (Kleman *et al.,* 2006).

Streaming flow in the Mackenzie lobe was fed by Fs228 and Fs199, which lie south of Great Bear Lake. The large ice stream flow-set along the Amundsen Gulf coast (Fs272) remained active at the same time.

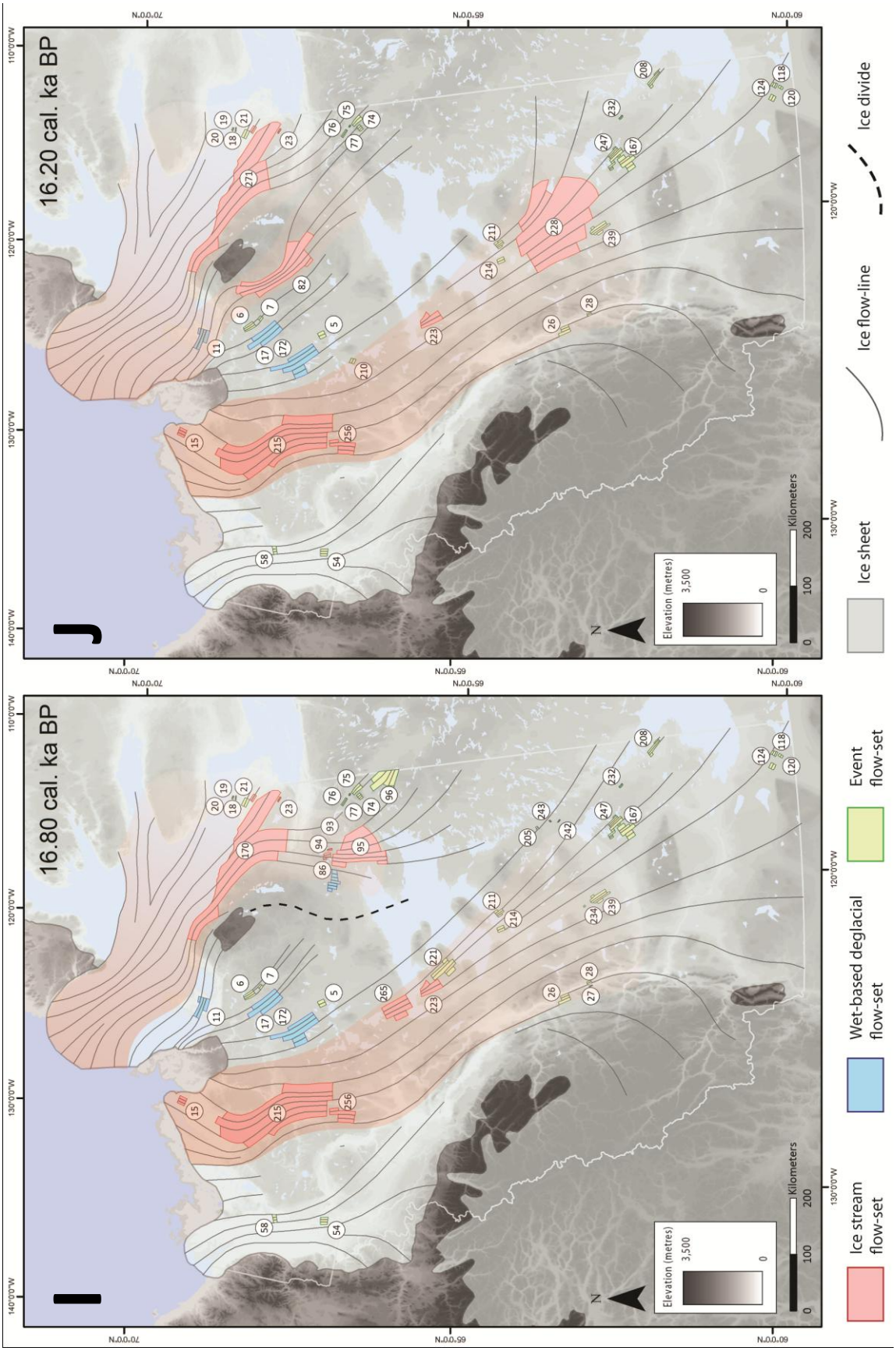

Figure 5-4 (cont.): Reconstructed ice sheet and ice stream dynamics in the north-west sector of the LIS during Late Wisconsinan glaciation.

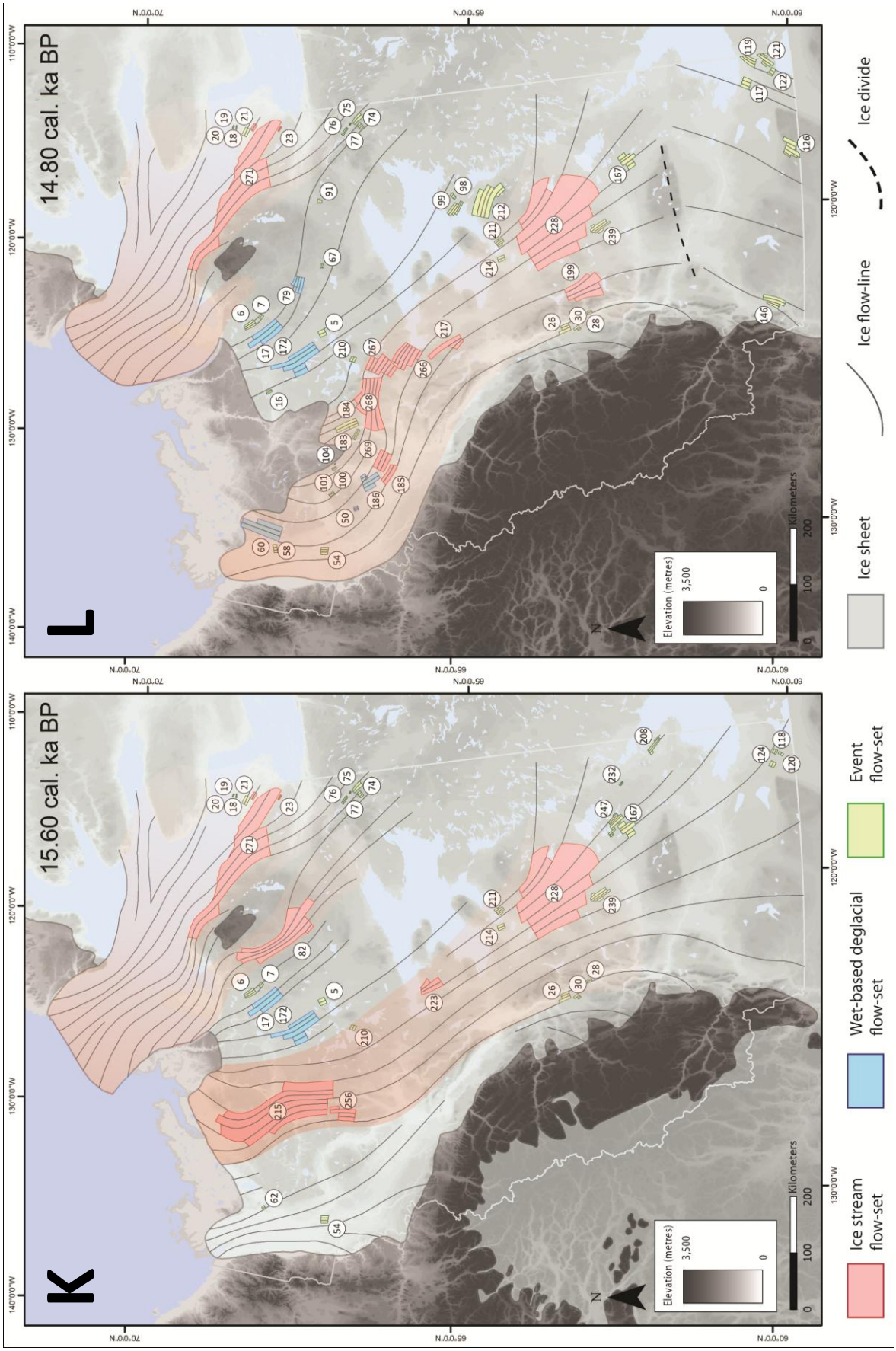

Figure 5-4 (cont.): Reconstructed ice sheet and ice stream dynamics in the north-west sector of the LIS during Late Wisconsinan glaciation.

5.6.3 14.8 – 14.1 cal. ka BP

At 14.25 cal. ka BP, ice stream Fs270 became active and the Mackenzie lobe retreated further south (see Figure 5-4M). A series of wet-based deglacial flow-sets were active along the ice margin and streaming flow to the south and along the Amundsen Gulf Coast persisted. By 14.10 cal. ka BP (Figure 5-4N), the ice margin had taken a more linear form and retreat had shifted to a west-east orientation. While streaming flow on the south-western side of Great Bear Lake continued, it became represented by a different group of flow-sets: Fs216, Fs240, Fs217 and Fs223. At this point, ice began originating from a more easterly position on the Canadian Shield. A lobe of ice containing a series of event flow-sets, whose geomorphological signature includes elongate flow traces without convergent or divergent arrangements, occupied the foot of the Rocky Mountains at 65°N. Streaming flow persisted along the Amundsen Gulf coast, as denoted by Fs272. South of the ice divide at 62°N, 23 flow-sets were active and indicate ice flow to the south-west. The activity of five wet-based deglacial flow-sets with abundant elongate glacial lineations and aligned eskers, indicate warm based deglacial conditions near to the ice margin. With subsequent retreat of the ice margin the ice divide shut down between 14.10 and 13.80 cal. ka BP (Figure 5-4M-O). In the southern part of the study area, ice retreated to the north-east and was accompanied by the operation of Fs252; a large wet-based deglacial flow-set. Streaming flow in the central portion of the study area remains represented by a similar arrangement of flow-sets. However, in the north, Fs272 was no longer operational.

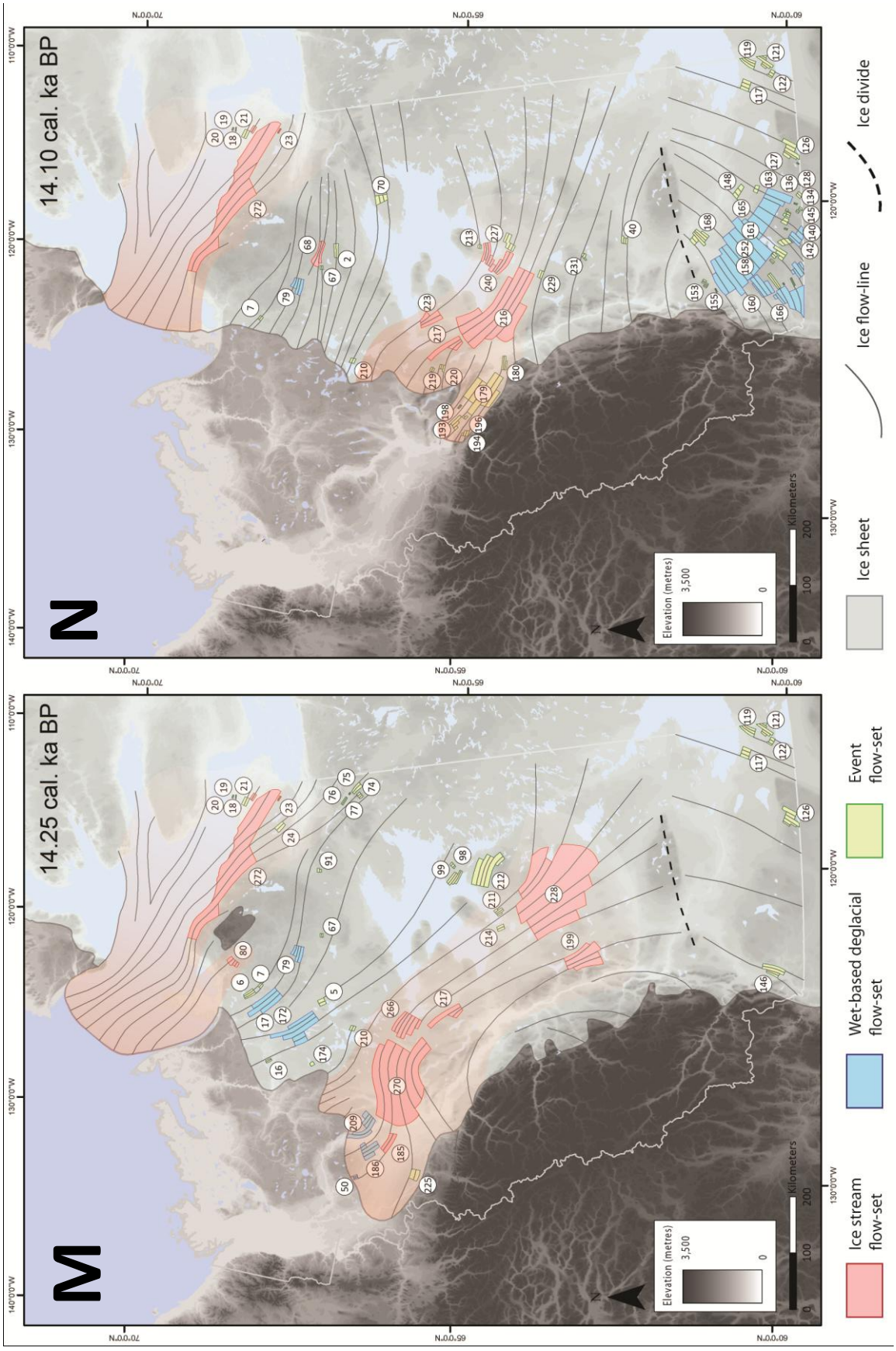

Figure 5-4 (cont.): Reconstructed ice sheet and ice stream dynamics in the north-west sector of the LIS during Late Wisconsinan glaciation.

5.6.4 14.1 – 11.45 cal. ka BP

At 13.80 cal. ka BP a small lobe developed to the east of Paulatuk and ice stream Fs66 switched on. Ice from the Amundsen Gulf in the vicinity of Kugluktuk continued to flow north-west into this small lobe at 13.80 cal. ka BP but also came onshore, flowing to the south-west (Figure 5-4O). This switch in flow is represented by a collection of flow-sets north of Great Bear Lake. The geomorphological signature of these flow-sets is complex and includes Fs1; a lone ice stream flow-set which has been previously documented as the Haldane palaeo-ice stream (Winsborrow *et al.,* 2004; Kleman and Glasser, 2007). The geomorphology associated with this flow-set includes abundant highly elongate glacial lineations and aligned eskers which strongly converge into a 50 km wide corridor. Unlike many of the other areas of streaming flow identified within this reconstruction, this area of streaming appears to be represented by just a single flow-set.

Fs1 only appears active during one time-step of the reconstruction: 13.80 cal. ka BP. After 13.80 cal. ka BP, the area occupied by Fs1 began to rapidly deglaciate. However, three wet-based deglacial flow-sets (Fs89, Fs83 and Fs92) along with five event flow-sets provide evidence for continued ice flow inland and south-west from Kugluktuk. South of Great Bear Lake, evidence for ice stream activity becomes limited to just Fs216 and Fs240 which fed a small lobe near Norman Wells. At 13.00 cal. ka BP (Figure 5-4Q), as the ice margin approached the Canadian Shield, a series of large wet-based deglacial flow-sets became active and fed a small area of streaming flow in Fs206. Fs88 indicates the final onset of streaming flow, again, near Kugluktuk. At 12.70 cal. ka BP, this fed a lobe on the southern side of the Melville Hills. At the same time, further large wet-based deglacial flow-sets fed two lobes; one which occupied the current outflow from great Slave Lake and one further north. By 12.0 cal. ka BP only small wet-based deglacial flow-sets were present along the ice margin and the study area rapidly became ice-free soon after this (Figure 5-4S).

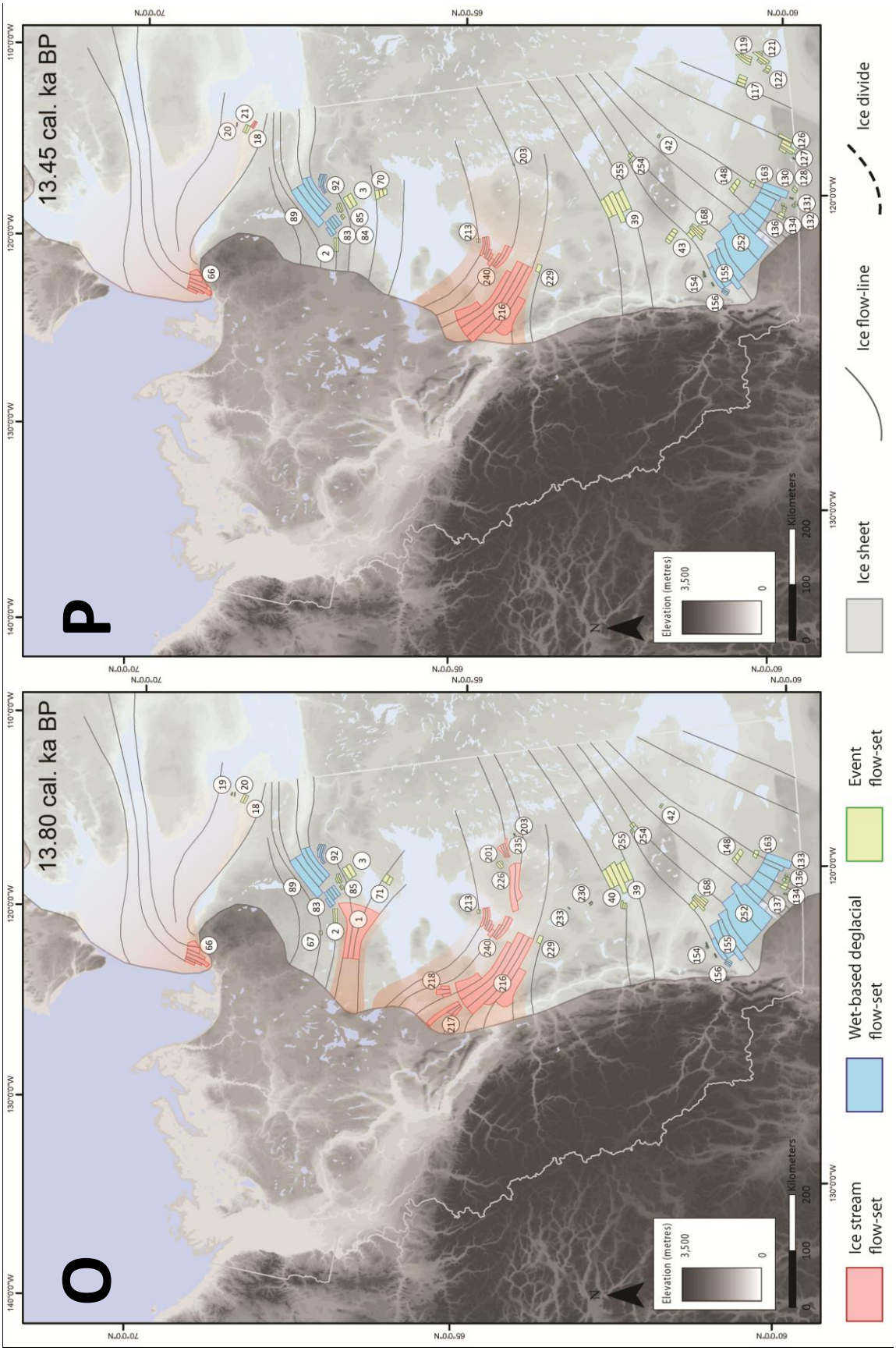

Figure 5-4 (cont.): Reconstructed ice sheet and ice stream dynamics in the north-west sector of the LIS during Late Wisconsinan glaciation.

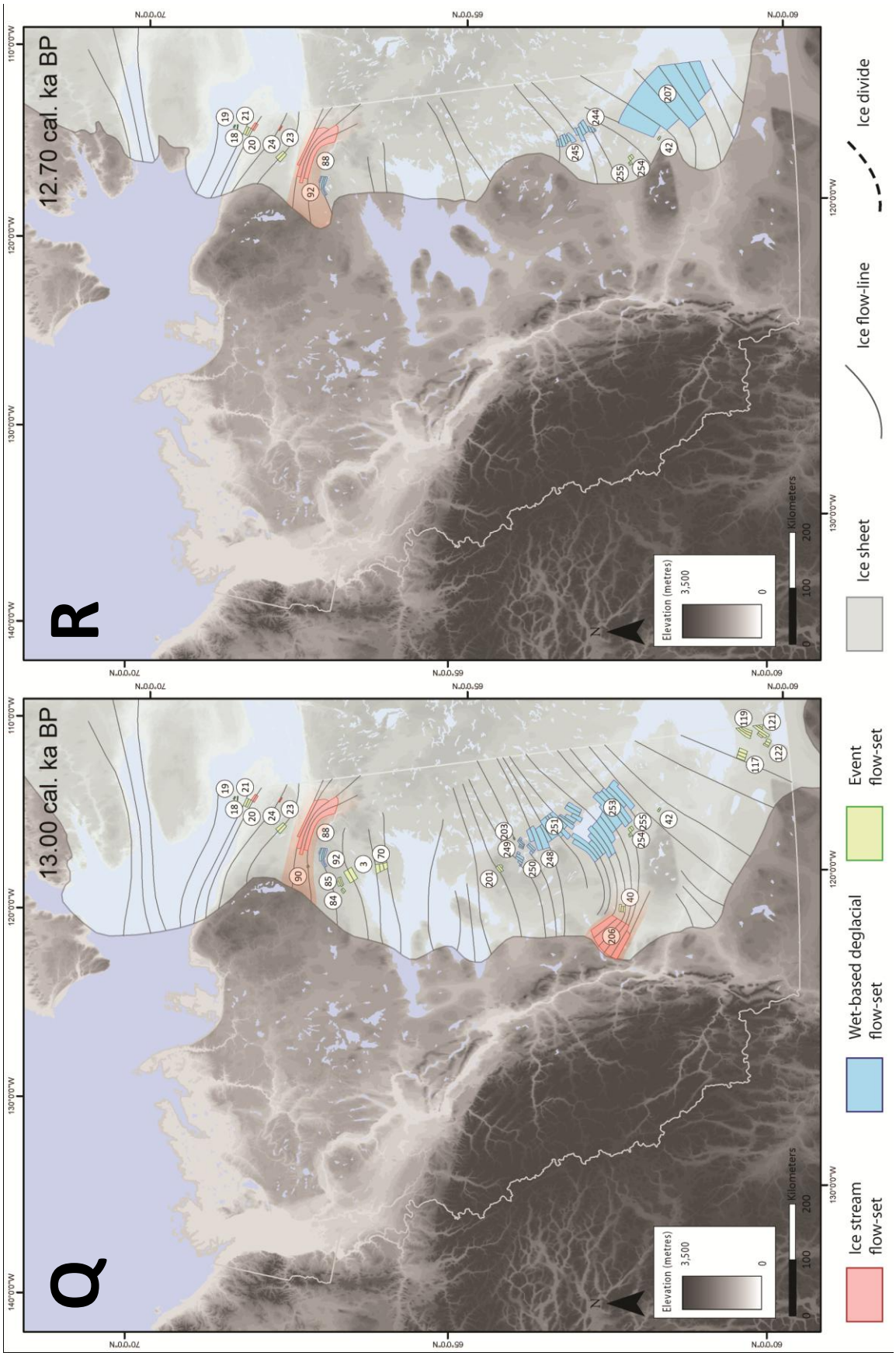

Figure 5-4 (cont.): Reconstructed ice sheet and ice stream dynamics in the north-west sector of the LIS during Late Wisconsinan glaciation.

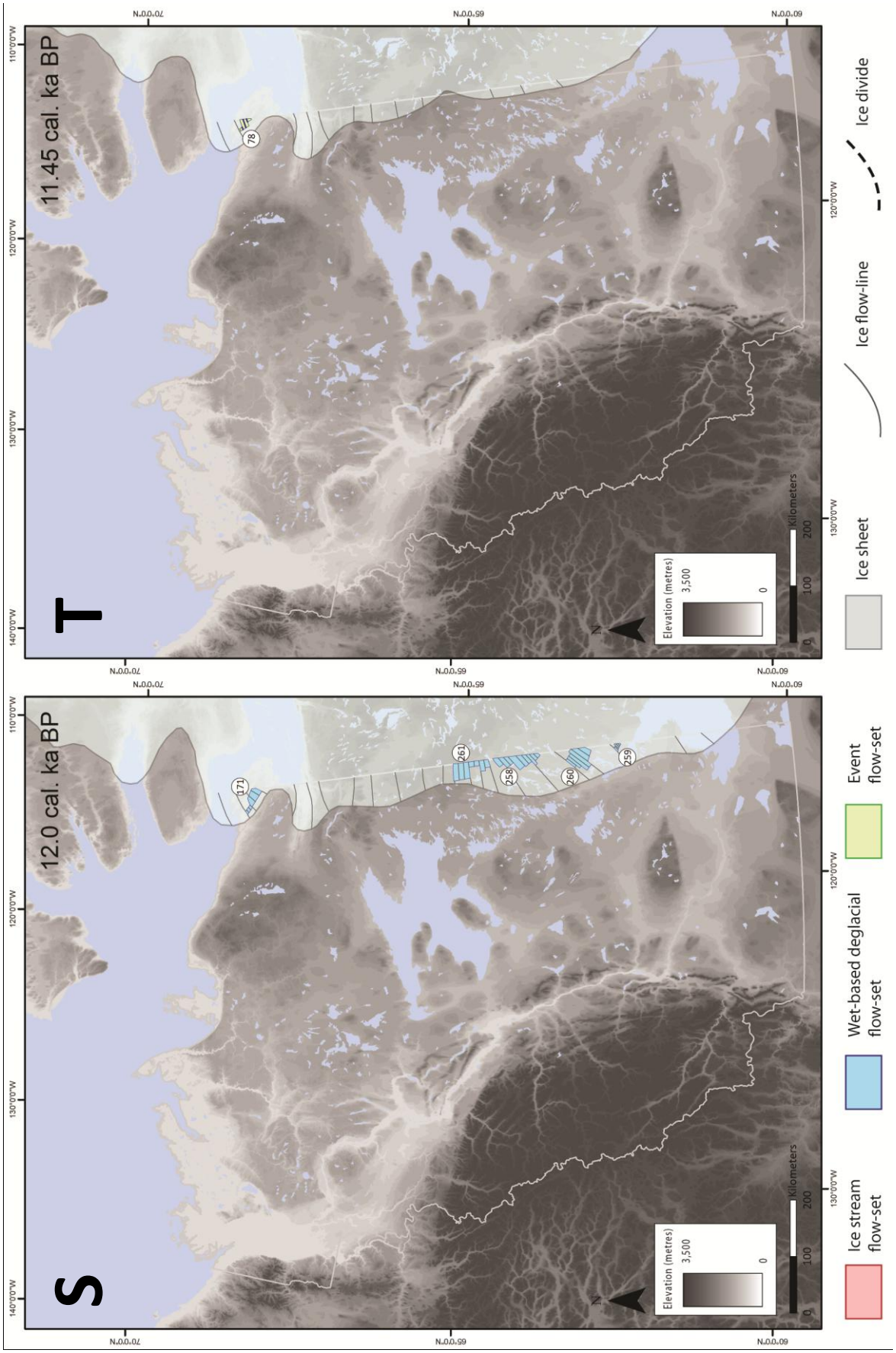

Figure 5-4 (cont.): Reconstructed ice sheet and ice stream dynamics in the north-west sector of the LIS during Late Wisconsinan glaciation.

5.6.5 Additional flow-sets

Forty-three flow-sets have been identified which are not easy to fit into the ice sheet reconstruction presented above, see Figure 5-4 There are a number of reasons for this which are explained below. Firstly, twenty-six of the flow-sets shown in Figure 5-5 are orientated north-east to south-west across the northern part of the study area (from Amundsen Gulf towards the Yukon Mountains). They therefore lie almost perpendicular to the dominant ice flow direction during Late Wisconsinan deglaciation (south-east to north-west). Large-scale, almost implausible, ice sheet reorganisation would have been required following the LGM in order to generate this spatial arrangement of flow traces during the Late Wisconsinan. It is therefore likely that these flow-sets were formed during an earlier glacial phase possibly during ice sheet build up when a dispersal centre may have existed over the Canadian Arctic. Indeed, Kleman *et al.* (2010) indicate that a dispersal centre over the central Arctic produced a radial flow pattern which included ice flow from north-east to south-west across the study area (Figure 5-6). The preservation of pre-LGM flow-sets has also been documented by Kleman (1994) who confirm that the preservation of landforms which predate the last glacial event is possible, not just in areas characterised by cold based ice. Indeed, such landforms have been identified in the areas covered by both the Fennoscandian and Laurentide ice sheets (Kleman, 1994).

Further flow-sets which do not fit into the reconstruction may have existed at intermediary time-steps between those documented in Section 5.6. Examples include Fs28 and Fs52, which are classified as wet-based deglacial flow-sets based on their geomorphological signature. Along the southern margin of the study area at 60°N, Fs144, Fs146, Fs169 and Fs186, indicate flow to the south-west. These flow-sets cannot have formed isochronously with neighbouring flow-sets due to subtle differences in the orientation of their associated flow traces. They are also therefore assumed to have formed at intermediary time-steps between those shown in the reconstruction and during periods of localised ice sheet reorganisation during deglaciation.

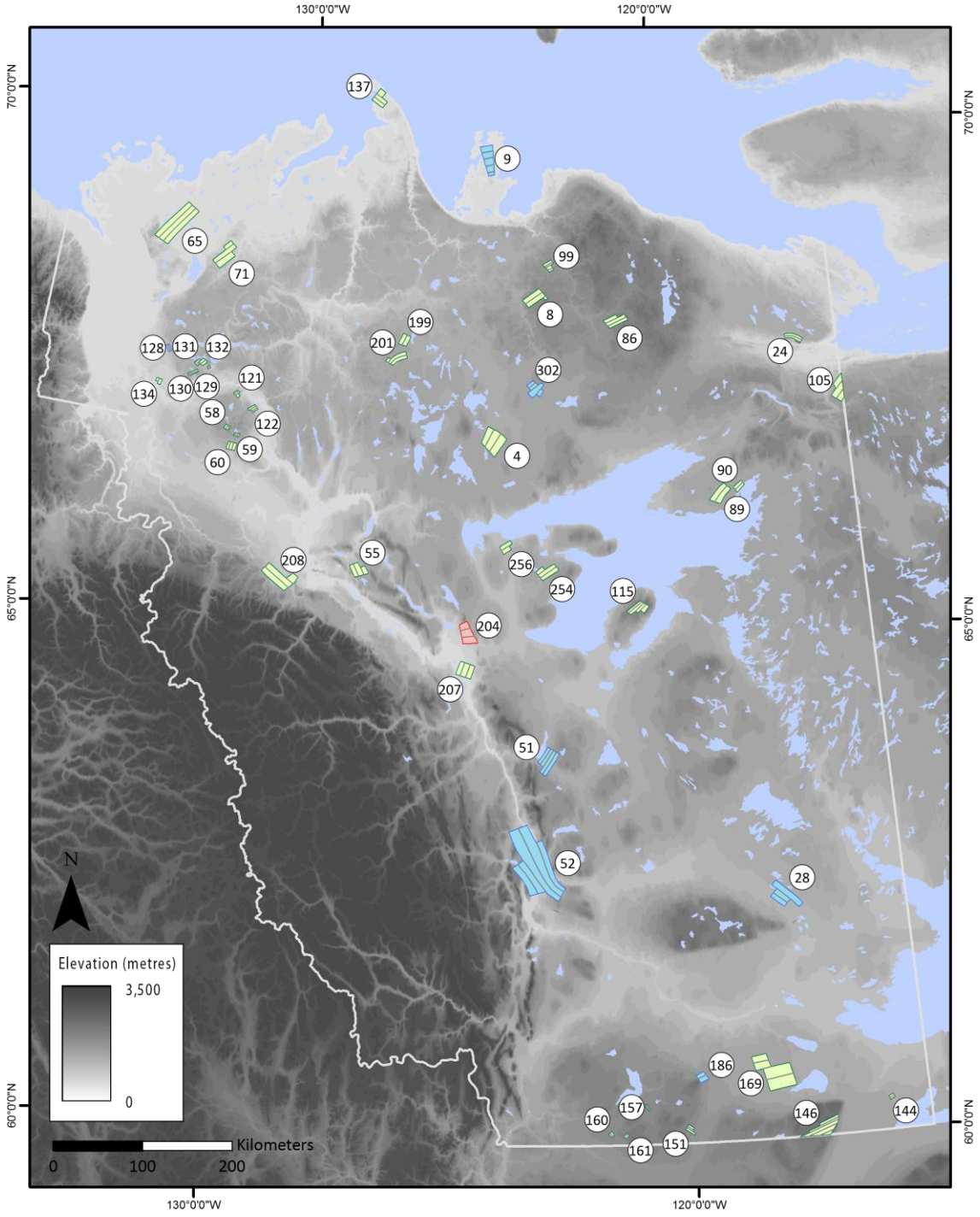

Figure 5-5: Additional flow-sets which cannot be reconciled with the reconstruction shown in Section 5.6.

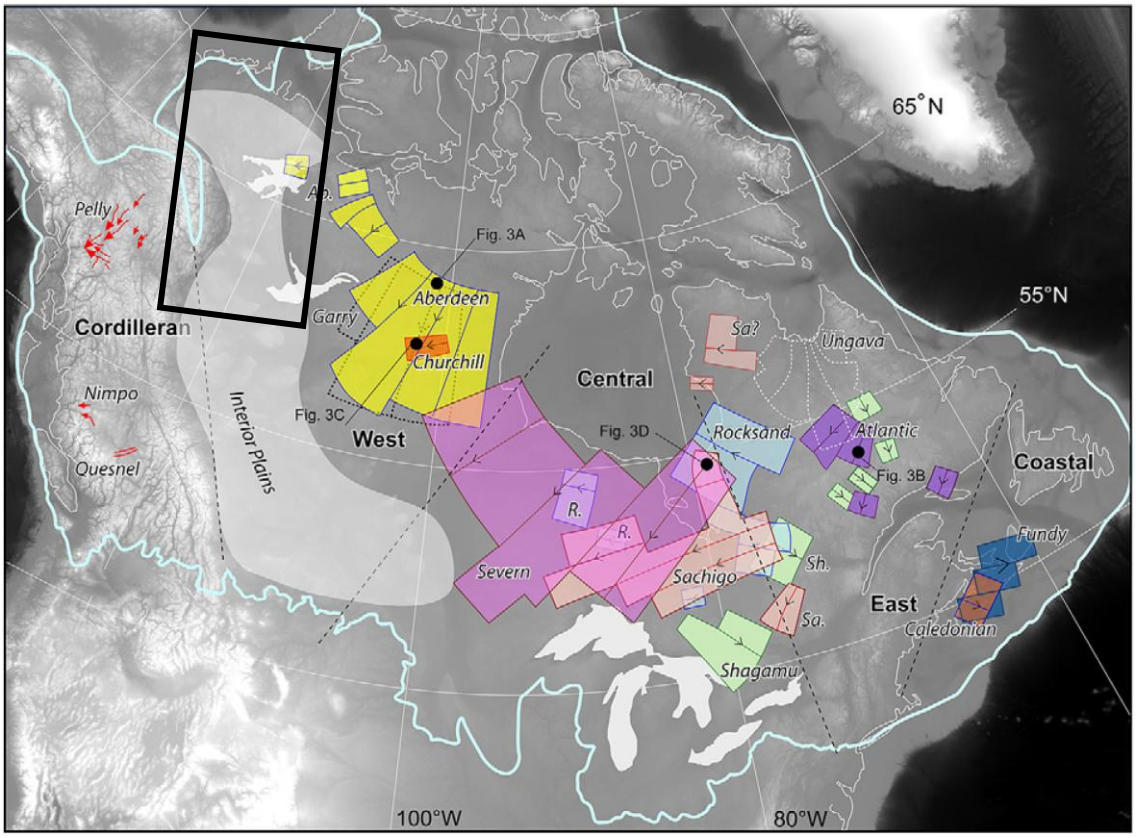

Figure 5-6: Landform flow-sets suggested by Kleman et al. (2010) to be older than the LGM. In the north-west LIS, the yellow flow-sets indicate radial ice flow away from the central Canadian Arctic and from north-east to south-west across the study area. This is a similar ice flow orientation to that suggested by some of the flow-sets shown in Figure 5-5 which are also suggested to be of pre-LGM origin. Figure taken from Kleman et al. (2010). The study area is marked by a black box.

5.7 Ice stream activity

Thirty-five flow-sets display a geomorphological signature associated with ice stream activity (see Stokes and Clark, 1999). Together, these ice stream flow-sets document the operation of seven ice streams in the north-west sector of the LIS throughout Late Wisconsinan deglaciation, hereafter named the Mackenzie (east and west branches), Amundsen, Paulatuk, Kugluktuk, Haldane and Fort Simpson. Figure 5-7 schematically illustrates the location of these ice streams.

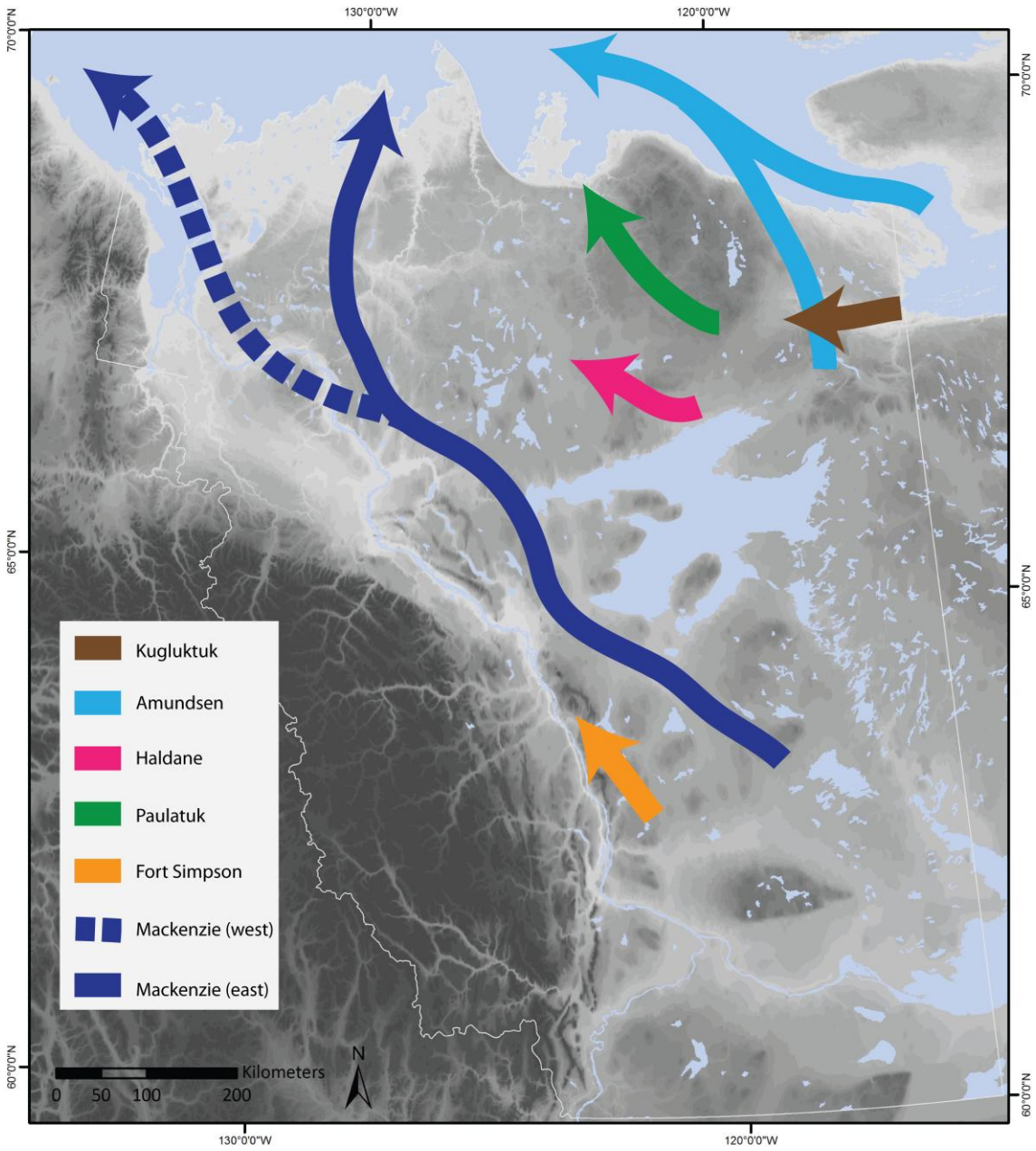

Figure 5-7: A schematic illustration of the seven ice streams which were active in the north-west sector of the LIS during Late Wisconsinan deglaciation.

In some cases, multiple flow-sets together document the activity of an ice stream. However, each individual flow-set was required to display the characteristics of ice stream activity in order to be classified as an ice stream flow-set. This allowed for a more rigorous and less subjective methodology in which the location of ice stream activity was not identified until the reconstruction shown in Section 5.6 was completed. The geomorphological signature and activity of each of the seven ice streams identified in the north-west sector of the LIS will be discussed in turn below.

5.7.1 Amundsen Gulf palaeo-ice stream

The Amundsen Gulf palaeo-ice stream has previously been documented by Stokes *et al.* (2006; 2009). The ice stream was approximately 600 km long and was fed by ice from the Keewatin Dome of the LIS. As shown in the LIS reconstructions of Dyke *et al.* (2003), it terminated in a lobate ice margin on the continental shelf edge, west of Banks Island. It was comparable in size to the M'Clure Strait palaeo-ice stream that occupied the trough to the north of Victoria Island (see Stokes *et al.,* 2005). The location of the ice stream was controlled by topography with the ice stream occupying a trough with an average depth of 200 m. The ice stream was active for a large part of overall LIS deglaciation following the LGM. According to Lakeman *et al.* (2012), the Amundsen Gulf ice stream was up to 700 m thick and began to retreat from its maximum position prior to 13 cal. ka BP. In the study area, the ice stream is represented by a single flow-set located along the northern coast of the study area (Fs170). This large flow-set is ~ 300 km long and comprised of abundant elongate bedforms. In the east, these bedforms trend south to north before shifting to a south-east to north-west orientation as they converge towards Amundsen Gulf (see Chapter 4, Figure 4-3). As noted by Stokes *et al.* (2006), the glacial geomorphology on the southern side of Victoria Island is also characterised by highly elongate bedforms which converge towards the gulf. Furthermore, Lakeman *et al.* (2012) indicate the presence of glacial flutings on the floor of Amundsen Gulf and a series of moraines at the western mouth of the trough which mark the temporary ice positions of a retreating ice margin.

5.7.2 Mackenzie palaeo-ice streams (east and west)

The Mackenzie palaeo-ice stream supplied ice to the north-western most margin of the LIS. It followed a meandering pathway west of Great Bear Lake around the base of the adjacent Yukon, Richardson and Mackenzie Mountains (see Figure 5-7). At 67° N, the ice stream split into an eastern and western branch although these were not coincident in time. The eastern branch of the ice stream was located in the vicinity of the present day Anderson River, while the western branch delivered ice to the margin over the present day Mackenzie Delta. The ice stream was subject to limited topographic control, having occupied a broad low-lying region in which it migrated laterally throughout deglaciation. The Mackenzie palaeo-ice stream switched on and off during deglaciation (see Figure 5-4). The western branch of the ice stream was the first to become active ~ 18.50 cal. ka BP and remained operational until 14.80 cal. ka BP. The eastern branch of the ice stream became active ~ 17.35 cal. ka BP and operated in two phases, both of which were complete by 13 cal. ka BP. The ice stream has previously been hypothesised by Clark (*unpublished*, cited in Winsborrow *et al.,* 2004) but detailed geomorphological evidence has not been presented. As shown in Figure 5-8, mapping indicates

that south of Great Bear Lake, strongly convergent, elongate bedforms and aligned eskers are arranged to form a 'fan-shaped' flow-set (Fs228). This flow-set represents the onset zone of the Mackenzie palaeo-ice stream and contains some of the most closely spaced and elongate bedforms that were mapped in the study area. Additional examples of geomorphology associated with the Mackenzie ice streams are shown in Figure 4-5A and Figure 4-5B. Further west, an additional flow-set (Fs199) also represents part of the southern limit of the Mackenzie palaeo-ice stream (Figure 5-9).

Between 64 and 67° N, elongate drumlins with aligned eskers trend south-east to north-west and continue to dominate the geomorphology. These bedforms cross-cut the surrounding perpendicular glacial lineations to form a corridor of elongate bedforms with abrupt lateral margins. Beyond 67° N, the eastern and western branches of the Mackenzie ice stream are represented by different geomorphological signatures. The geomorphological signature of the eastern branch of the ice stream ice characterised by abundant glacial lineations which form a sinuous corridor between 67° N and the Arctic Ocean coast (Fs215). In contrast, geomorphological evidence for the western branch of the ice stream is more subdued and bedforms are sparse. While the eastern branch of the ice stream is represented by just a single flow-set (Fs215), the western branch has been reconstructed based on a larger number of much smaller ice stream flow-sets.

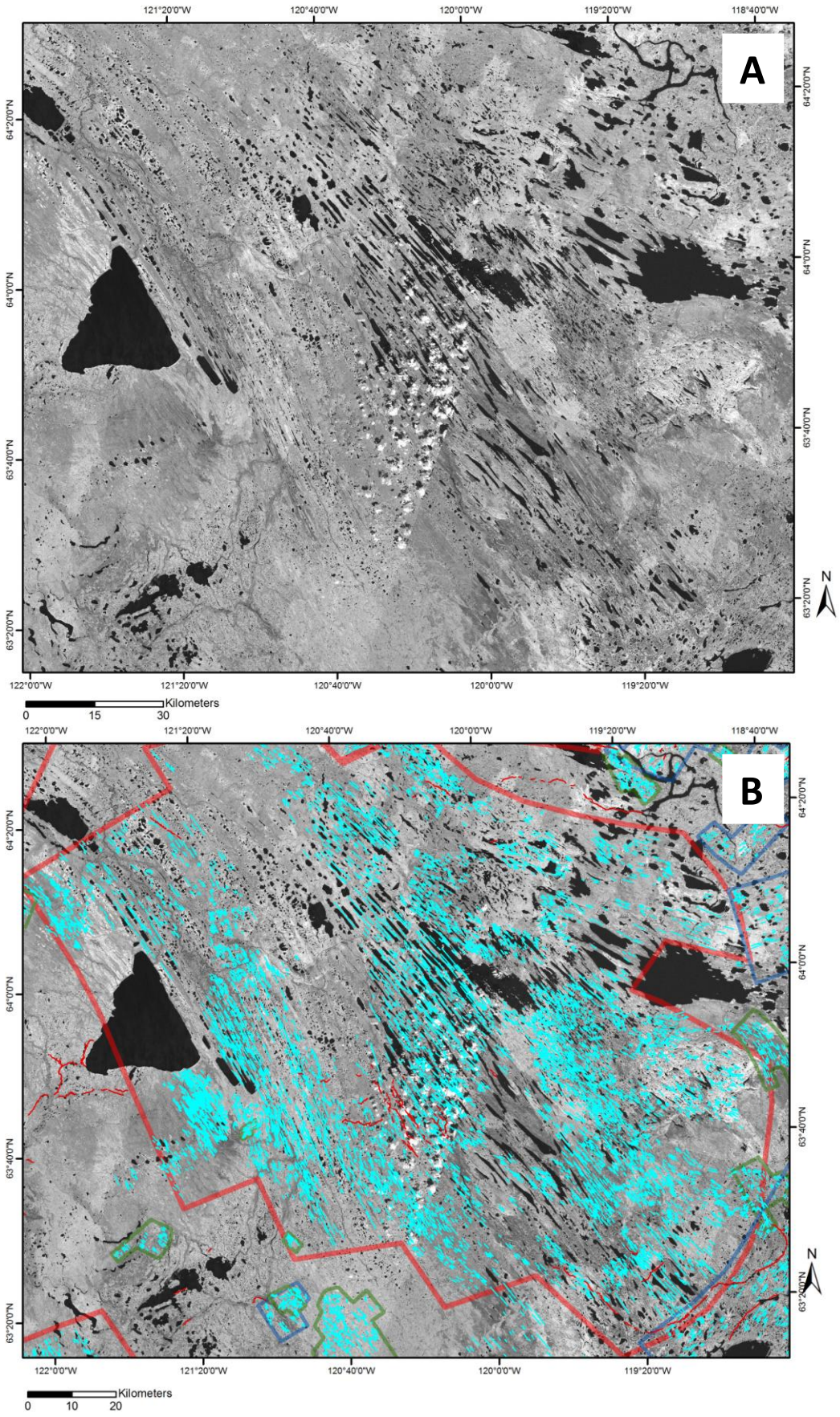

Figure 5-8: Fs228, the onset zone of the Mackenzie palaeo-ice stream (both eastern and western branches). A: the geomorphology associated with Fs228. B: the flow-set is outlined by

a thick red line, glacial lineations are shown in aqua blue, and eskers are the fine red lines. Other flow-sets are shown around the periphery of Fs228 which correspond in colour to those shown on Figure 5-2. The flow-set includes abundant highly elongate bedforms which trend south-east to north-west and also converge in the same direction. While some eskers are aligned with the surrounding glacial lineations, others are perpendicular. This can be attributed to the complex switches in ice flow orientation which occurred in this sector of the LIS, particularly during deglaciation, i.e. the ice stream operated from south to north but deglaciation later progressed from west to east.

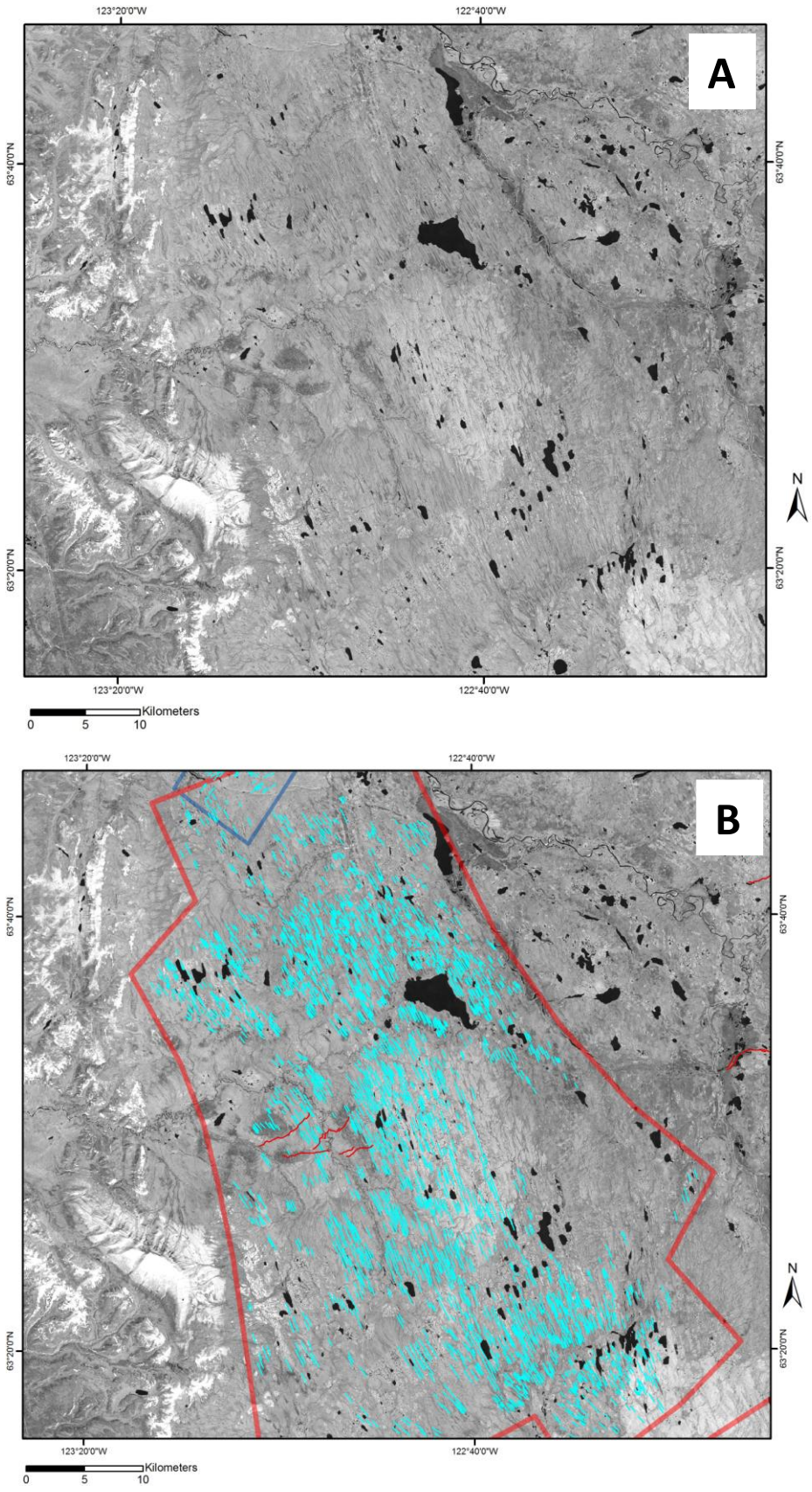

Figure 5-9: A smaller flow-set (Fs199), also located at the southern end of the Mackenzie palaeo-ice stream. A: the geomorphology associated with Fs199. B: the flow-set is outlined by a thick red line, glacial lineations are shown in aqua blue and eskers are the fine red lines. Fs199 includes abundant glacial lineations. Although the bedforms display only a moderate level of

convergence towards the north-west, they do form a corridor with an abrupt lateral margin, particularly on the eastern side of the flow-set.

5.7.3 Paulatuk palaeo-ice stream

Located on the southern side of the Melville Hills, the Paulatuk palaeo-ice stream occupied a shallow topographic trough (see Figure 5-7). The location of the ice stream may therefore have been controlled by topography. The geomorphological signature of the ice stream is encompassed in a single flow-set (Fs82), which trends south-east to north-west. This flow-set contains abundant elongate bedforms which are arranged in a convergent pattern at the up-ice end of the flow-set, and a divergent pattern at the down-ice end. Fs82 is ~ 150 km long and indicates that streaming flow took place in the area between ~ 16.20 and ~ 15.60 cal. ka BP, following the break-down of an ice divide on the south-eastern corner of the Melville Hills. This ice stream fed ice into Amundsen Gulf and can therefore be thought of as a tributary to the Amundsen Gulf palaeo-ice stream as discussed in Section 5.7.1. Despite evidence for the Amundsen Gulf palaeo-ice stream having been well documented (see Stokes *et al.,* 2005; Winsborrow *et al.,* 2004 and Kleman and Glasser, 2007), evidence for its tributary (the Paulatuk ice stream) has not.

5.7.4 Fort Simpson palaeo-ice stream

The Fort Simpson palaeo-ice stream is represented by a single ice stream flow-set (Fs206) which is orientated parallel to the foot of the Yukon Mountains at ~ 63° N. It was the most short-lived of the seven ice streams identified and is depicted in just one of the time-steps shown in the reconstruction in Section 5.6 (13.00 cal. ka BP). This ice stream, which has not previously been identified, does not occupy a topographic trough, so topography is not thought to have exerted a control on its activity. The clear geomorphological signature of this ice stream includes highly elongate bedforms with aligned eskers, and a divergent down-ice zone, all of which are suggested by Stokes and Clark (1999) to be characteristic of ice stream activity. Given the proximity of this ice stream to the neighbouring Mackenzie ice stream, its comparable orientation, and its activity immediately following the shut-down of the Mackenzie ice stream, it is suggested that this ice stream represents a final phase of ice streaming towards the north-west during deglaciation. Furthermore, the ice stream was active during a transitional phase when ice flow switched towards the south-west. This is indicated in the reconstruction in Section 5.6 by a group of wet-based deglacial flow-sets along the periphery of the Canadian Shield which became active ~ 13.00 cal. ka BP (see Figure 5-4).

5.7.5 Haldane palaeo-ice stream

The Haldane palaeo-ice stream has previously been hypothesised by Clark (*unpublished*, cited in Winsborrow *et al.,* 2004). It was located on the northern shore of Great Bear Lake and was a topographically controlled ice stream having occupied a short (~ 100 km), 30 km wide valley. While the larger ice streams in the study area are represented in the geomorphological record by several flow-sets (e.g. the Mackenzie ice streams), the geomorphological signature of the Haldane ice stream is contained within a single flow-set (Fs1). The geomorphology associated with this flow-set is shown in Figure 5-10.

Fs1 is characterised by closely spaced, highly elongate glacial lineations which converge strongly at the eastern end of the flow-set and mirror the 'bottle-neck' provided by the local topography. The activity of the Haldane ice stream was short-lived (< 650 years). Indeed, it is only depicted in one time-step of the reconstruction shown in Section 5.6 (13.80 cal. ka BP).

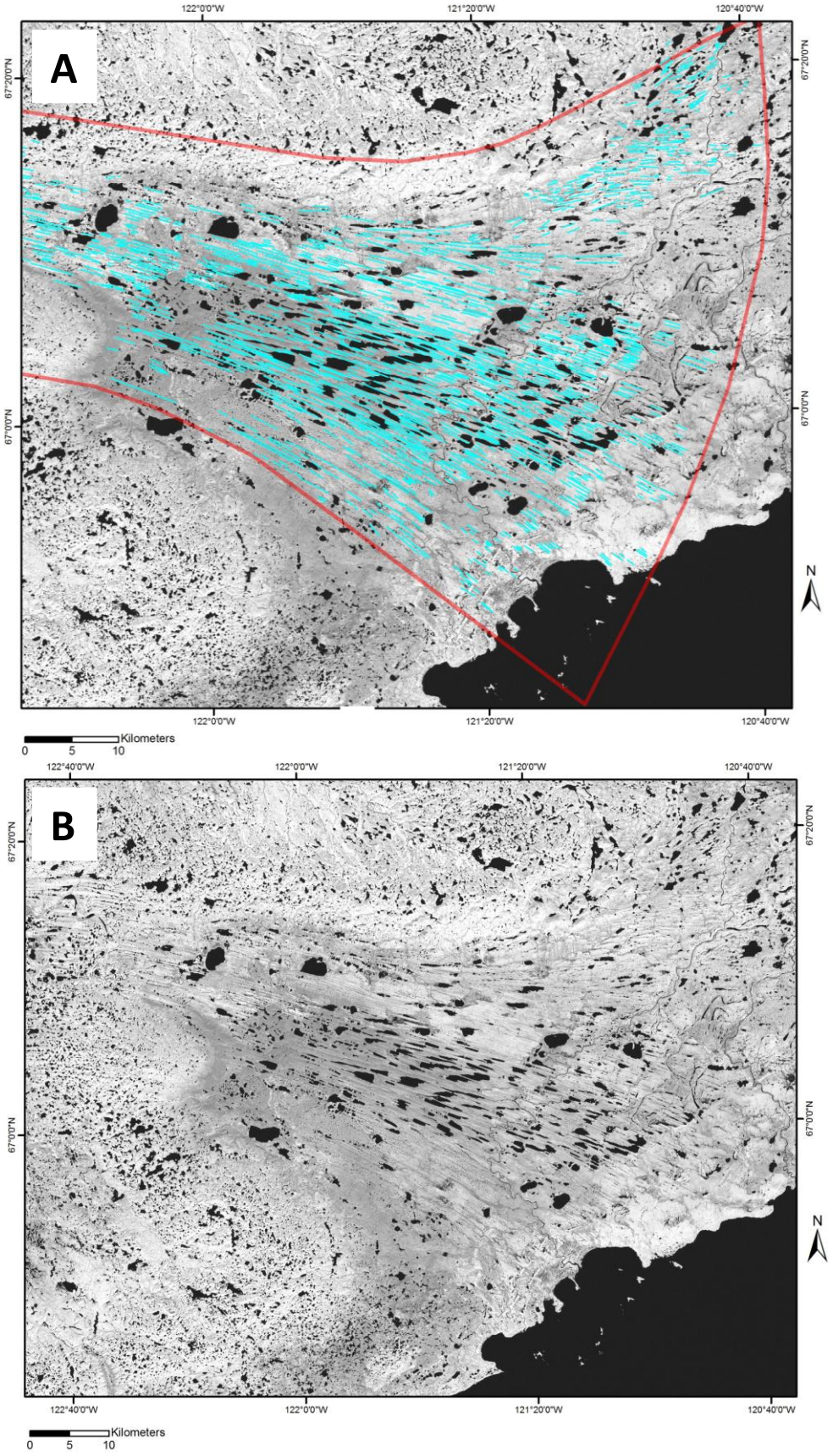

Figure 5-10: The Haldane palaeo-ice stream is located on the northern side of Great Bear Lake and is represented in the geomorphological record by abundant glacial lineations which converge strongly into a corridor of lineations with abrupt lateral margins. Together these

closely spaced bedforms form Fs1. A: the flow-set is outlined by a thick red line and glacial lineations are shown in aqua blue. B: the geomorphology associated with Fs1.

5.7.6 Kugluktuk palaeo-ice stream

The Kugluktuk palaeo-ice stream is represented in the geomorphological record by Fs88. Previous compilations of ice stream activity in the LIS have not identified an ice stream in this location (see Winsborrow *et al.,* 2004). The glacial geomorphology associated with this flow-set is shown in Figure 5-11. The flow-set trends roughly east to west on the south-eastern side of the Melville Hills and displays characteristics indicative of having formed under streaming flow, e.g. highly elongate bedforms which converge strongly into a corridor of bedforms with an abrupt lateral margin. The Kugluktuk ice stream was active between ~ 13.00 and ~ 12.70 cal. ka BP as shown in Figure 5-4, and its location was not controlled by the underlying topography. At the eastern end of the flow-set, lineations converge into a corridor of glacial lineations with abrupt lateral margins. However, unlike the Haldane ice stream, the geomorphology associated with Fs88 is underlain by cross-cutting glacial lineations associated with earlier ice flow orientations (see Section 5.6). During the early stages of deglaciation, ice flow in the vicinity of Fs88 was orientated south to north into Amundsen Gulf. However, as deglaciation progressed, and the ice divide on the southern side of the Melville Hills diminished, ice flow shifted to an east-west orientation towards Fs1 (the Haldane ice stream). The Kugluktuk ice stream was operational following the shut-down of the Haldane ice stream and fed ice to a lobate ice margin at ~ 67° N.

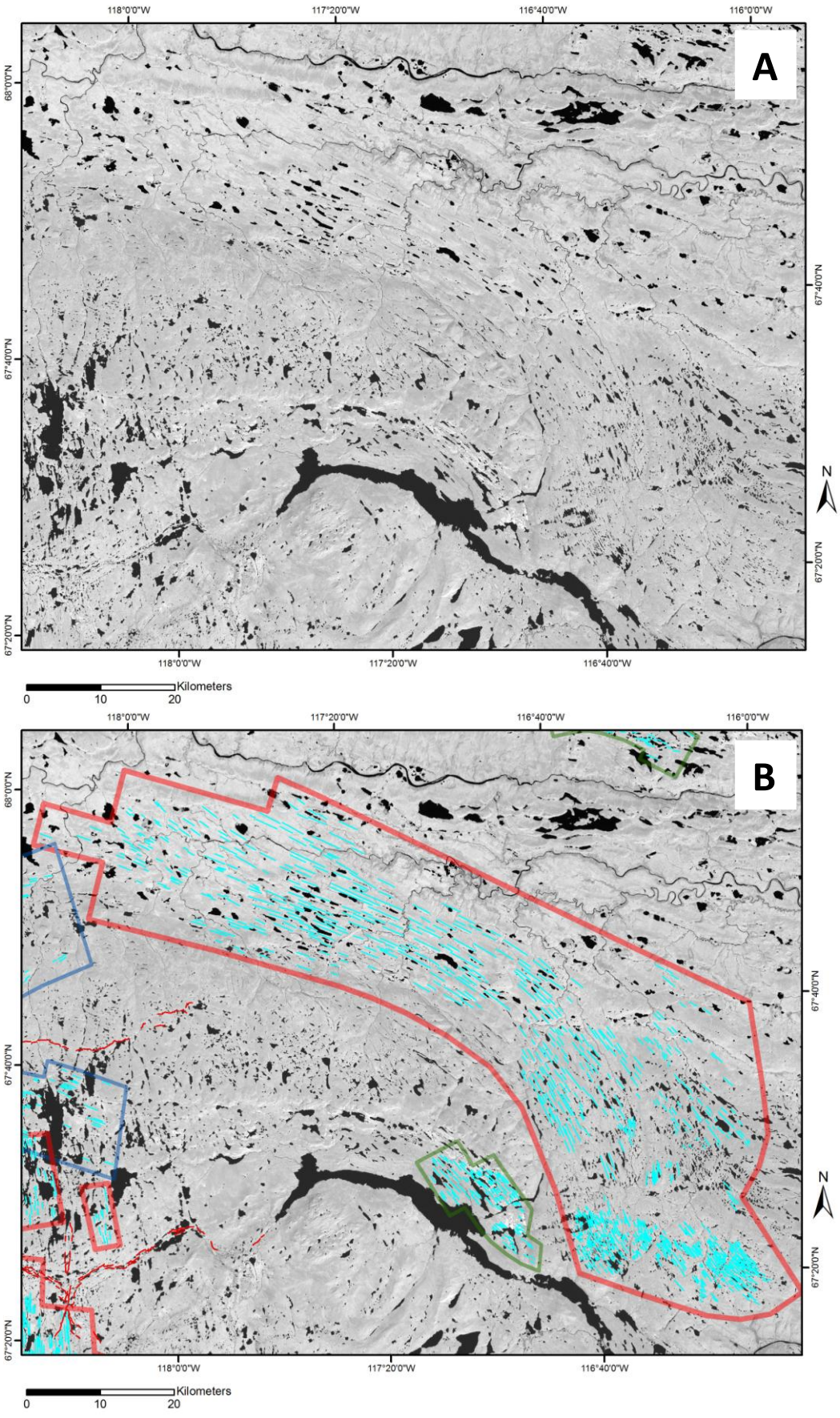

Figure 5-11: The flow-set shown above is Fs88 which represents the Kugluktuk palaeo-ice stream. A: the geomorphology associated with Fs88. B: the flow-set is comprised of glacial lineations which are particularly closely spaced at the eastern end of the flow-set. At the

eastern end of the flow-set, lineations indicate ice flow towards the north-west while in the west, the flow-set indicates more westerly flow. The flow-set is outlined by a thick red line, glacial lineations are shown in aqua blue and eskers are the fine red lines. Other flow-sets are shown around the periphery of Fs88 which correspond in colour to those shown on Figure 5-2.

A summary of ice stream activity in the north-west sector of the LIS is provided in Figure 5-12 and indicates a peak in ice stream activity between 15 and 13 cal. ka BP. Some ice streams persisted over millennial timescales throughout deglaciation such as the Mackenzie (east and west) and Amundsen ice streams. However, other ice streams existed as just short pulses of streaming flow (500 years) during deglaciation, for example, the Haldane, Fort Simpson and Kugluktuk ice streams. Furthermore, while the Haldane ice stream is represented in the reconstruction by just one flow-set, the Mackenzie ice stream is represented by many, but sometimes smaller, flow-sets. The arrangement and geometry of the multiple flow-sets associated with some ice streams, indicates that these ice streams underwent sustained reorganisation during deglaciation. This is particularly evident from the Mackenzie ice stream, which initially fed a lobe over the Mackenzie Delta (Mackenzie west: phase 1) before switching flow direction to the Anderson River (Mackenzie east) and then, in turn back to its westerly position (Mackenzie west: Phase 2). While the location of streaming at the margin switched position, the source of streaming flow along the western side of Great Bear Lake remained intact.

Streaming flow during deglaciation appears to have been dominated by a small number of large ice streams such as the Mackenzie and Amundsen ice streams, particularly during its early stages. The Mackenzie ice streams (east and west) were both in excess of 900 km long and had onset zones deep within the ice sheet. Consequently, these larger ice streams were probably crucial to sustained large-scale mass loss from this sector of the ice sheet when the ice margin remained relatively stable and offshore. In contrast, the smaller ice streams were often closer to the ice margin and played a key role in the reorganisation of the ice sheet over shorter time-scales during the periods of most rapid eastward retreat of the LIS.

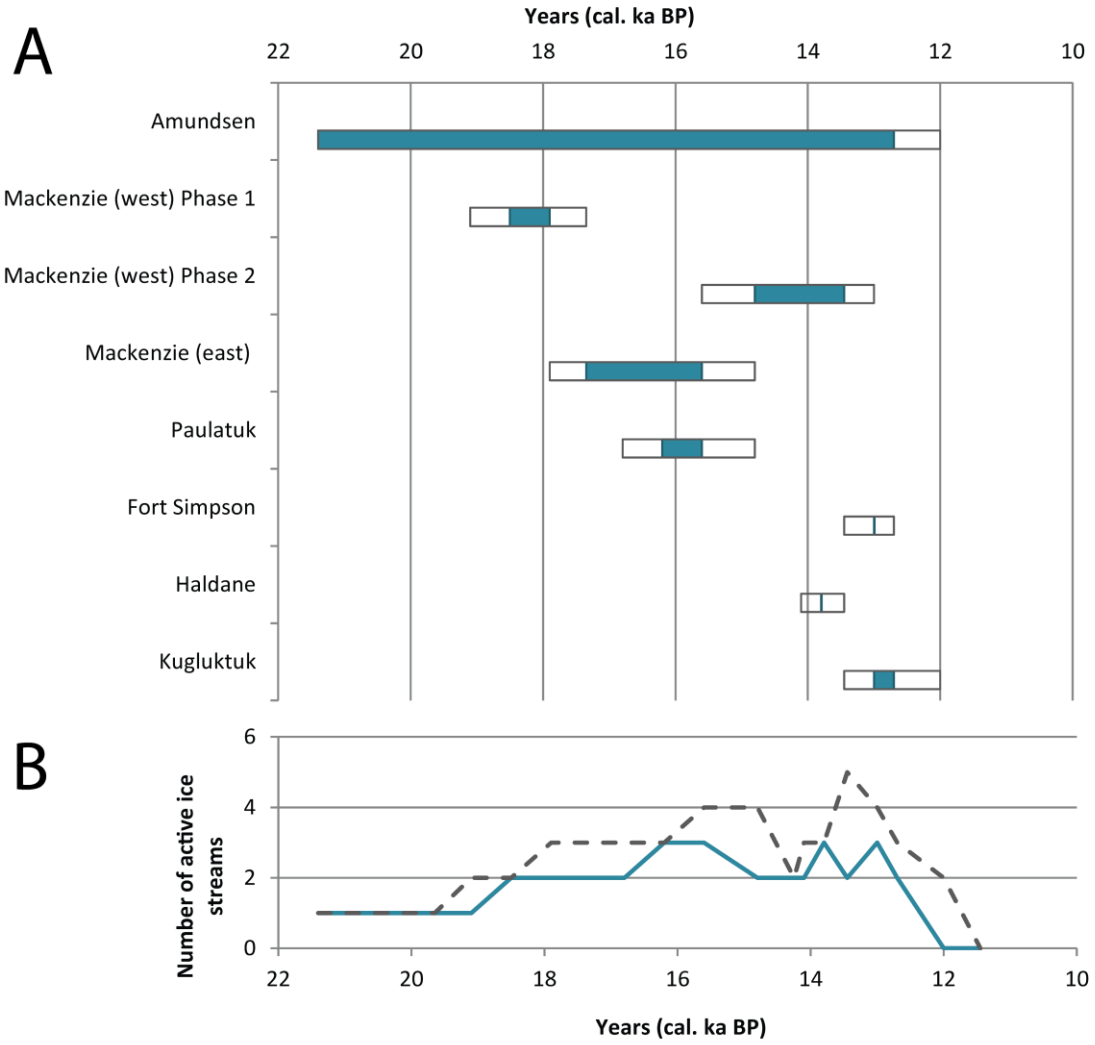

Figure 5-12: The timing of ice stream activity in the north-west LIS during Late Wisconsinan deglaciation. A: the activity of seven individual ice streams. The blue/green bars indicate the time-steps for which each ice stream is active in the reconstruction shown in Section 5.6 (minimum durations), while the grey boxes indicate the maximum duration of ice stream activity by assuming that any one flow-set could remain active up until the next time-step of the reconstruction. B: the minimum and maximum number of ice streams that were active in the north-west sector of the LIS during deglaciation. The green line is based on the green bars shown in A, while the grey dashed line corresponds with the grey boxes on A. The green line can be thought of as a minimum number of ice streams, and the grey line as a maximum number of ice streams.

5.8 Summary

- The mapped glacial geomorphology has been used to delimit 272 flow-sets. Three different types of flow-set have been identified based on the local geomorphological signature; wet-based deglacial flow-sets, event flow-sets and ice stream flow-sets.
- More than 35 ice stream flow-sets have been identified. These flow-sets are comprised of highly elongate bedforms, often with aligned eskers. The bedforms also strongly

converge into corridors with abrupt lateral margins. These characteristics are similar to those reported by Stokes and Clark (1999) as being typical ice stream imprints.

- The reconstruction of ice sheet activity indicates extensive ice stream activity in this sector of the LIS during deglaciation. Thirty-five flow-sets record the activity of seven ice streams.
- Flow-sets have also been identified which cannot be reconciled with the reconstruction shown in Figure 5-4. Many of these flow-sets are orientated perpendicular to the dominant ice flow direction in this sector of the LIS during the Late Wisconsinan (south-east to north-west). These flow-sets may have formed during an earlier glacial phase, possibly pre-LGM. Other flow-sets which cannot be reconciled with the reconstruction may have formed at intermediate stages, between the time-steps presented here.
- The ice margins used in the reconstruction have been taken from Dyke *et al.* (2003). These margins are based on a radiocarbon chronology of 71 radiocarbon dates from across the study area. However, several modifications have been made to these ice margins in order to match with the location of major moraine ridges, account for local topography and to incorporate the full extent of the relevant flow-sets.
- The Mackenzie palaeo-ice stream was located west of Great Bear Lake and occupied a broad low-lying region along the foot of the Yukon Mountains. The onset zone of the ice stream was between Great Bear Lake and Fort Simpson and the ice stream fed an eastern and western branch of the ice stream further north. The ice stream switched between activity in its eastern and western branches meaning that the two branches were not active concurrently. The Mackenzie ice stream was active from the LGM and switched on and off until its final demise ~ 13 cal. ka BP. Highly elongate bedforms characterise the bed of this ice stream.
- Another large ice stream present in the NW LIS was the Amundsen Gulf palaeo-ice stream. This ice stream has been previously documented by Stokes *et al.* (2005) but its geomorphological signature in the study area has not hitherto been mapped. The Amundsen Gulf palaeo-ice stream occupied a large topographic trough between the Canadian mainland and Victoria Island. As the longest lived ice stream in the study area, the Amundsen Gulf palaeo-ice stream was active from the LGM until ~ 12 cal. ka BP.
- Four smaller ice streams were present in this sector of the LIS during deglaciation. While the Paulatuk, Fort Simpson and Kugluktuk palaeo-ice streams have not previously been documented, the Haldane ice stream has been recognised by Clark

(unpublished, cited in Winsborrow *et al.,* 2004) and Kleman and Glasser (2007). These ice streams became active later in deglaciation from ~ 17 cal. ka BP and causes the number of active ice streams to peak between 13 and 16 cal. ka BP.

Chapter 6: Pro-glacial lake evolution

6.1 Introduction

The method employed to reconstruct pro-glacial lakes in this thesis is outlined in Chapter 3. Principally, this method involves the use of the ice margins from Dyke *et al.* (2003), a DEM of North America (GTOPO30 DEM), and a representation of SED during deglaciation taken from ICE-5G, each of which is discussed below. This Chapter documents the evolution of pro-glacial lakes along the mainland North American margin of the Laurentide Ice Sheet (LIS) from the LGM to 8.45 cal. ka BP; when the study area became completely ice free (see Dyke *et al.*, 2003). Section 6.2 discusses the influence of Solid Earth Deformation (SED) on lake evolution before introducing the patterns of SED over North America during LIS deglaciation. New bathymetric maps are presented for Great Bear Lake and Great Slave Lake in Section 6.3. These are the two largest lakes within the study area and therefore likely to have influenced the configuration of pro-glacial lakes. Section 6.4 follows with a continental reconstruction of pro-glacial lake evolution during the Late Wisconsinan.

6.2 The influence of SED on pro-glacial lake evolution

Previous reconstructions of pro-glacial lake extent have been limited to: 1) regional scale reconstructions which have largely been based on field evidence (Craig, 1965; Fisher and Lowell, *In press*); 2), GIS based approaches that account for the effects of SED (Dyke *et al.*, 2003; Fisher and Souch, 1998; Kehew *et al.*, 2009); or, 3), GIS based approaches that do not account for spatial changes in SED throughout deglaciation (Leverington *et al.*, 2000; Teller and Kehew, 1994). Figure 6-1 schematically illustrates the concept of SED and its associated impact on pro-glacial lake evolution.

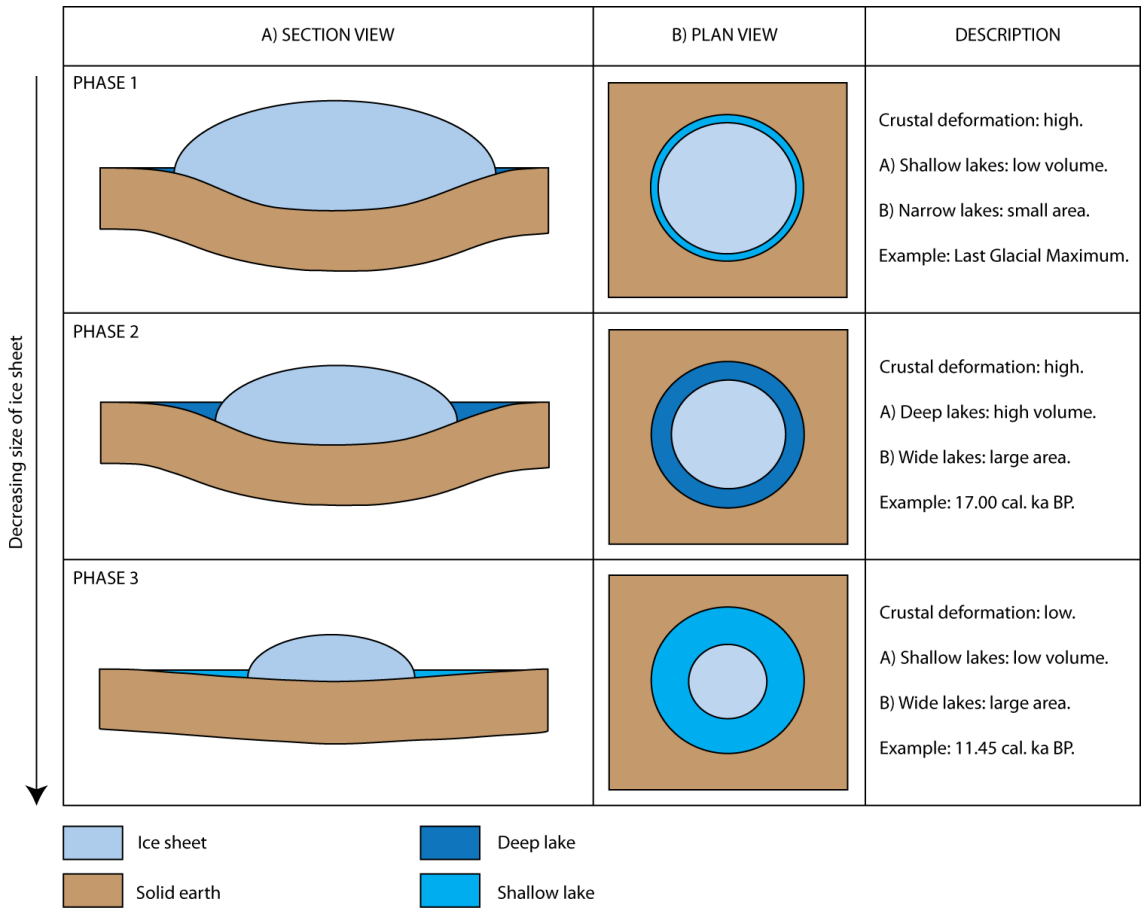

Figure 6-1: A schematic illustration of pro-glacial lake evolution during deglaciation and the influence of solid earth deformation by crustal loading. The diagram does not quantify the horizontal or vertical extent of crustal deformation as a function of loading, and assumes a delay in crustal rebound following unloading i.e. from Phase 1 to Phase 2.

Depression of the solid earth across North America reflected the changing geometry of the LIS. As outlined in Chapter 3, ICE-5G is a global ice sheet model, which provides a 3D topographic representation of the solid ice-age earth by incorporating SED or Glacio-Isostatic Adjustment (GIA) (Peltier, 2004). During the LGM, deformation values of up to 1200 m are indicated on the Canadian Shield at ~ 108° W, while later in deglaciation, deformation of < 800 m is indicated for the same location as shown in Chapter 3. Deformation tilted the crust towards the centre of loading and therefore aided the formation of pro-glacial lakes. The effects of this are shown in Figure 6-2 reveals two reconstructions of pro-glacial lake evolution along the north-west margin of the LIS; one which does not incorporate SED (Figure 6-2A) and one which does (Figure 6-2B). In not accounting for SED, pro-glacial lakes were much smaller, discontinuous, and rarely in contact with the ice margin. In contrast, the reconstruction shown in Figure 6-2B indicates the growth of large pro-glacial lakes along the ice margin which extended well beyond 120°W. This highlights the importance of SED in reconstructions of pro-glacial lake

extent and evolution. A series of maps displaying the reconstructed pro-glacial lakes around the LIS which incorporate SED are presented in Section 6.4.

The difference between the topography of the north-west LIS both with and without the addition of data from ICE-5G is shown in Figure 6-3. SED lowered the topography as a whole but, in particular, depressed the land more, closer to the centre of loading (the ice sheet). Figure 6-3 shows that, prior to the addition of the ICE-5G data, the basin of Great Bear Lake and the western end of Great Slave Lake were much more pronounced. By accounting for SED, the topography appears more subdued and the two major lake basin are not as easily distinguished. In addition, profile graphs across the peripheral depression at the ice sheet margin again indicate that when ICE-5G is added to a DEM of North America, the tilt of the land towards the ice sheet increases. This therefore increases the size of the lake basins along the ice margin and has a significant impact on the configuration of pro-glacial lakes. For example, along the north-west margin of the LIS, the basin of Glacial Lake McConnell is depressed by up to 400 m by incorporating GIA into the reconstructions (Figure 6-3). This is the case throughout the Lake McConnell basin. Further south, the two profile graphs for the Lake Agassiz basin again suggest that GIA made a significant contribution to the configuration and volume of the lakes. For example, in both profile graphs from Lake Agassiz, the depression of the solid earth along the ice margin is between 400 and 500 m (Figure 6-4).

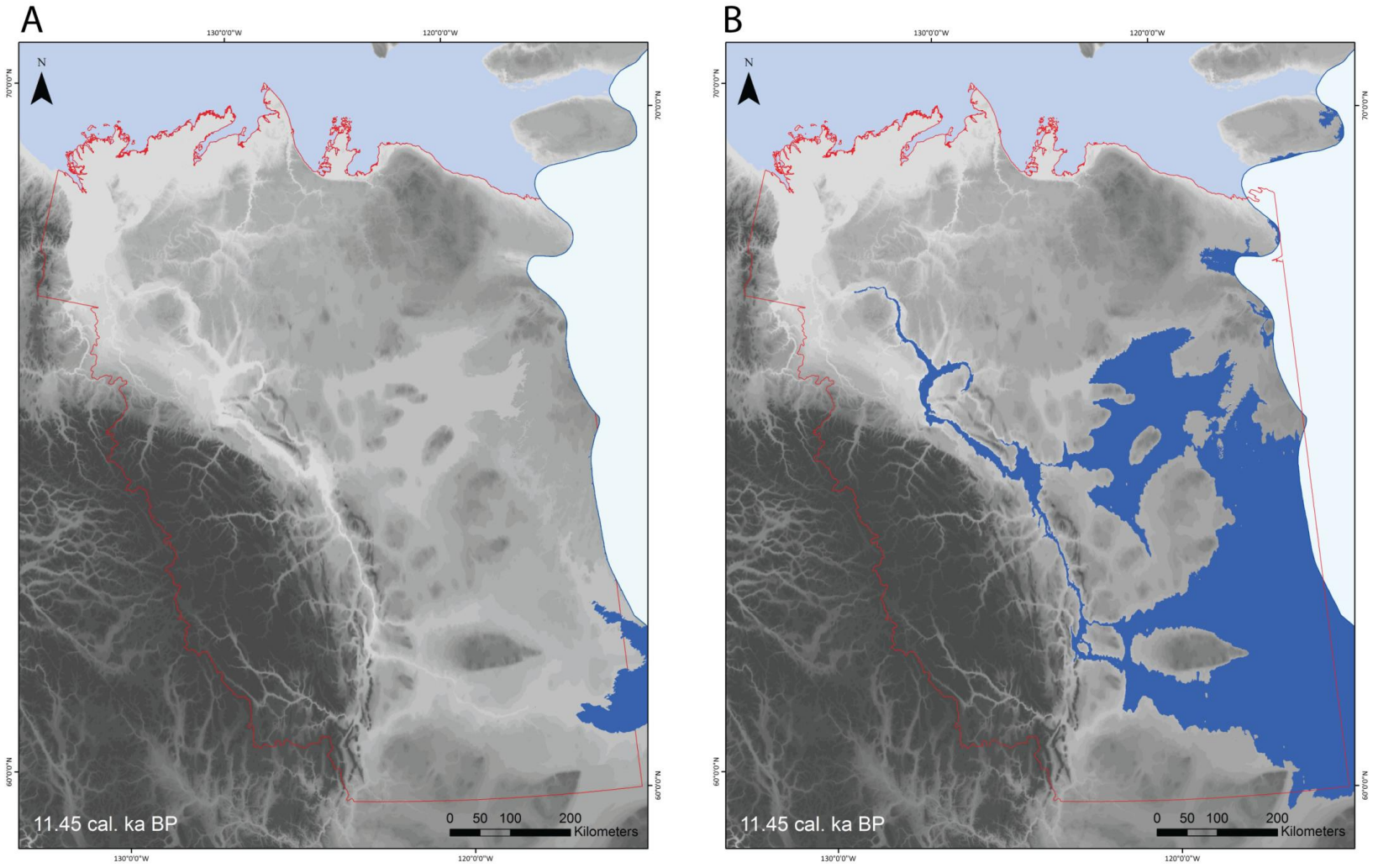

Figure 6-2: Pro-glacial lakes along the north-west mainland LIS margin at 11.45 cal. ka BP. A) The reconstructed pro-glacial lakes without the incorporation of ICE-5G SED into the DEM. Unlike Figure 6-6, all ponded water is shown in this reconstruction rather than just lakes which were in contact with the ice margin. B) For comparison, the reconstructed pro-glacial lakes with the incorporation of SED.

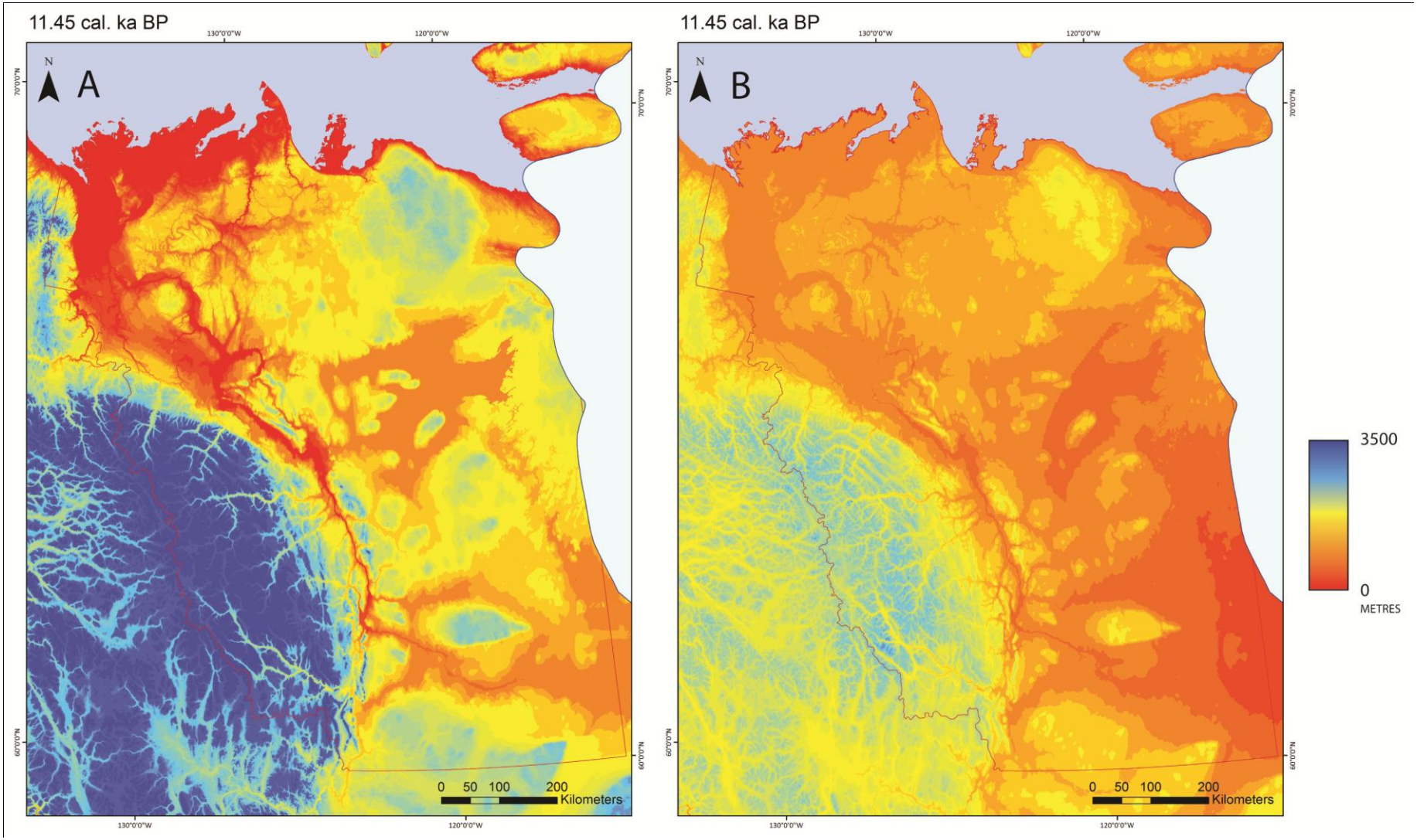

Figure 6-3: The topography of the north-west LIS with the ice sheet at 11.45 cal. ka BP and the study area outlined. A: the present day topography from GTOPO-30, and B: the topography with the addition of SED data from ICE-5G.

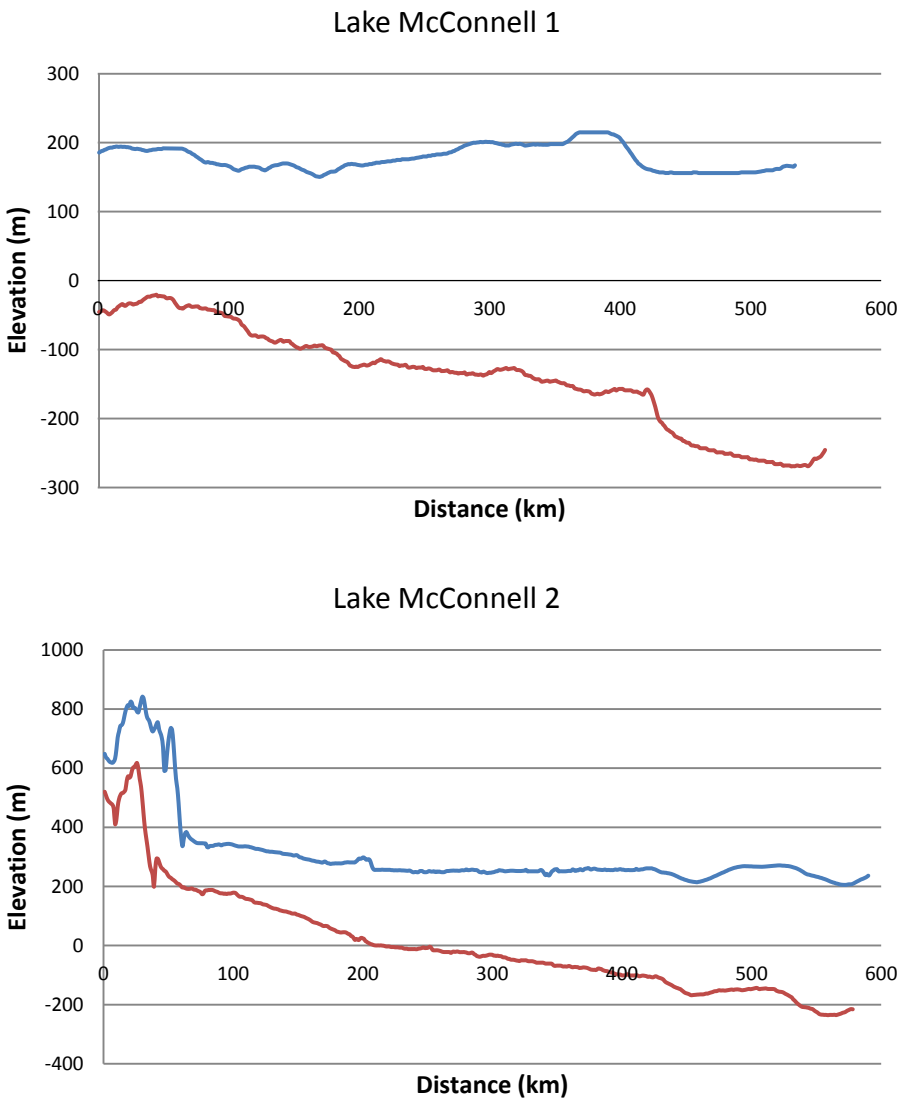

Figure 6-4: Profiles across the peripheral depression at the ice margin where pro-glacial lakes have been reconstructed. The blue lines show the present day topography with no account for SED. The red line shows the topography when data from ICE-5G is added to the DEM. The ice margin is not shown on the graphs but is located on the right hand side of the graphs at the point where the topographic profile ends. In all cases, the land elevation therefore decreases towards the ice margin.

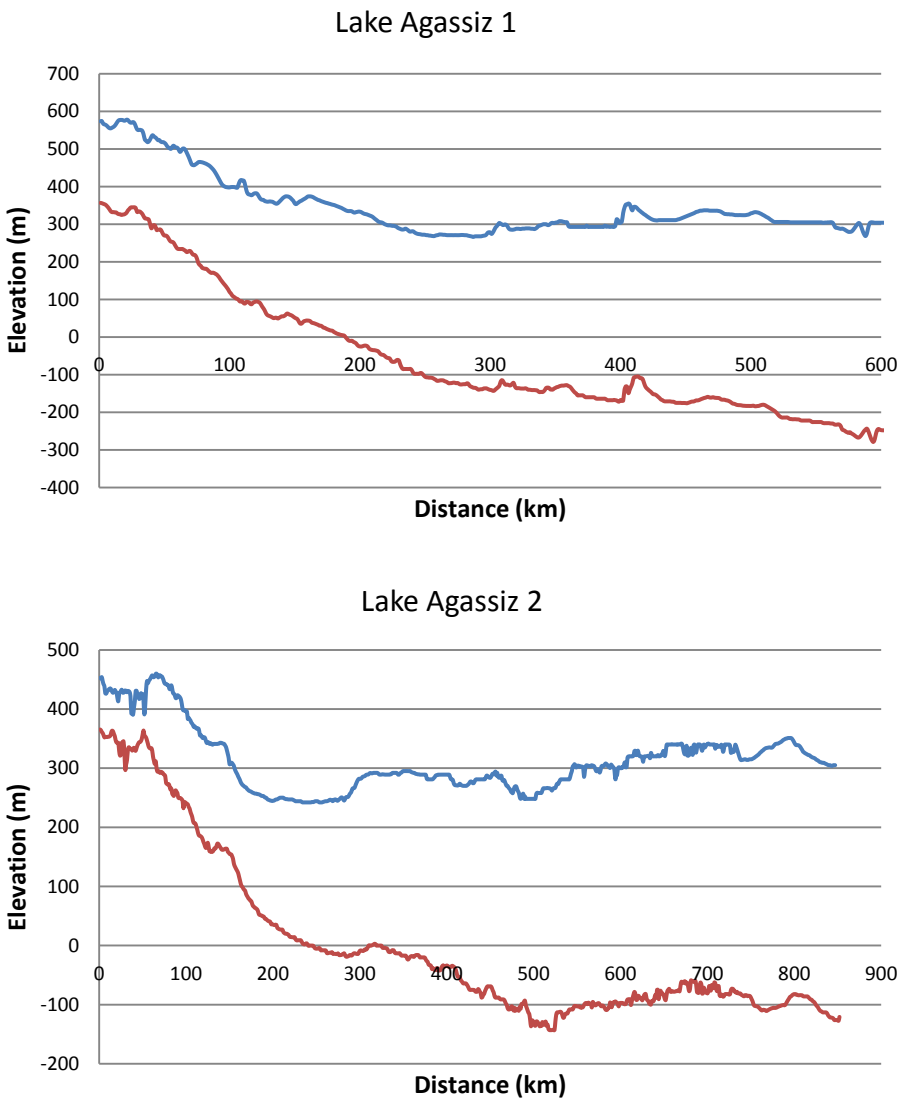

Figure 6-4 (continued): Profiles across the peripheral depression at the ice margin where pro-glacial lakes have been reconstructed. The blue lines show the present day topography with no account for SED. The red line shows the topography when data from ICE-5G is added to the DEM. The ice margin is not shown on the graphs but is located on the right hand side of the graphs at the point where the topographic profile ends. In all cases, the land elevation therefore decreases towards the ice margin.

6.3 Lake Bathymetry

Present day water bodies, represented by flat surfaces within the DEM, prevented the accumulation of water in topographic depressions where accumulations of water would be otherwise expected. It was therefore necessary to incorporate the bathymetry of major present-day water bodies into the DEM before flooding to establish the extent and depth of pro-glacial lakes. This was done for the two largest lakes in the north-west sector of the LIS: Great Bear Lake (GBL) and Great Slave Lake (GSL). Since digital bathymetry data was not available for these two lakes, it was necessary to digitise a series of nautical charts (see

Chapter 3 for further details). Points on the charts were interpolated to produce the bathymetry shown in Figure 6-5 and Figure 6-6. The basin occupied by GBL is dominated by a 200 km long trough which reaches a maximum depth of -236 m OD (420 m deep from the shoreline). When GBL bathymetry data is added to the DEM, a basin with a volume of 406 km^3 is produced. The basin of GSL is 247 km^3.

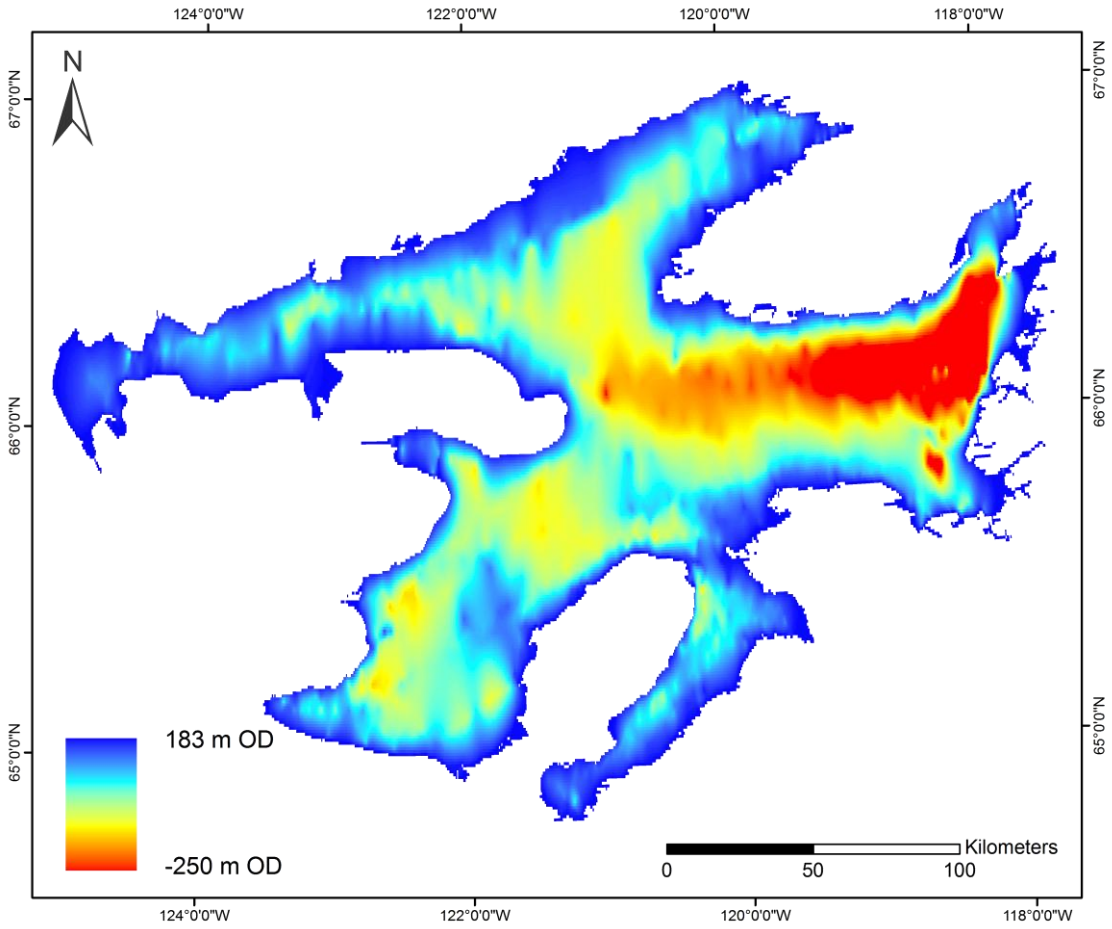

Figure 6-5: The bathymetry of Great Bear Lake as digitised and interpolated using the nearest neighbour technique from Nautical Charts obtained from the Canadian Hydrographic Service.

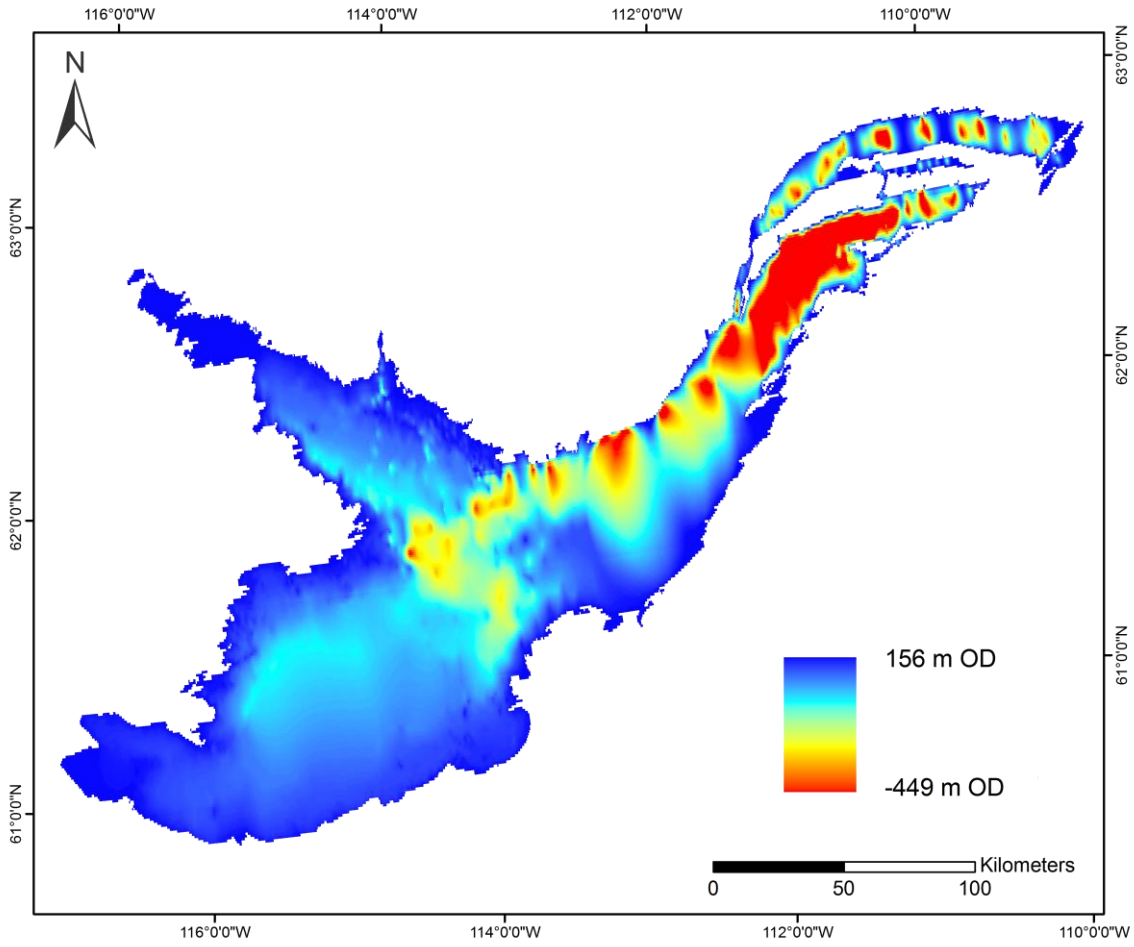

Figure 6-6: The bathymetry of Great Slave Lake as digitised and interpolated using the nearest neighbour technique from Nautical Charts obtained from the Canadian Hydrographic Service. While Christoffersen et al. (2008) present some bathymetric date for Great Slave Lake, it is limited to the eastern end of the lake and covers a small area. The data shown above has been compared to that of Christoffersen et al. (2008) for the eastern end of the lake and the two data sets have been found to be comparable.

6.4 Pro-glacial lake evolution

Pro-glacial lakes were present around the terrestrial margins of the LIS throughout deglaciation. However, at the LGM and during the early stages of Late Wisconsinan deglaciation, the lakes did not extend far from the ice margin. Dyke *et al.* (2003) depict the evolution of these lakes as documented by previous authors such as Craig (1965), Smith (1992) and Couch and Eyles (2008) (see Chapter 2). These reconstructions are based primarily on geomorphological evidence. As documented in Chapter 3, the reconstruction of pro-glacial lake evolution presented in this chapter uses the reconstructed LIS margins from Dyke *et al.* (2003), patterns of SED from ICE-5G, newly digitised lake bathymetry data, and the GTOPO30 DEM. The new reconstructions are shown below in Figure 6-7. In the north-west sector of the LIS, the reconstructions shown in Figure 6-7 allowed for a direct comparison between ice

stream activity and pro-glacial lake evolution throughout deglaciation. This comparison is discussed in Chapter 7.

6.4.1 21.40 – 19.10 cal. ka BP

Between 21.40 cal. ka BP and 19.65 cal. ka BP the margins of the LIS remained relatively stable, not only in the north-west, as noted in Chapter 5, but also along its southern margin. As a result, ICE-5G indicates a very small change in SED during this period which can be accounted for by assuming a greater change in the vertical (ice thickness), rather than lateral, ice sheet geometry. The resulting pro-glacial lake reconstructions for the time steps between 21.40 cal. ka BP and 19.65 cal. ka BP, therefore, show minimal change in pro-glacial lake configuration. These small changes in lake configuration are reflected in the consistent area of the lakes shown in Figure 6-7A-D for the early stages of deglaciation.

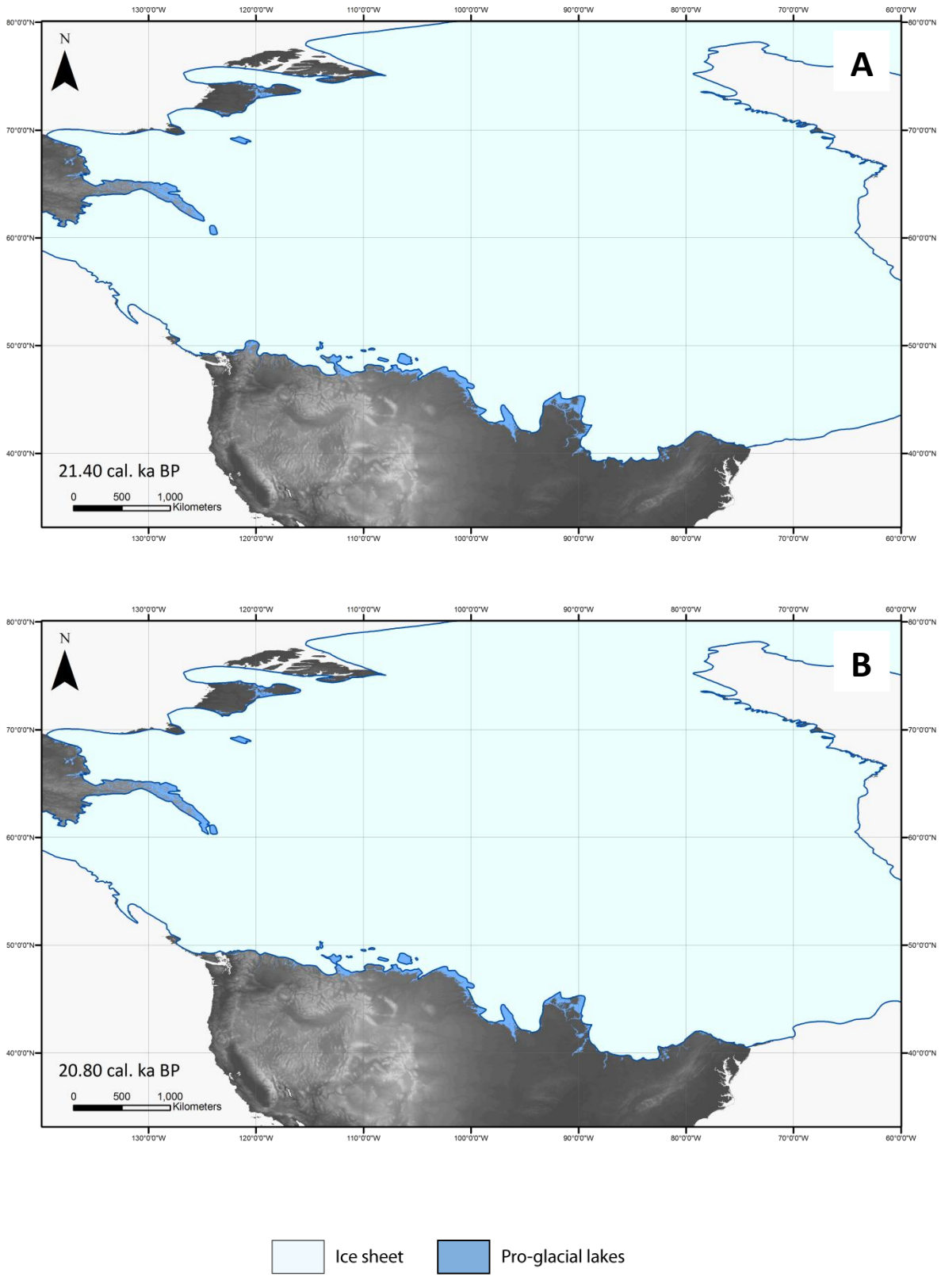

Figure 6-7: The reconstructed pro-glacial lakes along the LIS mainland margin during the Late Wisconsinan. Where present, Glacial Lake Agassiz is labelled as 'GLA', Glacial Lake McConnell is labelled as 'GLMc' and the routeway which joins the two lakes is highlighted with a red box.

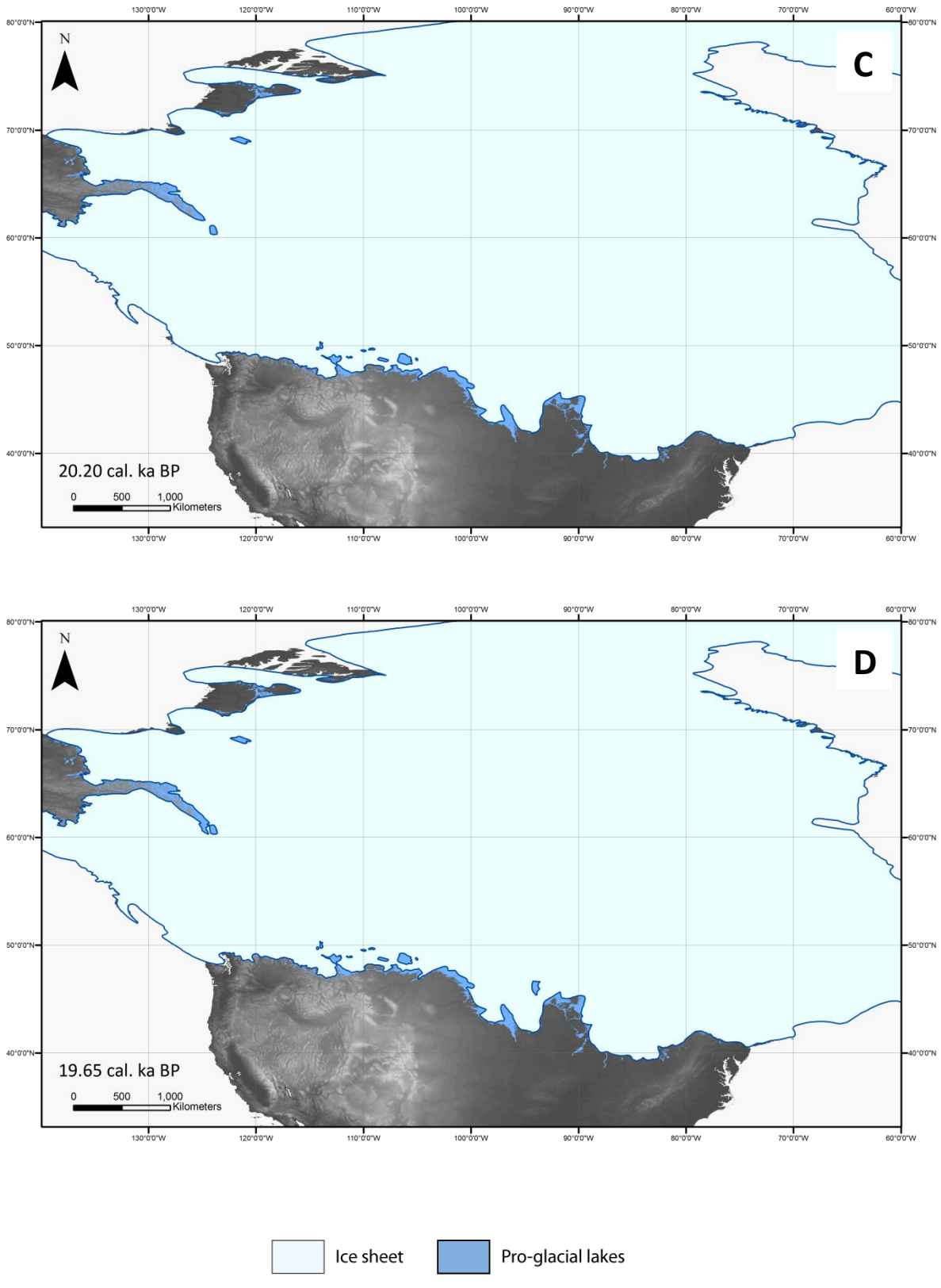

Figure 6-7 (cont.): The reconstructed pro-glacial lakes along the LIS mainland margin during the Late Wisconsinan. Where present, Glacial Lake Agassiz is labelled as 'GLA', Glacial Lake McConnell is labelled as 'GLMc' and the routeway which joins the two lakes is highlighted with a red box.

6.4.2 19.10 – 16.80 cal. ka BP

Between 19.10 cal. ka BP and 18.50 cal. ka BP the reconstructions shown in Figure 6-7E-H indicate an increase in pro-glacial lake area; the first marked increase since the LGM. In the suture zone between Cordilleran ice and Laurentide ice, pro-glacial lakes formed around the foot of the Yukon Mountains. Pro-glacial lakes also developed between 80 and 90° W in the basins now occupied by the Great Lakes (Lakes Superior, Ontario, Michigan and Erie) following the northward retreat of the ice margin. Lakes also developed around the southern lobes of the LIS (Des Moines and James lobes) at ~ 95° W. By 17.90 cal. ka BP, the ice margin reconstructions of Dyke *et al.* (2003) indicate a readvance of ice in the Great Lakes region (see Figure 6-7G). This resulted in a reduction of pro-glacial lake area along this portion of the ice margin as ice once again occupied the major topographic depressions now occupied by the Great Lakes. From 17.90 cal. ka BP the Des Moines and James lobes began to decrease in width (east to west) and pro-glacial lakes developed along their retreating margins. This is most pronounced on the eastern side of the Des Moines lobe where ice retreated north to form an embayment at ~ 47° N.

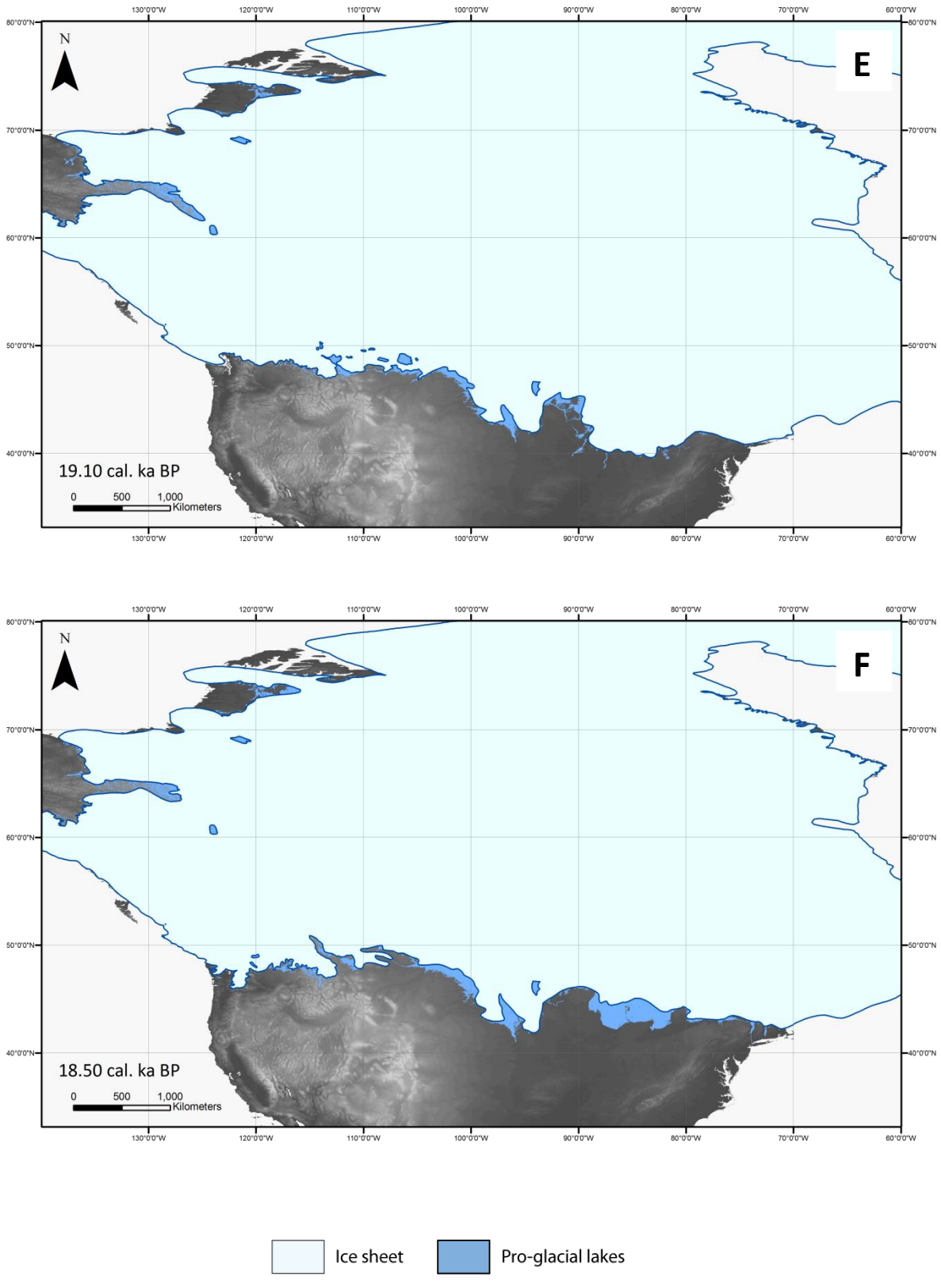

Figure 6-7 (cont.): The reconstructed pro-glacial lakes along the LIS mainland margin during the Late Wisconsinan. Where present, Glacial Lake Agassiz is labelled as 'GLA', Glacial Lake McConnell is labelled as 'GLMc' and the routeway which joins the two lakes is highlighted with a red box.

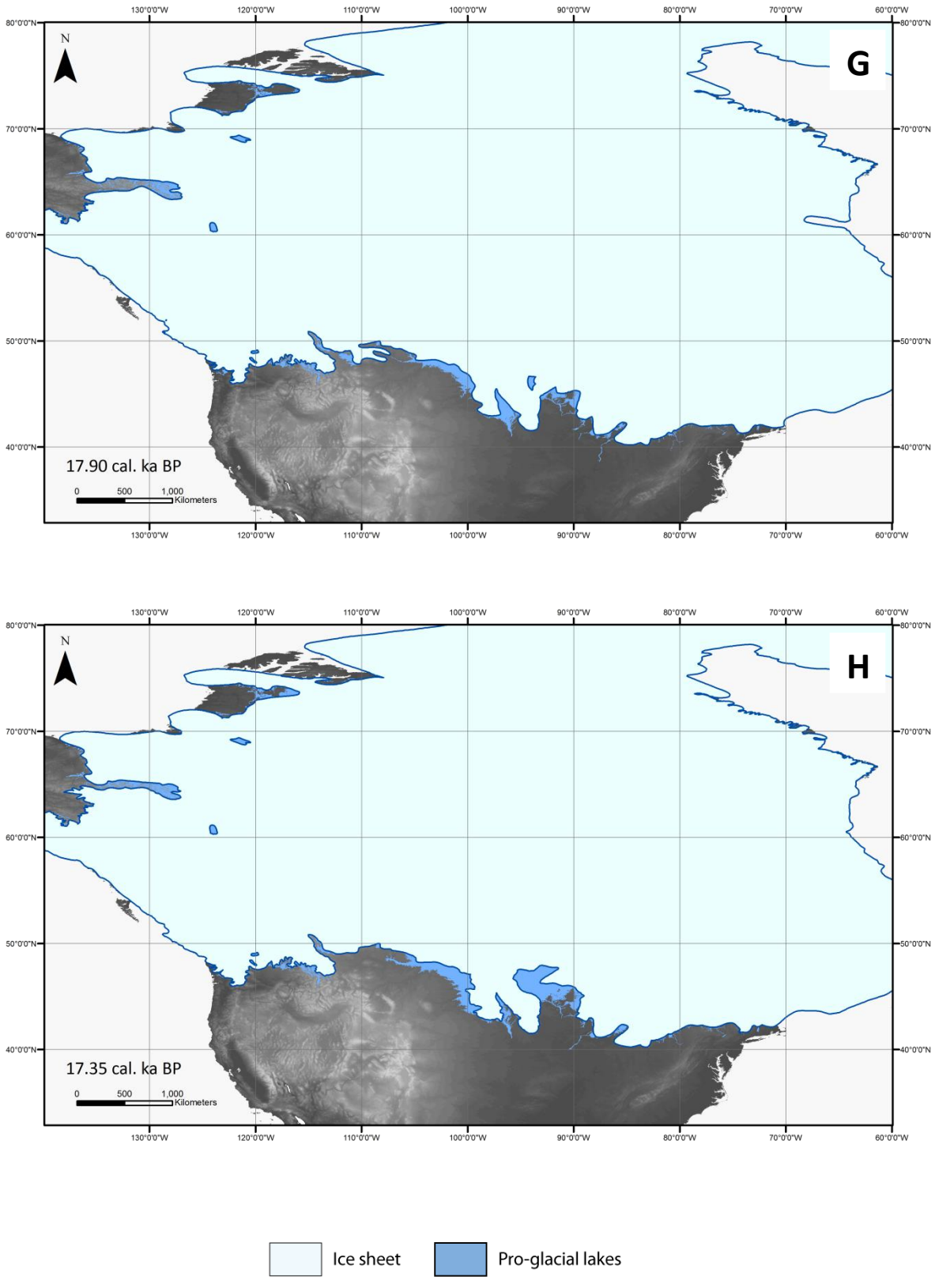

Figure 6-7 (cont.): The reconstructed pro-glacial lakes along the LIS mainland margin during the Late Wisconsinan. Where present, Glacial Lake Agassiz is labelled as 'GLA', Glacial Lake McConnell is labelled as 'GLMc' and the routeway which joins the two lakes is highlighted with a red box.

6.4.3 16.80 – 14.25 cal. ka BP

By 16.80 cal. ka BP, pro-glacial lakes along the southern margin of the LIS had become far more extensive, and the suture zone between Cordilleran Ice and Laurentide Ice along the Rocky Mountains began to open. Laurentide ice became separated from Cordilleran ice by 14.80 cal. ka BP (Dyke *et al.,* 2003; Tarasov *et al.,* 2012). Pro-glacial lakes subsequently began developing along the western margin of the LIS as shown in Figure 6-7I-L. At 14.80 cal. ka BP, these lakes were largely located within the foothills of the Rocky Mountains and were dammed by ice to east (Figure 6-7L). The onshore retreat of the mainland north-western margin of the LIS by 14.80 cal. ka BP initiated the expansion of pro-glacial lakes in the study area.

In the Great Lakes region, the growth of pro-glacial lakes was most prominent between 16.80 and 16.20 cal. ka BP. However, further west, large changes in the configuration of pro-glacial lakes occurred between 15.60 and 14.80 cal. ka BP as a result of the retreat and readvance of the southern lobes (Des Moines and James lobes).

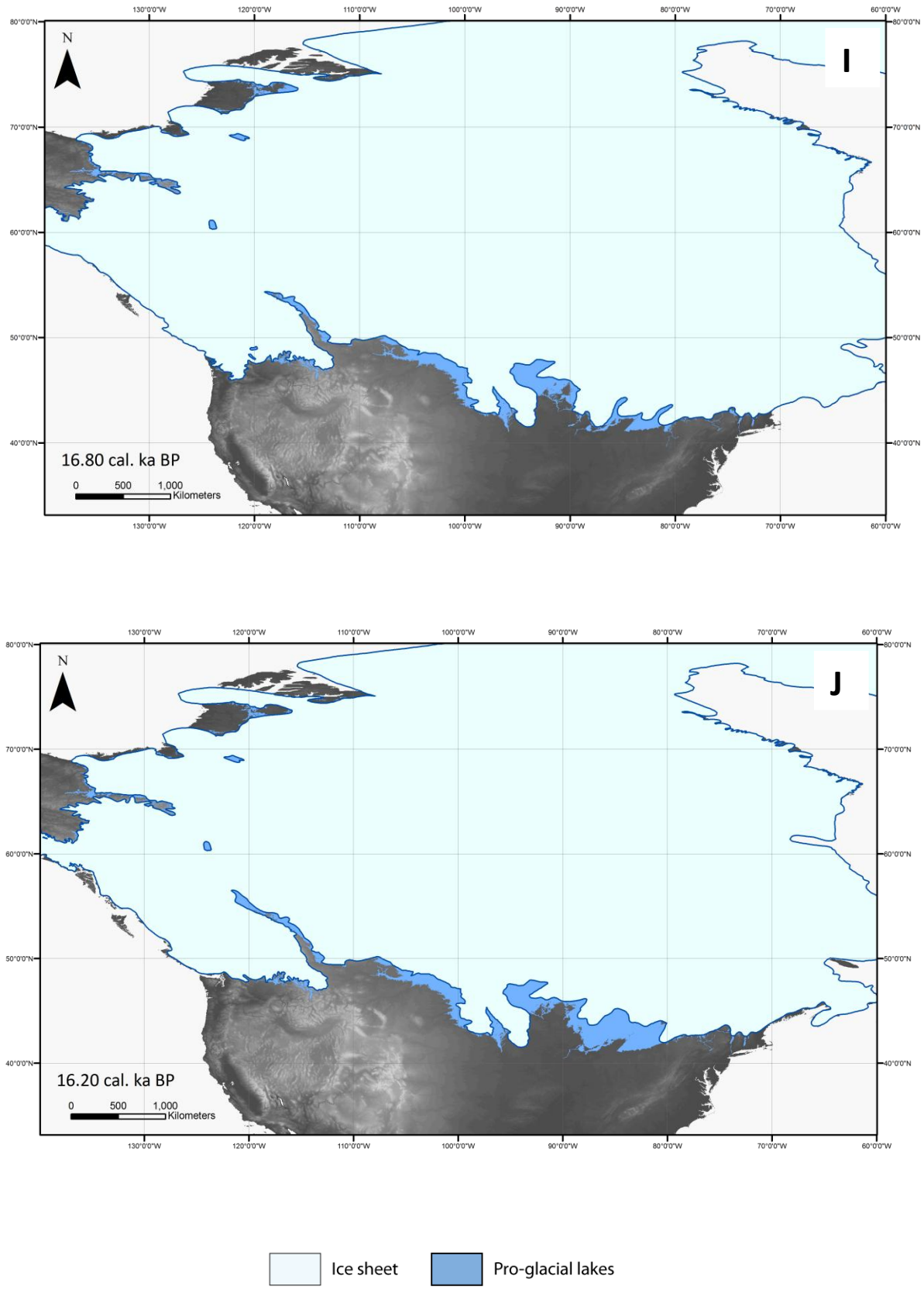

Figure 6-7 (cont.): The reconstructed pro-glacial lakes along the LIS mainland margin during the Late Wisconsinan. Where present, Glacial Lake Agassiz is labelled as 'GLA', Glacial Lake McConnell is labelled as 'GLMc' and the routeway which joins the two lakes is highlighted with a red box.

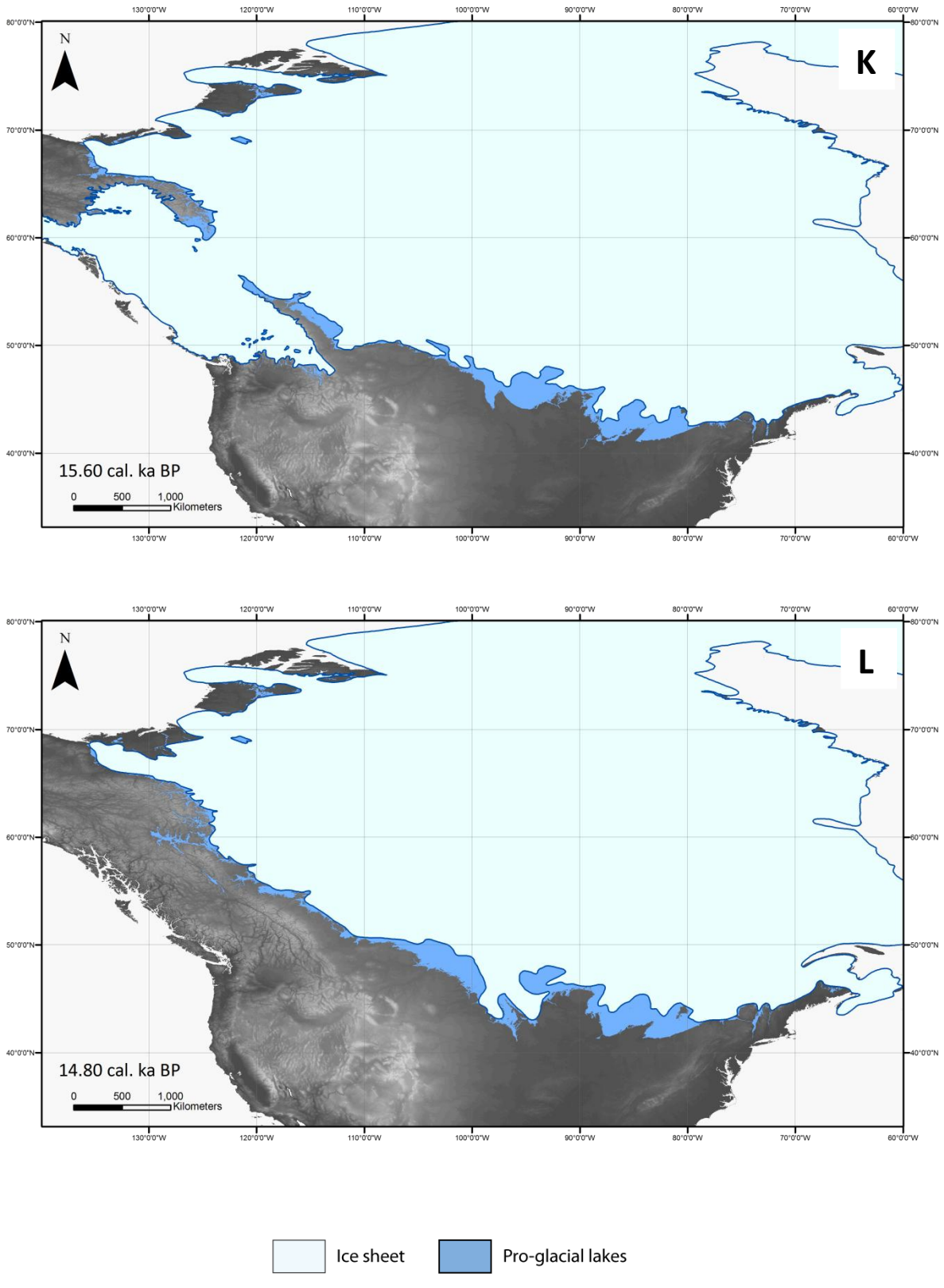

Figure 6-7 (cont.): The reconstructed pro-glacial lakes along the LIS mainland margin during the Late Wisconsinan. Where present, Glacial Lake Agassiz is labelled as 'GLA', Glacial Lake McConnell is labelled as 'GLMc' and the routeway which joins the two lakes is highlighted with a red box.

6.4.4 14.25 – 13.00 cal. ka BP

As shown below in Figure 6-7M-P, by 14.25 cal. ka BP, the lobe of ice which previously extended over the present day Mackenzie delta had retreated south to 67°N. From 14.25 cal. ka BP, the reconstructions shown in Figure 6-7M-P indicate the development of a lake over the delta. This is most likely to be an artefact of the methodology employed (detailed in Chapter 2), and in particular the resolution of the DEM used to generate the reconstruction. Indeed, the 1 km resolution DEM was not capable of resolving the subtle positive relief features of the delta. Furthermore, the delta is a post-glacial feature and the pre-glacial and glacial landscape of the region would have been significantly different to today in this area. Therefore, the lakes indicated in this area on the reconstructions shown below most likely did not evolve as shown.

By 14.10 cal. ka BP, lakes began to form closer to the ice margin. In particular, water ponded around Fort Good Hope. This lake, hereafter known as Lake Good Hope, represented the earliest phase of lake evolution in the study area and, more specifically, Glacial Lake McConnell (GLMc – see Figure 6-7).

The final demise of the southern lobes had occurred by 14.10 cal. ka BP (see Figure 6-7N). In retreating north, these lobes exposed a large basin along the southern LIS margin which subsequently allowed the initiation of a large lake dammed by the ice margin: Glacial Lake Agassiz (Upham, 1895; Thorleifson, 1996). 14.10 cal. ka BP is the first time step which illustrates a coherent large water body along the southern LIS margin which is isolated by ice dams and topographic highs.

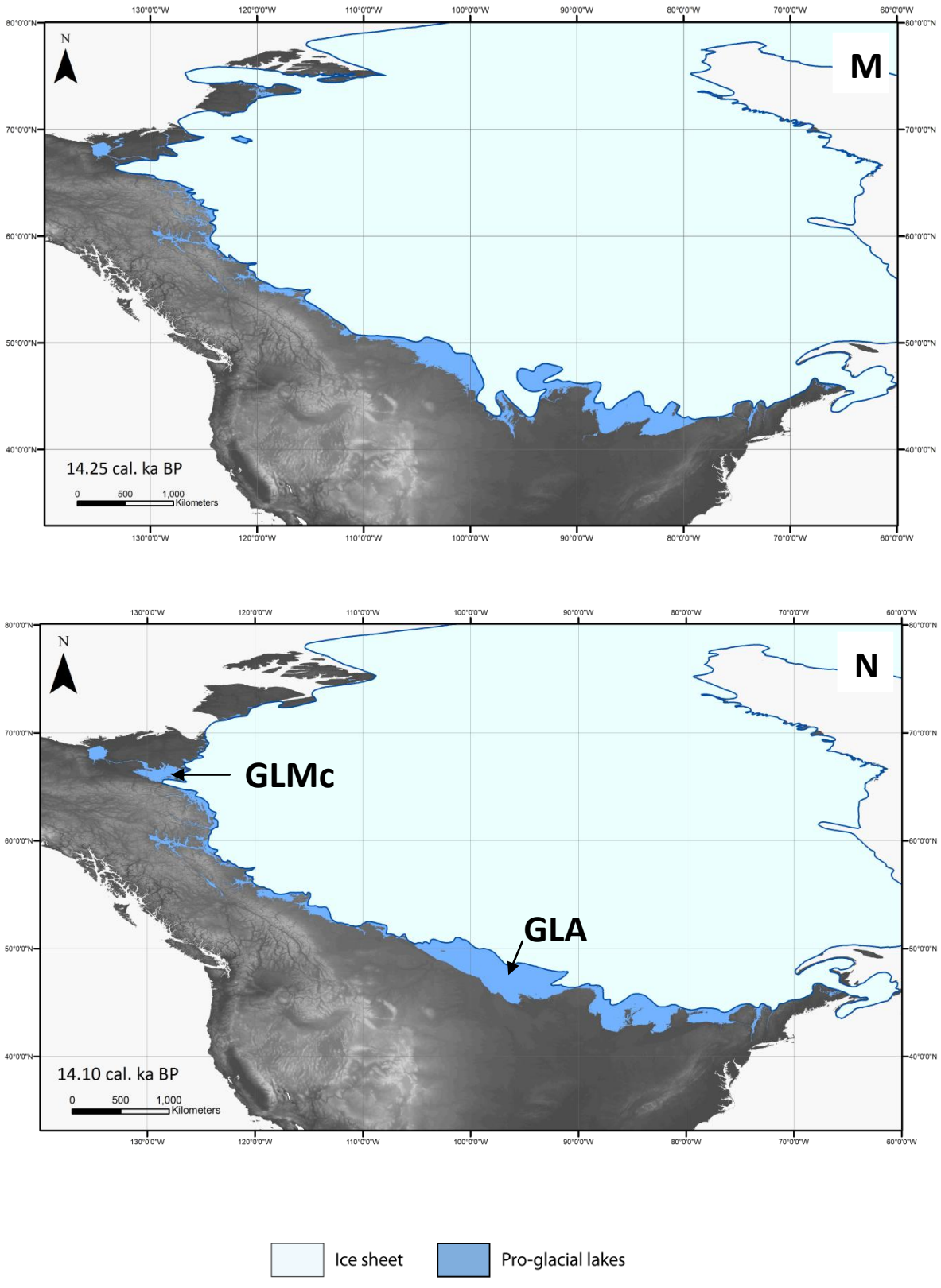

Figure 6-7 (cont.): The reconstructed pro-glacial lakes along the LIS mainland margin during the Late Wisconsinan. Where present, Glacial Lake Agassiz is labelled as 'GLA', Glacial Lake McConnell is labelled as 'GLMc' and the routeway which joins the two lakes is highlighted with a red box.

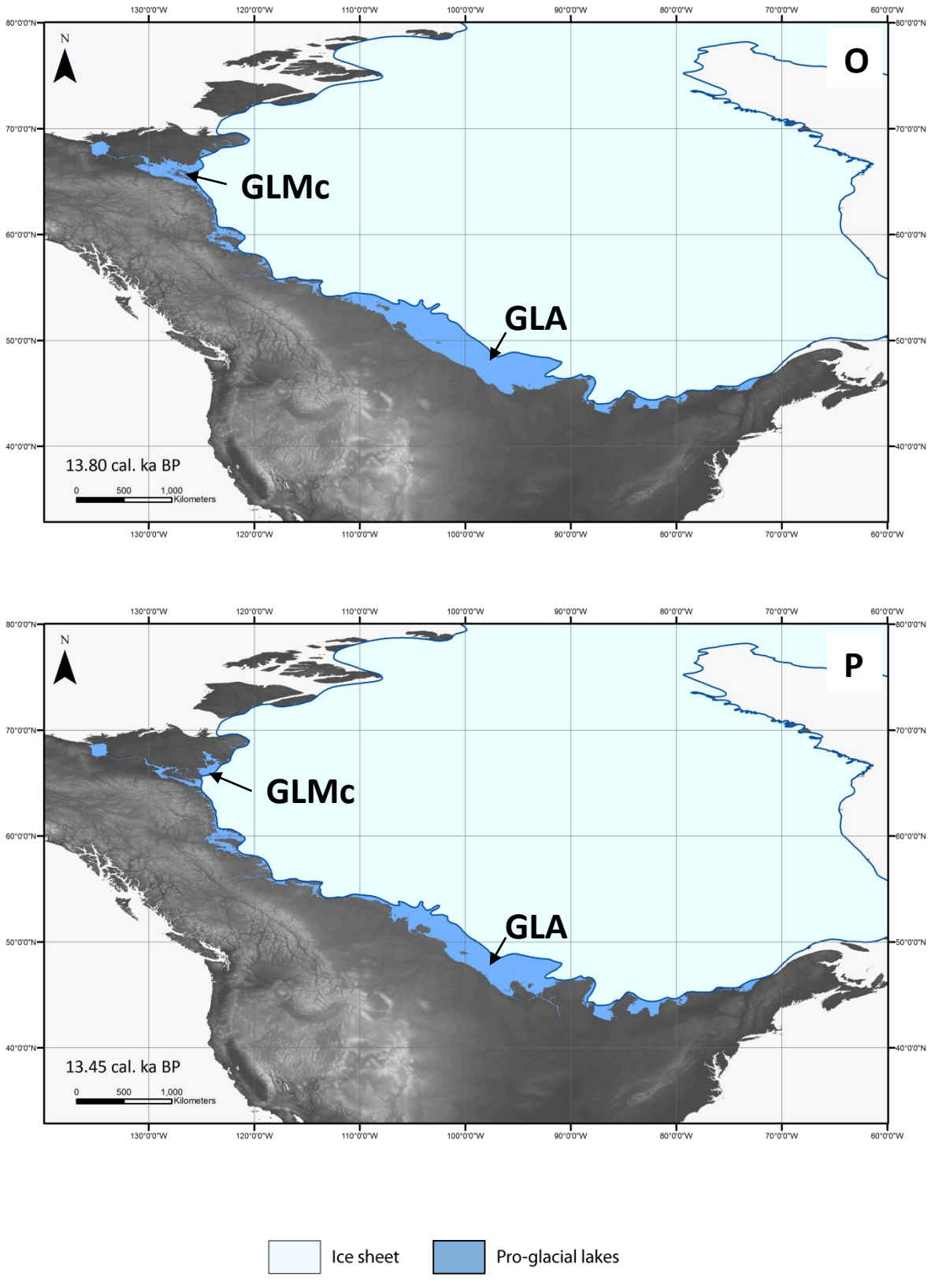

Figure 6-7 (cont.): The reconstructed pro-glacial lakes along the LIS mainland margin during the Late Wisconsinan. Where present, Glacial Lake Agassiz is labelled as 'GLA', Glacial Lake McConnell is labelled as 'GLMc' and the routeway which joins the two lakes is highlighted with a red box.

6.4.5 13.00 – 11.00 cal. ka BP

As eastward ice retreat continued, pro-glacial lakes along the north-western margin of the LIS continued to expand (see Figure 6-7Q-T). By 12.70 cal. ka BP, Glacial Lake McConnell had expanded to form a large pro-glacial lake along the mainland north-western margin of the LIS (see Figure 6-7R). According to Smith (1994), Lake McConnell was present between 11.8 and 8.3 cal. ka BP. This is nearly 1000 years later than that indicated by the reconstructions presented in this thesis. As such, the lifetime of Glacial Lake McConnell may have been longer than previously believed (discussed further in Chapter 2).

Elsewhere, pro-glacial lakes were extensive along the southern margin of the LIS during this period. In particular, Glacial Lake Agassiz (shown on Figure 6-7 as 'GLA') expanded further towards the north-west between 110 and 120°W. By 12.70 cal. ka BP, a connection had developed between Glacial Lake Agassiz and the lakes along the north-western margin. This connection was a 2 km wide spillway in the vicinity of the present-day Clearwater River, which straddles the northern Alberta-Saskatchewan border. This spillway has previously been identified as an outlet for Glacial Lake Agassiz by numerous authors including Smith and Fisher (1993), Fisher and Souch (1998), Teller *et al.* (2005) and Kehew *et al.* (2009). However, the timing of lake drainage through this outlet has not previously been established as part of a continental-scale systematic reconstruction of pro-glacial lake evolution throughout the Late Wisconsinan (discussed in Chapter 7).

In the Great Lakes region, lakes reached their maximum extent at 12.00 cal. ka BP before rapidly decreasing in size by 11.45 cal. ka BP. This can be explained by isostatic rebound of the solid earth as the LIS retreated towards Hudson Bay. Glacio-isostasy reduced the tilt of the earth's crust towards the centre of loading/the ice margin and thus reduced the area and volume of the lakes. The rapid reduction in the size of pro-glacial lakes in the Great Lakes region may indicate that the lakes drained between 12.00 and 11.45 cal. ka BP (see Figure 6-7S and T). The most obvious routeway for this drainage was to the east through the Gulf of St Lawrence and into the North Atlantic. This routeway has long been hypothesised in the literature by Teller and Thorleifson (1983), Coleman *et al.* (1994), Clark *et al.* (2001), Leverington and Teller (2003), Teller *et al.* (2005), and others. Crucially, however, a connection between Glacial Lake Agassiz and the lakes described above in the Great Lakes region has not been identified in any of the timesteps in the reconstructions presented in this thesis. This would have significantly limited the amount of freshwater able to drain into the North Atlantic through the Gulf of St Lawrence (Condron and Winsor, 2011, Li *et al.*, 2009).

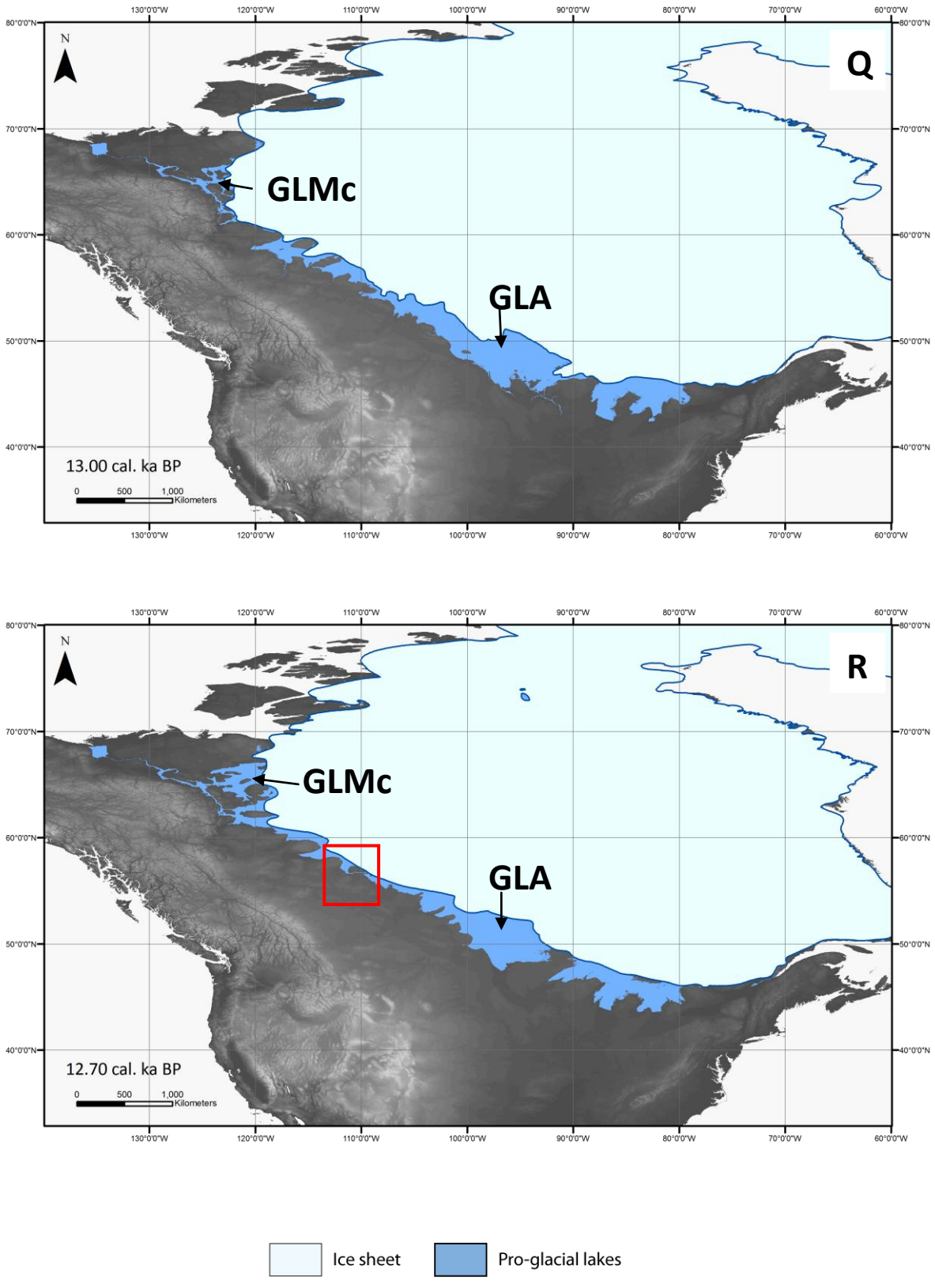

Figure 6-7 (cont.): The reconstructed pro-glacial lakes along the LIS mainland margin during the Late Wisconsinan. Where present, Glacial Lake Agassiz is labelled as 'GLA', Glacial Lake McConnell is labelled as 'GLMc' and the routeway which joins the two lakes is highlighted with a red box.

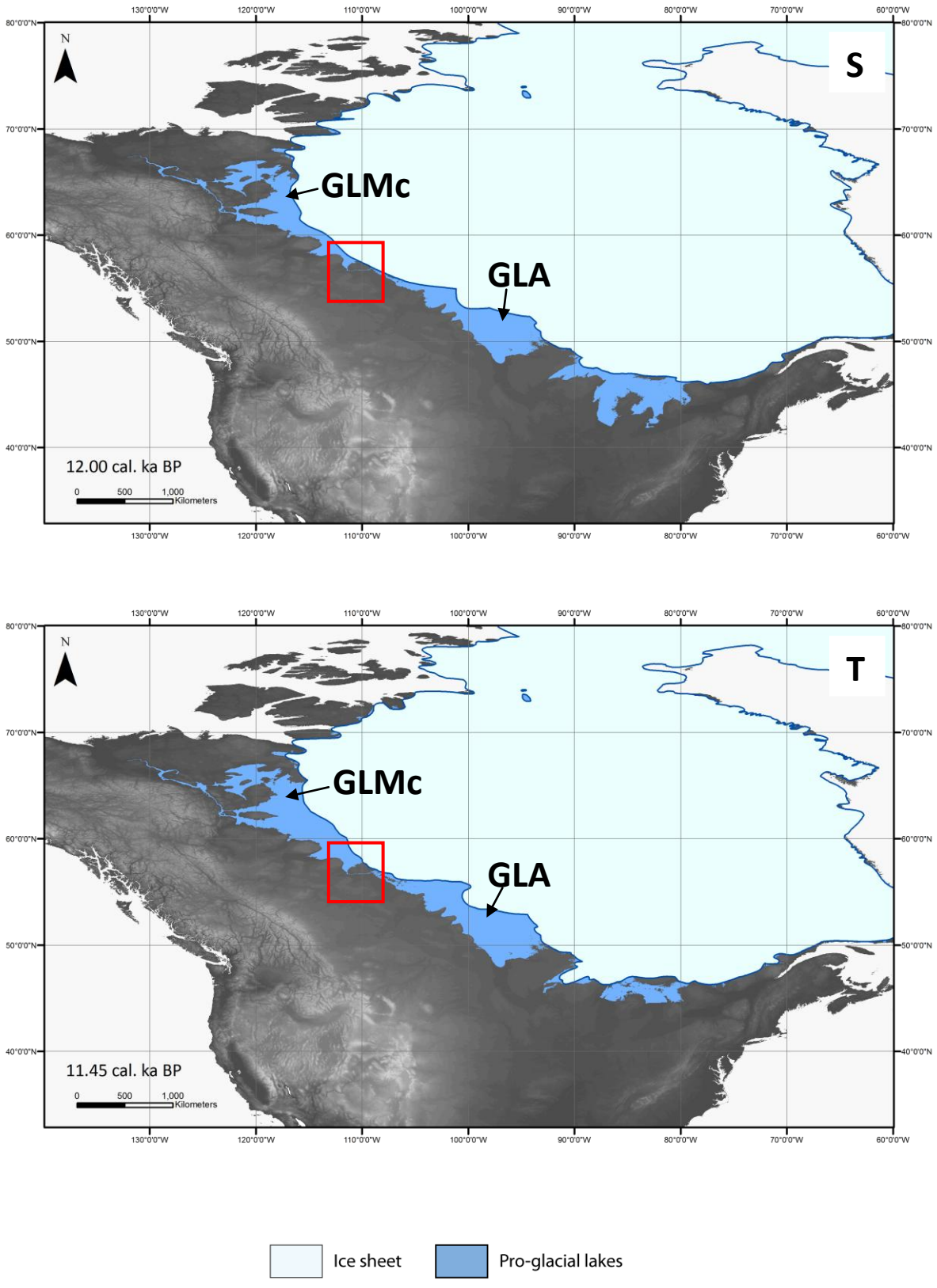

Figure 6-7 (cont.): The reconstructed pro-glacial lakes along the LIS mainland margin during the Late Wisconsinan. Where present, Glacial Lake Agassiz is labelled as 'GLA', Glacial Lake McConnell is labelled as 'GLMc' and the routeway which joins the two lakes is highlighted with a red box.

6.4.6 11.00 – 9.00 cal. ka BP

Between 11.45 and 11.00 cal. ka BP, pro-glacial lakes continued to expand along the north-western margin of the LIS. In particular, Glacial Lake McConnell expanded west to form a wider connection with water which occupied the basin of Great Bear Lake (see Figure 6-7T and U). Glacial Lake Mackenzie also began to develop around the foot of the Yukon Mountains between 120 and 130° W and continued to grow until 10.20 cal. ka BP (see Figure 6-7U-X). As shown in Chapter 2, Glacial Lake Mackenzie was a narrow lake which occupied the valley of the present day Mackenzie River.

Further south, lakes expanded along the outflow from Great Slave Lake and a connection to the lakes along the southern margin of the LIS, including Glacial Lake Agassiz, formed (see Figure 6-7U). This connection persisted as a narrow corridor which was ~ 2 km wide and 200 m deep until 10.20 cal. ka BP. The corridor was located approximately 200 km from the ice margin. Between 10.20 and 9.50 cal. ka BP, the LIS retreated towards the north-east and major changes to the configuration of pro-glacial lakes around the mainland margin of the ice sheet occurred (see Figure 6-7X). The narrow connection between lakes along the north-western margin of the LIS and Glacial Lake Agassiz was abandoned and a much wider connection formed along the ice margin. By 9.50 cal. ka BP, the basins of Glacial Lakes Mackenzie and McConnell had both been abandoned with a pro-glacial lake re-locating further east (see Figure 6-7U). However, Glacial Lake Agassiz remained along the southern margin of the LIS.

In the Great Lakes region, the configuration of pro-glacial lakes remained very similar between 11.00 and 10.20 cal. ka BP (see Figure 6-7U, Figure 6-7V and Figure 6-7W). However, between 10.20 and 9.50 cal. ka BP, pro-glacial lakes in the Great Lakes region decreased in size dramatically. By 9.50 cal. ka BP, the ice margin had retreated north beyond the present location of the Great Lakes. The resulting pro-glacial lakes were located close to the ice margin and were not connected to Glacial Lake Agassiz. Pro-glacial lakes were minimal in this region due to the presence of an eastern drainage routeway into the Gulf of St Lawrence.

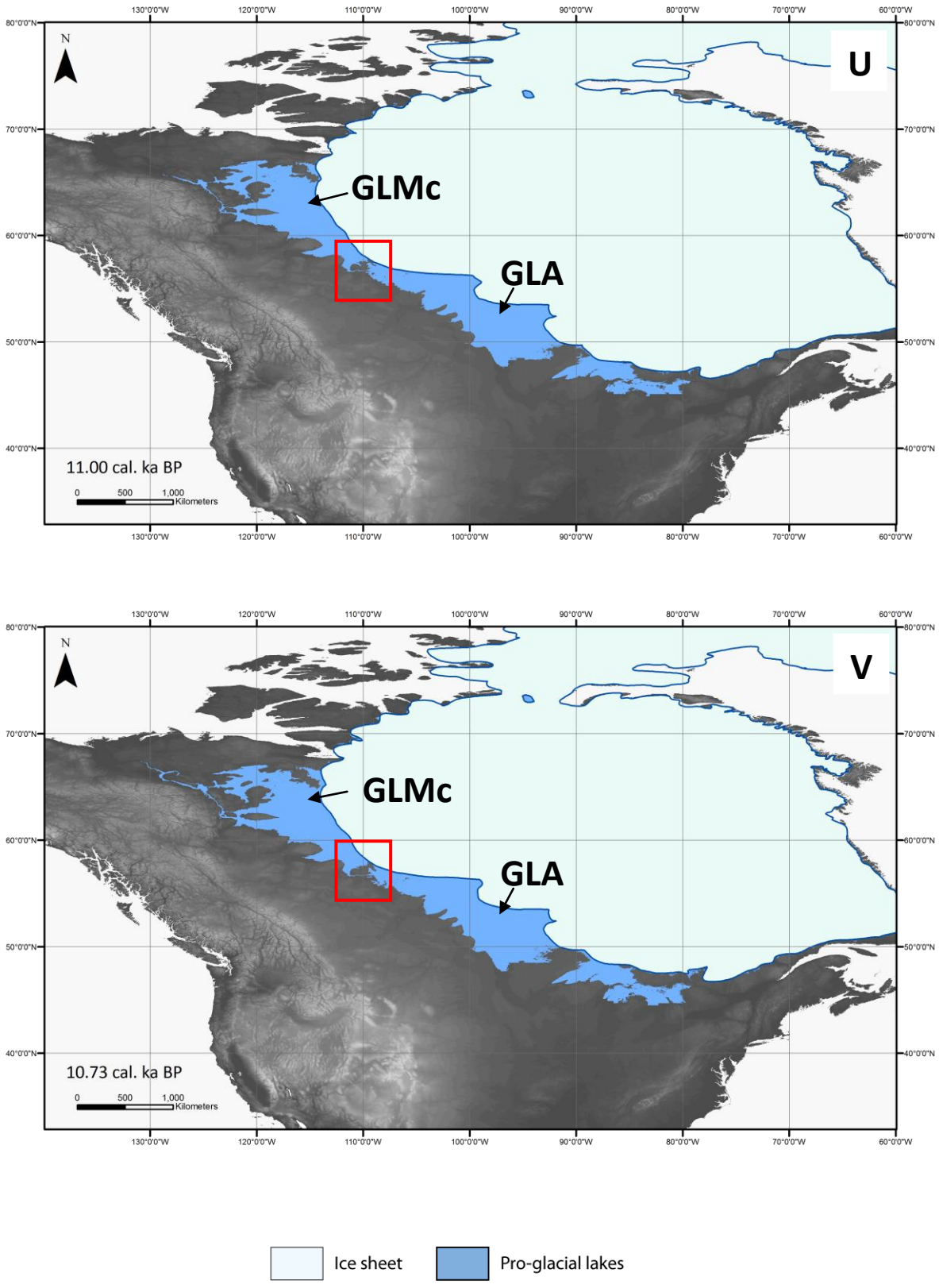

Figure 6-7 (cont.): The reconstructed pro-glacial lakes along the LIS mainland margin during the Late Wisconsinan. Where present, Glacial Lake Agassiz is labelled as 'GLA', Glacial Lake McConnell is labelled as 'GLMc' and the routeway which joins the two lakes is highlighted with a red box.

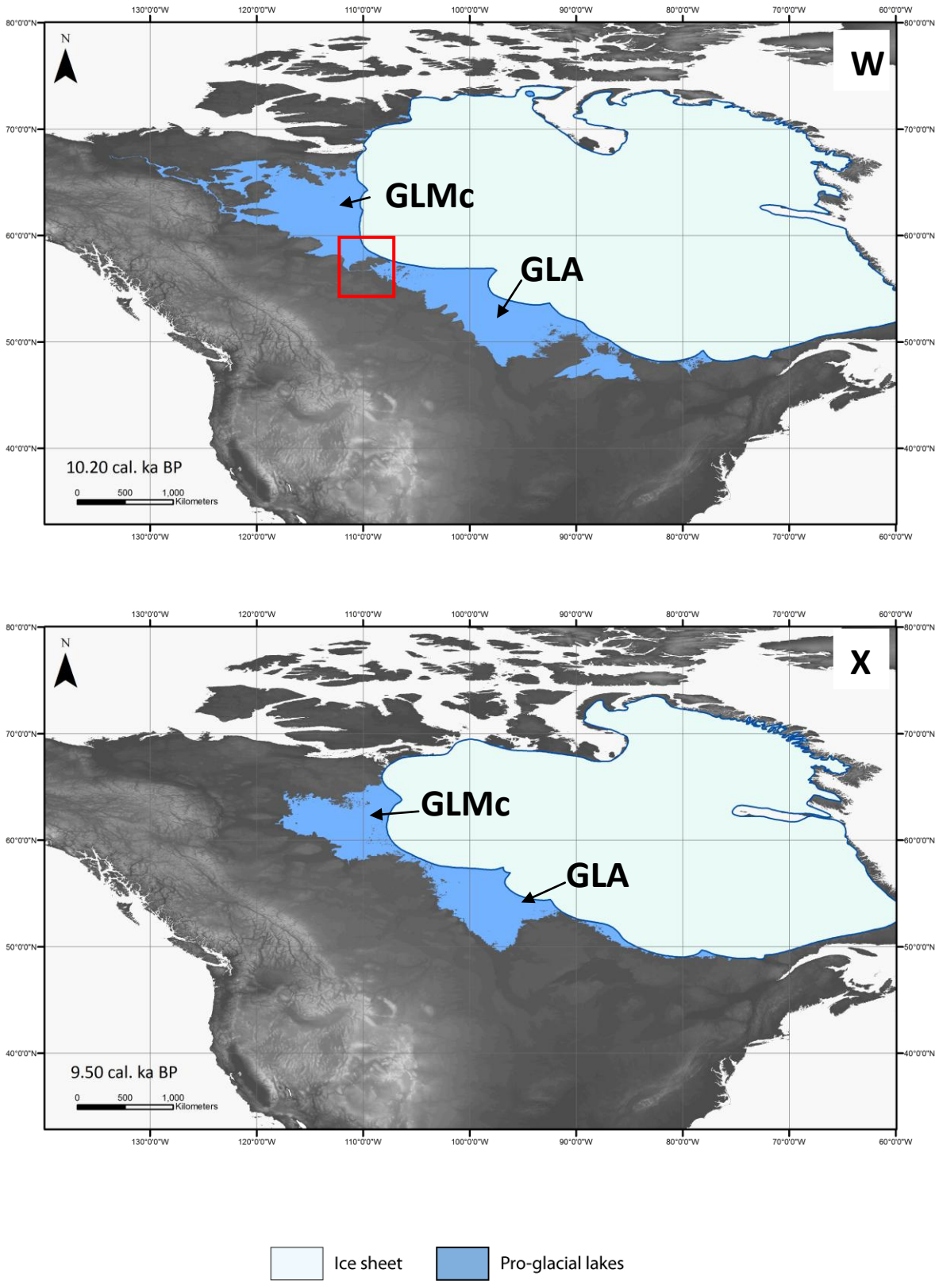

Figure 6-7 (cont.): The reconstructed pro-glacial lakes along the LIS mainland margin during the Late Wisconsinan. Where present, Glacial Lake Agassiz is labelled as 'GLA', Glacial Lake McConnell is labelled as 'GLMc' and the routeway which joins the two lakes is highlighted with a red box.

6.4.7 9.00 – 8.45 cal. ka BP

By 9.00 cal. ka BP, pro-glacial lakes no longer occupied the study area. The retreat of the LIS towards the east was accompanied by the initiation of two sutures zones in the ice sheet; one along Hudson Strait, and the second at the south-eastern corner of Hudson Bay (see Figure 6-7Y). The changing configuration of the LIS was accompanied by a dramatic reduction in pro-glacial lake extent between 9.00 and 8.45 cal. ka BP. This was partly due to the opening of the Hudson Bay suture zone which may have allowed pro-glacial lakes to drain sub-glacially, particularly those along the southern margin of the LIS (see Fisher *et al.,* 2002). As shown below in Figure 6-7Y, ~ 9.00 cal. ka BP, pro-glacial lakes were most extensive along the north-western margin of the LIS. Between 60 and 70° N, a narrow lake extended ~ 1000 km from the ice margin towards the basin of Great Slave Lake. Between 9.00 and 8.60 cal ka BP, this lake drained towards the north-east. During this period, a drainage pathway became available because of a small regional shift of the ice margin to the south (see Figure 6-7Z). Further south, Glacial Lake Agassiz persisted until 8.60 cal. ka BP, having rapidly decreased in size between 9.50 and 8.60 cal. ka BP. By 8.45 cal. ka BP, Glacial Lake Agassiz had drained and only a small pro-glacial lake remained along the mainland margin of the LIS. This small lake was located between 60 and 70° N on the Canadian Shield, just east of the study area (see Figure 6-7Aa).

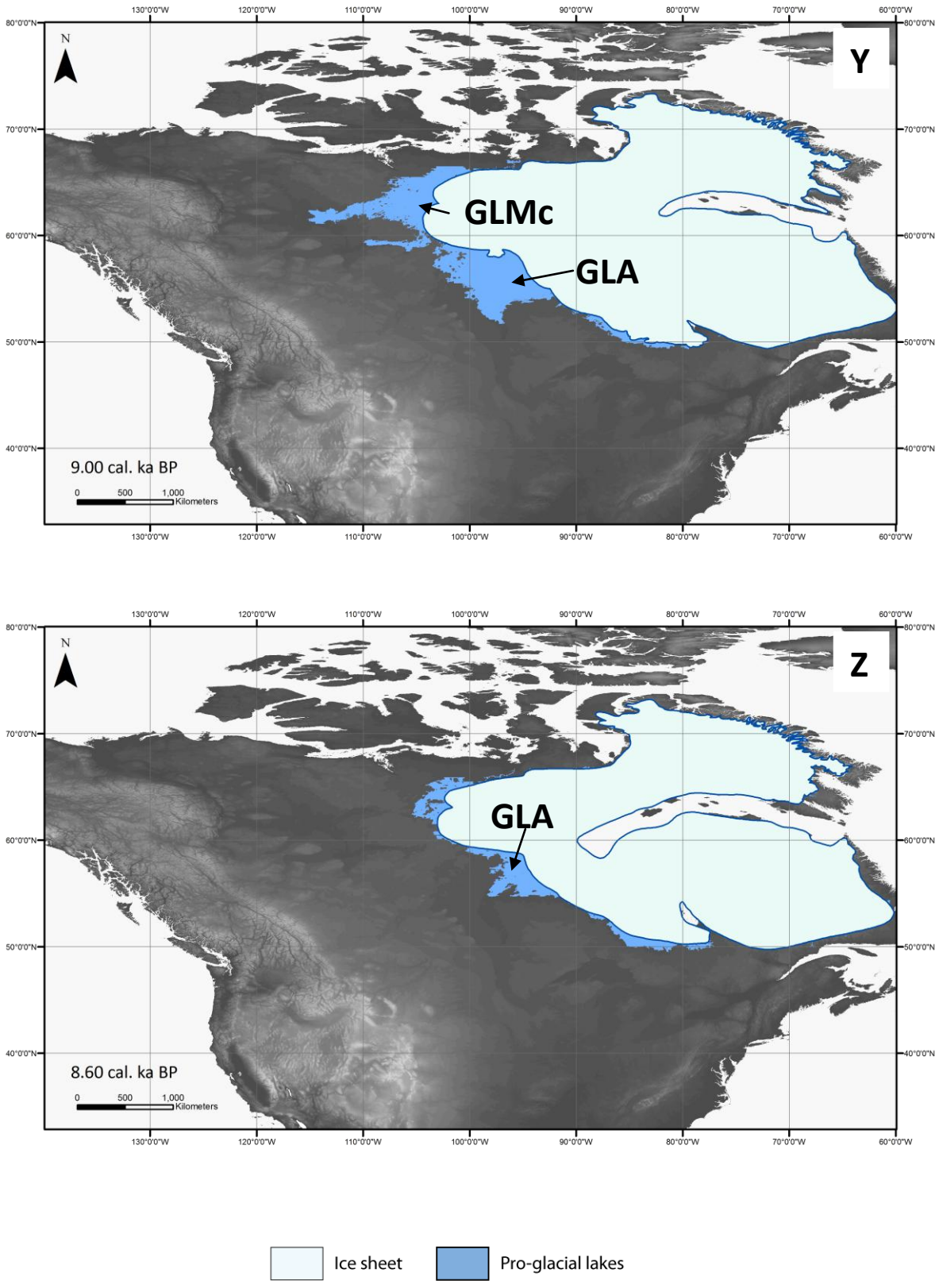

Figure 6-7 (cont.): The reconstructed pro-glacial lakes along the LIS mainland margin during the Late Wisconsinan. Where present, Glacial Lake Agassiz is labelled as 'GLA', Glacial Lake McConnell is labelled as 'GLMc' and the routeway which joins the two lakes is highlighted with a red box.

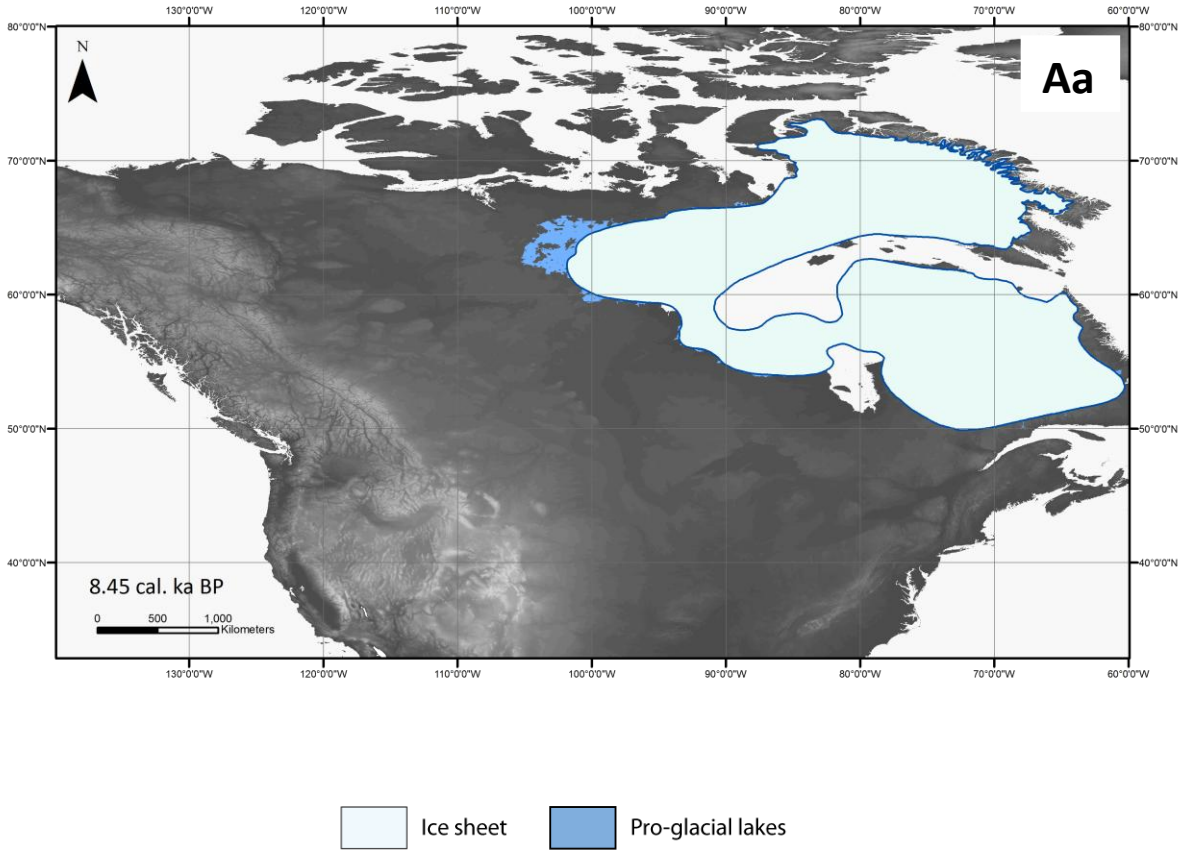

Figure 6-7 (cont.): The reconstructed pro-glacial lakes along the LIS mainland margin during the Late Wisconsinan. Where present, Glacial Lake Agassiz is labelled as 'GLA', Glacial Lake McConnell is labelled as 'GLMc' and the routeway which joins the two lakes is highlighted with a red box.

6.5 Pro-glacial lake area and volume

Time-series of both total lake area and volume are presented below in Figure 6-8 and Figure 6-9. A gradual increase in the area of pro-glacial lakes surrounding the LIS occurred following the LGM, before reaching a peak at ~ 10.20 cal. ka BP (Figure 6-8). Indeed, visual inspection of the pro-glacial lake reconstructions in Section 6.4 also allow for the identification of the largest pro-glacial lakes ~ 10.20 cal. ka BP. Pro-glacial lake area then decreased rapidly until 8.45 cal. ka BP which marks the end of the time-series for which pro-glacial lakes have been reconstructed. In particular, as noted above, Glacial Lake Agassiz, the largest pro-glacial lake along the margin of the LIS, drained between 8.60 and 8.45 cal. ka BP. This drainage is likely to have been towards the east, either into the North Atlantic or into Hudson Bay because by this stage of deglaciation, the ice margin had moved away from the north-western outlet through the study area. Small drops in lake area are also noted between 14 and 13 cal. ka BP and 12.5 and 11.5 cal. ka BP.

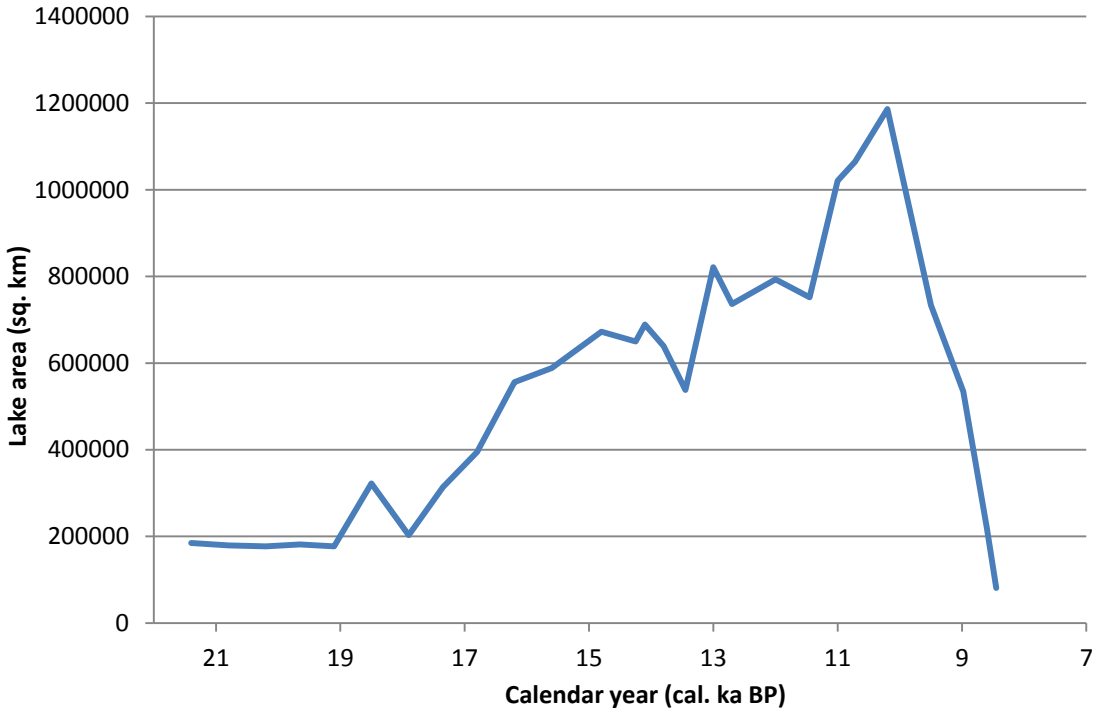

Figure 6-8: The area of pro-glacial lakes along the mainland margin of the LIS during deglaciation.

The record of pro-glacial lake volume during deglaciation is more complex. According to Figure 6-9, pro-glacial lake volume peaked three times during deglaciation. The first two peaks occurred early in deglaciation at 18.5 cal. ka BP and 17.35 cal. ka BP when lake volumes reached 66978 km^3 and 70349 km^3 respectively. However, inspection of the reconstructions of pro-glacial lakes shown in Section 6.4 and the area of pro-glacial lakes shown in Figure 6-8, suggests that lake area was limited until later in deglaciation when the LIS had begun to retreat. These peaks, and the intermediate drop in lake volume ~ 18 cal. ka BP, are therefore attributed to changes in the configuration of the southern margin of the LIS during this period; in particular, the formation of pro-glacial lakes in the Great Lakes region. Despite their relatively small area, these lakes must have been very deep in order to achieve the volumes shown in Figure 6-9. This was a result of high levels of crustal loading which caused the solid earth to deform, thus tilting the surface of the earth towards the ice margin to form an ice dammed lake basin. GIA during the early stages of deglaciation had a long lag time behind crustal unloading. The solid earth was therefore unable to readjust to small and localised changes in ice volume rapidly. Deep pro-glacial lakes exploited this lag time by developing in depressions along the ice margin where GIA had not yet responded to crustal unloading. This concept is schematically illustrated in Figure 6-1.

Later in deglaciation, further peaks in pro-glacial lake volume occurred ~ 13 cal. ka BP and ~ 10.72 cal. ka BP. The reconstructed pro-glacial lakes shown in Section 6.4, and their area shown in Figure 6-8, both suggest that pro-glacial lake area remained relatively stable ~ 13 cal. ka BP. The peak in lake volume ~ 13 cal. ka BP is therefore attributed to large amounts of SED which again produced very deep lakes with high volumes despite their modest area. The later peak in lake volume ~ 10.72 cal. ka BP occurred immediately prior to the peak in lake area ~ 10.2 cal. ka BP. At this time, the solid earth was rebounding after crustal loading during overall LIS retreat which explains why peaks in lake area and volume do not directly correlate. At 10.72 cal. ka BP, the lakes had a volume of 62880 km^3. Changes in pro-glacial lake area and volume are both discussed further in Chapter 7.

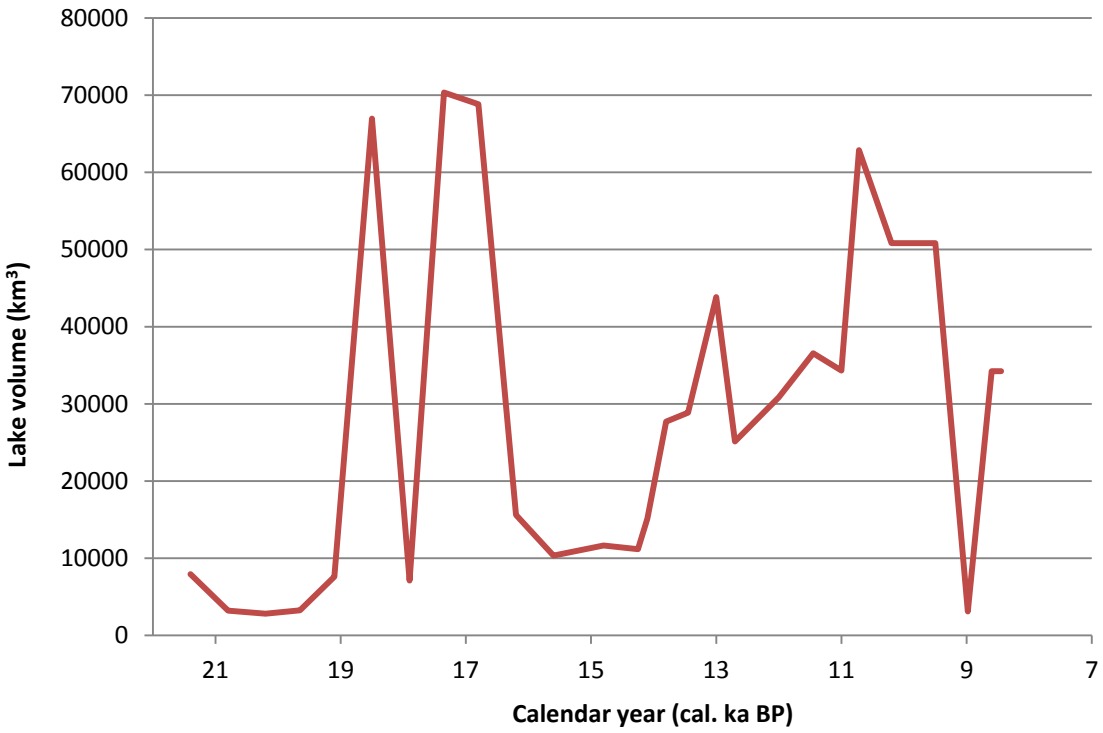

Figure 6-9: The volume of pro-glacial lakes along the mainland margin of the LIS during deglaciation.

6.6 Summary

- The extent of pro-glacial lakes along the mainland margin of the LIS has been established by flooding a DEM of North America. This has been carried out at twenty-seven time steps throughout Late Wisconsinan deglaciation from 21.4 cal. ka BP to 8.45 cal. ka BP.

- Data from the ICE-5G model of the glaciated earth surface was added to the DEM at each time step. This incorporates the effects of SED into the reconstructions of pro-glacial lakes.
- The reconstructions indicate that the extent of pro-glacial lakes remained minimal and relatively constant until 16.80 cal ka BP, particularly along the north-western margin of the LIS. After 16.80 cal. ka BP, the lakes initially expanded along the southern margin of the LIS around the James and Des Moines lobes. Subsequent expansion of pro-glacial lakes occurred in the Great Lakes region following the northward retreat of ice in the basins now occupied by Lakes Superior, Michigan, Ontario and Erie.
- By 15.60 cal. ka BP, ice had retreated onshore along the north-western mainland margin of the LIS and pro-glacial lakes began to form. Lakes continued to expand along the north-western margin of the LIS until they reached their maximum extent at ~ 10.72 cal. ka BP.
- A possible drainage routeway has been identified between Glacial Lake Agassiz and the lakes along the north-western margin of the LIS. The routeway opened ~ 12.7 cal. ka BP and persisted until 10.20 cal. ka BP.
- From 10.71 cal. ka BP, the LIS retreated rapidly and pro-glacial lakes decreased in both area and volume. During this period, routeways became available for lake drainage as the configuration of the LIS margin evolved.
- Pro-glacial lake area increased gradually during deglaciation, while pro-glacial lake volume change was more complex. The relationship between pro-glacial lake area and volume can be explained by changes in SED which often allowed for the formation of deep lakes near the ice margin which covered small areas but had high volumes.

Chapter 7: Discussion

7.1 Introduction

This chapter provides a synthesis of Chapters 4, 5 and 6, draws links between the contents of each chapter, and discusses the wider implications of this thesis for north-west LIS history and palaeo-ice stream dynamics. The timing and controls on ice stream activity in the north-west LIS will first be examined. The latter part of the chapter discusses a possible north-west drainage routeway for Glacial Lake Agassiz and its associated geomorphological signature. Finally, the chapter will provide recommendations for future work.

7.2 Causes of streaming flow in the north-west LIS

According to Winsborrow *et al.* (2010), the location of ice streams is controlled by a number of factors as detailed below in Figure 7-1. Each of these possible controls will be discussed below with respect to the north-west LIS with the aim of establishing why the temporal and spatial patterns of ice streaming are particularly complex in this sector of the LIS. The relationship between ice stream activity and deglacial climate will also be discussed. Figure 7-1 summarises the hierarchy of key controls on ice stream activity.

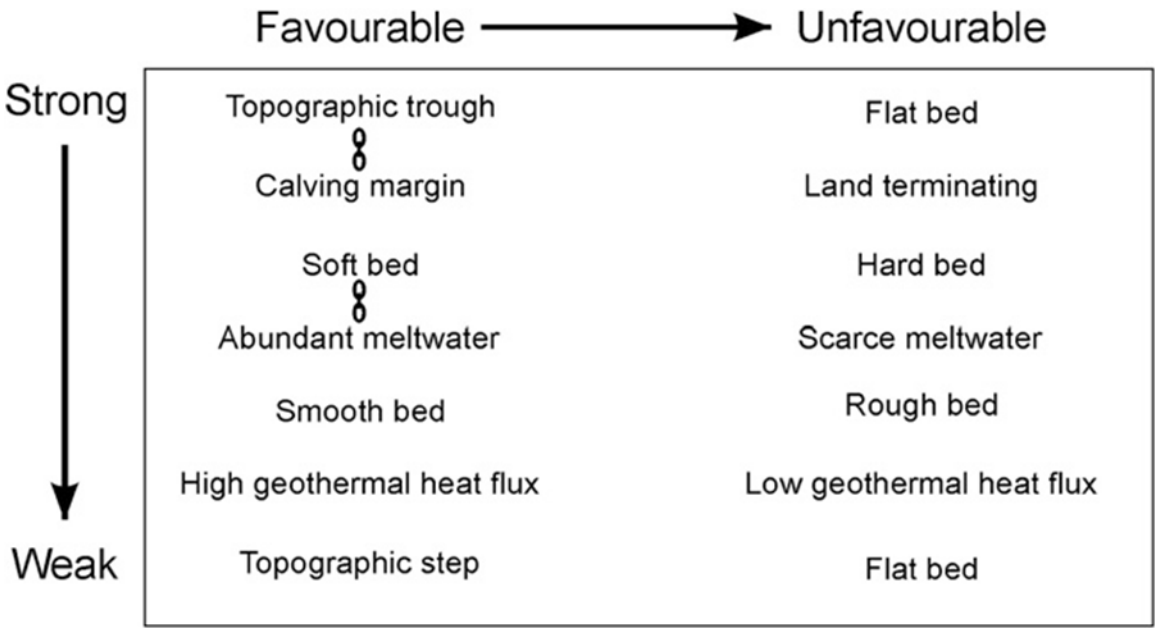

Figure 7-1: The hierarchy of controls on the location of ice streams. Taken from Winsborrow et al. (2010). The chains between some of the factors on the left-hand side of the diagram indicate that these factors may be of equal importance.

7.2.1 Regional topography

As noted by Winsborrow *et al.* (2010), streaming flow may be controlled by topography via two mechanisms. Firstly, constriction of ice through a topographic trough requires an increase in velocity in order to maintain a constant discharge, and secondly, an increase in velocity aids basal melting which subsequently lubricates the bed and aids further rapid flow (Patterson, 1994; Winsborrow *et al.,* 2010).

The area covered by the north-west LIS is characterised by low-lying, undulating topography which is neighboured to the west by the contrasting steep terrain of the Rocky Mountains (Reed *et al.*, 2003). To the north is Amundsen Gulf, a deep marine tough which is approximately 3 km wide at its narrowest point. According to the reconstruction presented in Chapter 5, the trough was occupied by an ice stream during the Late Wisconsinan, the location of which was controlled by the regional topography (see also Stokes and Clark, 2006 and Stokes, 2000). Onshore, the topography is more subtle but a number of small topographic troughs are present. In particular, on the northern shore of Great Bear Lake, a small trough ~ 7 km long, 1.5 km wide, and up to 200 m deep, trends east to west. This trough was occupied by the Haldane ice stream during deglaciation; an ice stream that is documented in this thesis but also previously by Kleman and Glasser (2007) and Winsborrow *et al.,* (2004) based on Clark (*unpublished*, cited in Winsborrow *et al.,* 2004). However, elsewhere, ice streams have been reconstructed which did not occupy topographic troughs. This includes ice streams which defected around topographic high points such as the Mackenzie ice streams (both east and west branches), and the Paulatuk ice stream which extended around the southern side of the Melville Hills. The Mackenzie ice streams originated south of Great Bear Lake and flowed north while extending around topographic highs at ~65°N, on the western side of the present day Mackenzie River, and on the western side of Great Bear Lake. These ice streams can be differentiated from ice streams such as the Haldane ice stream because they were at no point contained completely within a topographic trough. Therefore, while two ice streams in the north-west LIS occupied topographic troughs, a further three ice streams extended around topographic highs but were not constrained within troughs. In contrast, the Kugluktuk and Fort Simpson ice streams did not occupy topographic troughs or extend around topographic highs on either side of the ice streams. As such, it is likely that regional topography exerted only a moderate control on ice stream activity in this sector of the ice sheet.

7.2.2 Calving margin

A calving margin provides an effective means of drawing down ice from an ice sheet and removing mass (Benn and Evans, 2010). Subsequent ice draw-down lowers the ice sheet

surface and allows the catchment area of an ice stream to expand. Hughes (1992) termed this 'ice stream pulling power'. Water at the terminus of an ice stream also increases the subglacial water pressure which in turn reduces basal shear stresses and aids streaming flow up-ice of the terminus (Nye, 1959; Winsborrow *et al.*, 2010). Of the ice streams reconstructed in this thesis, four were terrestrially terminating while the other three (Amundsen, Mackenzie East and Mackenzie West) terminated in the present day Beaufort Sea. However, with global sea level approximately 120 m lower than present at the LGM (eustatic component), the coastline of north-west Canada would have been located several hundreds of kilometres offshore near the edge of the continental shelf. However, glacio-isostasy will have also depressed the lithosphere and therefore reduced the impact of this. It is therefore possible that ice streams were able to calve into the ocean, but only during the very early stages of deglaciation when the LIS was near its maximum extent with a margin well away from the present day coastline.

The only scenario in which a calving margin could have been established is if pro-glacial lakes developed along the ice margin. Along the north-western margin of the LIS, pro-glacial lakes McConnell and Mackenzie formed (see Chapter 6). As shown in Figure 7-2, the volume and area of pro-glacial lakes along the north-west margin of the LIS remained relatively low until 13.0 cal. ka BP when they both began to increase rapidly. A peak in lake volume occurred ~ 12.7 cal. ka BP. However, as previously noted, ice stream activity in the north-west LIS peaked before this, between 13 and 15 cal. ka BP. This suggests that ice streaming in the north-west LIS was not controlled by the growth of pro-glacial lakes which aided calving at the ice stream terminus.

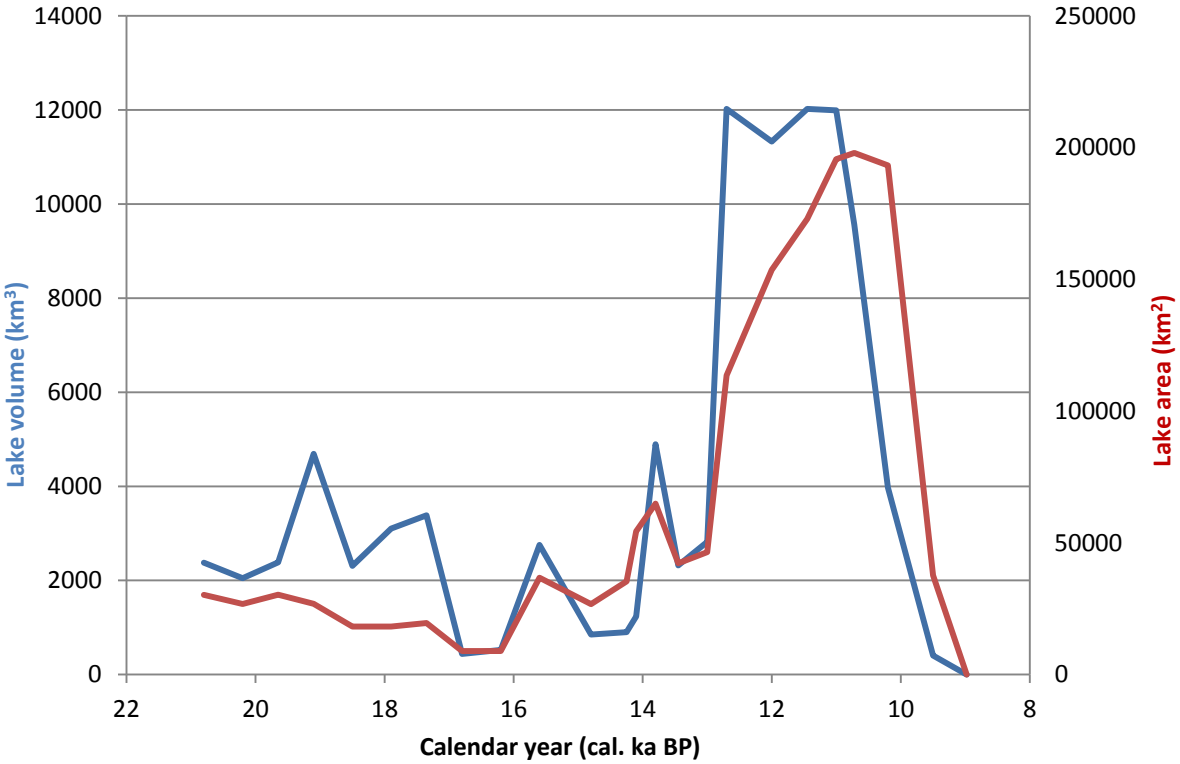

Figure 7-2: The volume and area of pro-glacial lakes in the study area along the north-western margin of the LIS (the study area) during Late Wisconsinan deglaciation. While the reconstructions of pro-glacial lakes presented in Chapter 6 indicate that pro-glacial lakes along the north-west margin of the LIS continued to increase after 10 cal. ka BP, it should be noted that the lake volumes and area shown in Figure 7-3 only include lakes within the study area. Therefore, as deglaciation progressed, the ice margin and associated pro-glacial lakes retreated east. This reduced the area of the lake within the study area, despite an overall increase in lake area and volume along the north-western margin of the LIS. This accounts for the drop in pro-glacial lake area and volume shown in Figure 7-3 ~ 10.5 cal. ka BP.

7.2.3 Relationship to underlying geology

The occurrence of soft-sediment has often been assumed as a prerequisite for ice stream activity. This is particularly the case in an ice stream onset zone, since it allows for ice sheet motion via subglacial sediment deformation (Clark, 1992; Patterson, 1998; Anandakrishnan *et al.,* 1998; Engelhardt *et al.,* 1990 MacAyeal, 1992; Peters *et al.*, 2006; Siegert *et al.,* 2004; Ó Cofaigh *et al.,* 2005). Examples include the ice streams of the Siple Coast, Antarctica which are located on soft unconsolidated sediment > 2 m thick (Engelhardt *et al.,* 1990; Alley *et al.,* 2007). However, Stokes and Clark (2003) have indicated that while the presence of abundant soft-sediment remains favourable for ice stream activity, it is not essential. Indeed, Winsborrow *et al.* (2010) identify a soft-bed as a control on ice stream activity but do not assume it to be vital.

Mainland north-west Canada is dominated by a thick blanket of till which is underlain by soft-sedimentary sequences deposited in shallow inland seas (Reed *et al.,* 2003) (Figure 7-3). To the west of the study area, the solid surficial geology of the Rocky Mountains contrasts with the abundant soft sediment in the central study area (units Tb and Tv on Figure 7-3). In the east, the metamorphosed Precambrian Shield, with its limited sediment cover, rises gently towards the Northwest Territories – Nunavut border (unit R). Soft-sediment is therefore likely to have been abundant in the north-west LIS during the Late Wisconsinan, even prior to the deposition of the thick blanket of till which presently accounts for a large area of the region's surficial geology. This would have aided fast ice flow via subglacial sediment deformation. Because the till blanket in north-west Canada is so extensive, each of the ice streams identified in this thesis were located on it. Therefore, while it is not possible to identify the degree to which subglacial sediment deformation influenced the activity of individual ice streams within the north-west LIS, it is likely that, regionally, ice stream activity is likely to have been facilitated by an abundant supply of soft-sediment in this location, as opposed to further east.

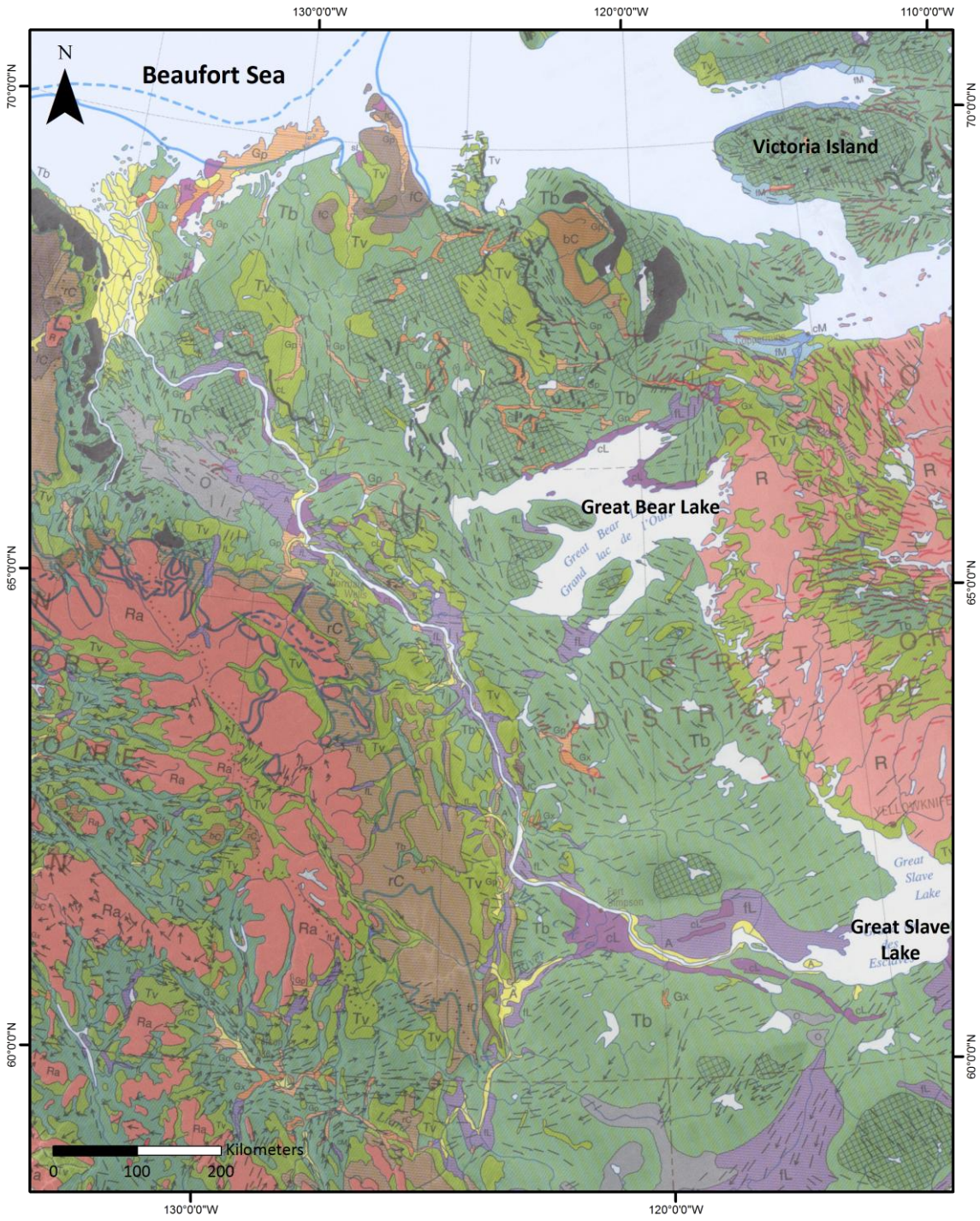
130°0'0"W
120°0'0"W
110°0'0"W
70°0'0"N
65°0'0"N
60°0'0"N
N
Beaufort Sea
Victoria Island
Great Bear Lake
Great Slave Lake
Kilometers
0
100
200

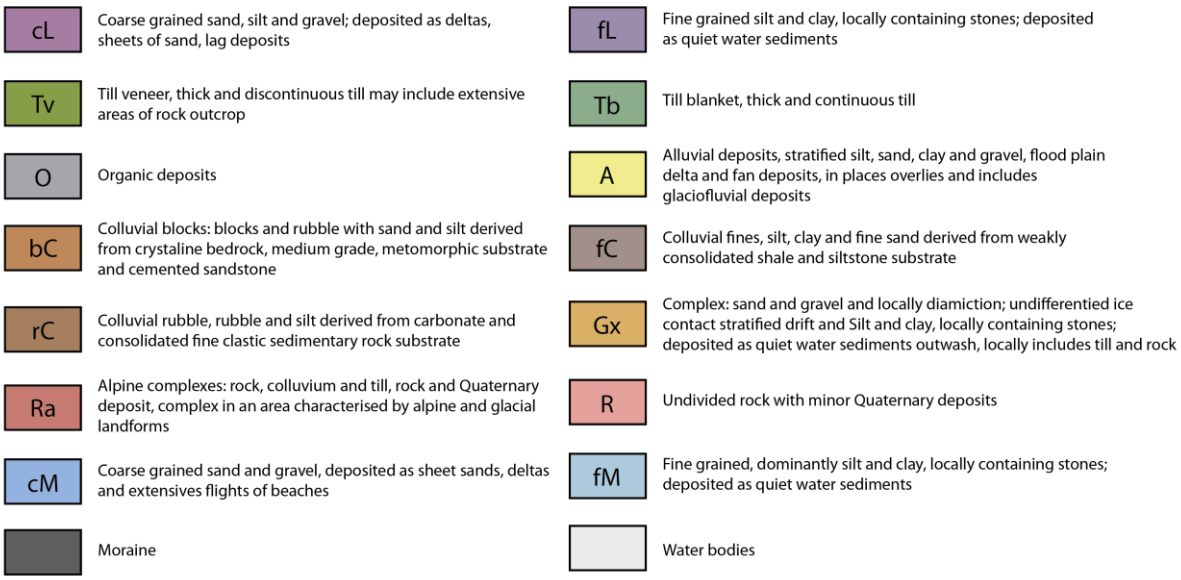

Figure 7-3: The surficial geology of north-west Canada. Extract taken from Fulton (1995). Note that the majority of the study area is covered with a till blanket (Tb), or fine grained silt and clay (fL).

7.2.4 Geothermal heat sources

Greater geothermal heat flux has been shown to increase the temperature of basal ice and therefore promote faster ice flow (Blankenship *et al.,* 1993; van der Veen *et al.,* 2007; Rogozhina *et al.,* 2012). Across North America, present day geothermal heat flux is highly variable. According to Blackwell and Richards (2004), the greatest geothermal heat flux in Canada occurs along the Rocky Mountains along the western seaboard (Figure 7-4). In contrast, in Hudson Bay, a more tectonically stable region with much older geologic origins (Bastow *et al.,* 2011), a relatively low geothermal heat flux is indicated (Blackwell and Richards, 2004). The study area lies between these two regions with high geothermal heat fluxes consistently in excess of 65 mW/m^2 and a maximum geothermal heat flux of 110 mW/m^2. This is comparable to the contemporary geothermal heat flux below Jakobshavns Isbrae, Greenland which is suggested by van der Veen *et al.* (2007) to be approximately 115 mW/m^2, and thought to be crucial to the occurrence of streaming flow in the Jakobshavns trough. Within the study area, regions of high geothermal heat flux match the area occupied by the Mackenzie east and Mackenzie west ice streams. Furthermore, the area surrounding the Anderson River in the northern part of the study area should be noted as an area of more isolated high geothermal heat flux.

High geothermal heat flux such as that presently recorded within the study area is likely to have introduced basal melting and therefore abundant meltwater to the subglacial

environment. This would have aided faster ice flow, including streaming flow, by enhanced basal sliding. Therefore, assuming that the geothermal heat flux during the Late Wisconsinan was not dissimilar to that of the present, geothermal heat flux appears to have exerted a strong control on the location of ice streaming in the north-west sector of the LIS.

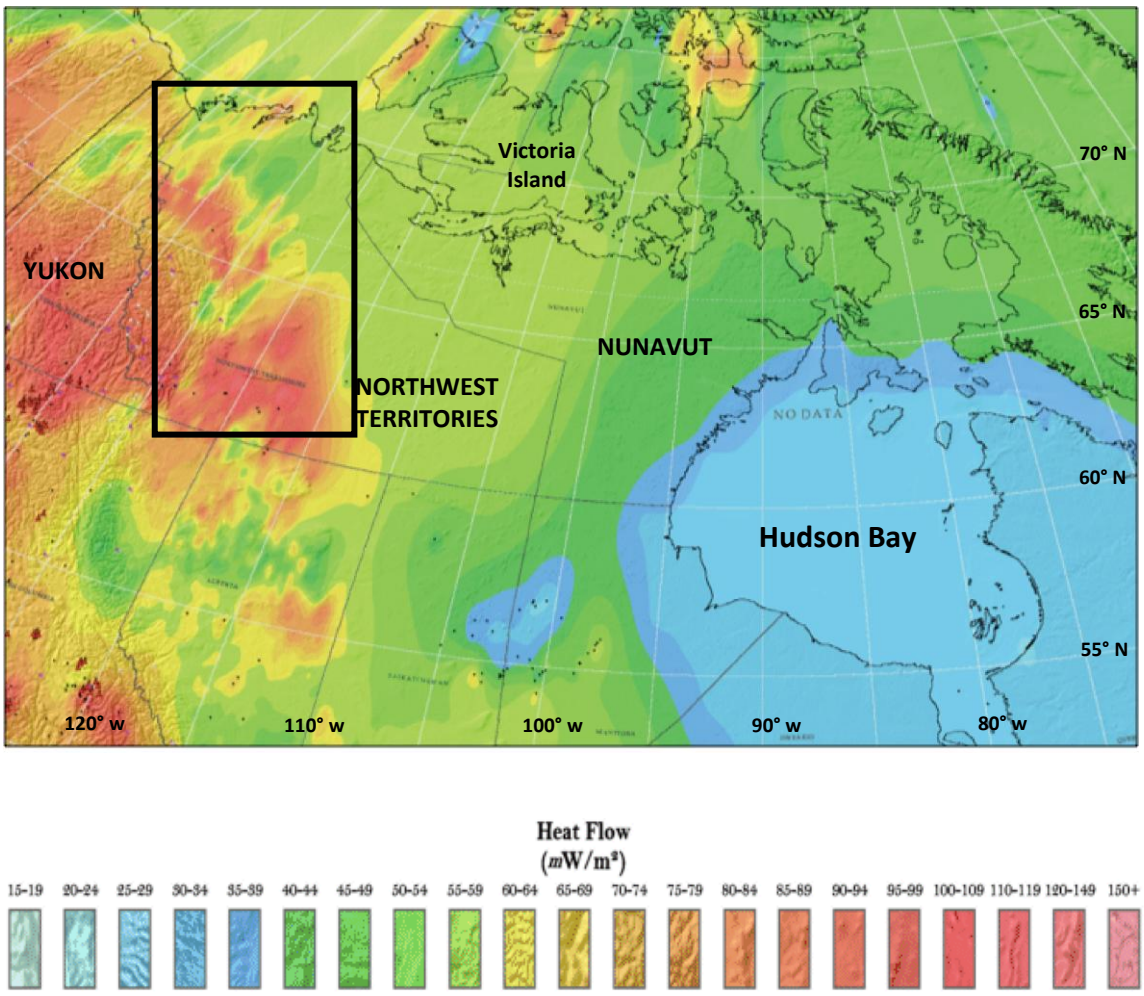

Figure 7-4: Present day relative geothermal heat over Canada taken from Blackwell and Richards (2004). The study area is located in the north-west portion of the map and along its western margin follows the Yukon – Northwest Territories border. The study area is highlighted with a black box.

7.2.5 Meltwater supply

Subglacial meltwater in the north-west LIS was principally controlled by two factors; geothermal heat flux as previously discussed, and meltwater resulting from changing internal ice sheet dynamics and feedback mechanisms. The Keewatin Dome was the largest dome of the LIS and contained ice up to 3 km thick (Argus and Peltier, 2010). It was located to the west of Hudson Bay on the Canadian Shield and was the major source of ice for the north-west LIS (Carlson *et al.,* 2009). According to Tarasov and Peltier (2006), the overburden pressure of ice

within the dome induced pressure melting at the ice bed interface. This, in turn, reduced the basal shear stress, increased ice velocity by basal sliding, and resulted in a net draw-down of ice which lowered the ice surface profile. Abundant meltwater would have also increased the pore-water pressure of soft subglacial sediments and thus supported increased ice velocities by subglacial sediment deformation (Alley *et al.,* 1987; Clayton and Mickelson, 1989; Hicock and Dreimanis, 1992; Clark, 1994; Tulaczyk *et al.,* 2000). Moreover, as deglaciation progressed, LIS subglacial meltwater became more abundant and accumulated in topographic depressions to form subglacial lakes (Marshall and Clark, 2002). Christoffersen *et al.* (2008) have reconstructed a subglacial lake close to the study area around the eastern arm of Great Slave Lake based on sedimentological evidence. The lake was 130 km^2 and may have acted as a slippery spot in which ice could not become grounded (Christoffersen *et al.,* 2008). This therefore facilitated basal sliding and increased ice velocity, possibly to a velocity comparable to that of streaming flow (Christoffersen *et al.,* 2008). The presence of subglacial lakes such as this therefore provide further evidence for an abundance of meltwater in the north-west LIS. In accordance with Winsborrow *et al.* (2010), an abundance of meltwater may also explain why this sector of the ice sheet was subject to such extensive ice stream activity during the Late Wisconsinan.

7.2.6 Topographic steps

McIntyre (1985) first suggested that topographic steps of the order of 100 m may control the location of streaming flow. This occurs through a strain-heating feedback loop in which strain heating of the ice occurs as it flows over a step and is forced to accelerate (McIntyre, 1985). It causes a decrease in ice viscosity and therefore enables ice to deform more readily and thus flow faster (McIntyre, 1985; Winsborrow *et al.*, 2010). Further increases in basal ice temperatures then occur through frictional heating at the ice-bed interface. This initiates further ice-draw down over the step and achieves a positive thermo-mechanical loop (Winsborrow *et al.,* 2010). Extensional flow within ice as ice moves over a convex bed or topographic high, can also aid basal sliding and therefore increase ice velocity by opening crevasses which provide water with access to the ice-bed interface (Nye, 1952).

In the north-west sector of the LIS, the seven ice streams occupied a region of low-lying, relatively flat topography. The ice streams occurred over distances > 1000 km and were, therefore, comparable in size to the ice streams reconstructed by De Angelis and Kleman (2007) in the Foxe/Baffin sector of the LIS, or the ice streams along the southern margin of the LIS in the St James and Des Moines lobes (Patterson, 1998; Jennings, 2006). However, over the entire length of the Mackenzie ice streams, the ice stream bed descends by only 300 m. In the

case of the smaller ice streams, similar shallow bed profiles have been identified. For example, in the case of the Haldane ice stream, a change in bed elevation of < 150 m is observed from the up-ice to down-ice end of the ice stream. When considering the distances over which the ice streams were flowing, it is unlikely that such subtle changes in bed elevation would influence ice stream operation. In addition, as noted in Section 7.3.3, the regional topography is dominated by abundant soft sediment which would also have provided ice streams in the north-west LIS with smooth beds. According to Winsborrow *et al.* (2010) a smooth bed is preferable for streaming flow as this reduces friction at the ice-bed interface.

7.2.7 Climate oscillations

Contemporary ice streams have been found to respond to changes in ocean temperature induced by decadal atmospheric temperature oscillations (Pritchard *et al.,* 2009; Joughin *et al.,* 2010; White *et al.,* 2011). During Late Wisconsinan deglaciation, an abrupt climate warming occurred ~ 14.7 cal. ka BP. This lasted until ~ 12.7 cal. ka BP and is known as the Bolling-Allerød (Figure 7-5). Around the time of the Bolling-Allerød, the north-west LIS underwent rapid eastward retreat. The Anderson lobe, which was fed by the Mackenzie east ice stream, retreated, and ice stream flow switched to the western branch of the Mackenzie ice stream. The ice stream fed a lobe of ice over the present day Mackenzie delta before this lobe also retreated east. Following the loss of these two major lobes, and the relocation of the ice margin further east, streaming flow continued and was accompanied by the onset of the smaller Haldane, Paulatuk and Fort Simpson ice streams from 13.80 cal. ka BP. This group of smaller ice streams provided short pulses of streaming flow during the latter part of deglaciation compared to their larger counterparts. Ice stream activity therefore remained relatively constant in the north-west sector of the LIS despite periods of abrupt climate change during deglaciation and the associated retreat of the ice margin. A positive link between climate and ice stream activity is therefore difficult to discern. However, it is likely that ice streams in the north-west LIS played a key role in mass loss from this sector of the ice sheet during periods of ice sheet retreat. This may have been achieved by an increase in the intensity of streaming flow within the existing ice streams rather than a change in the number of active ice streams during periods of climate warming. Indeed, according to Carlson *et al.* (2011), the north-west sector of the LIS was unusual because it retained a positive surface mass balance throughout periods of climate warming during the Late Wisconsinan. This will have sustained ice streams in the north-west sector of the LIS despite overall margin retreat.

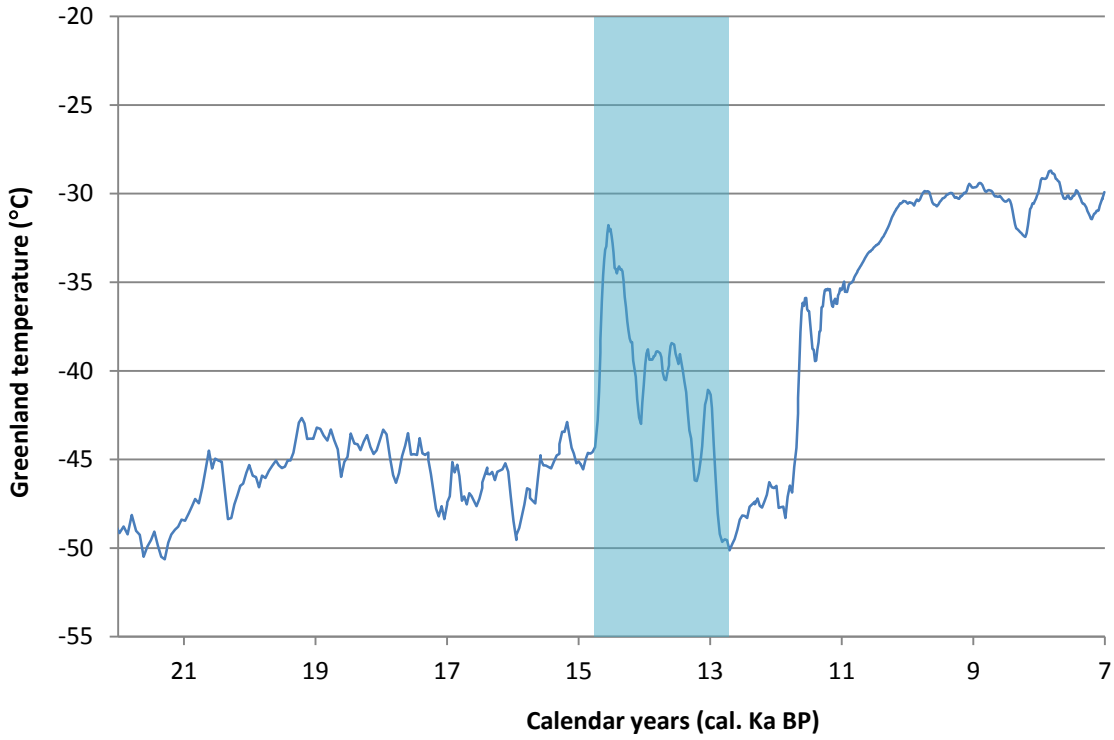

Figure 7-5: The record of northern hemisphere atmospheric temperature taken from the Greenland Ice Core Project 2 core. Data sourced from NOAA (www.ncdc.noaa.gov). The Bolling-Allerød is highlighted in blue.

This section has identified the relative importance of the controls on ice stream activity in the north-west LIS. The principal controls on the operation of the seven ice streams in this sector of the LIS were the underlying geology, relatively high geothermal heat flux, and a probable meltwater supply. However, it should be acknowledged that these factors are unlikely to have operated in isolation but rather, they worked together to result in a compound effect. In comparison to other sectors of the LIS, this is another reason why ice stream activity was so extensive in the study area.

7.3 Ice stream activity in the north-west LIS

Ice streams in the north-west LIS are represented in the post-glacial landscape by a distinct geomorphological signature. This signature includes groups of highly elongate bedforms with abrupt lateral margins and glacial lineations which are arranged in convergent patterns in the ice stream head-zone, and in downstream locations, divergent patterns. These characteristics are described in Chapter 5, and were suggested by Stokes and Clark (1999) as indicative of ice stream activity (see Chapter 2, Figure 2-5). Previous authors, including Clark (*unpublished*, cited in Winsborrow *et al.,* 2004), Winsborrow *et al.* (2004), Kleman and Glasser (2007), and Beget (1987), have hypothesised that ice streaming took place in the north-west LIS). Of the

ice streams reconstructed in this thesis, four equate to previously hypothesised ice streams: the Mackenzie ice stream (both east and west branches), Amundsen Gulf ice stream, and Haldane ice stream. However, as previously stated, geomorphological evidence for the activity of these ice streams has not hitherto been compiled, and their behaviour (including location, timing and mechanisms of flow) has therefore remained uncertain. The glacial geomorphology documented in both Chapter 4 and Brown *et al.* (2011) includes a complex arrangement of highly elongate and partially overprinted glacial lineations along with aligned and non-aligned eskers. Moreover, major moraine ridges are relatively sparse and large palaeo-channels dissect the region pattern of glacial geomorphology. The complex spatial arrangement of glacial geomorphology in this sector of the LIS is attributed to dynamic switches in ice sheet flow orientation during deglaciation.

During Late Wisconsinan deglaciation, changes between streaming flow and sheet flow occurred at a variety of time intervals and resulted in different durations and styles of streaming flow. In the early stages of deglaciation, streaming was dominated by the three large ice streams (Mackenzie East and West ice streams and the Amundsen Gulf ice stream). Later in deglaciation, streaming flow was dominated by a greater number of smaller ice streams. The larger ice streams are represented by multiple flow-sets which can be traced over large areas (several hundred kilometres). According to Jennings (2006) and Stokes and Tarasov (2010), terrestrially terminating ice streams, including those in the north-west LIS, do not persist throughout deglaciation but rather, switch on and off for short periods. However, the reconstruction presented in Chapter 5 suggests that the largest terrestrially terminating ice streams in the north-west LIS persisted for several thousand years during deglaciation, in particular between 21.4 and 16.0 cal. ka BP. Ice may have been evacuated from the termini of these ice streams immediately following the LGM by ice calving into the ocean (see Section 7.2.2). These ice streams include the Mackenzie ice streams and the Amundsen Gulf ice stream. As noted above in Section 7.3.2, each of these ice streams is likely to have been terrestrially terminating, particularly during the early stages of deglaciation, as a result of a lower sea level. However, while each of the larger ice streams persisted over millennial timescales, they were located in contrasting topographic settings.

As outlined by Bennett (2003), the physics which determine the operation of topographic and pure ice streams is very different. The ice streams identified in the north-west LIS are pure ice streams with the exception of the Haldane ice stream and Amundsen Gulf ice streams which occupied topographic troughs. Physiographically, the study area comprises a broad low-lying plain which allowed the boundaries of pure ice streams to migrate in response to changing ice

sheet dynamics (Kleman and Glasser, 2007). Thus, in this setting, major changes in the operation of ice streams can be partially explained by assuming that individual ice streams did not operate mutually exclusively of those around them. Rather, the seven ice streams documented in this thesis formed a web of interacting ice streams in the north-west sector of the LIS (cf. Kleman and Glasser, 2007). Examples of contemporary pure ice streams are limited and possibly restricted to the Siple Coast, West Antarctica (Alley *et al.,* 1986; Alley and Bentley, 1988; Payne, 1998; Joughin *et al.,* 2002; Siegert *et al.,* 2004).

The Siple Coast ice streams form a network of interacting ice streams comparable to those identified in this thesis in the north-west LIS (Payne, 1998). In the north-west LIS, dynamic switches in ice stream activity occurred during deglaciation, both within (e.g. the Mackenzie east and Mackenzie west ice streams), and between individual ice streams. However, unlike the Siple Coast ice streams, those of the north-west LIS did not stagnate as a result of changes in their onset zones, see Figure 5-4. As suggested by Stokes and Tarasov (2010), marked changes in the onset zones of ice streams occurred in this sector of the ice sheet, even in the absence of marked changes down-stream and vice versa. This is confirmed by the reconstruction of ice stream activity shown in Chapter 5. For example, the onset zone of the Mackenzie ice streams is represented by several flow-sets which indicate the switching on and off of the ice stream during deglaciation. However, these changes are not concurrent with switches downstream between the Mackenzie East and Mackenzie West ice streams. However, when the Mackenzie east ice stream shut down, the Mackenzie west ice stream became active again in a second phase. Therefore, unlike the Siple Coast ice streams, ice piracy does not appear to have initiated ice stream stagnation via 'reduced catchment-area' mechanism, but rather, it may have contributed to the internal downstream re-configuration of the Mackenzie ice streams as ice switched from the east to west branches and vice versa. Furthermore, water piracy may have contributed to this switching behaviour by changing the location and pathways of subglacial meltwater. This will have enhanced basal sliding and therefore promoted streaming flow in different part of the ice sheet. Therefore, along with the controls identified in Section 7.2, water piracy is likely to also have been influential in promoting ice streaming in the north-west sector of the LIS.

7.4 Lake Agassiz drainage

The drainage of LIS pro-glacial lakes during deglaciation has been hypothesised as a trigger for abrupt climate and sea level changes such as Bolling-Allerød, the Younger Dryas (YD), Preboreal Oscillation (PBO) and 8.2 event (Broecker *et al.,* 1988; Broecker *et al.*, 1999; Teller

and Leverington, 2002; Lowell *et al.,* 2005; Tarasov and Peltier, 2005; Murton *et al.*, 2010; Condron and Winsor, *unpublished*).

Event	Date of onset	Duration	Published in:
Bolling-Allerød	14.6 cal. ka BP	340 years	Deschamps *et al.* (2012)
Younger Dryas	12.9 cal. ka BP	1300 years	Carlson (2010); Broecker *et al.* (2010)
Preboreal Oscillation	11.3 cal. ka BP	150 – 250 years	Fisher *et al.* (2002)
8.2 event	8.2 cal. ka BP	100 years	Rohling and Pälike (2005)

Table 7-1: The timing of key changes in global climate during deglaciation taken from the most recently published sources.

As outlined in Chapter 2, pro-glacial lake drainage has been suggested via a number of different routeways (see Chapter 2, Table 2-1 and Figure 2-18). Most recently, a north-western outlet for Glacial Lake Agassiz has been suggested by Murton *et al.* (2010) who describe two fluvial boulder gravels along the Tuktoyaktuk Peninsula which have been dated using OSL to between 13.06 ± 0.2 ka BP and 11.67 ± 0.1 ka BP (event 1), and 11.76 ± 0.1 ka BP and 9.36 ± 0.7 ka BP (event 2). These gravels are located between 1 and 30 m. a. s. l.. They therefore cannot be explained by a high post-glacial discharge from the Mackenzie River, nor meltwater sourced directly from the ice margin because the elevation attained by water from these sources would not have been sufficient to reach 30 m. a. s. l. (Murton *et al.,* 2010). A large distant meltwater source which provided two 'flood' events towards the north-west is therefore favoured, the most obvious of which is Glacial Lake Agassiz via Glacial Lake McConnell.

The reconstruction of pro-glacial lakes at ~ 11.45 cal. ka BP, as shown in Chapter 6, indicates that a routeway existed between Glacial Lake Agassiz and the lakes along the mainland north-west margin of the LIS e.g. Glacial Lake McConnell. According to the reconstructions presented in this thesis, the routeway opened ~ 12.70 cal. ka BP, and persisted until 10.20 cal. ka BP. These dates coincide with those of Murton *et al.* (2010) for two 'flood' events through the study area as described above. At its narrowest point and maximum depth, the channel was 2 km wide and 200 m deep, and occupied the present day valley of the Clearwater River. Indeed, Fisher and Lowell (*In press)* and Fisher *et al.* (2009), both suggest that the Clearwater-Lower Athabasca Spillway is the geomorphic feature which is most likely to have supported the drainage of Glacial Lake Agassiz towards the north-west.

With respect to the drainage of Glacial Lake Agassiz, the reconstructions presented in Chapter 6 can be thought of as 'maximum' lake extents in that they identify all areas in which water could pond. These reconstructions are therefore realistic in a scenario in which the meltwater supply during deglaciation was sufficient to fill the basins until their spillways were breached.

Murton *et al.* (2010) suggest that in order for flow of water from Glacial Lake Agassiz towards the Beaufort Sea to occur, it is necessary to move the LIS margin of Dyke *et al.* (2003) inland by ~ 10 km in the vicinity of the Clearwater River. Dyke (*Pers. Comm*.) has subsequently suggested that this modification to the ice margin is plausible. Although the shift in the ice margin would have increased discharge towards the Beaufort Sea, the reconstructions shown in Chapter 6 suggest that it was still possible for water to evacuate Lake Agassiz via a north-western routeway with the margin in its original configuration as reconstructed by Dyke *et al.* (2003). It was only possible to detect the narrow routeway shown in Figure 7-6 by incorporating a DEM into the method of lake reconstruction, as outlined in Chapter 3. Murton *et al.* (2010) do not identify this routeway because their reconstruction was based on OSL dates and sedimentological evidence located much further north of the connection between Glacial Lake Agassiz and Glacial Lake McConnell shown in Figure 7-6.

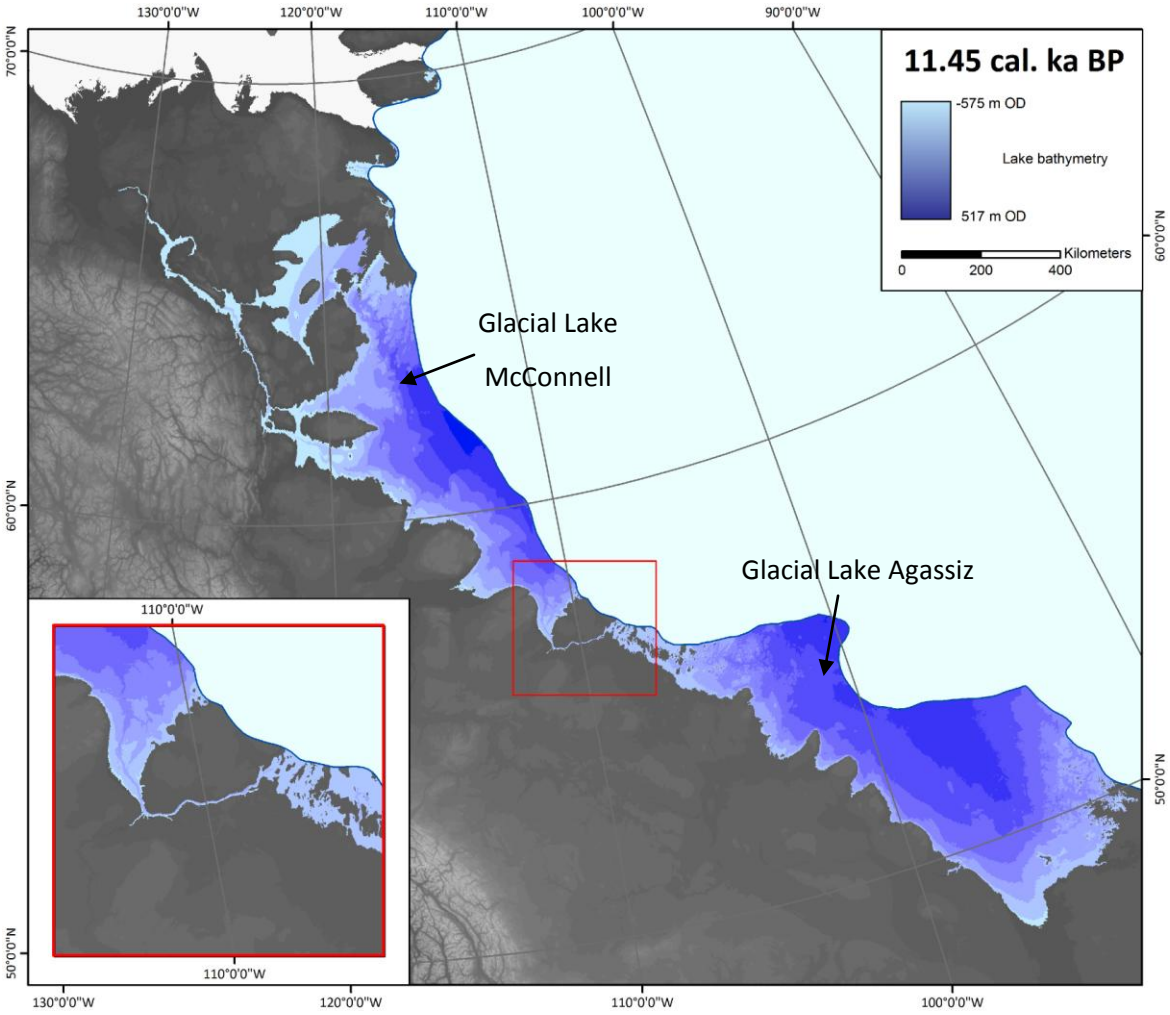

Figure 7-6: The reconstructed pro-glacial lakes along the LIS mainland margin at 11.45 cal. ka BP. A clear drainage routeway is identified between Glacial Lake Agassiz and the pro-glacial lakes along the north-western margin of the LIS.

The opening of the north-west routeway as shown in Figure 7-6, occurred immediately prior to the Younger Dryas (see Table 7-1). The routeway is not depicted after 10.20 cal. ka BP in the reconstruction of pro-glacial lakes presented in Chapter 6. According to Fisher *et al.* (2002), the north-west routeway closed after the Preboreal Oscillation. Indeed, as outlined in Chapter 2, the drainage of pro-glacial lakes into the Arctic Ocean via a north-west routeway has been hypothesised by numerous authors including Fisher *et al.* (2002), Murton *et al.* (2010), Condron and Winsor (2011) as a trigger for the Younger Dryas and/or Preboreal Oscillation. Moreover, Condron and Winsor (2011) suggest that input of freshwater into the ocean via a north-west routeway would be the most effective means of interrupting ocean circulation sufficiently to cause abrupt climate change.

Whilst this investigation does not falsify an eastern drainage routeway for Glacial Lake Agassiz, it does confirm the plausibility of a north-western outlet into the Beaufort Sea based on the regional topography during deglaciation. Indeed, within the current literature, many authors discredit the north-western outlet, instead strongly favouring drainage to the east through the Gulf of St Lawrence (Teller and Leverington, 2002; Lowell *et al.,* 2005; Tarasov and Peltier, 2005). While the focus of this thesis remains on the north-west routeway for Glacial Lake Agassiz, it is acknowledged that the amount of water flowing north-west may have been affected by coeval drainage towards the east if both routeways became available at the same time. While this thesis does not identify a link between Glacial Lake Agassiz and the lakes further to the east around the same time that the north-western routeway appears to have been available, there are two possible explanations for this. Firstly, the reconstruction of pro-glacial lakes does not account for water flowing either over or under the ice. This may have enabled water to flow to the east during the Younger Dryas, for example. Alternatively, if the bathymetry data for the Great Lakes in eastern Canada was to be added to this reconstruction, this may significantly change the configuration of the lakes and thus, drainage routeways, to the east of Glacial Lake Agassiz. Again, this hypothesis may result in drainage to the east during periods which have not been identified in this reconstruction. Therefore, with the possibility of eastern drainage remaining, it should not be assumed that the north-west routeway was the only drainage pathway available to pro-glacial lakes during this time. This has implications for estimates of the volume of water entering both the Beaufort Sea and North Atlantic at any given time during deglaciation and should be considered carefully by those who use such estimates to drive ocean circulation models (see Condron and Windsor, 2011).

7.5 Geomorphological evidence for lake drainage

In order to verify the reconstruction of pro-glacial lakes shown in Chapter 6, it is necessary to reconcile the reconstructed lakes with geomorphological evidence (strandlines and palaeo-channels). Since extensive geomorphological mapping has been carried out as part of this project in north-west Canada, this section will provide a comparison between lake extent and geomorphology for that area. As shown in Figure 7-7, a dendritic network of palaeo-channels emanates from the northern most point of ponding in the valley now occupied by the Mackenzie River. While it has not been possible to assign an age to the channels, they appear to emanate from the edge of the lakes at their maximum extent, for example, at 11.45 cal. ka BP as shown in Figure 7-7. As discussed in Chapter 4, these channels are large channels occupied by misfit streams which are suggested to have been cut by meltwater during Late Wisconsinan deglaciation (Brown *et al.*, 2011). Assuming that water draining north-west from

the reconstructed pro-glacial lakes exited the region via these palaeo-channels, then freshwater would have been delivered to the Beaufort Sea between 128 and 130° W.

As part of the present study, strandlines have been mapped along the north-western margin of the LIS (see Chapter 4). In some areas (e.g. the valley now occupied by outflow from Great Slave Lake), the strandlines coincide closely with the lake extent shown in Figure 7-7 at 11.45 cal. ka BP. Elsewhere (i.e. between the basins of Great Bear and Great Slave Lakes), the shorelines are located up to 150 km from the reconstructed lake extent and at a lower altitude. The strandlines depicted in Figure 7-7 therefore did not form during the same lake phase. However, since the shorelines do, in places, coincide with the 'maximum' possible lake extents shown in Chapter 6 and Figure 7-7, lakes of this magnitude must have existed during Late Wisconsinan deglaciation. Geomorphological inheritance of the shorelines from a previous glaciation of this area is unlikely given the fresh and well preserved nature of the features and the fact that the study area was completely glaciated during the Late Wisconsinan.

Despite the close agreement of the geomorphological evidence with the modelled lakes, we are unable to assign an absolute age to the strandlines or palaeo-channels. However, Fisher and Lowell (*In press*) have used dated strandlines in Alberta and Saskatchewan to reconstruct the history of lake outlets and strandlines along the north-west margin of the LIS. They conclude that the ice margins of Dyke *et al.* (2003) combined with their radiocarbon strandline ages do not support a flood of Younger Dryas age towards the north-west from Glacial Lake Agassiz. Instead, they infer a later period of drainage between 10.6 and 10.1 cal. ka BP. This conclusion assumes lower lake levels than those depicted in Chapter 6. While this thesis cannot falsify the dated strandlines presented by Fisher and Lowell (*In press*), it is plausible that additional standlines were present in the region which have been post-glacially eroded and therefore, not dated. Furthermore, strandlines pertaining to periods when pro-glacial lakes were more extensive may; 1) not have formed due to the short-lived nature of a particular lake level, or, 2) not have been mapped due to limitations associated with the 30 m resolution of the National Elevation Dataset from which Fisher and Lowell (*In press*) chose to map. Indeed, during a high lake level phase when catastrophic outflow is hypothesised from Glacial Lake Agassiz towards the north-west (Murton *et al.,* 2010; Teller *et al.,* 2005), it is reasonable to suppose that downstream strandlines may not be well preserved.

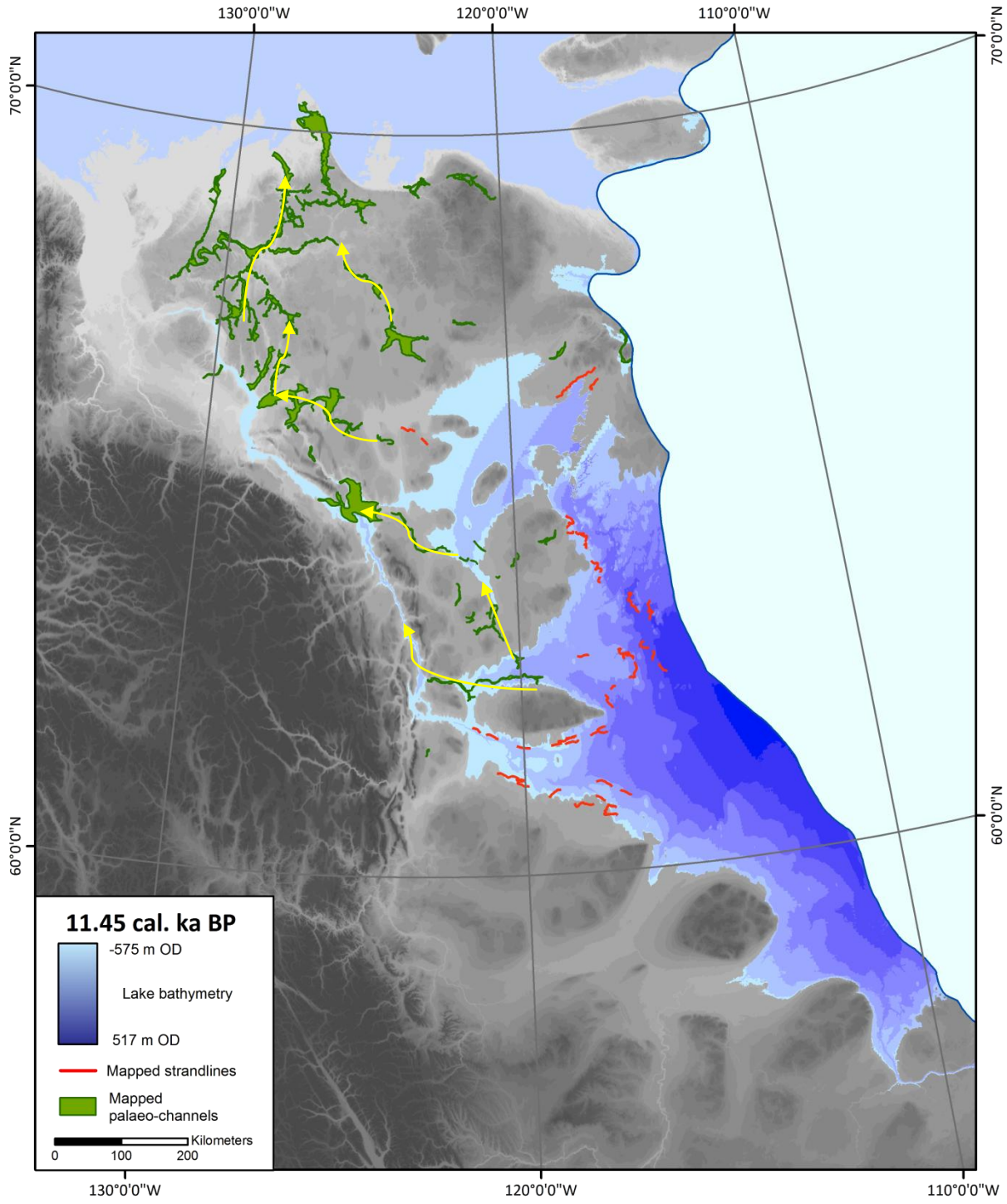

Figure 7-7: The reconstructed pro-glacial lakes along the north-western LIS mainland margin at 11.45 cal. ka BP along with the locations of mapped strandlines and palaeo-channels. The yellow arrows indicate the probable drainage routes of water from the pro-glacial lakes through the network of mapped palaeo-channels towards the Arctic Ocean.

Further south, Great Slave Lake has been hypothesised by Christoffersen et al. (2008) as a subglacial lake. Given that ice retreat towards the east during the Late Wisconsinan it is suggested that subglacial lake Great Slave drained towards the west as the lake basin deglaciated. Interestingly, directly to the west of the present-day Great Slave Lake, Figure 4-1

documents a landscape almost void of geomorphology. This is likely to have been a result of outflow from subglacial Lake Great Slave which subdued or eradicated the bedforms in this region. The outflow from the lake was channelled through a broad valley between two prominent topographic highs to the east of Fort Simpson. According to the reconstruction presented in Chapter 5, the pro-glacial lakes also developed in this valley which may have also contributed to the subdued, and apparent lack of, glacial geomorphology in the area.

7.6 Limitations

7.6.1 High resolution imagery and Digital Elevation Models

Imagery from the Landsat ETM+ satellite is beneficial because it provides freely available, widespread coverage of the earth's surface a consistent horizontal resolution of 30 m for bands 1 – 7 and 15 m for band 8. This allows for rapid and systematic mapping over large areas, as has been carried out here. However, for localised mapping which requires high resolution imagery, Landsat ETM+ may be unsuitable. Indeed, as noted in Chapter 4, small meltwater channels have not been mapped because they cannot be clearly and consistently resolved by the imagery. Similarly, for the reconstruction of pro-glacial lakes, the topography used was from the GTOPO-30 DEM and had a horizontal resolution of 1 km. This allowed for the identification of major spillways between and away from lakes. However, narrower spillways are likely to have existed which could not be resolved by the DEM. While higher resolution DEMs are available, they either do not cover the high Arctic regions or, in the case of the ASTER GDEM, would have required large amounts of processing power in order to mosaic each of the required individual tiles. This was not realistic given the time and resources available. Future work should incorporate DEMs of a higher resolution than GTOPO-30 in order to provide more complete mapping, and accurate reconstructions of pro-glacial lakes. This may require investigators to mosaic the currently available ASTER GDEM or wait until future generations of higher resolution DEMs, with large spatial coverage, become available.

7.6.2 Ice margin chronology

The ice margin chronology of Dyke *et al.* (2003) provides the most comprehensive account of changes in LIS margin geometry during the Late Wisconsinan to date. The reconstructions are based on over 4000 radiocarbon dates from across North America. Despite this, the distribution of the radiocarbon control across North America is not regular, with some areas remaining devoid of, or sparsely populated by, radiocarbon dates. Such areas include the north-west sector of the LIS as shown in Chapter 5, the Canadian Shield to the west of Hudson Bay, and Ungava. Furthermore, the dates have been obtained from a wide variety of datable

materials and many come from already published work. Therefore, despite attempts to 'retire' spuriously old dates, inconsistencies in the choice of datable product, the method of age derivation, reservoir correction and the subsequent calibration to calendar ages, have all brought about uncertainties within the Dyke *et al.* (2003) reconstructions. Refinements to the ice margin chronology are particularly imperative with respect to the drainage of pro-glacial lakes, because the position of the ice margin determines the drainage routeways available at each stage of deglaciation. Improvements to the ice margin chronology in the study area could include further dates around Great Bear Lake, along the edge of the Canadian Shield between Great Bear Lake and Great Slave Lake, but in particular, along the path of the Mackenzie Ice Streams (both eastern and western branches). Furthermore, existing dates require increased consistency in their provenance and age derivation. In the north-west LIS, a greater number of radiocarbon dates would help to constrain the ice margins in the central portion of the study area where dates are currently limited. In particular, the new ice margins introduced in this thesis, which have been demarcated by major moraine ridges rather than geochronology could also be made more robust should further dates become available.

7.6.3 Lake bathymetry data

Bathymetric data for Great Bear Lake and Great Slave Lake were incorporated into the reconstruction of pro-glacial lakes because they occupy two major topographic basins within the mapped study area which filled with water during pro-glacial lake formation. They were therefore influential upon the extent and volume of pro-glacial lakes. Subsequently, work would ideally also incorporate the bathymetry of all lake basins. The incorporation of these data into a reconstruction of pro-glacial lakes would not only increase the volume of the lakes, but would also allow for a more accurate understanding of pro-glacial lake extent and drainage to be realised (see also section 7.4).

7.6.4 Errors associated with ICE-5G

Absolute gravity measurements, GPS data and records of Relative Sea Level (RSL) change can provide a useful means of calibrating and testing models of SED such as ICE-5G. However, the value of GPS studies is often limited by the poor spatial coverage of the data points which are insufficient to test model predictions of SED, particularly around the area/s of greatest uplift (Lambert *et al.,* 2001; Sella *et al.,* 2007). The fit of ICE-5G to the updated absolute gravity rates of Mazzotti *et al.* (2011) is reasonable, but becomes weaker at higher latitudes. However, since the data presented by Mazzotti *et al.* (2011) are small in number, there are again issues over the spatial coverage of the data (Lambert *et al.* 2001; Argus and Peltier, 2010). Similarly,

studies of RSL change are often localized and confined to coastal areas. This makes it difficult to determine the broad pattern of SED over the continental interior.

As depicted in ICE-5G, the multi-domed LIS caused SED to become focused beneath the two largest areas of mass on either side of Hudson Bay (Peltier, 2009). Compared to its predecessor ICE-4G, ICE-5G contains significantly more ice in western Canada within the Keewatin Dome which was located to the west of Hudson Bay (Argus and Peltier, 2010). However, GPS measurements of vertical crustal motion across North America indicate that the LIS may have been thinner than indicated by ICE-5G across the Canadian Prairies but thicker in the east over Quebec and in the west along the British Colombia-Alberta border (Argus and Peltier, 2010). While these data indicate that ice in the north-west LIS was intermediate in mass between that of ICE-4G and ICE-5G, GRACE gravity data suggest that the volume of the western LIS was nearly equivalent to that of ICE-5G but mass was distributed more broadly across north-west Canada (Argus and Peltier, 2010). Indeed, across the whole of North America, GRACE data broadly agree with the patterns and magnitudes of SED shown by ICE-5G (Tamisea *et al.,* 2007; Peltier, 2009; Paulson *et al.*, 2007).

The LIS ice margins of Dyke *et al.* (2003) were used in the development of ICE-5G. Therefore, despite the additions to the Dyke *et al.* (2003) data recommended above, the combination of ICE-5G data with Dyke *et al.* (2003) in order to reconstruct ice stream activity and pro-glacial lake evolution in this thesis, can be deemed appropriate. In order to improve ICE-5G, further widespread records of absolute gravity change, GPS data of present day SED, sea-level change and horizontal ice extent are required to refine the vertical and horizontal profiles of the LIS, which can be input into subsequent generations of SED models.

7.7 Further work

Four key areas of the project have been identified which would benefit from further work beyond that presented in this thesis.

- While the impact of loading from the LIS has been thoroughly considered in the reconstruction of pro-glacial lakes (Chapter 6), the impact of the lakes themselves on the deformation of the solid earth, has not. Loading from water contained within pro-glacial lakes will have caused additional deformation of the lithosphere which remains unaccounted for in this study. In turn, increased deformation caused by the lakes will have increased the capacity of the lake basins. This will not only have increased lake

volume but also altered the configuration of the lakes and therefore the drainage routeways available throughout the various stages of deglaciation. The quantification of SED resulting from the lakes is therefore a crucial next step towards producing the most realistic reconstruction of pro-glacial lakes around the LIS.

- The reconstruction of pro-glacial lakes currently ends at 8.45 cal. Ka BP. Future work should consider extending this reconstruction for another 2 or 3 timesteps in order to provide a reconstruction of pro-glacial lakes around the time of the 8.2 ka BP event. This event involved a decrease in global temperature which lasted for 200 – 400 years. The drainage of pro-glacial lakes around the LIS has been hypothesised as a trigger for the 8.2 ka BP event Teller *et al.,* 2005: Hoffman *et al.,* 2012). Therefore, a reconstruction of pro-glacial lake evolution around this time which identifies changes in the volume and configuration of the lakes during the later stages of deglaciation would allow for the above hypothesis to be tested.
- Figure 4-1 provides comprehensive documentation of the geomorphological signature of ice sheet and ice stream activity in the north-west mainland sector of the LIS. However, the offshore record of ice sheet/stream activity has not yet been explored with respect to ice sheet dynamics in the region. An extension to the work presented in this thesis would be to carefully examine the offshore geomorphological record to extend the mapping campaign. This would not only provide additional information about ice stream activity in this sector of the ice sheet but may also facilitate the refinement of the ice margin geometry. In particular, during the early stages of deglaciation when the ice margin was located offshore, the ice margin geometry remained consistent according to Dyke *et al*. (2003). In reality, it is unlikely that the ice margin did not change geometry at all during this period. Inspection of the offshore geomorphological record may therefore be valuable in teasing out subtle changes in the ice margin geometry during the early stages of Late Wisconsinan deglaciation.
- This thesis has determined the location and timing of ice streams in the north-west LIS. However, in order to understand the impact of these ice streams on overall ice sheet mass balance and their comparative contribution to deglaciation across all of the LIS ice streams, the next step in this research should be to calculate estimates of ice stream discharge. This could also be used to inform numerical models of ice stream activity (see Stokes and Tarasov, 2010) and, furthermore, could be used to compare the LIS ice streams with contemporary ice streams in Antarctica and Greenland.

7.8 Summary

- Of the controls on ice stream activity outlined by Winsborrow *et al.* (2010), ice streams in the north-west LIS are proposed to have been primarily controlled by high geothermal heat flux, the presence of a smooth sediment rich bed, and a large meltwater supply. Ice and water piracy may also have been influential.
- With the exception of the Haldane and Amundsen Gulf palaeo-ice streams which occupied topographic troughs, the ice streams in the north-west LIS were pure ice streams. They were located on thick sediment which may have aided bed lubrication and thus, ice stream activity.
- A drainage routeway for pro-glacial lakes has been identified along the Clearwater-Athabasca spillway. The spillway is 2 km wide and 200 m deep and directed water towards the Arctic Ocean from 12.70 cal. ka BP, around the time of the Younger Dryas. However, this does not falsify an eastern drainage routeway for Glacial Lake Agassiz.
- Within the mapped area, a series of strandlines have been identified which coincide with maximum extent of pro-glacial lakes along the north-western margin of the LIS as depicted by the reconstruction in Chapter 6.
- Palaeo-channels have also been mapped in the north-west LIS. These large, abandoned channels emanate from the most northern point of ponded water in the reconstruction of pro-glacial lakes. Assuming that these channels drained water from the lakes, they would have delivered freshwater to the Arctic Ocean between 128 and 130°N.
- A number of recommendations for future work have been outlined in the final section of this chapter. These include higher resolution imagery and DEMs, a more robust ice margin chronology, the introduction of more bathymetry data, and a reduction in the errors associated with ICE-5G.

Chapter 8: Conclusions

An extensive mapping campaign was undertaken in Northwest Territories, Canada: the area covered by the north-west LIS. The study area is ~ 800,000 km^2. All mapping was carried out remotely from a selection of spaceborne and airborne imagery, but principally Landsat ETM+ images. Remote mapping was advantageous as it allowed mapping to take place at a variety of scales and imagery could be manipulated for optimum visualisation of the geomorphology.

More than 94,000 landforms have been mapped including lineations, eskers, moraine ridges, ribbed moraine, hummocky moraine and palaeo-channels. Lineations are the most abundant landform and vary greatly in morphology from drumlins to mega-scale lineations. The most elongate lineations are found along the Amundsen Gulf coast, around the Anderson River, south-west of Great Bear Lake and on the northern shore of Great Bear Lake.

The distribution of landforms is complex and non-uniform. Lineations are clustered into corridors with abrupt lateral margins, convergent head-zones and divergent down-stream limits. Geomorphological signatures such as these have been identified by Stokes and Clark (1999) and suggested to be indicative of ice stream activity. Cross-cutting and partially over-printed landforms have been mapped which suggest that major periods of ice reorganisation occurred in this sector of the LIS during deglaciation.

The mapped glacial geomorphology has been used to delimit 272 flow-sets. Three types of flow-set were identified, each with different geomorphological signatures; wet-based deglacial flow-sets, event flow-sets and ice stream flow-sets. The location and relative orientation of these flow-sets means that they cannot all have formed synchronously during deglaciation.

The LIS margins of Dyke et al. (2003) were used as a basis for reconstructing ice stream activity in the north-west LIS. Between 21.4 cal. ka BP and 11.45 cal. ka BP, ice margins were used at time-steps with ~ 500 year intervals. Within the study area, these margins were based on 71 radiocarbon dates. Some modifications were made to these margins in order to; 1), match with the location of major moraine ridges; 2), reconcile the ice margins with the extent of nearby flow-sets, and 3), to account for local topography. Two new ice margins have been added to those of Dyke *et al.* (2003) at 13.8 cal. ka BP and 14.25 cal. ka BP.

More than 35 ice stream flow-sets have been identified which demarcate the extent of 7 ice streams. While some of these ice streams have previously been hypothesised (the Mackenzie

and Haldane ice streams), others have not (the Kugluktuk, Fort Simpson and Paulatuk ice streams). Throughout the study area ice streams switched on and off dynamically during deglaciation. Some ice streams are represented by a single flow-set (e.g. the Haldane ice stream) while others are represented by multiple flow-sets (e.g. the Mackenzie East and Mackenzie West ice streams). Furthermore, the largest ice streams also reorganised during deglaciation to operate in a number of different configurations.

Streaming flow was dominated by the activity of a small number of large ice streams during the early stages of deglaciation. These ice streams were the Mackenzie East, Mackenzie West and Amundsen Gulf ice streams. Later in deglaciation, a larger number of smaller ice streams operated and a peak in ice stream activity occurred between 15 and 13 cal. Ka BP.

The abundant soft sediment in the study area, relatively high geothermal heat flux and abundance of meltwater were the principal controls on ice stream activity in the north-west LIS. The study area is dominated by thick sedimentary sequences which aided streaming flow principally by subglacial sediment deformation. Assuming that Late Wisconsinan geothermal heat flux in the study area was akin to that of the present day, then geothermal heat flux was consistently high and in places comparable to that below contemporary ice streams in Greenland. Meltwater resulting from high ice overburden pressures and frictional basal heating was also a key control on ice stream activity in this sector of the ice sheet. Basal meltwater promoted streaming flow by enhancing basal sliding and subglacial sediment deformation.

Pro-glacial lakes surrounding the LIS have been reconstructed using a new GIS approach. This involved warping a DEM of North America to take into account SED throughout deglaciation. This information was obtained from ICE-5G. The ice margins were then elevated and merged with the warped DEMs before being flooded with water to establish the locations of pro-glacial lakes.

Large palaeo-channels have been identified in north-west Canada which may demarcate the drainage routeway of pro-glacial lakes. The channels emanate from the most northerly point of ponded water, as shown in the reconstructions in Chapter 6. They form a dendritic network and many are currently occupied by mis-fit streams such as the Anderson River. Assuming that they drained pro-glacial lakes during the Late Wisconsinan, they would have delivered water to the Arctic Ocean between 128 and 130° W. While the formation of the channels remains uncertain, they appear emanate from the edge of the lakes reconstructed at 11.45 cal. ka BP.

Strandlines in north-west Canada match with the extent of the reconstructed pro-glacial lakes. In particular, the reconstruction of pro-glacial lakes at 11.45 cal. ka BP matches closely with the location of mapped strandlines. This indicates that the reconstructions shown in Chapter 6 are realistic despite being 'maximum extent' reconstructions which assume a sufficient meltwater supply during deglaciation in order to fill areas of ponding to their maximum extent.

A north-west drainage routeway for pro-glacial lakes has been identified. According to the reconstruction presented in Chapter 6, the routeway became available ~ 12.7 cal. ka BP which agrees with the previously published dates of Smith and Fisher (1993). The opening of the routeway is coincident with a major flood event through the study area as suggested by Murton *et al.* (2010). The routeway opened along the present day Clearwater-Athabasca spillway and was 2 km wide and 200 m deep. As proposed by Murton *et al.* (2010), an eastward shift of the ice margin in the vicinity of the spillway would allow for further lake drainage along the ice margin towards the north-west.

This work has wider implications for a range of geographical applications. The thesis has identified seven ice streams in the north-west LIS, and established the temporal controls on their activity. This knowledge has implication for work targeted at testing numerical models against geological evidence (e.g. Stokes and Tarasov, 2010), particularly at a detailed regional scale. Future work could also investigate the sediments and basal processes on each of these ice stream beds with the aim of establishing their mechanisms of flow. Indeed, examination of the geomorphological record on the neighbouring continental shelf may provide additional insights into ice stream activity in the north-west LIS, particularly during the early stages of deglaciation, and its synchrony with adjacent ice streams throughout the Canadian Arctic Archipelago. The plausibility of a north-west drainage routeway for Glacial Lake Agassiz has also been presented in this thesis. With further chronological control, this may be of interest to research which explores the impact of pro-glacial lake drainage from around the LIS on ocean circulation, and subsequently global climate.

Appendix

In the pages that follow, the dates associated with the ice margin chronology of Dyke *et al.* (2003) are presented as a series of tables. The ID of each date corresponds to the numbers shown on the location map below.

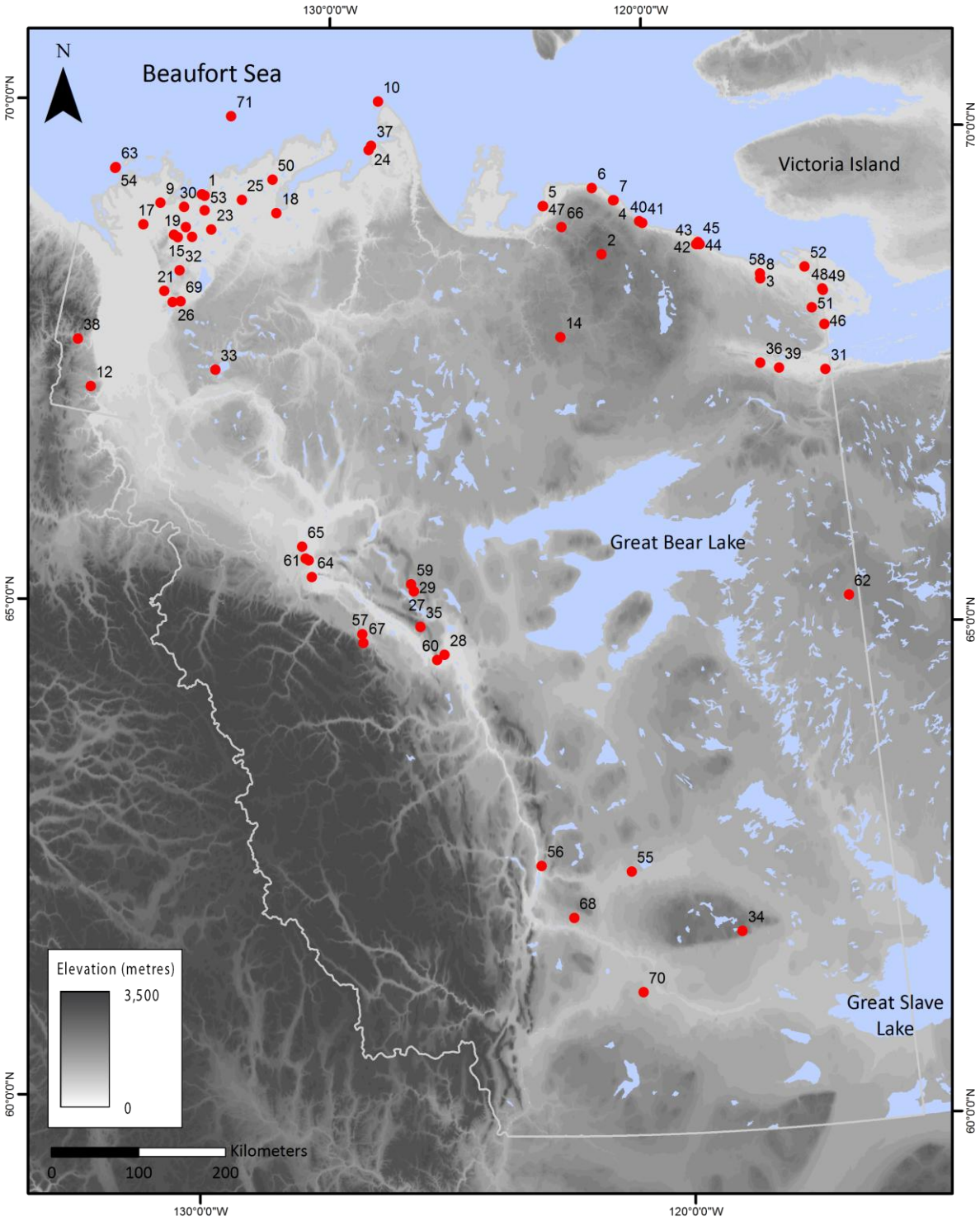

DATE ID	REGION	UNCERTAINTY	LAB CODE FROM DYKE ET AL. (2003)	LATITUDE	LONGITUDE	MATERIAL	AGE IN CALENDAR YEARS	CITATION	SITE
1	W Arctic Mainland	0.100	AA-13013	69.41	-133.14	biogenic CO	13.860	Moorman, 1998	Peninsula Pt
2	W Arctic Mainland	0.095	AA-44353	69.08	-121.43	moss in lake	9.744	Beierle et al., 2002	Melville Hills
3	W Arctic Mainland	0.240	AECV-474Cc	68.73	-116.93	Macoma sp.	10.440	Kerr, 1996	C Young
4	W Arctic Mainland	0.180	AECV-642Cc	69.63	-121.05	Hiatella arct	10.740	Kerr, 1996	Buchanan R
5	W Arctic Mainland	0.160	AECV-643Cc	69.58	-123.13	Hiatella arct	12.190	Kerr, 1996	Darnley B
6	W Arctic Mainland	0.180	AECV-644Cc	69.77	-121.67	Hiatella arct	11.240	Kerr, 1996	Buchanan R
7	W Arctic Mainland	0.150	AECV-645Cc	69.63	-121.03	shells	10.810	Kerr, 1996	Buchanan R
8	W Arctic Mainland	0.540	AECV-713Cc	68.73	-116.93	Mya sp., Hia	10.820	St-Onge & McMartin, 1995	C Young
9	W Arctic Mainland	0.080	Beta-	69.25	-134.30	wood	11.700	Dallimore et al., 2000	Cabin Creek L
10	W Arctic Mainland	0.160	Beta-25119	70.58	-128.25	Saiga tataric	14.920	Harington & Cinq-Mars, 1995	Baillie I
11	W Arctic Mainland	0.210	Beta-34312	69.25	-133.00	organic lake	14.020	Hill et al., 1985	Topkak Marsh
71	W Arctic Mainland	0.630	Beta-6276	70.25	-132.67	wood & herb	21.600	Hill et al., 1985	Uviluk
12	W Arctic Mainland	0.080	BGS-139	67.27	-135.23	limnic peat	9.960	Pettapiece & Zoltai, 1974; D	Ft Macpherson
13	W Arctic Mainland	0.130	BGS-240	68.95	-133.75	peat in marl	9.890	Delorme et al., 1977	Parsons L
14	W Arctic Mainland	0.150	GSC-1139	68.23	-122.63	peat	10.800	Fulton in GSC Paper 71-7	Erly L
15	W Arctic Mainland	0.160	GSC-1160	68.93	-133.63	twigs & peat	11.400	Fyles in GSC Paper 73-7	Parsons L
16	W Arctic Mainland	0.180	GSC-1214	69.41	-133.15	peat	12.800	Fyles in GSC Paper 71-7; Ram	Peninsula Pt
17	W Arctic Mainland	0.160	GSC-1286	69.00	-134.67	basal peat	11.000	Rampton, 1988	Tununuk
18	W Arctic Mainland	0.160	GSC-1303	69.33	-130.92	basal? peat	10.900	Rampton, 1988	Kugaluk R
19	W Arctic Mainland	0.170	GSC-1321	69.05	-133.45	lake sed	12.900	Ritchie & Hare, 1971	Tuk-5
20	W Arctic Mainland	0.180	GSC-1469	68.96	-133.23	basal peat	9.790	Rampton and Bouchard, 1975	Zed L
21	W Arctic Mainland	0.160	GSC-1514	68.37	-133.74	peat	11.500	Kuc in GSC Paper 73-7; Rampt	Twin L
22	W Arctic Mainland	0.220	GSC-1573	65.82	-129.00	wood	11.200	Mackay & Mathews, 1973	Sans Sault Rapids
23	W Arctic Mainland	0.150	GSC-1784-2	69.07	-132.72	grass/sedge	12.900	Rampton, 1988	Eskimo L
24	W Arctic Mainland	0.080	GSC-1989	70.08	-128.40	basal peat	9.020	Rampton, 1988	Mackenzie D
25	W Arctic Mainland	0.090	GSC-2023	69.42	-131.98	wood base c	9.180	Rampton in GSC Paper 86-7	Eskimo L
26	W Arctic Mainland	0.090	GSC-2075	68.27	-133.47	lake sed	11.100	Ritchie, 1977	M Lake
27	W Arctic Mainland	0.110	GSC-2320	65.58	-126.33	basal? peat	9.570	Savigny & Rutter in GSC Pape	Kelly L
28	W Arctic Mainland	0.260	GSC-2328	64.94	-125.50	organic detr	10.600	Hughes, 1987	Great Bear R
29	W Arctic Mainland	0.080	GSC-2379	65.58	-126.33	peat, not bas	9.600	Savigny & Rutter in GSC Pape	Kelly L

DATE ID	REGION	UNCERTAINTY	LAB CODE FROM DYKE ET AL. (2003)	LATITUDE	LONGITUDE	MATERIAL	AGE IN CALENDAR YEARS	CITATION	SITE
30	W Arctic Mainland	0.110	GSC-3302	69.25	-133.60	gyttja	12.500	Spear, 1993	Sleet L
31	W Arctic Mainland	0.090	GSC-3327	67.73	-115.42	Macoma cal	10.220	St-Onge in GSC Paper 83-7	Coppermine R
32	W Arctic Mainland	0.150	GSC-3387	68.60	-133.42	lake sed	13.000	Ritchie, 1977	Twin Tamarack L
33	W Arctic Mainland	0.100	GSC-3419	67.65	-132.02	lake sed	9.520	Ritchie, 1984	Sweet Little L
34	W Arctic Mainland	0.200	GSC-3524	62.05	-118.70	lake sed	10.500	MacDonald, 1987	L Demain
35	W Arctic Mainland	0.340	GSC-3536	65.22	-126.12	lake sed	11.000	MacDonald, 1987	L Mélèze
36	W Arctic Mainland	0.240	GSC-3663	67.87	-117.17	Macoma cal	10.700	St-Onge in GSC Paper 83-7	Richardson R
37	W Arctic Mainland	0.080	GSC-3763	70.12	-128.34	basal peat	9.400	Vincent, unpublished	Liverpool B
38	W Arctic Mainland	0.240	GSC-3813	67.72	-135.83	organic detr	21.200	Catto, 1996	Rat R
39	W Arctic Mainland	0.110	GSC-3941	67.80	-116.67	Mya truncat	9.830		Cox L
40	W Arctic Mainland	0.100	GSC-4318	69.41	-120.30	Hiatella arct	11.100	St-Onge & McMartin, 1995	Buchanan R
41	W Arctic Mainland	0.120	GSC-4339	69.39	-120.22	Hiatella arct	11.000	St-Onge & McMartin, 1995	Buchanan R
42	W Arctic Mainland	0.000	GSC-4390	69.14	-118.68	Hiatella arct	11.000	St-Onge & McMartin, 1995	Clifton Pt
43	W Arctic Mainland	0.100	GSC-4390	69.14	-118.68	Hiatella arct	11.100	St-Onge & McMartin, 1995	Clifton Pt
44	W Arctic Mainland	0.100	GSC-4402	69.13	-118.58	Hiatella arct	10.700	Kerr, 1996	Clifton Pt
45	W Arctic Mainland	0.100	GSC-4424	69.16	-118.63	Hiatella arct	10.760	Kerr, 1996	Clifton Pt
46	W Arctic Mainland	0.170	GSC-4747	68.19	-115.30	Hiatella arct	10.040	St-Onge & McMartin, 1995	Klengenberg B
47	W Arctic Mainland	0.100	GSC-4757	69.58	-123.12	Hiatella arct	11.600	Vincent, unpublished	Brock Lagoon
48	W Arctic Mainland	0.090	GSC-4823	68.56	-115.23	gyttja	7.040	St-Onge in GSC Paper 90-7	Coppermine
49	W Arctic Mainland	0.110	GSC-4842	68.54	-115.21	gyttja	7.010	McMartin & St-Onge in GSC Pa	Coppermine
50	W Arctic Mainland	0.140	GSC-4905	69.67	-131.17	lake sed	13.800	Ritchie in GSC Paper 91-7	Tuk NE
51	W Arctic Mainland	0.100	GSC-4916	68.38	-115.58	shells	11.150	St-Onge & McMartin, 1995	NW Klengenberg B
52	W Arctic Mainland	0.000	GSC-4926	68.80	-115.65	Hiatella arct	11.000	St-Onge & McMartin, 1995	Stapylton B
53	W Arctic Mainland	0.440	GSC-512	69.40	-133.07	peat	14.130	Fyles in GSC Paper 73-7	Ibyuk Pingo
54	W Arctic Mainland	0.150	GSC-516	69.51	-135.79	basal? peat	10.300	Kerfoot in GSC Paper 71-7	Garry I
55	W Arctic Mainland	0.110	GSC-5750	62.72	-121.10	basal peat	9.190	Kettles in GSC List unpub	Fort Simpson
56	W Arctic Mainland	0.090	GSC-6111	62.79	-123.12	basal peat	9.380	Kettles in GSC List unpub	Willowlake R
57	W Arctic Mainland	0.110	GSC-6249	65.11	-127.53	basal peat	10.300	Kettles in GSC List unpub	Norman Wells
58	W Arctic Mainland	0.260	I(GSC)-25	68.78	-116.93	Macoma bal	10.930	Craig, 1960	Harding R
59	W Arctic Mainland	0.160	I-14619	65.65	-126.40	basal peat	9.380	Smith, 1992	Kelly L

DATE ID	REGION	UNCERTAINTY	LAB CODE FROM DYKE ET AL. (2003)	LATITUDE	LONGITUDE	MATERIAL	AGE IN CALENDAR YEARS	CITATION	SITE
60	W Arctic Mainland	0.170	I-15020	64.88	-125.67	wood	11.530	Smith, 1992	Little Bear R
61	W Arctic Mainland	0.170	I-3734	65.83	-129.08	wood	11.530	Mackay & Mathews, 1973	Fort Good Hope
62	W Arctic Mainland	0.360	I-3957	65.40	-115.52	charcoal	6.970	Nobel, 1971	Acasta L
63	W Arctic Mainland	0.250	S-277	69.52	-135.78	wood base c	11.700	Rampton, 1988	Garry I
64	W Arctic Mainland	0.090	TO-1190	65.65	-128.88	wood	11.760	Smith, 1992	Mountain R
65	W Arctic Mainland	0.090	TO-1191	65.95	-129.20	wood	11.440	Smith, 1992	Hume R
66	W Arctic Mainland	0.100	TO-217	69.37	-122.58	Hiatella arct	11.680	Kerr, 1996	Brock R
67	W Arctic Mainland	0.150	TO-2375	65.02	-127.48	wood	10.230	Szeicz et al., 1995	Bell's L
68	W Arctic Mainland	0.110	WAT-2351	62.25	-122.40	lake sed	9.050	McLeod & MacDonald, 1997	Rugged L
69	W Arctic Mainland	0.080	WAT-3027	68.29	-133.25	basal peat	9.060	Vardy et al., 2000	CC-P
70	W Arctic Mainland		WAT-405	61.47	-120.92	basal peat	10.380	Chatwin, 1983	Fort Simpson

References

Alley, R. B. and C. R. Blankenship (1986). "Deformation of till beneath ice stream B, West Antarctica." Nature **322**: 57 - 59.

Alley, R. B. and C. R. Bentley (1988). "Ice-core analysis on the Siple Coast of West Antarctica." Annals of Glaciology **11**: 1 - 7.

Alley, R. B. and A. M. Águstsdóttir (2005). "The 8k event: cause and consequences of a major Holocene abrupt climate change." Quaternary Science Reviews **24**: 1123 - 1149.

Alley, R. B., D. D. Blankenship, S. T. Rooney and C. R. Bentley (1987). "Continuous till deformation beneath ice sheets". The Physical Basis of Ice Sheet Modelling Proceedings of the Vancouver Symposium, August 1987

Alley, R. B., S. Anandakrishnan, T. K. Dupont, B. R. Parizek and D. Pollard (2007). "Effect of Sedimentation on Ice-Sheet Grounding-Line Stability." Science **315**(5820): 1838-1841.

Anandakrishnan, S. D., D. Blankenship, R. B. Alley and P. L. Stoffa (1998). "Influence of subglacial geology on the position of a West Antarctica ice stream from seismic measurements." Nature **394**: 62 - 65.

Andersson, G. (1998). "Genesis of hummocky moraine in the Bolmen area, southwestern Sweden. ." Boreas **27**: 55-67.

Andrews, J. T. and B. MacLean (2003). "Hudson Strait ice streams: a review of stratigraphy, chronology and links with North Atlantic Heinrich events." Boreas **32**(1): 4-17.

Argus, D. F. and W. R. Peltier (2011). "Constraining models of postglacial rebound using space geodesy: A detailed assessment of model ICE-5G (VM2) and its relatives." Geophysical Journal International **181**(697 - 723).

Aylsworth, J. M. and W. W. Shilts (1989). "Bedforms of the Keewatin Ice Sheet, Canada." Sedimentary Geology **62**: 407-428.

Bader, H. (1965). "The Greenland Ice Sheet." U.S. Army, Corps of Engineers, Cold Regions Research and Engineering Laboratory **I-B2**: 18 p.

Bamber, J. L., D. G. Vaughan and I. Joughin (2000). "Widespread Complex Flow in the Interior of the Antarctic Ice Sheet." Science **287**(5456): 1248-1250.

Bamber, J. L., R. B. Alley and I. Joughin (2007). "Rapid response of modern day ice sheets to external forcing." Earth and Planetary Science Letters **257**: 1-13.

Bannerjee, I. and B. C. MacDonald, Eds. (1975). Nature of esker sedimentation. Glaciofluvial and glaciolacustrine sedimentation. Tulsa, Oklahoma Society of Economic Paleontologists and Mineralogists Special Publication.

Barendregt, R. W. and A. Duk-Rodkin (2004). Chronology and Extent of Late Cenozoic Ice Sheets in North America: A magnetostratigraphic Assessment. Quaternary Glaciations-Extent and Chronology Part II. J. Ehlers and G. P. L, Elsevier**:** 1-17.

Bastow, I. D., J.-M. Kendall, D. B. Brisbourne, D. B. Snyder, D. Thompson, D. Hawthorne, G. R. Helffrich, J. Wookey, A. Holeston and D. Eaton (2011). "The Hudson Bay Lithospheric Experiment." Astronomy and Geophysics **6**: 21 - 24.

Beget, J. (1987). "Low profile of the northwest Laurentide ice sheet." Arctic and Alpine Research **19**(1): 81-88.

Benn, D. I. and S. Lukas (2006). "Younger Dryas glacial landsystems in North West Scotland: an assessment of modern analogues and palaeoclimatic implications." Quaternary Science Reviews **25**(17-18): 2390-2408.

Benn, D. I. and D. J. A. Evans (2010). Glaciers and Glaciation. London, Arnold.

Benn, D. I., M. P. Kirkbride, L. A. Owen and V. Brazier, Eds. (2003). Glaciated Valley Landsystems. Glacial Landsystems, Arnold.

Bennett, G. L., D. J. A. Evans, P. Carbonneau and R. Twigg (2010). "Evolution of a debris-charged glacier landsystem, Kviárjökull, Iceland." Journal of Maps **6**(1): 40-67.

Bennett, M. R. (2003). "Ice streams as the arteries of an ice sheet: their mechanics, stability and significance." Earth Science Reviews **61**: 309-339.

Bentley, C. R. (1987). "Antarctic Ice Streams: a review." Journal of Geophysical Res **92**(B9): 8843-8858.

Bentley, C. R., N. Lord and C. Liu (1998). "Radar reflections reveal a wet bed beneath stagnant Ice Stream. C and a frozen bed beneath ridge BC, West Antarctica." Journal of Glaciology **44**(146): 149 - 156.

Bernard, L., D. Lacelle, M. St-Jean, I. D. Clark and G. D. Zazula (2010). "Late Quaternary paleoenvironments and growth of intrusive ice in eastern Beringia (Eagle River valley, northern Yukon, Canada)." Canadian Journal of Earth Sciences **47**: 941 - 955.

Bindschadler, R. A. and T. Scambos (1991). "Satellite-image-derived velocity field of and Antarctic ice stream." Science **252**(5003): 242 - 246.

Bindschadler, R. and P. Vornberger (1998). "Changes in the West Antarctic Ice Sheet Since 1963 from Declassified Satellite Photography." Science **279**(5351): 689-692.

Blackwell, D. D. and M. Richards (2004). "Geothermal map of North America." American Association of Petroleum Geologists, scale: 1:6,500,000.

Blake, J. (1966). "End moraines and deglaciation chronology in northern Canada with special reference to southern Baffin Island." Geological Survey of Canada **Paper 66** 26 - 31.

Blankenship, D. D., R. E. Bell, S. M. Hodge, J. M. Brozena, J. C. Behrendt and C. A. Finn (1993). "Active volcanism beneath the West Antarctic ice sheet and implications for ice-sheet stability." Nature **361**: 526 - 529.

Bond, G., W. Broecker, S. Johnsen, J. McManus, L. Labeyrie, J. Jouzel and G. Bonani (1993). "Correlations between climate records from North Atlantic sediments and Greenland ice." Nature **365**: 143-147.

Bostock, H. S. (1948). "Physiography of the Canadian Cordillera, with special reference to the area north of the fifty-fifth parallel." Geological Survey of Canada Memoir **247**: Report and Map 922 A, 106 p.

Boulton, G. S. (1972). "Modern Arctic glaciers as depositional models for former ice sheets." Journal of the Geological Society **128**(4): 361-393.

Boulton, G. S. (1987). A theory of drumlin formation by subglacial deformation. Drumlins Symposium. Rose. J and Menzies. J. Rotterdam, Balkema**:** 25 - 80.

Boulton, G. S. and C. D. Clark (1990). "The Laurentide ice sheet through the last glacial cycle: the topology of drift lineations as a key to the dynamic behaviour of former ice sheets." Earth and Environmental Science Transactions of the Royal Society of Edinburgh **81**(04): 327-347.

Boulton, G. and M. Hagdorn (2006). "Glaciology of the British Isles Ice Sheet during the last glacial cycle: form, flow, streams and lobes." Quaternary Science Reviews **25**(23–24): 3359-3390.

Boulton, G. S., G. Smith, A. S. Jones and J. Newsome (1985). "Glacial geology and glaciology of the last mid-latitude ice sheets." Journal of the Geological Society **142**: 447-474.

Boyce, I. and N. Eyles (1991). "Drumlins carved by deforming till streams below the Laurentide ice sheet." Geology **19**(8): 787-790.

Brennand, T. A. (2000). "Deglacial meltwater drainage and glaciodynamics: inferences from Laurentide eskers, Canada." Geomorphology **32**(3-4): 263-293.

Broecker, W. S. (2000). "Abrupt climate change: causal constraints provided by the paleoclimate record." Earth-Science Reviews **51**(1–4): 137-154.

Broecker, W. S., M. Andree, W. Wolfli, H. Oeschger, G. Bonani, J. Kennett and D. Peteet (1988). "The chronology of the last deglaciation: Implications to the cause of the Younger Dryas event." Paleoceanography **3**: 1 - 19.

Broecker, W. S., G. H. Denton, R. L. Edwards, H. Cheng, R. B. Alley and A. E. Putnam (2010). "Putting the Younger Dryas cold event into context." Quaternary Science Reviews **29**(9–10): 1078-1081.

Brook, S. J. and H. J. B. Birks (2000). "Chironomid-inferred Late-glacial air temperatures at Whitrig Bog, southeast Scotland." Journal of Quaternary Science **15**: 759-764.

Brown, V. H., D. J. A. Evans and I. S. Evans (2011). "The glacial geomorphology and surficial geology of the south-west English Lake District." Journal of Maps **7**(1): 221-243.

Brown, V. H., C. R. Stokes and C. O. Cofaigh (2011). "The glacial geomorphology of the north-west Laurentide Ice Sheet." Journal of Maps **7**(1): 409-428.

Bryson, R. A., W. A. Wendland, J. D. Ices and J. T. Andrews (1969). "Radiocarbon isochrones on the distintegration of the Laurentide Ice Sheet." Arctic and Alpine Research **1**(1): 1 - 13.

Cameron, A. E. (1922). "Post-Glacial Lakes in the Mackenzie River Basin, North West Territories, Canada." The Journal of Geology **30**(5): 337-353.

Carlson, A. E. (2010). "What caused the Younger Dryas Cold Event?" Geology **38**: 383-384.

Carlson, A. E., A. N. LeGrande, D. W. Oppo, R. E. Came, G. A. Schmidt, F. S. Anslow, J. M. Licciarda and E. A. Obbink (2008). "Rapid early Holocene deglaciation of the Laurentide ice sheet." Nature Geoscience **1**(9): 620-624.

Carlson, A. E., P. U. Clark and S. W. Hostetler (2009). "Comment: Radiocarbon deglaciation chronology of the Thunder Bay, Ontario area and implications for ice sheet retreat patterns." Quaternary Science Reviews **28**(23-24): 2546-2547.

Carlson, A. E., D. J. Ullman, F. S. Anslow, F. He, P. U. Clark, Z. Liu and B. L. Otto-Bliesner (2012). "Modeling the surface mass-balance response of the Laurentide Ice Sheet to Bølling warming and its contribution to Meltwater Pulse 1A." Earth and Planetary Science Letters **315–316**(0): 24-29.

Christoffersen, P., S. Tulaczyk, J. Wattrus, N. Peter, N. Quintana-Krupinski, C. D. Clark and C. Sjunneskog (2008). "Large subglacial lake beneath the Laurentide Ice Sheet during the last glacial maximum." Geology **36**(7): 563-566.

Clark, C. D. (1993). "Mega-scale glacial lineations and cross-cutting ice-flow landforms." Earth Surface Processes Landforms **18**(129): 1-29.

Clark, C. D. (1997). "Reconstructing the evolutionary dynamics of former ice sheets using multi-temporal evidence, remote sensing and GIS." Quaternary Science Reviews **16**: 1067-1092.

Clark, C. D. (1999). "Glaciodynamic context of subglacial bedform generation and preservation." Annals of Glaciology **28**(23-32).

Clark, C. D., J. K. Knight and J. T. Gray (2000). "Geomorphological reconstruction of the Labrador Sector of the Laurentide Ice Sheet." Quaternary Science Reviews **19**: 1343-1366.

Clark, C. D., S. M. Tulaczyk, C. R. Stokes and M. Canals (2003). "A groove-ploughing theory for the production of mega-scale glacial lineations, and implications for ice-stream mechanics " Journal of Glaciology **49**(165): 240-256.

Clark, C. D., A. L. Hughes, S. L. Greenwood, M. Spagnolo and F. S. L. Ng (2009). "Size and shape characteristics of drumlins, derived from a large sample, and associated scaling laws " Quaternary Science Reviews **28**(7-8): 677-692.

Clark, P. U. and J. S. Walder (1994). "Subglacial drainage, eskers, and deforming beds beneath the Laurentide and Eurasian ice sheets." Geological Society of America Bulletin **106**(2): 304-314.

Clark, P. U. and A. C. Mix (2002). "Ice sheets and sea level of the Last Glacial Maximum." Quaternary Science Reviews **21**(1-3): 1-7.

Clark, P. U., R. B. Alley and D. Pollard (1999). "Northern Hemisphere Ice-Sheet Influences on Global Climate Change." Science **286**(5442): 1104-1111.

Clark, P. U., S. J. Marshall, G. K. C. Clarke, S. W. Hostetler, J. M. Licciardi and J. T. Teller (2001). "Freshwater Forcing of Abrupt Climate Change During the Last Glaciation." Science **293**(5528): 283-287.

Clark, R. (1992). Quaternary Features north of the Kirkstone Pass. Lakeland rocks and landscape. M. Dodd. Oxford, Cumberland Geological Society**:** 37-49.

Clayton, L. and S. R. Moran, Eds. (1974). A glacial process-form model. Glacial geomorphology. Binghamton, State University of New York.

Colman, S. M., L. D. Keigwin and R. M. Forester (1994). "Two episodes of meltwater influx from glacial Lake Agassiz into the Lake Michigan basin and their climatic contrasts." Geology **22**(6): 547-550.

Condron, A. and P. Winsor (2011). "A subtropical fate awaited freshwater discharged from glacial Lake Agassiz." Geophysical Research Letters **38**(L03705): 1-5.

Côté, M. M. and C. R. Burn (2002). "The oriented lakes of Tuktoyaktuk Peninsula, Western Arctic Coast, Canada: a GIS-based analysis." Permafrost and Periglacial Processes **13**(1): 61-70.

Couch, A. G. and N. Eyles (2008). "Sedimentary record of glacial Lake Mackenzie, Northwest Territories, Canada: Implications for Arctic freshwater forcing." Palaeogeography, Palaeoclimatology, Palaeoecology **268**: 26-38.

Coulthard, R. D., M. F. A. Furze, A. J. Pieńkowski, F.C. Nixon and J. H. England (2010). "New marine ΔR values for Arctic Canada." Quaternary Geochronology **5**(4): 419-434.

Cowan, W. R. (1968). "Ribbed moraine: till-fabric analysis and origin." Canadian Journal of Earth Sciences **5**: 1145-1159.

Craig, B. G. (1960). Surficial geology of north-central District of Mackenzie, Northwest Territories, Geological Survey of Canada**:** Paper 60 -18, Map 24-1960.

Craig, B. G. (1965). Glacial Lake McConnell, and the surficial geology of parts of Slave River and Redstone River map-areas, District of Mackenzie. D. o. M. a. T. Surveys, Geological Survey of Canada Bulletin **122**.

Dallimore, S. R. and J. V. Matthews (1997). The Mackenzie Delta borehole project. Environmental Studies Research Funds. **135:** 1 CDROM.

Darby, D. A., J. F. Bischof, R. F. Spielhagen, S. A. Marshall and S. W. Herman (2002). "Arctic ice export events and their potential impact on global climate during the late Pleistocene." Paleoceanography **15**(2): 1 - 17.

De Angelis, H. and J. Kleman (2005). "Palaeo-ice streams in the northern Keewatin sector of the Laurentide ice sheet." Annals of Glaciology **42**(1): 135-144.

De Angelis, H. and J. Kleman (2007). "Palaeo-ice streams in the Foxe/Baffin sector of the Laurentide Ice Sheet." Quaternary Science Reviews **26**: 1313-1331.

De Angelis, H. and J. Kleman (2008). "Palaeo-ice-stream onsets: examples from the north-eastern Laurentide Ice Sheet." Earth Surface Processes and Landforms **33**(4): 560-572.

Deschamps, D., Durand, N., Bard, E., Hamelin, B., Camolin, G., Thomas, A. L., Henderson, G. M., Okuno, J., Yokoyama, Y., 2012. "Ice-sheet collapse and sea-level rise at the Bölling warming 14,600 years ago". Nature **483**: 559-564.

Duk-Rodkin, A. and O. L. Hughes (1995). "Quaternary geology of the northeast part of the central Mackenzie Valley corridor, Northwest Territories." Geological Survey of Canada Bulletin **458**.

Duk-Rodkin, A. and C. S. Lemmen (2000). Glacial history of the Mackenzie region. The physical environment of the Mackenzie Valley. Northwest Territories: a base line for the assessment of environmental change. L. D. Dyke and G. R. Brooks, Geological Survey of Canada Bulletin. **547:** 11-20.

Dunlop, P. and C. D. Clark (2006). "The morphological characteristics of ribbed moraine." Quaternary Science Reviews **25**(13-14): 1668-1691.

Dunlop, P., C. D. Clark and R. C. Hindmarsh (2008). "Bed Ribbing Instability Explanation: testing a numerical model of ribbed moraine formation arising from coupled flow of ice and subglacial sediment." Journal of Geophysical Research **113**: F03005.

Dyke, A. S. and V. K. Prest (1987). "Late Wisconsinan and Holocene History of the Laurentide Ice Sheet." Geographie Physique et Quaternaire **41**(2): 237-263.

Dyke, A. S. and T. F. Morris (1988). "Drumlin fields, dispersal trains, and ice streams in Arctic Canada." Canadian Geographer **32**(1): 86 - 90.

Dyke, A. S. and J. M. Savelle (2000). "Major end moraines of Younger Dryas age on Wollaston Peninsula, Victoria Island, Canadian Arctic: implications for paleoclimate and the formation of hummocky moraine." Canadian Journal of Earth Sciences **37**(4): 601-619.

Dyke, A. S. and D. J. A. Evans, (2003). Ice-marginal terrestrial landsystems: northern Laurentide and Innuitian ice sheet margins. Eds. D. J. A., Evans. Glacial Landsystems, Hodder Arnold.

Dyke, A. S., L. A. Dredge and J. Vincent (1982). "Configuration and dynamics of the Laurentide Ice Sheet during the Late Wisconsin Maximum." Geographie Physique et Quaternaire **36**(1-2): 5-14.

Dyke, A. S., J. T. Andrews, P. U. Clark, J. H. England, G. H. Miller, J. Shaw and J. J. Veillette (2002). "The Laurentide and Innuitian ice sheets during the Last Glacial Maximum." Quaternary Science Reviews **21**(1–3): 9-31.

Dyke, A. S., A. Moore and L. Robertson (2003). "Deglaciation of North America." Geological Survey of Canada, Open File 1574.

Engelhardt, H. and B. Kamb (1997). "Basal hydaulic system of a West Antarctic ice stream: constraints from borehole observations." Journal of Glaciology **43**(144): 207 - 230.

Engelhardt, H., N. Humphrey, B. Kamb and M. Fahnestock (1990). "Physical Conditions at the Base of a Fast Moving Antarctic Ice Stream." Science **248**(4951): 57-59.

England, J. and M. Furze (2008). "New evidence from the western Canadian Arctic Archipelago for the resubmergence of Bering Strait." Quaternary Science Reviews **70**: 60 - 67.

England, J. H., M. F. A. Furze and J. P. Doupe (2009). "Revision of the NW Laurentide Ice Sheet: implications for palaeoclimate, the northeast extremity of Beringia, and Arcitc Ocean sedimentation." Quaternary Science Reviews **28**: 1573-1596.

Evans, D. J. A. (2003). "Glaciers." Progress in Physical Geography **27**(2): 261-274.

Evans, D. J. A. (2009). "Controlled moraines: origins, characteristics and palaeoglaciological implications." Quaternary Science Reviews **28**(3–4): 183-208.

Evans, D. J. A. and A. J. Russell (2002). "Modern and ancient ice-marginal landsystems." Sedimentary Geology **149**.

Evans, D. J. A. and D. R. Twigg (2002). "The active temperate glacial landsystem: a model based on Breiðamerkurjökull and Fjallsjökull, Iceland." Quaternary Science Reviews **21**(20–22): 2143-2177.

Evans, D. J. A., D. R. Twigg and M. Shand (2006). "Surficial geology and geomorphology of the þorisjokull plateau icefield, west-central Iceland." Journal of Maps **2**(1): 17 - 29.

Evans, D. J. A., Brice R., Hiemstra, J. F., O´ Cofaigh, C., (2006) “A critical assessment of subglacial mega-floods: a case study of glacial sediments and landforms in south-central Alberta, Canada.” Quaternary Science Reviews **25**: 1638–1667

Evans, D. J. A., D. R. Twigg, B. R. Rea and M. Shand (2007). "Surficial geology and geomorphology of the Bruajokull surging glacier landsystem." Journal of Maps **3**(1): 349 - 367.

Evans, D. J. A., C. D. Clark and B. R. Rea (2008). "Landform and sediment imprints of fast glacier flow in the southwest Laurentide Ice Sheet." Journal of Quaternary Science **23**: 249-272.

Eyles, N., J. I. Boyce and R. W. Barendregt (1999). "Hummocky moraine: sedimentary record of stagnant Laurentide Ice Sheet lobes resting on soft beds." Sedimentary Geology **123**: 163-174.

Fairbanks, R. G. (1989). "A 17,000-year glacio-eustatic sea level record: influence of glacial melting rates on the Younger Dryas event and deep-ocean circulation." Nature **342**(6250): 637-642.

Fawcett, P. J., A. M. Águstsdóttir, R. B. Alley and C. A. Shuman (1997). "The Younger Dryas termination and North Atlantic Deep Water Formation: Insights from climate model simulations and Greenland ice cores." Paleoceanography **12**(1): 23-38.

Fisher, T. G. (1993). Glacial Lake Agassiz: the northwest outlet and paleoflood spilway, N W Saskatchewan and N E Alberta. PhD, University of Calgary.

Fisher, T. G. (2007). "Abandonment chronology of glacial Lake Agassiz's Northwestern outlet." Palaeogeography, Palaeoclimatology, Palaeoecology **246**: 31-44.

Fisher, T. G. and C. Souch (1998). "Northwest outlet channels of Lake Agassiz, isostatic tilting and a migrating continental drainage divide, Saskatchewan, Canada." Geomorphology **25**(1-2): 57-73.

Fisher, T. G. and J. Shaw (1992). "A depositional model for Rogen moraine, with examples from the Avalon Peninsula, Newfoundland." Canadian Journal of Earth Sciences **29**: 669-686.

Fisher, T. G. and T. V. Lowell (2012). "Testing northwest drainage from Lake Agassiz using extant ice margin and strandline data." Quaternary International **260**(0): 106-114.

Fisher, T. G., D. G. Smith and J. T. Andrews (2002a). "Preboreal oscillation caused by a glacial Lake Agassiz flood." Quaternary Science Reviews **21**: 873-878.

Fisher, T. G., J. J. Clague and J. T. Teller (2002b). "The role of outburst floods and glacial meltwater in subglacial and proglacial landform genesis." Quaternary International **90**: 1-4.

Fookes, P. G., D. L. Gordon and I. E. Higginbottom (1978). Glacial landforms, their deposits and engineering characteristics. Geoabstracts, Proceedings of Symposium, University of Birmingham.

Fulton, R. J. (1995). Surficial Materials of Canada Scale 1:5,000000. M. 1880A.

Fulton, R. J. and V. K. Prest (1987). "The Laurentide Ice Sheet and its significance." Geographie Physique et Quaternaire **XLI**(2): 181-186.

Glasser, N. F., M. R. Bennett and D. Huddart (1999). "Distribution of glaciofluvial sediment within and on the surface of a high arctic valley glacier: Marthabreen, Svalbard." Earth Surface Processes and Landforms **24**(4): 303-318.

Goldstein, R. M., H. Engelhardt, B. Kamb and R. M. Frolich (1993). "Satellite radar interferometry for monitoring ice sheet motion: application to an Antarctic Ice Stream." Science **262**: 1525 - 1530.

Golledge, N. R. (2007). "An ice cap landsystem for palaeoglaciological reconstructions: characterizing the Younger Dryas in western Scotland." Quaternary Science Reviews **26**(1–2): 213-229.

Greenwood, S. L. and C. D. Clark (2009a). "Reconstructing the last Irish Ice Sheet 1: changing flow geometries and ice flow dynamics deciphered from the glacial landform record." Quaternary Science Reviews **28**(27–28): 3085-3100.

Greenwood, S. L. and C. D. Clark (2009b). "Reconstructing the last Irish Ice Sheet 2: a geomorphologically-driven model of ice sheet growth, retreat and dynamics." Quaternary Science Reviews **28**(27–28): 3101-3123.

Greenwood, S. L., C. D. Clark and A. L. C. Hughes (2007). "Formalising an inversion methodology for reconstructing ice-sheet retreat patterns from meltwater channels: application to the British Ice Sheet." Journal of Quaternary Science **22**(6): 637-645.

Hart, J. K. (1999). "Identifying fast ice flow from landform assemblages in the geological record: A discussion. ." Annals of Glaciology **28**(5966).

Hattestrand, C. and J. Kleman (1999). "Ribbed Moraine Formation." Quaternary Science Reviews **18**: 43-61.

Hess, D. and J. P. Briner (2009). "Geospatial analysis of controls on subglacial bedform morphometry in the New York Drumlin Field." Earth Surface Processes and Landforms **34**: 1126 - 1135.

Hicock, S. R. (1988). "Calcareous till facies north of Lake Superior, Ontario: implications for Laurentide ice streaming." Géographie Physique et Quaternaire **42**(2): 120 - 135.

Hicock, S. R. and A. Dreimanis (1992). "Deformation till in the Great Lakes region: implications for rapid flow along the south-central margin of the Laurentide Ice Sheet." Canadian Journal of Earth Sciences **29**(7): 1565-1579.

Hoffman, J. S., A. E. Carlson, K. Winsor, G. P. Klinkhammer, A. N. LeGrande, J. T. Andrews, and J. C. Strasser (2012), "Linking the 8.2 ka event and its freshwater forcing in the Labrador Sea", *Geophys. Res. Lett.*, **39**: L18703.

Hodgson, D. A. (1994). "Episodic ice streams and ice shelves during retreat of the northwesternmost sector of the late Wisconsinan Laurentide Ice Sheet over the central Canadian Arctic Archipelago." Boreas **23**(1): 14-28.

Hughes, O. L. (1972). "Surficial geology of northern Yukon Territory and northwestern district of MacKenzie, Northwest Territories." Geological Survey of Canada Paper **69 - 36**: 11.

Hughes, O. L. (1987). "Late Wisconsinan Laurentide glacial limits of Northwestern Canada: The Tutsieta Lake and Kelly Lake phases." Geological Survey of Canada, Paper **85 - 25**: 4.

Hughes, T. J. (1992). "On the pulling power of ice streams." Journal of Glaciology **38**(128): 125 - 151.

Jacobel, R. W., T. A. Scambos, C. F. Raymond and A. M. Gades (1996). "Changes in the configuration of ice stream flow from the West Antarctic Ice Sheet." Journal of Geophysical Research **101**(B3): 5499-5504.

Jansson, K. N. and N. F. Glasser (2005). "Using Landsat 7 ETM+ imagery and Digital Terrain Models for mapping glacial lineaments on former ice sheet beds." International Journal of Remote Sensing **26**(18): 3931-3941.

Jansson, K. N., A. P. Stroeven and J. Kleman (2003). "Configuration and timing of Ungava Bay ice streams, Labrador–Ungava, Canada." Boreas **32**(1): 256-262.

Jennings, C. E. (2006). "Terrestrial ice streams—a view from the lobe." Geomorphology **75**(1–2): 100-124.

Josenhans, H. W. and J. Zevenhuizen (1990). "Dynamics of the Laurentide Ice Sheet in Hudson Bay, Canada." Marine Geology **92**: 1-26.

Joughin, I. and R. B. Alley (2011). "Stability of the West Antarctic ice sheet in a warming world." Nature Geoscience **4**(8): 506-513.

Joughin, I., S. Tulaczyk, R. Bindschadler and S. F. Price (2002). "Changes in west Antarctic ice stream velocities: Observation and analysis." Journal of Geophysical Research **107**(B11): 2289.

Joughin, I., S. Tulaczyk, J. L. Bamber, D. Blankenship, J. W. Holt, T. Scambos and D. G. Vaughan (2009). "Basal conditions for Pine Island and Thwaites Glaciers, West Antarctica, determined using satellite and airborne data." Journal of Glaciology **55**(190): 245-257.

Joughin, I., B. E. Smith and D. M. Holland (2010). "Sensitivity of 21st century sea level to ocean-induced thinning of Pine Island Glacier, Antarctica." Geophysical Research Letters **37**(L20502).

Joughin, I., B. E. Smith, I. M. Howat, D. Floricioiu, R. B. Alley, M. Truffer and M. Fahnestock (2012). "Seasonal to decadal scale variations in the surface velocity of Jakobshavn Isbrae, Greenland: Observation and model-based analysis." Journal of Geophysical Research **117**(F2): F02030.

Kaplan, M. R., G. H. Miller and E. J. Steig (2001). "Low-gradient outlet glaciers (ice streams?) drained the Laurentide ice sheet." Geology **29**(4): 343-346.

Kehew, A. E., M. L. Lord, A. L. Kozlowski and T. G. Fisher, Eds. (2009). Proglacial megaflooding along the margins of the Laurentide Ice Sheet Megaflooding on Earth and Mars, Cambridge University Press.

King, E. C., R. C. Hindmarsh and C. R. Stokes (2009). "Formation of mega-scale glacial lineations observed beneath a West Antarctic ice stream." Nature Geoscience **2**: 585-596.

Klassen, R. W. (1971). "Surficial geology, Brock River and Franklin Bay, District of Mackenzie, Northwest Territories." Geological Survey of Canada Open File **48**(1:250,000 scale).

Kleman, J. (1992). "The palimpsest glacial landscape in northwestern Sweden - Late Weichselian deglaciation landforms and traces of older west-centered ice sheets." Geografiska Annaler Series A - Physical Geography **74A**(4): 305 - 325.

Kleman, J. (1994). "Preservation of landforms under ice sheets and ice caps." Geomorphology **9**(1): 19-32.

Kleman, J. and I. Börgstrom (1996). "Reconstruction of palaeo-ice sheets: the use of geomorphological data." Earth Surface Processes and Landforms **21**: 893-909.

Kleman, J. and C. Hättestrand (1999). "Frozen-bed Fennoscandian and Laurentide ice sheets during the last glacial maximum." Nature **402**: 63-66.

Kleman, J. and N. F. Glasser (2007). "The subglacial thermal organisation (STO) of ice sheets." Quaternary Science Reviews **26**: 585-597.

Kleman, J., I. Borgström and C. Hättestrand (1994). "Evidence for a relict glacial landscape in Quebec-Labrador." Palaeogeography, Palaeoclimatology, Palaeoecology **111**(3–4): 217-228.

Kleman, J., D. Marchant and I. Borgström (2001). "Geomorphic Evidence for Late Glacial Ice Dynamics on Southern Baffin Island and in Outer Hudson Strait, Nunavut, Canada." Arctic, Antarctic, and Alpine Research **33**(3): 249-257.

Kleman, J., C. Hättestrand, A. P. Stroeven, K. J. Jansson, H. De Angelis and I. Borgström, Eds. (2006). Reconstruction of paleo-ice sheets – inversion of their glacial geomorphological record. Glacier Science and Environmental Change. Oxford, Blackwell Publishing.

Kleman, J., K. N. Jansson, H. De Angelis, A. P. Stroeven, C. Hättestrand, G. Alm and N. F. Glasser (2010). "North American Ice Sheet build-up during the last glacial cycle, 115-21 kyr." Quaternary Science Reviews **29**: 2036 - 2051.

Lakeman, T. R. and J. H. England (2012). "Paleoglaciological insights from the age and morphology of the Jesse moraine belt, western Canadian Arctic" Quaternary Science Reviews **47**: 82 - 100.

Lambert, A., N. Courtier, G. S. Sasagawa, F. Klopping, D. Winester, T. S. James and J. O. Liard (2001). "New constraints on Laurentide postglacial rebound from absolute gravity measurements." Geophysical Research Letters **28**(10): 2109-2112.

Laymon, C. (1992). "Glacial geology of western Hudson Strait, Canada, with reference to Laurentide Ice Sheet dynamics." Geological Society of America Bulletin **104**(9): 1169-1177.

Lemmen, D. S., A. Duk-Rodkin and J. M. Bednarski (1994). "Late glacial drainage systems along the northwestern margin of the Laurentide Ice Sheet." Quaternary Science Reviews **13**(9-10): 805-828.

Leverington, D. W. and J. T. Teller (2003). "Paleotopographic reconstructions of the eastern outlets of glacial Lake Agassiz." Canadian Journal of Earth Sciences **40**: 1259-1278.

Leverington, D. W., J. D. Mann and J. T. Teller (2000). "Changes in the Bathymetry and Volume of Glacial Lake Agassiz between 11,000 and 9,300 ^{14}C yr BP." Quaternary Research **54**: 174-181.

Lewis, C. F. M., A. A. L. Miller, E. Levac, D. J. W. Piper and G. V. Sonnichsen (2012). "Lake Agassiz outburst age and routing by Labrador Current and the 8.2 cal ka cold event." Quaternary International **260**(0): 83-97.

Li, Y.-X., H. Renssen, A. P. Wiersma and T. E. Tornqvist (2009). "Investigating the impact of Lake Agassiz drainage routes on the 8.2 ka cold event with a climate model." Climate of the Past **5**: 471-480.

Lillesand, T. M., R. W. Kiefer and J. W. Chipman (2008). Remote Sensing and Image Interpretation. New Jersey, John Wiley and Sons.

Linden, M., P. Moller and L. Adrielsson (2008). "Ribbed moraine formed by subglacial folding, thrust stacking and lee side cavity infill." Boreas **37**(102-131).

Livingstone, S. J., C. Ó Cofaigh and D. J. A. Evans (2008). "Glacial geomorphology of the central sector of the last British-Irish Ice Sheet." Journal of Maps **4**(1): 358 - 377.

Livingstone, S. J., C. Ó Cofaigh, C. R. Stokes, C.-D. Hillenbrand, A. Vieli and S. S. R. Jamieson (2012). "Antarctic palaeo-ice streams." Earth-Science Reviews **111**(1–2): 90-128.

Lloyd, J.M., M. Moros, K. Perner, R. J. Telford, A. Kuijpers, E. Jansen and D. McCarthy (2011). "A 100 yr record of ocean temperature control on the stability of Jakobshavn Isbrae, West Greenland." Geology **39**(9): 867-870.

Lovell, H., C. R. Stokes, M. J. Bentley and D. I. Benn (2012). "Evidence for rapid ice flow and proglacial lake evolution around the central Strait of Magellan region, southernmost Patagonia." Journal of Quaternary Science **27**(6): 625-638.

Lowell, T., N. Waterson, T. Fisher, H. Loope, K. Glover, G. Comer, I. Hajdas, G. Denton, J. Schaefer, V. Rinterknecht, W. Broecker and J. Teller (2005). "Testing the Lake Agassiz meltwater trigger for the Younger Dryas." Eos Trans. AGU **86**(40).

Lucchitta, B. K. and H. M. Ferguson (1986). "Antarctica: measuring glacier velocity from satellite images." Science **234**(4780): 1105 - 1108.

Lundqvist, J. (1989). "Rogen (ribbed) moraine – identification and possible origin." Sedimentary Geology **62**: 281-292.

MacAyeal, D. R. (1992). "The basal stress distribution of ice stream E, Antarctica, inferred by control methods." Journal of Geophysical Research **97**(B1): 595 - 603.

Mackay, J. R. (1956). "Deformation by glacier-ice at Nicholson Peninsula, N.W.T., Canada." Arctic **9**(4): 218 - 228.

Mackay, J. R. (1958). "The valley of the lower Anderson River, N. W. T. " Geographical Bulletin **11**: 36 - 56.

Mackay, J. R. (1959). "Glacier ice-thrust features of the Yukon Coast." Geographical Bulletin **13**: 5 - 21.

Mackay, J. R. (1963). "The Mackenzie Delta area, N.W.T." Geographical Branch Memoir , Ottawa Ontario: Department of Mines and Technical Surveys**. 8**: 202 p.

Mackay, J. R. and W. H. Matthews (1973). "Geomorphology and Quaternary history of the Mackenzie River Valley near Fort Good Hope, N.W.T. Canada." Canadian Journal of Earth Sciences **10**: 26-41.

Mäkinen, J. (2003). "Time-transgressive deposits of repeated depositional sequences within interlobate glaciofluvial (esker) sediments in Köyliö, SW Finland." Sedimentology **50**(2): 327-360.

Manley, W. F. (1996). "Late-glacial flow patterns, deglaciation, and postglacial emergence of south-centra Baffin Island and the north-central coast of Hudson Strait, eastern Canadian Arctic." Canadian Journal of Earth Sciences **33**: 1499 - 1510.

Marich, A., M. Batterson and T. Bell (2005). "The Morphology and Sedimentological Analysis of Rogen Moraines, Central Avalon Peninsula, Newfoundland. Newfoundland and Labrador " Department of Natural Resources Geologic Survey **5**(1): 1-14.

Marshall, S. J. and P. U. Clark (2002). "Basal temperature evolution of North American ice sheets and implications for the 100-kyr cycle." Geophysical Research Letters **29**(24): 2214.

Marshall, S. J., G. K. C. Clarke, A. S. Dyke and D. A. Fisher (1996). "Geologic and topographic controls on fast flow in the Laurentide and Cordilleran Ice Sheets." Journal of Geophysical Research **101**(B8): 17827-17839.

Mazzotti, S., A. Lambert, J. Henton, T. S. James and N. Courtier (2011). "Absolute gravity calibration of GPS velocities and glacial isostatic adjustment in mid-continent North America." Geophysical Research Letters **38**(24): L24311.

McConnell, R. G. (1890). "Glacial features of parts of the Yukon and Mackenzie basins." Geological Society of, America.

McIntyre, N. F. (1985). "The dynamics of ice-sheet outlets." Journal of Glaciology **31**(108): 99 - 107.

Meissner, K. J. and P. U. Clark (2006). "Impact of floods versus routing events on the thermohaline circulation." Geophysical Research Letters **33**: 1-4.

Menzies, J. (1979). "A review of the literature on the formation and location of drumlins." Earth Science Reviews **14**(315-359).

Mickelson, D. M. and P. M. Colgan, Eds. (2003). The southern Laurentide Ice Sheet in the United States. Quaternary History of the United States, International Quaternary Association (INQUA) Special Volume for 2003 International Meeting in Reno, Nevada.

Mitchell, W. A. and J. M. Riley (2006). "Drumlin map of the Western Pennines and southern Vale of Eden, Northern England, UK." Journal of Maps **2**(1): 10 - 16.

Möller, P. (2010). "Melt-out till and ribbed moraine formation, a case study from south Sweden. ." Sedimentary Geology **232**: 161-180.

Morgan, V. L., T. H. Jacka, G. J. Akerman and A. L. Clarke (1982). "Outlet glacier and mass-balance studies in Enderby, Kemp and MacRobertson Lands, Antarctica." Annals of Glaciology **3**: 204 - 210.

Munro, M. J. and J. Shaw (1997). "Erosional origin of hummocky terrain in south-central Alberta, Canada." Geology **25**: 1027-1030.

Munro-Stasiuk, M. J. and D. B. Sjogren (1999). "Hummocky moraine: sedimentary record of stagnant Laurentide ice lobes resting on soft beds - commen." Sedimentary Geology **129**: 165-168.

Murton, J. B. (1996). "Thermokarst-lake-basin sediments, Tuktoyaktuk Coastlands, western arctic Canada." Sedimentology **43**(4): 737-760.

Murton, J. B., M. D. Bateman, S. R. Dallimore, J. T. Teller and Z. R. Yang (2010). "Identification of Younger Dryas outburst flood path from Lake Agassiz to the Arctic Ocean." Nature **464**(7289): 740-743.

Ó Cofaigh, C., J. A. Dowdeswell, C. S. Allen, J. F. Hiemstra, C. J. Pudsey, J. Evans and D. J.A Evans (2005). "Flow dynamics and till genesis associated with a marine-based Antarctic palaeo-ice stream." Quaternary Science Reviews **24**(5-6): 709-740.

Ó Cofaigh, C., J. A. Dowdeswell, E. C. King, J. B. Anderson, C. D. Clark, D. J. A. Evans, J. Evans, R. C. A. Hindmarsh, R. D. Larter, C. R. Stokes (2008) Comment on Shaw J., Pugin, A. and Young, R. "A meltwater origin for Antarctic shelf bedforms with special attention to megalineations." Geomorphology **102**, 364–375

Ó Cofaigh, C., Evans, D.J.A. & Smith, I.R. (2010) "Large-scale reorganization and sedimentation of terrestrial ice streams during late Wisconsinan Laurentide Ice Sheet deglaciation" Geological Society of America Bulletin **122**:743-756.

Occhietti, S., Ed. (1989). Quaternary Geology of St. Lawrence Valley and Adjacent Appalachian Subregion. Quaternary Geology of Canada and Greenland, Geology of Canada, 1. Ottawa, Geological Survey of Canada.

Oerlemans, J. and C. J. van der Veen (1984). Ice sheets and climate change. Dorecht/Boston/Lancaster, D. Reidel Publishing Company.

Patterson, C. J. (1997). "Southern Laurentide ice lobes were created by ice streams: Des Moines Lobe in Minnesota, USA." Sedimentary Geology **111**(1-4): 249-261.

Patterson, C. J. (1998). "Laurentide glacial landscapes: The role of ice streams." Geology **26**(7): 643-646.

Patterson, C. J. and R. L. Hooke (1995). "Physical environment of drumlin formation." Journal of Glaciology **41**(137): 30 - 38.

Patterson, C. J. and T. J. Boerboom (1999). "The significance of preexisting deeply weathered crystalline rock in interpreting the effects of glaciation in the Minnesota River valley, USA." Annals of Glaciology **28**(53 -58).

Patterson, W. S. B. (1994). The Physics of Glaciers. Oxford, Butterworth-Heinemann.

Paulson, A., A. S. Zhong and J. A. Wahr (2007). "Inference of mantle viscosity from GRACE and relative sea level data." Geophysical Journal International **171**: 497 - 508.

Payne, A. J. (1998). "Dynamics of the Siple Coast ice streams, West Antarctica: results from a thermomechanical ice sheet model." Geophysical Research Letters **25**(16): 3173 - 3176.

Payne, A. J., A. Vieli, A. P. Shepherd, D. J. Wingham and E. Rignot (2004). "Recent dramatic thinning of largest West Antarctic ice stream triggered by oceans." Geophysical Research Letters **31**(23): L23401.

Peltier, W. R. (2004). "Global Glacial Isostasy and the surface of the Ice-Age Earth: The ICE-5G (VM2) Model and GRACE." Annual Reviews of Earth and Planetary Science **32**: 111-149.

Peltier, W. R. (2009). "Closure of the budget of global sea level rise over the GRACE era: the importance and magnitudes of the required corrections for global glacial isostatic adjustment." Quaternary Science Reviews **28**: 1658 - 1674.

Peters, L. E., S. Anandakrishnan, R. B. Alley, J. P. Winberry, D. E. Voigt, A. M. Smith and D. L. Morse (2006). "Subglacial sediments as a control on the onset and location of two Siple Coast ice streams, West Antarctica." Journal of Geophysical Research **111**(B1): B01302.

Phillips, E., J. Everest and D. Diaz-Doce (2010). "Bedrock controls on subglacial landform distribution and geomorphological processes: Evidence from the Late Devensian Irish Sea Ice Stream." Sedimentary Geology **232**(3–4): 98-118.

Prest, V. K., D. R. Grant and V. N. Rampton (1968). Glacial map of Canada. Map 1253, Geological Survey of Canada.

Pritchard, H. D., R. J. Arthern, D. G. Vaughan and L. A. Edwards (2009). "Extensive dynamic thinning on the margins of the Greenland and Antarctic ice sheets." Nature **461**(971-975).

Rampton, V. N. (1982). "Quaternary geology of the Yukon Coastal Plain." Geological Survey of Canada Bulletin **317**.

Rampton, V. N. (1988). "Quaternary Geology of the Tuktoyaktuk Coastlands, Northwest Territories." Geological Survey of Canada **Memoir 423**.

Raup, H. M. (1946). "Phytogeographic studies in the Athabasca-Great Slave Lake region II." Journal Arnold Arboretum **27**(1): 1 - 84.

Rea, B. R. and D. J. A. Evans (2007). "Quantifying climate and glacier mass balance in North Norway during the Younger Dryas." Palaeogeography, Palaeoclimatology, Palaeoecology **246**(2-4): 307-330.

Reed, J. C., J. O. Wheeler, K. E. Barton, D. G. Howell and J. F. Vigil (2003). The North America Tapestry of Time and Terrain. Investigations Series 1-2781 (Version 1.0), United States Geological Survey.

Rhine, J. L. and D. G. Smith (1988). "Sedimentology and paraglacial eolian influence of the Late Pleistocene Athabasca fan-delta, northeast Alberta, Canada". Fan deltas: sedimentology and tectonic settings. W. Nemec and R. J. Steel. Glasgow, Blackie**:** 158-169.

Rignot, E., I. Velicogna, M. R. van den Broeke, A. Monaghan and J. Lenaerts (2011). "Acceleration of the contribution of the Greenland and Antarctic ice sheets to sea level rise." Geophysical Research Letters **38**(5): L05503.

Rogozhina, I., J. M. Hagedoorn, Z. Martinec, K. Fleming, O. Soucek, R. Greve and M. Thomas (2012). "Effects of uncertainties in the geothermal heat flux distribution on the Greenland Ice Sheet: An assessment of existing heat flow models." Journal of Geophysical Research **117**(F2): F02025.

Rohling, E. J., and H. Pälike. (2005). "Centennial-scale climate cooling with a sudden cold event around 8,200 years ago". Nature **434**: 975-979.

Ross, M., J. E. Campbell, M. Parent and R. S. Adams (2009). "Palaeo-ice streams and the subglacial landscape mosaic of the North American mid-continental prairies." Boreas **38**(3): 421-439.

Ross, M., P. Lajeunesse, and K. G. A. Kosar. (2011). "The subglacial record of northern Hudson Bay: insights into the Hudson Strait Ice Stream catchment". Boreas. **40**(1), 73-91.

Rutter, N. W. (1974). Surficial geology and landforms, Williston Lake area (Map 1), British Colombia. G. S. o. Canada, Geological Survey of Canada**:** Map 1381A, scale :1125,1000.

Rydningen, T. A., T. O. Vorren, J. S. Laberg and V. Kolstad (2012). The marine-based NW Fennoscandian Ice Sheet: glacial and deglacial dynamics as reconstructed from submarine landforms. Geophysical Research Abstracts. EGU General Assembly 2012. **14**.

Sella, G. F., S. Stein, T. H. Dixon, M. Craymer, T. S. James, S. Mazzotti and R. K. Dokka (2007). "Observation of glacial isostatic adjustment in ‘‘stable’’ North America with GPS." Geophysical Research Letters **34**(L02306).

Shaw, J., and D. Kvill, (1984).”A glaciofluvial origin for drumlins of the Livingstone Lake area, Saskatchewan.” Canadian Journal of Earth Sciences **21:** 1442-1459.

Shaw, J., and Sharpe, D. R., (1987) “Drumlin formation by subglacial meltwater erosion.” Canadian Journal of Earth Sciences, **24:** 2316-2323.

Shaw, J., D. Kvill, and B. Rains, (1989) “Drumlins and catastrophic subglacial floods.” Sedimentary Geology **62:** 177-202.

Shaw, J. (2003). "Submarine moraines in Newfoundland coastal waters: implications for deglaciation of Newfoundland and adjacent areas." Quaternary International **99-100**: 115-134.

Shaw, J., D. Sharpe and J. Harris (2010). "A flowline map of glaciated Canada based on remote sensing data." Canadian Journal of Earth Sciences **47**: 89-101.

Shreve, R. L. (1985). "Esker characteristics in terms of glacier physics, Katahdin esker system, Maine." Geological Society of America Bulletin **96**: 639-646.

Siddall, M. and M. R. Kaplan (2008). "Climate science: A tale of two ice sheets." Nature Geoscience **1**(9): 570-572.

Siegert, M. J., B. Welch, D. Morse, A. Vieli, D. D. Blankenship, I. Joughin, E. C. King, G. J.-M. C. L. Vieli, A. J. Payne and R. Jacobel (2004). "Ice Flow Direction Change in Interior West Antarctica." Science **305**(5692): 1948-1951.

Smith, D. G. (1992). "Glacial Lake Mackenzie, Mackenzie Valley, Northwest Territories, Canada." Canadian Journal of Earth Sciences **29**(8): 1756-1766.

Smith, D. G. (1994). "Glacial lake McConnell: Paleogeography, age, duration, and associated river deltas, mackenzie river basin, western Canada." Quaternary Science Reviews **13**(9–10): 829-843.

Smith, D. G. and T. G. Fisher (1993). "Glacial Lake Agassiz: The northwestern outlet and paleoflood." Geology **21**: 9-12.

Smith, M. J. and J. Knight (2011). "Palaeoglaciology of the last Irish ice sheet reconstructed from striae evidence." Quaternary Science Reviews **20**(1 - 2): 147 - 160.

Smith, M. J., J. Rose and S. Booth (2006). "Geomorphological mapping of glacial landforms from remotely sensed data: an evaluation of the principal data sources and an assessment of their quality." Geomorphology **76**(1 - 2): 148 - 165.

Sollid, J. L. and L. Sørbel (1994). "Distribution of Glacial Landforms in Southern Norway in Relation to the Thermal Regime of the Last Continental Ice Sheet." Geografiska Annaler Series A - Physical Geography **76**(1/2): 25 - 35.

Spagnolo, M., C. D. Clark and A. L. C. Hughes (2012). "Drumlin relief." Geomorphology **153–154**(0): 179-191.

Spedding, N. and D. J. A. Evans (2002). "Sediments and landforms at Kvarjokull, southeast Iceland: a reappraisal of the glaciated valley landsystem." Sedimentary Geology **149**(1): 21-42.

Speight, J. G. (1963). "Late Pleistocene historical geomorphology of the Lake Pukaki area, New Zealand." New Zealand Journal of Geology and Geophysics **6**(160 - 188).

Stokes, C. R. (2000). The geomorphology of palaeo-ice streams: identification, characteristics and implications for ice stream functioning. PhD, University of Sheffield.

Stokes, C. R. and C. D. Clark (1999). "Geomorphological criteria for identifying Pleistocene ice streams." Annals of Glaciology **28**: 67-74.

Stokes, C. R. and C. D. Clark (2001). "Palaeo-ice streams." Quaternary Science Reviews **20**: 1437-1457.

Stokes, C. R. and C. D. Clark (2002). "Are long subglacial bedforms indicative of fast ice flow?" Boreas **31**: 239-249.

Stokes, C. R. and C. D. Clark (2003). "Laurentide ice streaming on the Canadian Shield: A conflict with the soft-bedded ice stream paradigm?" Geology **31**(4): 347-350.

Stokes, C. R. and C. D. Clark (2004). "Evolution of late glacial ice-marginal lakes on the northwestern Canadian Shield and their influence on the location of the Dubawnt Lake palaeo-ice stream." Palaeogeography, Palaeoclimatology, Palaeoecology **215**: 155-171.

Stokes, C. R. and L. Tarasov (2010). "Ice streaming in the Laurentide Ice Sheet: A first comparison between data-calibrated numerical model output and geological evidence." Geophysical Research Letters **37**(1): L01501.

Stokes, C. R., C. D. Clark, D. Darby and D. A. Hodgson (2005). "Late Pleistocene ice export events into the Arctic Ocean from the M'Clure Strait Ice Stream, Canadian Arctic Archipelago." Global and Planetary Change **49**: 139-162.

Stokes, C. R., C. D. Clark, O. B. Lian and S. Tulaczyk (2006). "Geomorphological Map of Ribbed Moraines on the Dubawnt Lake Palaeo-Ice Stream Bed: A Signature of Ice Stream Shut-down?" Journal of Maps **2**(1): 1-9.

Stokes, C. R., A. B. Llan, S. Tulaczyk and C. D. Clark (2008). "Superimposition of ribbed moraines on a palaeo-ice-stream bed: implications for ice stream dynamics and shutdown." Earth Surface Processes and Landforms **33**(4): 593-609.

Stokes, C. R., C. D. Clark and R. Storrar (2009). "Major changes in ice stream dynamics during deglaciation of the north-western margin of the Laurentide Ice Sheet." Quaternary Science Reviews **28**(7-8): 721-738.

Stokes, C. R., M. Spagnolo and C. D. Clark (2011). "The composition and internal structure of drumlins: Complexity, commonality, and implications for a unifying theory of their formation." Earth-Science Reviews **107**(3-4): 398-422.

Storrar, R. and C. R. Stokes (2007). "A Glacial Geomorphological Map of Victoria Island, Canadian Arctic." Journal of Maps **3**(1): 191-210.

Stuiver, M., P. J. Reimer, E. Bard, J. W. Beck, G. S. Burr, K. A. Hughen, B. Kromer, G. McCormac, J. Van Der Plicht and M. Spurk (1998). "INTCAL98 Radiocarbon age calibration, 24,000-0 cal BP." Radiocarbon **40**(3): 1041-1083.

Sugden, D. E. (1977). "Reconstruction of the morphology, dynamics and thermal characteristics of the Laurentide Ice Sheet at its maximum." Arctic and Alpine Research **9**(1): 21 - 47.

Sugden, D. E. (1978). "Glacial erosion by the Laurentide Ice Sheet." Journal of Glaciology **20**(83): 367 - 391.

Tamisiea, M. E., J. X. Mitrovica and J. L. Davis (2007). "GRACE Gravity Data Constrain Ancient Ice Geometries and Continental Dynamics over Laurentia." Science **316**: 881 - 883.

Tarasov, L. and W. R. Peltier (2003). "Greenland glacial history, borehole constraints and Eemian extent." Journal of Geophysical Research **108**(B4): 2124 - 2143.

Tarasov, L. and W. R. Peltier (2005). "Arctic freshwater forcing of the Younger Dryas cold reversal." Nature **435**: 662-665.

Tarasov, L. and W. R. Peltier (2006). "A calibrated deglacial drainage chronology for the North American continent: evidence of an Arctic trigger for the Younger Dryas." Quaternary Science Reviews **25**: 659-688.

Tarasov, L., A. S. Dyke, R. M. Neal and W. R. Peltier (2012). "A data-calibrated distribution of deglacial chronologies for the North American ice complex from glaciological modeling." Earth and Planetary Science Letters **315–316**(0): 30-40.

Teller, J. T. and L. H. Thorleifson, (1983). The Lake Agassiz-Lake Superior connection. Glacial Lake Agassiz. St John's, Geological Association of Canada.

Teller, J. T. and A. E. Kehew (1994). " Introduction to the late glacial history of large proglacial lakes and meltwater runoff along the Laurentide ice sheet." Quaternary Science Reviews **13**: 795-799.

Teller, J. T., D. W. Leverington and J. D. Mann (2002). "Freshwater outbursts to the oceans from glacial Lake Agassiz and their role in climate change during the last deglaciation." Quaternary Science Reviews **21**: 879-887.

Teller, J. T., M. Boyd, Z. R. Yang, P. S. G. Kor and A. M. Fard (2005). "Alternative routing of Lake Agassiz overflow during the Younger Dryas: new dates, paleotopography, and re-evaluation." Quaternary Science Reviews **24**(16-17): 1890-1905.

Thorleifson, L. H., Ed. (1996). Review of Lake Agassiz history. Sedimentology, Geomorphology, and History of the Central Lake Agassiz Basin, Geological Association of Canada Field Trip Guidebook for GAC/MAC Joint Annual Meeting.

Truffer, M., K. A. Echelmeyer and W. D. Harrison (2001). "Implications of till deformation on glacier dynamics." Journal of Glaciology **47**(156): 123-134.

Tulaczyk, S., W. Kamb and H. Engelhardt (2000). "Basal mechanics of Ice Stream B, West Antarctica 1. Till mechanics." Journal of Geophysical Research **105**: B1.

Upham, W. (1895). "The Glacial Lake Agassiz." United State Geological Survey **Monograph 25**.

Upham, W. (1895). "Minor Time Divisions of the Ice Age." The American Naturalist **29**(339): 235-241.

van der Veen, C. J., T. Leftwich, R. von Frese, B. M. Csatho and J. Li (2007). "Subglacial topography and geothermal heat flux: Potential interactions with drainage of the Greenland ice sheet." Geophysical Research Letters **34**(12): L12501.

Viellette, J. J. (1995). "New evidence for northwestward glacial ice flow, James Bay region, Quebec." Commission Géologique du Canada, Current Research **1995 - C**: 249 - 258.

Vincent, J. S. (1982). "The Quaternary History of Banks Island, N. W. T., Canada." Geographie Physique et Quaternaire **XXXVI**(1-2): 209-232.

Vincent, J. S., Ed. (1989). Quaternary Geology of the North Canadian Interior Plains. Quaternary Geology of Canada and Greenland. Ottawa, Canada, Geological Survey of Canada.

Warren, W. P. and G. M. Ashley (1994). "Origins of the ice-contact stratified ridges (eskers) of Ireland." Journal of Sedimentary Research **64**(3a): 433-449.

Weertman, J. (1964). "Theory of Glacier Sliding." Journal of Glaciology **5**(39): 287-303.

White, D. A., D. Fink and D. B. Gore (2011). "Cosmogenic nuclide evidence for enhanced sensitivity of an East Antarctic ice stream to change during the last deglaciation." Geology **39**(1): 23-26.

Whitehouse, P. (2009). Glacial isostatic adjustment and sea-level change. Stockholm, Svensk Kärnbränslehantering AB, Swedish Nuclear Fuel, and Waste Management Co. Technical Report **TR-09-11**.

Winberry, J. P., S. Anandakrishnan, R. B. Alley, R. A. Bindschadler and M. A. King (2009). "Basal mechanics of ice streams: Insights from the stick-slip motion of Whillans Ice Stream, West Antarctica." Journal of Geophysical Research **114**: 1-11.

Winsborrow, M. C. M., C. D. Clark and C. R. Stokes (2004). "Ice Streams of the Laurentide Ice Sheet." Geographie physique et Quaternaire **58**(2-3): 26-280.

Winsborrow, M. C. M., C. D. Clark and C. R. Stokes (2010). "What controls the location of ice streams?" Earth-Science Reviews **103**(1–2): 45-59.

Winsborrow, M. C. M., C. R. Stokes and K. Andreassen (2012). "Ice-stream flow switching during deglaciation of the southwestern Barents Sea." Geological Society of America Bulletin **124**(3-4): 275-290.

Young, N. E., J. P. Briner, H. A. M. Stewart, Y. Axford, B. Csatho, D. H. Rood and R. C. Finkel (2011). "Response of Jakobshavn Isbræ, Greenland, to Holocene climate change." Geology **39**(2): 131-134.